

Spring 2017

# RURAL BROADBAND MOBILE COMMUNICATIONS: SPECTRUM OCCUPANCY AND PROPAGATION MODELING IN WESTERN MONTANA

Erin Wiles  
*Montana Tech*

Follow this and additional works at: [http://digitalcommons.mtech.edu/grad\\_rsch](http://digitalcommons.mtech.edu/grad_rsch)

 Part of the [Electrical and Electronics Commons](#), [Electromagnetics and Photonics Commons](#), and the [Other Electrical and Computer Engineering Commons](#)

---

## Recommended Citation

Wiles, Erin, "RURAL BROADBAND MOBILE COMMUNICATIONS: SPECTRUM OCCUPANCY AND PROPAGATION MODELING IN WESTERN MONTANA" (2017). *Graduate Theses & Non-Theses*. 119.  
[http://digitalcommons.mtech.edu/grad\\_rsch/119](http://digitalcommons.mtech.edu/grad_rsch/119)

This Thesis is brought to you for free and open access by the Student Scholarship at Digital Commons @ Montana Tech. It has been accepted for inclusion in Graduate Theses & Non-Theses by an authorized administrator of Digital Commons @ Montana Tech. For more information, please contact [sjuskiewicz@mtech.edu](mailto:sjuskiewicz@mtech.edu).

RURAL BROADBAND MOBILE COMMUNICATIONS:  
SPECTRUM OCCUPANCY AND PROPAGATION MODELING IN  
WESTERN MONTANA

by  
Erin Wiles

A thesis submitted in partial fulfillment of the  
requirements for the degree of

Masters of Science Electrical Engineering

Montana Tech

2017



## **Abstract**

Fixed and mobile spectrum monitoring stations were implemented to study the spectrum range from 174 to 1000 MHz in rural and remote locations within the mountains of western Montana, USA. The measurements show that the majority of this spectrum range is underused and suitable for spectrum sharing. This work identifies available channels of 5-MHz bandwidth to test a remote mobile broadband network. Both TV broadcast stations and a cellular base station were modelled to test signal propagation and interference scenarios.

Keywords: spectrum monitoring, propagation modeling, spectrum management, mobile communication, remote mobile broadband, spectrum occupancy

## **Dedication**

This work is dedicated to those who work hard and never give up.



## **Acknowledgements**

I would like to thank my thesis advisor, Kevin Negus for his guidance and encouragement. I am happy he came to Tech to start the Wireless Lab.

I would like to thank the Electrical Engineering Department at Montana Tech and Department Head Dan Trudnowski for providing the funding that allowed me to undertake this research and attend a conference.

I would like to thank my husband, Conor Cote, for his love and support as I completed my studies at Tech. I especially appreciate his help in editing and organizing my thesis manuscript.

## Table of Contents

<b>ABSTRACT .....</b>	<b>II</b>
<b>DEDICATION .....</b>	<b>III</b>
<b>ACKNOWLEDGEMENTS .....</b>	<b>IV</b>
<b>LIST OF TABLES .....</b>	<b>VII</b>
<b>LIST OF FIGURES.....</b>	<b>IX</b>
<b>LIST OF EQUATIONS .....</b>	<b>XIV</b>
<b>GLOSSARY OF ACRONYMS .....</b>	<b>XVII</b>
1. INTRODUCTION .....	1
2. LITERATURE REVIEW.....	6
3. TECHNICAL BACKGROUND .....	9
4. SPECTRUM MONITORING .....	26
4.1. <i>Methodology</i> .....	26
4.2. <i>Equipment</i> .....	27
4.3. <i>Locations</i> .....	37
4.4. <i>Procedure</i> .....	39
4.5. <i>Results</i> .....	50
4.6. <i>Analysis</i> .....	57
5. PROPAGATION MODELING.....	79
5.1. <i>Locations</i> .....	79
5.2. <i>Methodology</i> .....	83
5.2.1. Path Loss Parameters .....	84
5.2.2. ITM Algorithm .....	94
5.2.3. Propagation Mode Case Studies.....	103
5.3. <i>Results</i> .....	108

5.3.1. SPLAT! Irregular Terrain Parameter Calibration .....	108
5.3.2. ITM Predictions Compared to Measurements .....	115
5.3.3. Interference Simulations .....	118
6. CONCLUSION .....	137
<b>REFERENCES CITED.....</b>	<b>138</b>
<b>APPENDIX A: SUMMARY OF SPECTRUM MONITORING STUDIES.....</b>	<b>148</b>
<b>APPENDIX B: S21 MEASUREMENTS.....</b>	<b>150</b>
<b>APPENDIX C: OCCUPIED CHANNELS AT MONTANA TECH MUSEUM LOCATION.....</b>	<b>163</b>
<b>APPENDIX D: SPLAT! USER CONTROL.....</b>	<b>166</b>
<b>APPENDIX E: ANTENNA PATTERNS .....</b>	<b>173</b>

## List of Tables

Table I: Problematic Intermodulation Products .....	22
Table II: Equipment Summary.....	35
Table III: Time Duration for Each Hold.....	58
Table IV: Channel Occupancy Metrics.....	72
Table V: Occupied Channels at Moose Lake Road Location.....	74
Table VI: Mobile Communications at Museum and Moose Lake.....	77
Table VII: Summary of TV UHF Channels.....	81
Table VIII: Population Grid Summary .....	83
Table IX: Approximate Resolution for Each Elevation SDF File in Montana.....	88
Table X: SPLAT! Irregular Terrain Parameters .....	89
Table XI: Suggested Values for Electrical Ground Constants.....	90
Table XII: Radio Climates and Suggested Values.....	91
Table XIII: SPLAT! Test Input Parameters.....	94
Table XIV: Irregular Terrain Parameter for Various Terrains.....	101
Table XV: Propagation Mode Case Studies .....	103
Table XVI: Path Loss Predictions.....	109
Table XVII: Input Parameters Propagation Type .....	111
Table XVIII: Input Parameters Warning Code.....	113
Table XIX: Channel Power at Montana Tech Museum.....	117
Table XX: Summary of Channel Interference when EVM exceeds 5% .....	134
Table XXI: Summary of Spectrum Monitoring Studies .....	148
Table XXII: Occupied Channels at Montana Tech Museum Location .....	163

Table XXIII: Incompatible Latitudes for SPLAT! .....171

## List of Figures

Figure 1: Open Signal 2G/3G and LTE Coverage Map of USA .....	7
Figure 2: Open Signal 2G/3G and LTE Coverage Map of Montana .....	8
Figure 3: Modulation .....	10
Figure 4: Link Budget.....	12
Figure 5: Antenna Pattern of Omnidirectional in Azimuth .....	15
Figure 6: Dipole Pattern in Azimuth (left) and in Elevation (right) .....	15
Figure 7: Path Loss from a Transmitter .....	17
Figure 8: Signal Propagation .....	18
Figure 9: Receiver with Two Transmitters .....	20
Figure 10: Channel Interference: Adjacent Channel (top), Co-channel (bottom) .....	21
Figure 11: Error Vector Magnitude .....	23
Figure 12: Mobile Spectrum Monitoring Station.....	27
Figure 13: Station Equipment Schematic .....	28
Figure 14: Spectrum Analyzer Decompose Signal with Three Frequencies .....	29
Figure 15: Spectrum Analyzer Diagram.....	30
Figure 16: PSD Measurement without Shielding .....	36
Figure 17: PSD Measurement with Shielding .....	36
Figure 18: Map of Test Locations.....	37
Figure 19: Discone Antenna at Moose Lake Road Location.....	38
Figure 20: Museum Spectrum Monitoring Station at Montana Tech.....	38
Figure 21: Test Procedure Flow Chart.....	40
Figure 22: Data Acquisition Flow Chart.....	42

Figure 23: RTSA Device Initialization in Python.....	42
Figure 24: RTSA Sweep Settings and Initial Sweep .....	43
Figure 25: Frequency Interpolation .....	44
Figure 26: Gain Measurements on Network Analyzer .....	45
Figure 27: Equipment Gain Interpolation for Fixed Station Equipment .....	46
Figure 28: Equipment Gain Interpolation for Mobile Station Equipment.....	46
Figure 29: Gain Measurements of HP Filter Loss .....	47
Figure 30: D3000N Antenna Nominal Gain.....	47
Figure 31: Equipment Gain Interpolation.....	47
Figure 32: Typical Header File.....	49
Figure 33: Accessing Binary Data Efficiently .....	50
Figure 34: Montana Tech Wireless Lab YouTube Homepage .....	50
Figure 35: Typical Sweep for Montana Tech Museum Location.....	51
Figure 36: Typical Frame Non-Shielded Equipment at The M .....	53
Figure 37: Typical Frame Shielded Equipment at The M .....	54
Figure 38: The M Sweep with Spurious Emissions.....	55
Figure 39: Typical Frame at Moose Lake.....	56
Figure 40: Frame with Spurious Emissions at Moose Lake .....	57
Figure 41: Montana Tech Museum Hold Comparison .....	59
Figure 42: Moose Lake Road Hold Comparison .....	60
Figure 43: Noise Hold Comparison Analysis for Museum Setup .....	62
Figure 44: Noise Hold Comparison Analysis for Moose Lake Setup .....	63
Figure 45: Typical Idle Channel at Montana Tech.....	65

Figure 46: Active Channel 2G/3G Downlink at Museum Location .....	65
Figure 47: Active Channel with Noise, Verizon LTE Downlink, at Museum Location ...	66
Figure 48: Museum Location Typical Spurious Emissions Dominated Channel.....	67
Figure 49: Spurious Emissions Dominated Channel 14 at Moose Lake Road Location...	68
Figure 50: Spurious Emissions Dominated Channel 32 at Moose Lake Road Location...	68
Figure 51: Channel 43 at Moose Lake Road Location .....	69
Figure 52: Channel 98 at Moose Lake Road Location .....	70
Figure 53: Channel with RTSA 625 MHz Harmonic at Museum Location .....	71
Figure 54: Channel with RTSA 625 MHz Harmonic at Moose Lake Road Location.....	71
Figure 55: Museum Occupancy Plot for Each Frequency Bin .....	75
Figure 56: Moose Lake Occupancy Plot for Each Frequency Bin .....	76
Figure 57: UHF TV Channels within 242 km of Tech Museum .....	80
Figure 58: Map of Grid Locations .....	83
Figure 59: Distance between Tx and Rx on Earth .....	85
Figure 60: Python Azimuth Normalization.....	86
Figure 61: SRTM1 Coverage Area .....	87
Figure 62: SRTM3 Coverage Area .....	87
Figure 63: Surface Refractivity, <b>N<sub>s</sub></b> Mean August .....	92
Figure 64: Surface Refractivity, <b>N<sub>s</sub></b> Mean February .....	93
Figure 65: Geometry of Double Horizon Path.....	95
Figure 66: Typical Reference Attenuation.....	96
Figure 67: Horizon Distance.....	97
Figure 68: Reference Attenuation Test Case .....	100



Figure 69: Test Case for Quantile Attenuation .....	102
Figure 70: LOS Terrain Profile from Tech-Museum to K43DU-D.....	104
Figure 71: LOS Path Loss from K43DU-D to Montana Tech Museum.....	105
Figure 72: Diffraction Dominant Terrain Profile from Montana Tech Museum to K49KA-D .....	106
Figure 73: SPLAT! Diffraction Dominant Path Loss from K49KA-D to Montana Tech Museum .....	106
Figure 74: SPLAT! Troposcatter Dominant Terrain Profile form Montana Tech Museum to KTMF .....	107
Figure 75: SPLAT! Troposcatter Dominant Terrain Profile from KTMF to Montana Tech Museum.....	108
Figure 76: SPLAT! ITM Computation Warnings.....	112
Figure 77: K48MM-D Terrain Profile .....	114
Figure 78: RMS Smoothing of Channel Power .....	116
Figure 79: Matplotlib Contour Script .....	120
Figure 80: EVM Baseline for K27CD-D in Boulder, MT .....	121
Figure 81: EVM due Noise and Interference below 5% threshold in Boulder, MT .....	122
Figure 82: EVM due Noise and Interference above 5% threshold in Boulder, MT .....	122
Figure 83: EVM Baseline for KWYB at 79 dBm in Anaconda, MT .....	123
Figure 84: EVM Baseline for KWYB at 83 dBm in Anaconda, MT .....	124
Figure 85: EVM due Noise and Interference for KYWB at 79 dBm in Anaconda, MT .....	125
Figure 86: EVM due Noise and Interference for KYWB at 83 dBm in Anaconda, MT .....	125
Figure 87: EVM Baseline for KWYB at 79 dBm in Whitehall/Cardwell, MT .....	126

Figure 88: EVM Baseline for KWYB at 79 dBm in Whitehall/Cardwell, MT .....	127
Figure 89: EVM due Noise and Interference for KWYB at 79 dBm in Whitehall/Cardwell, MT .....	128
Figure 90: EVM due Noise and Interference for KWYB at 83 dBm in Whitehall/Cardwell, MT .....	128
Figure 91: EVM Baseline for KWYB at 83 dBm in Deer Lodge MT .....	129
Figure 92: EVM Baseline for KWYB at 83 dBm in Divide MT .....	130
Figure 93: EVM Baseline for KWYB at 79 dBm in Butte, MT .....	131
Figure 94: EVM Baseline for KWYB at 83 dBm in Butte, MT .....	131
Figure 95: EVM due Noise and Interference for KWYB at 79 dBm in Butte, MT.....	132
Figure 96: EVM due Noise and Interference for KWYB at 83 dBm in Butte, MT.....	133
Figure 97: Signal to Noise Ratio of WK9XUC Operating at 20 W ERP in Butte, Montana .....	135
Figure 98: Signal to Noise Ratio of WK9XUC Operating at 2 kW ERP in Butte, Montana .....	136
Figure 99: SPLAT! Command Line for ITM non-HD .....	166
Figure 100: SPLAT! Path Loss Report.....	167
Figure 101: SPLAT! Path Loss Report if Obstruction Detected .....	168
Figure 102: SPLAT! Command Line for ITM HD.....	168
Figure 103: KWYB Normalized Field Strength in Azimuth.....	169
Figure 104: Example SPLAT! Bash Script.....	170
Figure 105: Rx_names.txt Example.....	171
Figure 106: Grant Permission and Run Bash Script .....	172

## List of Equations

Equation (1) .....	9
Equation (2) .....	9
Equation (3) .....	10
Equation (4) .....	10
Equation (5) .....	11
Equation (6) .....	12
Equation (7) .....	13
Equation (8) .....	13
Equation (9) .....	13
Equation (10) .....	14
Equation (11) .....	14
Equation (12) .....	14
Equation (13) .....	16
Equation (14) .....	18
Equation (15) .....	19
Equation (16) .....	19
Equation (17) .....	22
Equation (18) .....	22
Equation (19) .....	22
Equation (20) .....	22
Equation (21) .....	23
Equation (22) .....	23

Equation (23) .....	24
Equation (24) .....	24
Equation (25) .....	24
Equation (26) .....	24
Equation (27) .....	24
Equation (28) .....	25
Equation (29) .....	31
Equation (30) .....	32
Equation (31) .....	41
Equation (32) .....	41
Equation (33) .....	43
Equation (34) .....	44
Equation (35) .....	48
Equation (36) .....	48
Equation (37) .....	72
Equation (38) .....	73
Equation (39) .....	81
Equation (40) .....	81
Equation (41) .....	85
Equation (42) .....	85
Equation (43) .....	86
Equation (44) .....	88
Equation (45) .....	88

Equation (46) .....	89
Equation (47) .....	90
Equation (48) .....	91
Equation (49) .....	92
Equation (50) .....	95
Equation (51) .....	96
Equation (52) .....	97
Equation (53) .....	97
Equation (54) .....	98
Equation (55) .....	98
Equation (56) .....	99
Equation (57) .....	99
Equation (58) .....	99
Equation (59) .....	100
Equation (60) .....	101
Equation (61) .....	102
Equation (62) .....	102
Equation (64) .....	103
Equation (65) .....	115
Equation (66) .....	115
Equation (67) .....	116
Equation (68) .....	169

## Glossary of Acronyms

<b>Term</b>	<b>Definition</b>
ACPR	adjacent channel power ratio
ADC	analog to digital converter
AGL	above ground level
AMSL	above mean sea level
BPSK	binary phase-shift keying
CBW	channel bandwidth
DFT	Discrete Fourier Transform
EIN	equivalent input noise
EIRP	equivalent isotropic radiated power
ERP	effective radiated power
EVM	error vector magnitude
FCC	Federal Communications Commission
FDD	frequency division duplex
FFT	Fast-Fourier Transform
FSPL	Free-Space Path Loss
GBE	Gigabit Ethernet
IF	intermediate frequency
IQ	in-phase quadrature
ISM	industrial, scientific and medical
ITM	Irregular Terrain Model
ITS	Institute for Telecommunication Scientists
ITU	International Telecommunication Union
ITWOM	Irregular Terrain with Obstruction Model
LNA	low noise amplifier
LO	local oscillator
LOS	line of sight
LTE	long-term evolution
NF	noise figure
NIST	National Institute of Standards and Technology
NTIA	National Telecommunications and Information Administration
PAPR	Peak to Average Power Ratio
PSD	power spectral density
RBW	resolution bandwidth
RF	radio frequency
RMS	Root Mean Square
RTSA	real-time spectrum analyzer
SAW	surface acoustic wave
SH	super-heterodyne
SNR	signal to noise ratio
SINR	signal to interference and noise ratio
SRTM	Shuttle Radio Topography Mission
UHF	ultra-high frequency
WLAN	wireless local area network

## 1. Introduction

The goal of this spectrum monitoring work is to demonstrate the viability of testing a remote land mobile wireless communication network. The results show that there is an abundance of underused spectrum in rural and remote areas across the span from 174 to 1000 MHz in western Montana. This work further identifies appropriate frequencies to optimize for mobile communications coverage in remote locations, specifically channels in the 500 MHz band.<sup>1</sup> The applications for using this spectrum to deliver mobile broadband communications will likely be modified technology designed for Long-Term Evolution (LTE) 4G wireless networks or the new 802.11ax standard for WLAN, therefore this work targets available 5-MHz channels<sup>2</sup>. Spectrum measurements are used to calibrate a popular propagation model, the Longley-Rice Path Loss, for locations in western Montana. Lastly, this work models the channel characteristics of a wireless broadband base station, whose call sign is WK9XUC, and TV stations located in this mountainous terrain.

Effective and efficient use of the spectrum is the aim of spectrum management policy. Various government agencies allocate spectrum to license holders on a long-term basis for large geographical regions. In the USA, the National Telecommunications and Information Administration (NTIA) administers federal communications, the Federal Communications Commission (FCC) administers non-federal communications. Currently, the 500 MHz band is designated by the FCC for TV broadcast.

---

<sup>1</sup> A band identifies a range of frequencies. Various agencies, International Telecommunications Union (ITU), IEEE, and NATO have different standards for designating bands across the spectrum. Since this paper covers frequency from 174 to 1000 MHz, each band is 100-MHz wide. The 200 MHz band ranges from 200 MHz to less than 300 MHz, the 300 MHz band ranges from 300 MHz to less than 400 MHz and so on. However, band is commonly used to refer to a specific communication channel. The bandwidth of a channel is the size of the band.

<sup>2</sup> When referencing a bandwidth the author will place a - between the value and frequency unit, e.g. 5-MHz. This designation does not identify the frequencies of the channel, but the size of the channel.

Wireless mobile networks have driven an increase in spectrum demand and a “scarcity” of spectrum in certain spectrum bands. Since spectrum has already been allocated from 9 kHz to 300 GHz, spectrum only becomes available by moving existing licenses to other bands or opening bands for shared use.

Wireless broadband networks are designed to meet capacity requirements in urban areas rather than eliminate coverage gaps in rural areas. A wireless mobile communication network is termed “broadband” because large amounts of data other than voice or text are being sent and received. What constitutes large is determined by the data rate. A mobile broadband network in a rural location must be designed to handle terrain, large geographical distances and a low density of users.

Compared to a channel at lower frequency, a channel at higher frequency is able to handle higher data rates. However, a signal with a higher frequency will more likely be absorbed or dispersed by objects or surfaces along the propagation path than a signal with a lower frequency. Therefore, a system with large data usage and higher frequency channels requires its base stations to be in close proximity to its mobile users.

The wireless industry shows a trend towards higher frequency in order to accommodate the large amounts of data consumed by mobile users. In July 2016, the FCC allocated nearly 11 GHz of spectrum for 5G mobile communications in 28 GHz, 37 GHz, and 39 GHz bands [1]. This 5G network planning aims to allow consumption of higher quantities of data by more users than LTE networks. It has been speculated that 5G will deliver data at 1 Gbit/sec in urban areas [2].

LTE is designated as broadband, and other 2G/3G wireless services are often designated as wireless mobile. LTE downlink speeds are typically between 5 and 15 Mbit/sec, and uplink



speeds between 3 and 9 Mbit/sec. 3G downlink speeds vary between less than 1 to 4 Mbit/sec, and average 3G uplink speeds vary from 0.300 to 1.1 Mbit/sec [3]. Uplinks are signals being transmitted from a mobile station to a base station. Downlinks are signals being transmitted from a base station to a mobile station.

A 5G system or even a current LTE system would be cost-prohibitive in a remote location. According to FCC statistics from 2013, the revenue potential for a wireless carrier in a major urban center is \$248,000 per square mile of service, whereas in remote areas the potential revenue may be as low as \$262 per square mile [4].

The most common bandwidths for LTE channels are 5-MHz and 10-MHz. In a given LTE band, multiple channels may be grouped together. In a frequency division duplex (FDD), the bands are paired as either uplink or downlink. Currently, the following bands (given in MHz) are used for LTE communication in North America: 700, 800, 1900, 1700/2100, 2300, 2500, 2600 [5]. In general, the spectrum allocations become larger (10-MHz to 80-MHz) as the band frequency increases.

In rural but populated areas, mobile cellular service is provided for 2G/3G legacy systems by Sprint, AT&T, and Verizon in the 800 MHz band. LTE coverage in rural but populated services is provided by carriers in the 700 MHz band, Verizon and AT&T currently.

Furthermore, sections of 600 MHz band were re-allocated by the FCC in 2014 from UHF (ultra-high frequency) TV channel to mobile communications [6]. These policy changes were in part meant to encourage competition for broadband wireless coverage in rural areas [7]. The 600 MHz wireless bands are going through several stages of auction, which will like conclude in 2017 [8].

A remote network with fewer base stations will require channels operating at a lower frequency with a larger bandwidth to cover fewer users across a larger area. This work targets channels below 600 MHz to operate a rural mobile broadband communication network.

Measured spectrum occupancy is useful to both policy makers and engineers, however, very little spectrum monitoring has been performed in remote and rural areas in the USA. A summary of these studies will be provided in the literature review that follows.

This work will give a sense of spectrum use in Butte, Montana and a remote location near Philipsburg, Montana. The strength of received signal is measured in power spectral density (PSD) with units of dBm/Hz (a dBm is power ratio in decibel in reference to a milliwatt, mW). These PSD measurements are made across a wide span from 174 to 1000 MHz with a resolution bandwidth (RBW) of 488 kHz resulting in 1692 frequency bins. The PSD measurements were made at each location for at least 2 weeks. Spectrum occupancy is quantified by several metrics in order to identify available 5-MHz channels, which include occupancy percentage above a threshold, mean shift, and max measurement. This work demonstrates the underuse of the spectrum in these rural and remote locations.

By identifying channels that may be available for shared use, the Wireless Lab applied for a license to transmit in several bands: 186 to 198 MHz, 510 to 550 MHz and 902 to 928 MHz (ISM band). As a consequence of this work, the Wireless Lab at Montana Tech was granted an experimental license to operate in each band at 20 W effective radiated power (ERP).

Additionally, this work characterizes the pathological spurious emissions that occur below 500 MHz. These emissions are likely due to electronic equipment, specifically computers. For this reason, the spectrum below 500 MHz is less valuable. Furthermore, devices that operate

in the ISM band must tolerate interference from other ISM applications. For these reasons, the 500 MHz band was chosen to model a cellular base station located in Butte, Montana.

The Longley-Rice Path Loss model was implemented to predict the channel characteristics of this 20 W ERP station, WK9XUC. This work tests the signal propagation of a base station and TV stations operating in these bands. Detailed predictions for receiver locations in western Montana will be provided.

## 2. Literature Review

While spectrum management policy is of interest to current academic researchers and industry professionals, there is no national comprehensive spectrum monitoring program in the USA. However, NTIA and National Institute of Standards and Technology (NIST) completed a pilot program in 2015. The aim of the program is to establish a national standard for spectrum monitoring data and architecture. Eventually, spectrum monitoring information would be shared by various host organizations, each with their own station(s) [9].

Depending on the purpose and method of acquisition, the spectrum monitoring data is varied and scattered. See Appendix A for a comparison of spectrum monitoring studies conducted worldwide by location, duration of recording, RBW and designation: urban, rural and/or suburban. Most spectrum monitoring studies focus on urban areas and collect data short-term either for several minutes or several days [10-28]. Other studies collect measurements for durations of several weeks, months or even years [29-36]. In general, studies demonstrate under-utilization of the spectrum, even in urban areas.

Current academic research in spectrum management has focused on cognitive radio. Cognitive radio is a scheme where a transceiver detects other licensed or unlicensed users in a communication channel, then selects another available channel to transmit or receive wireless communications. This scheme hopes to exploit any channel that is not occupied continuously (less than a 100% duty cycle). Since there is abundant spectrum available in the target rural and remote areas, evaluating the spectrum for cognitive radio development is not an aim of this project.

Long-term spectrum monitoring is a difficult task to complete in an urban location, but much harder in rural or remote locations due to limited resources. Short-term studies of twelve

locations within 100 km of Butte were conducted by the Wireless Lab of Montana Tech in 2015 [14]. These short-term measurements demonstrated that virtually the entire spectrum from 140 to 1000 MHz is unused in remote locations.

There is limited spectrum data collection for the majority of locations in rural and remote Montana. However, there are various data sets available to provide an idea of coverage. Open Signal is a private company that crowd sources data [37]. Users install an app that collects signal strength of the user's cellular service periodically. According to Open Signal reporting in 2016, LTE has been deployed in the USA with a time-coverage of 81%. Time coverage quantifies the amount of time that users have cellular (specifically LTE) network access [38]. Figure 1 depicts 2G/3G and LTE (4G) coverage maps nationwide retrieved on the 1<sup>st</sup> of May 2017 [39].

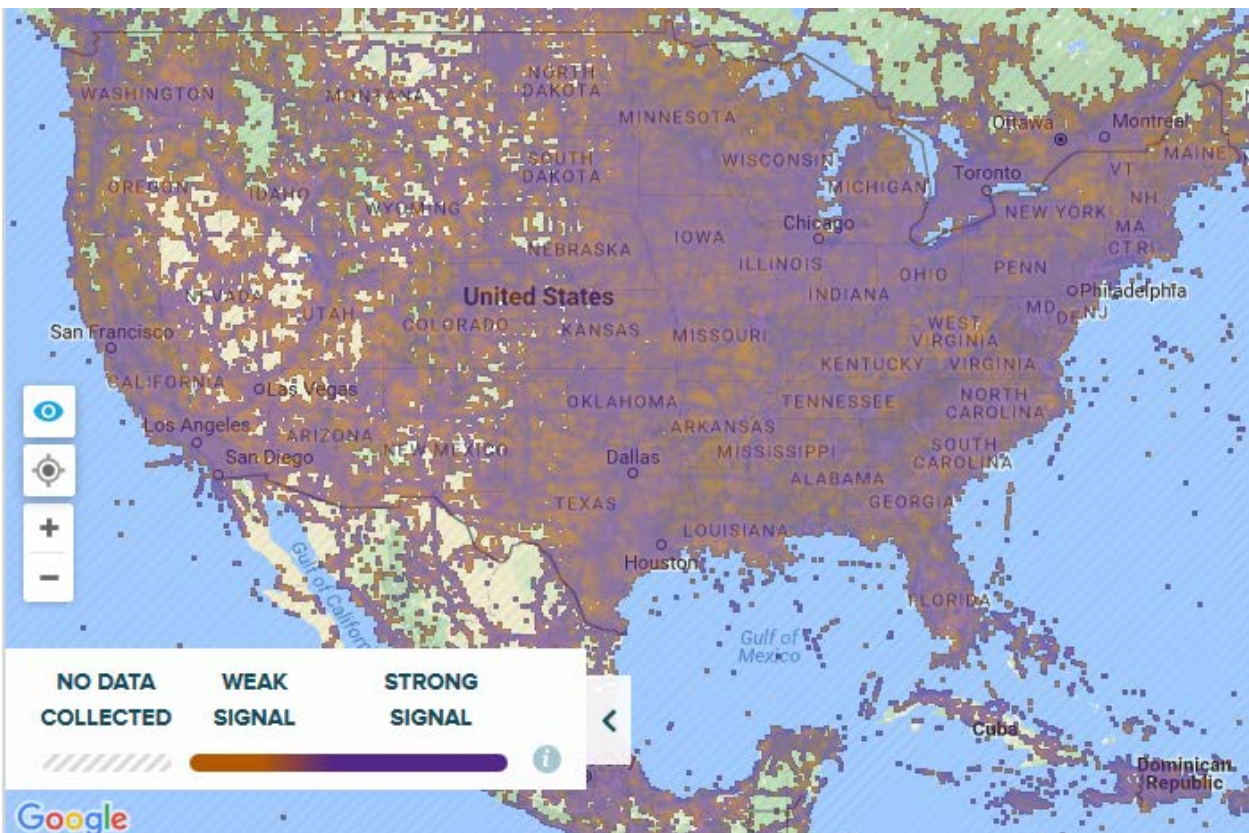


Figure 1: Open Signal 2G/3G and LTE Coverage Map of USA

Figure 2 depicts a coverage map for the state of Montana.

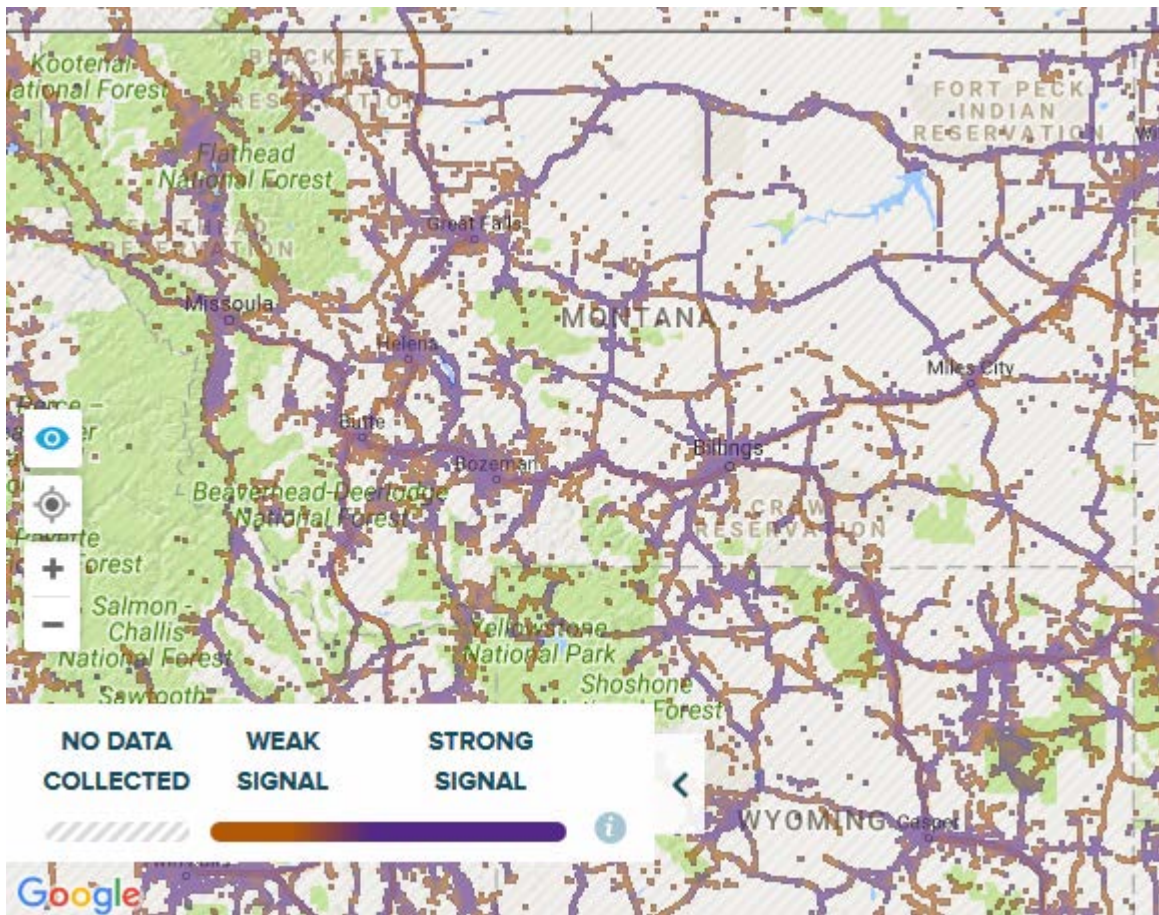


Figure 2: Open Signal 2G/3G and LTE Coverage Map of Montana

Note that most test locations are located in and around population centers and along highway and interstate systems. The majority of the state has no data collection as performed by Open Signal. It is likely that a majority of the state of Montana has no meaningful coverage.

### 3. Technical Background

In modern communication systems any given channel will have a carrier frequency that is modulated to convey information (data). A modulated carrier signal may have a time-varying amplitude, frequency and/or phase:

$$v(t) = A(t) \cos(\omega(t)t + \phi(t)) \quad (1)$$

The baseband message (or data) is conveyed in the carrier signal by changing the amplitude, frequency and/or phase of the carrier signal. This process is called modulation. At the transmitter, a device called a mixer modulates a carrier signal,  $c(t)$  with a baseband signal. Although a mixer is a non-linear device, it is assumed that the mixer multiplies the baseband and the carrier signal in Equation 2:

$$v(t) = c(t) \times A_{baseband}(t)(\cos 2\pi f_{baseband} + \phi_{baseband}(t)) \quad (2)$$

The mixer that multiplies the two signals is called an upconverter because the modulated signal has a higher frequency than the baseband signal (a downconverter would translate the incoming signal to a lower frequency). A simplified diagram of modulation, called binary phase-shift keying (BPSK) is pictured in Figure 3.



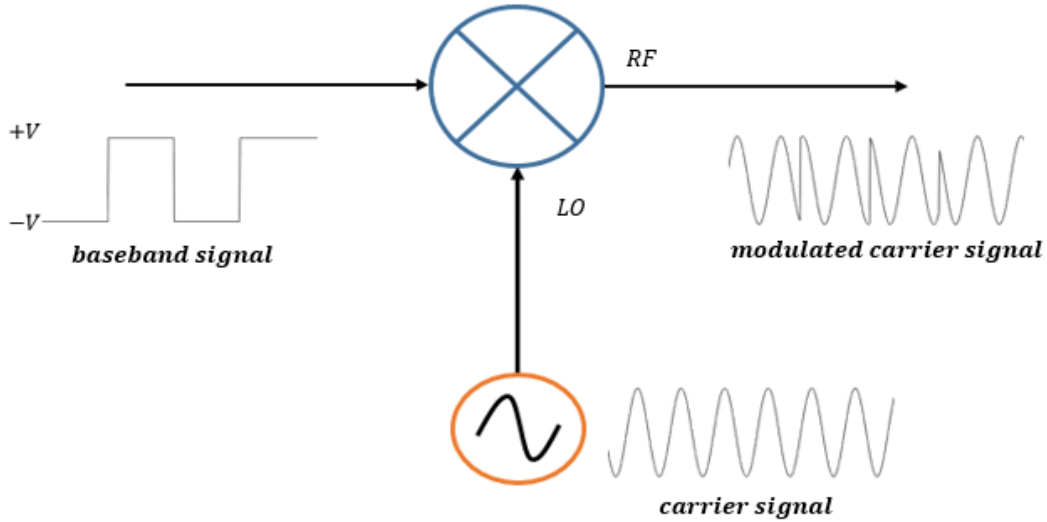


Figure 3: Modulation

The carrier signal is generated by what is called a local oscillator (LO). The baseband signal is the analog version of a bit stream: it is positive (+V) when the bit is 0, and negative (-V) when the bit is 1. The sign of the symbol changes the phase 180°. Recall that in the complex domain, a negative amplitude is equivalent to an amplitude with a phase of 180°: ( $-A = A\angle 180^\circ$ ). Product-to-sum trigonometric identities show how an LO frequency and a baseband frequency are combined:

$$\begin{aligned}
 v(t) &= \cos(2\pi f_{LO}t) A_{baseband}(t) \cos(2\pi f_{baseband}t + \varphi_{baseband}(t)) \\
 &= A_{baseband}(t) \left( \frac{1}{2} \cos(2\pi(f_{LO} - f_{baseband})t + \varphi_{baseband}(t)) \right. \\
 &\quad \left. + \frac{1}{2} \cos(2\pi(f_{LO} + f_{baseband})t + \varphi_{baseband}(t)) \right)
 \end{aligned} \tag{3}$$

In many modern systems, the baseband has a frequency of 0 Hz. As a result, the modulated carrier signal ('RF' in Figure 3) will have a phase that changes according to the phase of the baseband signal, and the modulated carrier frequency is the LO frequency:

$$y(t) = A_{baseband}(t) \cos(2\pi f_{LO}t + \varphi_{baseband}(t)) \tag{4}$$



A further consequence of sampling and filtering is that the modulated signal will occupy a range of frequencies, known as the channel bandwidth (CBW):

$$f_{modulated} = f_c \pm \frac{f_{bandwidth}}{2} \quad (5)$$

In general, the spectrum allocation restricts the channel to a bandwidth. Filters are implemented to adequately attenuate the sidebands. The bandwidth in turn limits the sampling rate and data rate of channel communications.

The simplest way to model a communication channel is to perform propagation analysis for a single link between a transmitter (Tx) and a receiver (Rx). A link budget is scaled in power decibels and accounts for the power of the signal from the transmitter to the receiver, which includes the transmit power,  $P_{Tx}$ , the gain or losses due to the Tx and Rx equipment, the path loss as the signal travels from the Tx, and to the Rx. Figure 4 pictures a link budget.

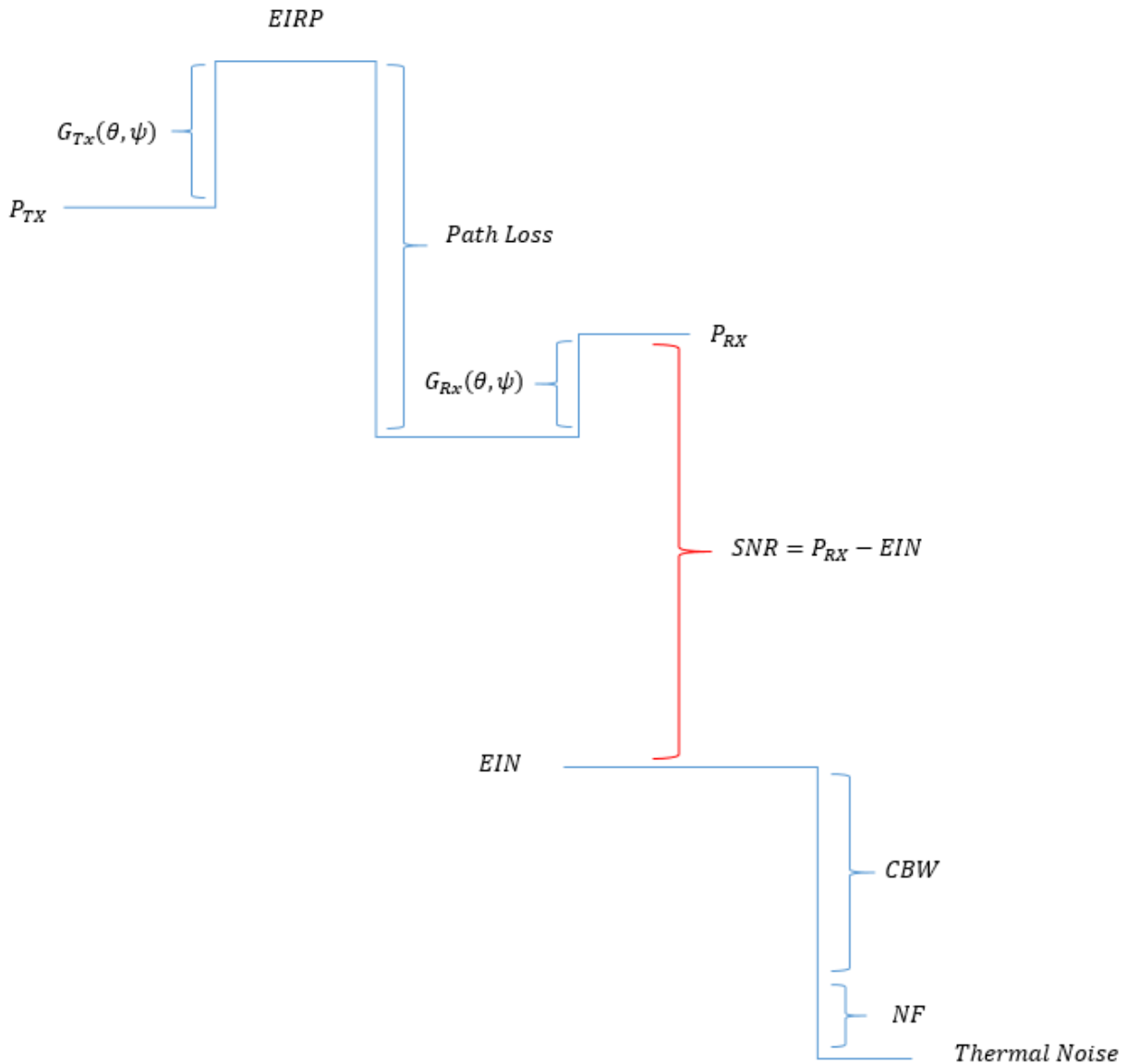


**Figure 4: Link Budget**

While it is simple to convert power values from linear to decibel:

$$P_{dB} = 10 \log_{10}(P_{linear}) \rightarrow P_{linear} = 10^{\frac{P_{dB}}{10}} \quad (6)$$

RF engineers prefer to report values in decibel and in a relatively small scale: dBm, which is the decibel version of milliwatts (mW). A gain in linear is the ratio between the output and input, in

decibel this is the difference between the output and input and is reported in dB. However, dB can also represent decibel watts, dBW (which is the decibel version of watt). Multiplication in linear is equivalent to addition in logarithmic, similarly linear division is the same as logarithmic subtraction. To convert from dBW to dBm simply add 30 dB:

$$P_{dBm} = P_{dBW} + 10 \log_{10} \left( 1000 \frac{mW}{W} \right) = P_{dBW} + 30 \text{ dB} \quad (7)$$

The equivalent isotropic radiated power (EIRP) is the sum of the transmit power and the gain of the Tx antenna. If the antenna has directivity, the relative position and orientation of the antenna in relation to the Rx, will alter the gain ( $G_{Tx}(\theta, \psi)$ ) of the Tx antenna. Here  $\theta$  represents the elevation angle and  $\psi$  represents the azimuth angle.

$$EIRP = P_{Tx} + G_{Tx}(\theta, \psi) \quad (8)$$

Additionally, the Rx may employ equipment to increase its sensitivity. These include but are not limited to the gain of the Rx antenna and of the amplifier. However, any loss due to filters or attenuators decreases sensitivity. Therefore, the power at the receiver is the decibel sum of EIRP, the path loss, and the losses or gains due Rx equipment:

$$P_{Rx} = EIRP + \text{Path Loss} - G_{Rx}(\theta, \psi) \quad (9)$$

The link budget figure is a visualization of power level at the receiver and the receiver sensitivity. The noise floor is a metric that describes the sensitivity of the receiver. It is the minimal detectable power level of the receiver. For a transmitter location and receiver location, engineers will determine the power of the received signal relative to noise floor. This is called

the signal to noise ratio (SNR), a useful metric that quantifies the quality of the received signal for a given scenario:

$$SNR_{linear} = \frac{P_{RX}}{EIN} \rightarrow SNR_{dB} = P_{RX_{dB}} - EIN_{dB} \quad (10)$$

For modern communication systems the SNR will in part determine the data rate. In general, a higher data rate requires a larger SNR.

The noise level depends on the environment for a given communication link, which includes but is not limited to the thermal noise of the channel and the internal noise of the Rx equipment. Thermal noise is the smallest amount of power that may exist in a given CBW. Thermal noise is calculated using the temperature (in Kelvins) and Boltzmann's constant,  $k_b$  ( $\frac{Joules}{Kelvin}$ ), where the CBW is assumed to be 1 Hz wide:

$$Noise_{thermal} = 10 \log_{10}(k_b T) \quad (11)$$

The internal noise of the equipment or noise figure (NF) is particular to each piece of equipment and must be measured. The channel bandwidth and NF will raise the noise floor according to the following equation, this metric is called the equivalent input noise (EIN):

$$EIN = Noise_{thermal} + 10 \log_{10}(CBW) + NF \quad (12)$$

The PSD of thermal noise has a limit of -174 dBm/Hz, when calculated in dBm, and a temperature of 300 K.

The gain of an antenna is a ratio relative to an isotropic antenna. An isotropic antenna has a gain of 1 in linear or 0 dBi in decibel. By changing an antenna's directivity, the gain is directed

towards a point (or points) in space and away from others. Figure 5 depicts an omnidirectional antenna in the azimuth direction that is shaped like a torus (donut). In contrast, an isotropic antenna would be shaped like a sphere.

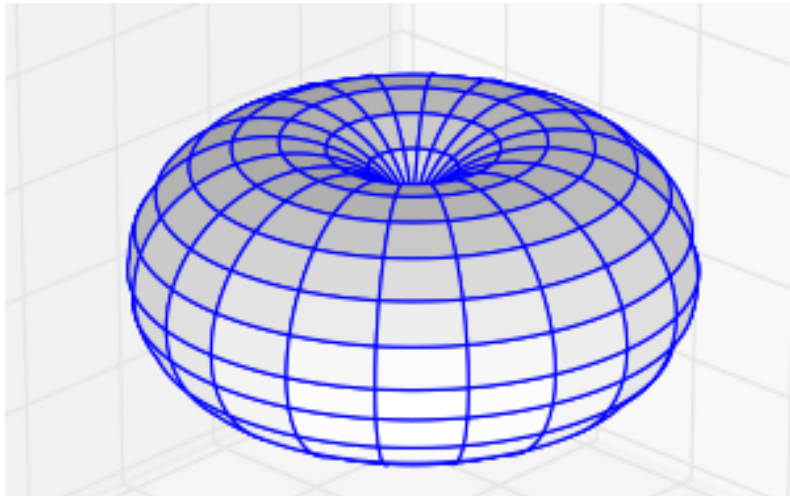


**Figure 5: Antenna Pattern of Omnidirectional in Azimuth**

Instead of modeling an antenna pattern in 3D, the antenna pattern is given in the azimuth direction (horizontal) and by elevation (vertical), see Figure 6. Depending on the relative location and position of the receiver to the transmitter, gain will be added or removed to the power of the transmission.

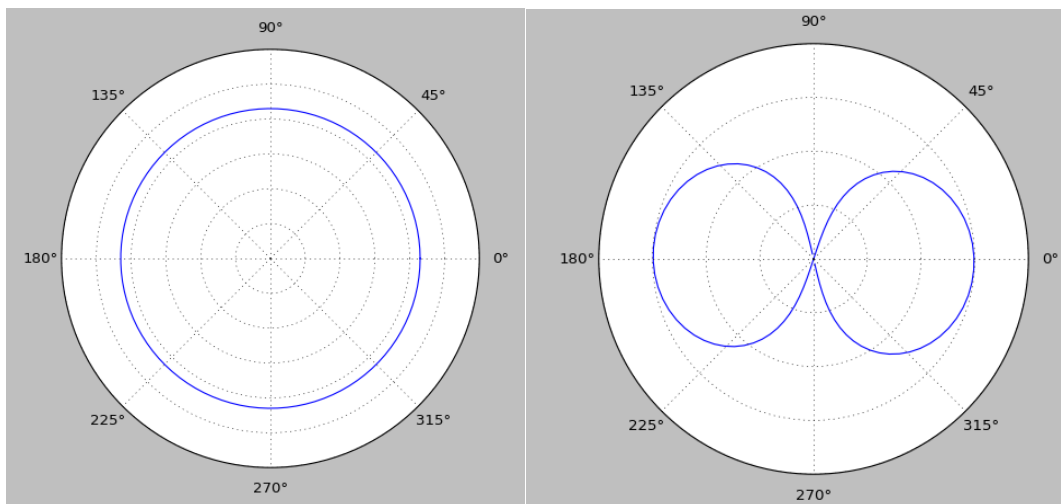


**Figure 6: Dipole Pattern in Azimuth (left) and in Elevation (right)**

When the direction of gain (either azimuth or elevation) is not given, the gain is understood to be in the direction of the peak value, in which case the EIRP is a maximum.

$$EIRP_{max} = P_{TX} + G_{Tx,max} \quad (13)$$

The power for transmitter is generally restricted to a CBW. For the TV channels the bandwidth is 6-MHz, and as discussed, the bandwidth of the target channels is 5-MHz.

Various models have been developed to model path loss for a given terrain and obstacles. Some of these models will be described in more detail below. The most simple are theoretical models operating in free-space (i.e. free of obstacles). A deterministic model would launch rays from a Tx, and trace the rays as they interact with the environment. Various empirical models have been developed by fitting collected data statistically. This work implements an empirical model called the Longley-Rice Path Loss model, and its algorithm is called the Irregular Terrain Model (ITM) [40].

A transmitter is often modeled as a point source, which emits a signal as rays in all directions (see Figure 7) [41]. Closer to the transmitter the rays are denser, further away they become sparser. The signal is said to “lose” power over a distance, but in reality the same amount of power becomes less dense as it propagates in three dimensions. The intensity or strength of the signal is inversely proportional to the surface area of a sphere ( $4\pi r^2$ ). This inverse square law is the basis for Free-Space Path Loss (FSPL) model.

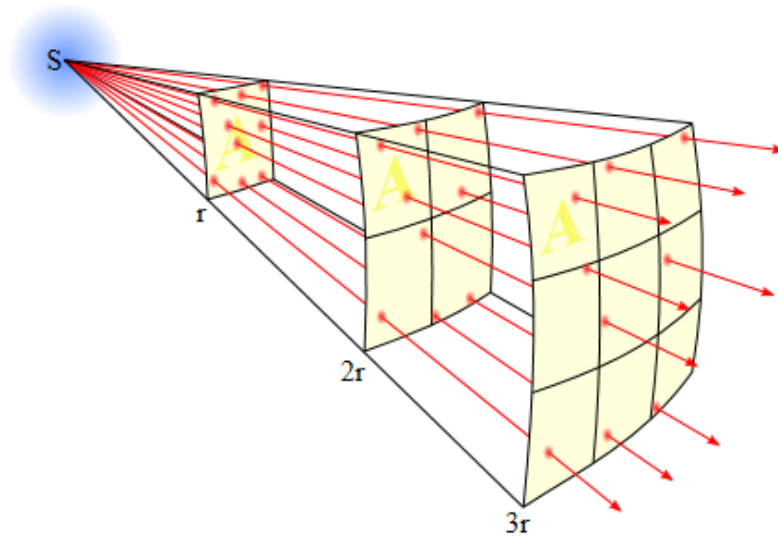


**Figure 7: Path Loss from a Transmitter**

As a signal propagates, the rays interact with the objects in the environment. How a signal propagates is determined by geometry and the materials in the environment. The materials may act like an insulator, a conductor or a ground. There are five basic mechanisms for signal propagation: direct transmission (commonly called line-of-sight (LOS)), reflection, refraction, diffraction and scattering. Figure 8 depicts each type of transmission (LOS-green, reflection-blue, refraction-purple, diffraction-orange and scattering-red).

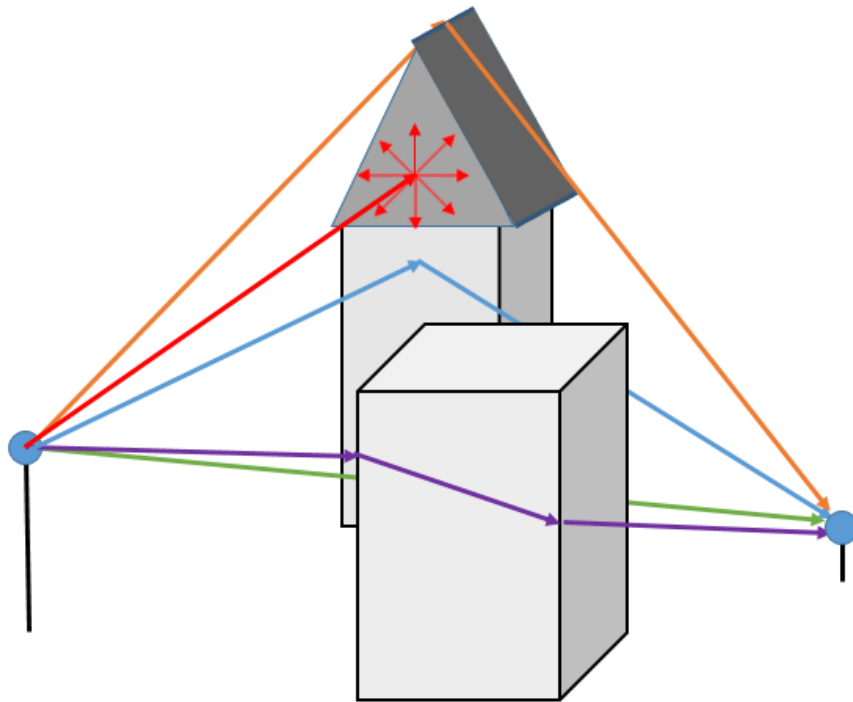


**Figure 8: Signal Propagation**

FSPL describes the theoretical power of a signal as it crosses a distance. As the distance between the transmitter and receiver increases, a two-ray path model is used when the signal reflects off the ground.

A LOS path (green line) travels through the air and is modeled with the FSPL equation that depends on the frequency of the carrier signal and the distance between the two antennas:

$$FSPL = \left(\frac{4\pi d f_c}{c}\right)^2 \rightarrow FSPL_{dB} = 20 \log_{10} \left(\frac{4\pi d f_c}{c}\right) \quad (14)$$

In decibels, the slope of signal across a distance is 20 dB/decade. When the distance between the transmitter and receiver are long enough, the path will reflect off the ground, in which case the slope is assumed to be 40 dB/decade. This inverse 4<sup>th</sup> power is a rule of thumb, and may change depending on the transmission environment. The distance at that the signal reflects is called the



cross-over (or critical) distance,  $d_c$ . This distance is determined by the height of the transmitter antenna,  $h_{TX}$  and the receiver antenna,  $h_{RX}$  and the wavelength of the carrier signal:

$$d_c = \frac{4\pi h_{tx} h_{rx}}{\lambda} \quad (15)$$

Increasing the height of either antenna will increase this distance, and lowering the frequency of the signal will decrease this distance. When the distance is greater than the cross-over distance the path loss is proportional to an inverse 4<sup>th</sup> power of distance,  $\propto \frac{1}{d^4}$ :

$$\begin{aligned} \mathbf{Path\ Loss}_{ground\ reflection} &= \frac{h_{tx}^2 h_{rx}^2}{d^4} \\ \rightarrow \mathbf{Path\ Loss}_{ground\ reflection_{dB}} &= 20 \log_{10}(h_{tx} h_{rx}) - 40 \log_{10}(d) \end{aligned} \quad (16)$$

Reflection is not limited to the ground, it can also reflect off of obstacles like buildings (blue line in Figure 8), in which case the path loss of each distance is summed.

A signal will also pass through a medium and refract (or change direction). Depending on the thickness of the material or type of material, refraction will likely result in absorption, i.e. the medium acts like a filter and dissipates the energy in the signal.

Diffraction, sometimes called knife-edge diffraction occurs when the signal is redirected by well-defined obstacle, like the roof of a building. When the object is rounded, the rays will diffract when the diameter of the object is larger than wavelength of the signal. Scattering occurs when the shape of the material is much smaller in diameter than the wavelength of the signal.

This ITM model assumes that the LOS is the dominant-path and does not account for multipath components directly. If there is an obstacle along the direct path, the algorithm determines additional attenuation to the direct path based on terrain parameters and elevation. In contrast, a ray-launching model would account for the multipath propagation but it requires

sufficient knowledge of the radio environment: location, geometry and material of the obstacles; ultimately, a ray launching program requires greater computation time and larger memory needs than a model like ITM.

Propagation modeling is an important component for planning a wireless network, but it requires accurate mapping of coverage of existing and planned networks. The key aim is to limit co-channel and adjacent channel interference between different transmitter stations. In both cases, an Rx receives a transmission (or emission) from each station: one is a desired signal and the other is interference, as pictured in Figure 9 below.

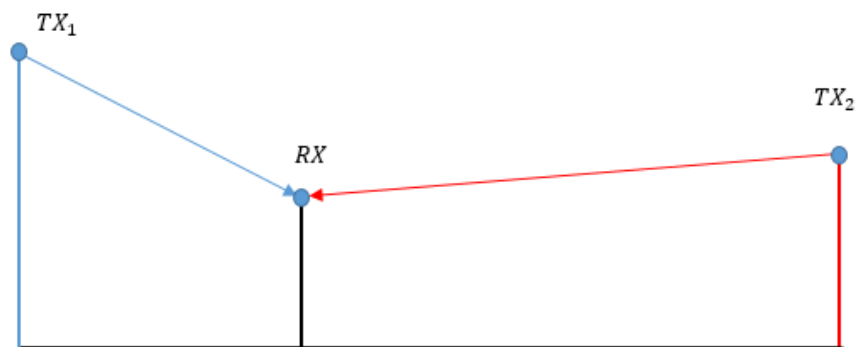


**Figure 9: Receiver with Two Transmitters**

Co-channel means at least two transmitter stations share the same channel at the same time but are separated by a geographical distance, as depicted in Figure 10 (bottom). These two stations may be a part of the same network (e.g. Verizon Base stations) or two different stations with the same frequency allocation. Adjacent channel interference occurs when a station transmits emissions into nearby channels, as depicted in Figure 10 (top).

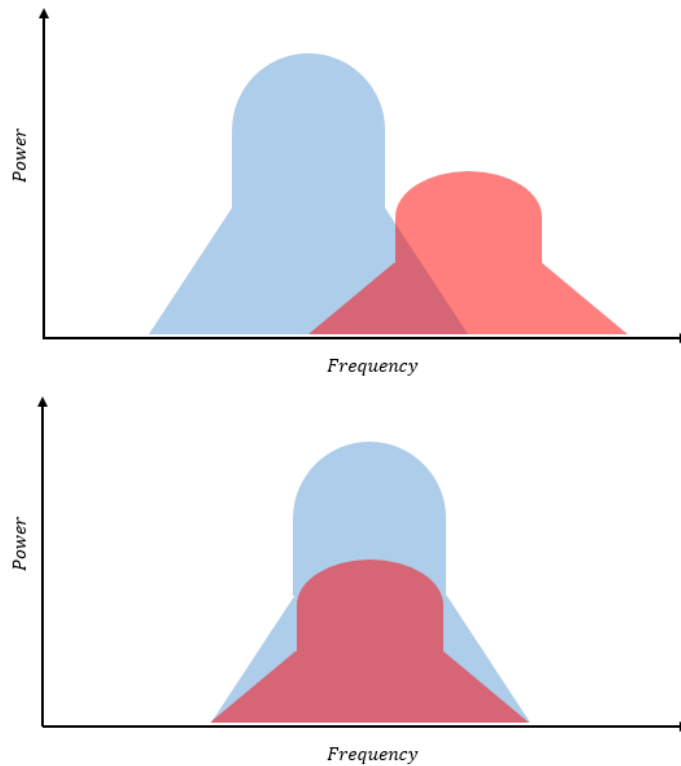


**Figure 10: Channel Interference: Adjacent Channel (top), Co-channel (bottom)**

The slopes off the main channel are meant to illustrate sideband emissions, these do not convey information but cause interference when they fall within the passband of a communication channel. These emissions are caused by intermodulation of amplifiers and to a certain extent the limitation of filters.

An amplifier has limited linear range, therefore when the amplifier operates non-linearly, it will generate intermodulation products. A signal that is saturated appears clipped and becomes more like a square wave. The effect of this is that the fundamental and harmonics of the signal will combine to produce intermodulation products.

In order to illustrate this phenomenon, an input voltage with only two tones is used. The output combination of these two tones may be written as a power series:

$$v_{out} = k_0 + k_1 v_{in} + k_2 v_{in}^2 + k_3 v_{in}^3 + \dots \quad (17)$$

where,

$$v_{in} = \cos(\omega_1 t) + \cos(\omega_2 t) \quad (18)$$

As a consequence, the frequencies present in the output signal are the sums and differences between integer multiples of the two tones:

$$f_{out} = |m f_1 \pm n f_2| \quad (19)$$

where  $m$  and  $n$  are integers that increment through the harmonics of each frequency. The signal is filtered to remove (most) of these intermodulation artifacts. However, the 3<sup>rd</sup> order intermods and 5<sup>th</sup> order intermods both fall within the passband of the channel:

**Table I: Problematic Intermodulation Products**

Intermodulation	Frequency
<i>IM3</i>	$[2f_1 - f_2 \quad 2f_2 - f_1]$
<i>IM5</i>	$[3f_1 - 2f_2 \quad 3f_2 - 2f_1]$

Depending on the degree of saturation, the channel power will be raised and potentially emit into other channels and/or interfere with itself.

There are several metrics to characterize interference. One is the signal to interference and noise ratio (SINR), it is similar to SNR, but the EIN and the power of the inference are summed linearly:

$$SINR_{dB} = P_{RX_{dB}} - 10 \log_{10}(EIN_{linear} + P_{interference}) \quad (20)$$

Another metric is the error vector magnitude (EVM). EVM is the ratio between the Root Mean Square (RMS) amplitude of the error,  $V_{error}$  and the RMS amplitude of the desired signal,

$V_{signal}$ . This is equivalent to the square root of the ratio between the average (RMS) power of the error and of the signal.

$$EVM_{linear} = \frac{V_{error}}{V_{signal}} = \sqrt{\frac{P_{error}}{P_{signal}}} \quad (21)$$

Since this is a ratio, the impedance is the same for both voltages, therefore these formulas are equal.

One way to picture this is to look at the signal in the complex domain as pictured in Figure 11.

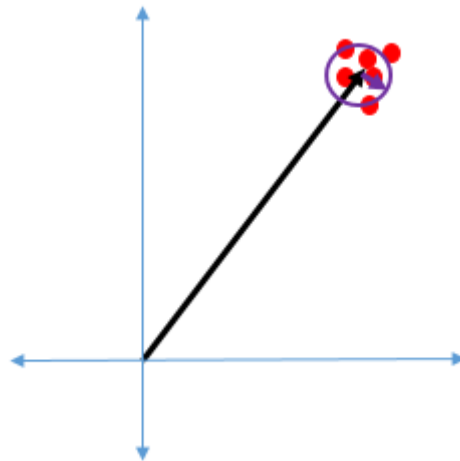


**Figure 11: Error Vector Magnitude**

The red dots depict six measurement samples of a voltage. The amplitude of the error vector (purple) is computed by finding the difference between the reference vector (black),  $V_{ref}$  and each measurement sample,  $V$ . The RMS amplitude of the error is calculated by applying the following equation:

$$V_{rms} = \sqrt{\frac{1}{n} (|V_{ref} - V_1|^2 + |V_{ref} - V_2|^2 + \dots + |V_{ref} - V_n|^2)} \quad (22)$$

where  $n$  is the number of samples and  $V_{ref}$  and  $V$  are complex numbers. The amplitude of the error can be determined with the following equation:

$$|V_k| = \sqrt{\text{Re}(V_k)^2 + \text{Im}(V_k)^2} = \sqrt{V_k V_k^*} \quad (23)$$

EVM may be given a percentage, in which case it is multiplied by 100, but it is also may be reported in dB, EVM is converted to a linear voltage with the following equation:

$$EVM_{dB} = -20 \log_{10}(EVM) \quad (24)$$

In mountainous rural terrain, the communication channel is likely to be noise-limited. In this case, the error is due to the thermal noise, NF and CBW:

$$EIN_{linear} = kT \times 1000 \frac{mW}{W} \times CBW \times 10^{\frac{NF_{dB}}{10}} \quad (25)$$

$$P_{error} = EIN_{linear} \rightarrow EVM = \sqrt{\frac{EIN_{linear}}{P_{signal}}} \quad (26)$$

However, the error may also be due to interference as well as noise, in which case the error is the linear sum of the power of the noise and of the interference. This is possible because the noise and the interference are treated as individual and independent waveforms, which add at the input of the Rx:

$$P_{error} = EIN_{linear} + P_{interference} \rightarrow EVM = \sqrt{\frac{(EIN_{linear} + P_{interference})}{P_{signal}}} \quad (27)$$

The EVM of the noise is the square root of the SINR, and the EVM of the SINR is the square root of the SINR.

$$\begin{aligned} EVM_{noise\ only} &= \frac{1}{\sqrt{SNR}} \\ EVM_{noise,interference} &= \frac{1}{\sqrt{SINR}} \end{aligned} \tag{28}$$

If the error due to the interfering station causes the EVM to exceed a threshold (5% and 10% are typically used by RF engineers), modifications would be made by the interfering station, which include but are not limited to lowering the transmitter power, adding filters at the Tx or employing a directive antenna at the Tx.

## **4. Spectrum Monitoring**

### **4.1. Methodology**

For this spectrum monitoring project, wireless communications are assessed by three parameters: frequency, time and power. For the propagation modeling, space will be an added parameter. This section provides technical information to explain how power measurements of signals at different frequencies are collected over time. For this thesis work the frequency span of interest is from 174 to 1000 MHz. The resolution bandwidth (RBW) is 488 kHz, resulting in 1692 frequency bins. This work collects the PSD dBm/Hz for each frequency bin.

The spectrum monitoring station, including the equipment and procedures at each location will be described in detail. The spectrum monitoring station may be implemented as either a fixed or mobile station; as such, this spectrum monitoring station may be adapted for measurements in remote, rural and urban locations. Figure 12 pictures the mobile spectrum monitoring station on site at a rural location.





**Figure 12: Mobile Spectrum Monitoring Station**

Since this work targets 5-MHz channels to demonstrate the viability of testing a remote land mobile wireless communication network, the frequency span is divided into 141 channels that contain 12 frequency bins, resulting in a channel bandwidth of 5.88-MHz. Lastly, the baseband message contained in the modulated signals is not identified.

## **4.2. Equipment**

A schematic of the equipment used is shown in Figure 13. The basic equipment for a spectrum monitoring station is an antenna and spectrum analyzer. The antenna receives the signals that are transmitted over the air and the spectrum analyzer identifies the power and the frequency content of those signals. The computer controls the spectrum analyzer and logs the data. The low noise amplifier (LNA) increases the sensitivity of the measurements, i.e. signals below the noise floor are amplified and may be subsequently processed by the spectrum

analyzer. Various filters are implemented to minimize device saturation. Filters remove (or attenuate) signals with undesired frequencies and pass signals with desired frequencies.

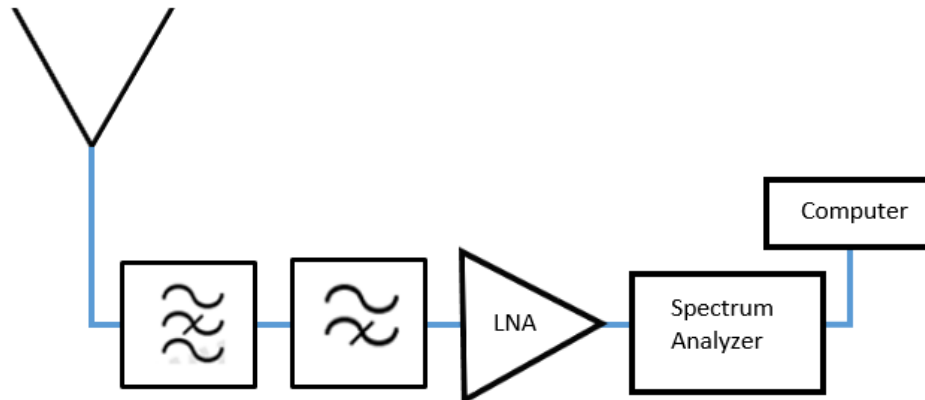


**Figure 13: Station Equipment Schematic**

Spectrum monitoring relies on the accuracy and sensitivity of a spectrum analyzer, which transforms time-domain voltage measurements to frequency-domain measurements. The device is used to characterize the spectra (frequencies) of signals present in a communication channel. In the frequency-domain representation of a modulated signal, the carrier frequency, its harmonics, mixing products and bandwidth can be identified.

Figure 14 shows a measured signal that is the combination of three signals with different amplitudes and frequencies [42]. A spectrum analyzer will take the signal and identify the amplitudes and frequencies of the signals present in the measured signal.

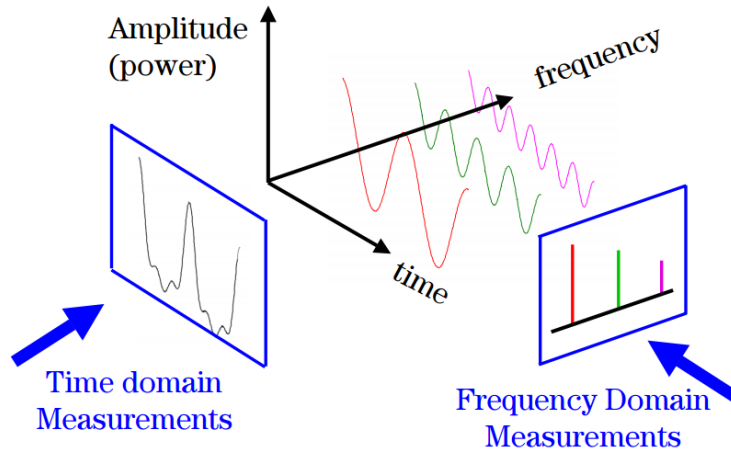


**Figure 14: Spectrum Analyzer Decompose Signal with Three Frequencies**

Voltage measurements made over time are transformed to the frequency-domain by applying a Fast-Fourier Transform (FFT). An FFT is an algorithm that rapidly computes the Discrete Fourier Transform (DFT). At its most basic, Fourier analysis represents the modulated voltage signal as a sum of sinusoid oscillations, each with its own amplitude and frequency.

The PSD measurements are made with a Berkeley Nucleonics Real-Time Spectrum Analyzer (RTSA-7500) [43]. This instrument is connected locally via Gigabit Ethernet (GbE) to a Windows OS computer that controls the RTSA-7500 and logs the recorded and processed data.

A spectrum analyzer is designed to optimize frequency-selectivity and prepare the signal for FFT analysis. Figure 15 depicts a simplified version of the real-time spectrum analyzer (RTSA) architecture this spectrum monitoring project employs, acting like a receiver and digitizer to process the input radio frequency (RF) signal.

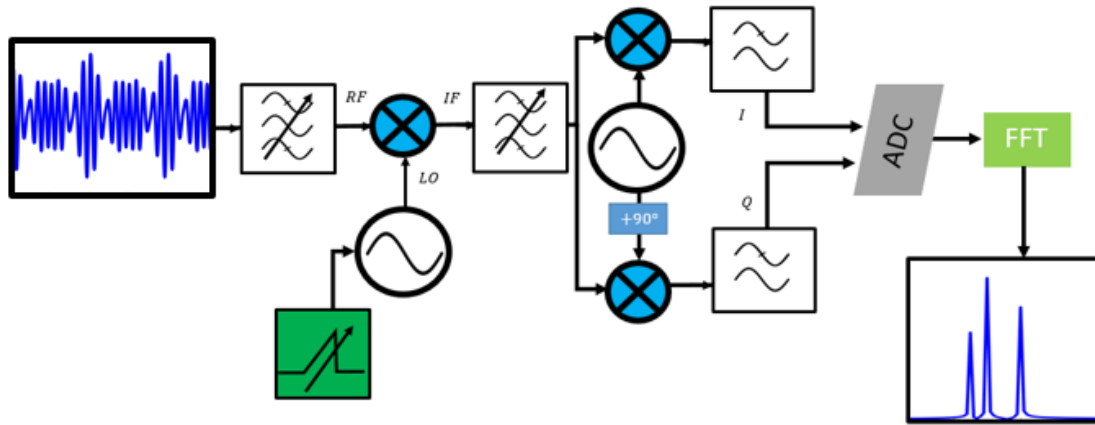


Figure 15: Spectrum Analyzer Diagram

The RTSA spectrum analyzer is able to handle frequencies from 100 kHz to 8 GHz. This wide span is made possible by its super-heterodyne (SH) architecture. The combination of filters and mixers allows the spectrum analyzer to analyze a specified frequency band with high accuracy. In heterodyne and super-heterodyne architecture, all signals are converted to and processed at an intermediate frequency (IF). The former processes signals at a single IF and the latter process the signals at two IFs.

The RTSA architecture is composed of two banks of tunable bandpass filters, and a mixer that multiplies the RF input with an LO. The RTSA will sweep the signals in the span of interest by adjusting the LO signal. The frequency of the LO is adjusted so that all signals are processed at the same fixed IF frequency. This allows the rest of the device to be optimized for the chosen IF frequency.

The RTSA contains a bank of bandpass filters to pre-select the desired frequency section. This occurs while the signal is still RF, before the mixing stage. The SH architecture changes the input RF signal to an IF by mixing the input signal with an LO.

The IF bandpass filter bank is made of surface acoustic wave (SAW) filters. It is best to avoid operating the mixer (or amplifier) non-linearly. If typical RF signals are too large for the

mixer, the operator would reduce the amplitude of the RF signal by lowering the gain of the internal or external amplifier and/or adding appropriate attenuators and filters.

After the first mixing stage the IF has either a higher or a lower frequency than the input RF signal, meaning it either up- or down-converted. For the frequency span of interest (174 to 1000 MHz), the frequencies are likely upconverted because the span of interest is on the lower end of frequencies that the RTSA is able to process.

The next stage is called demodulation because it isolates the baseband by undoing the modulation performed by the transmitter. RF engineers refer to the real part of the signal as I (for in-phase), and the imaginary part is Q (for quadrature). The real and imaginary parts of the signal are found by mixing the IF signal with another LO signal,  $LO2$ . The real part is found by multiplying the signal by a cosine,  $\cos(2\pi f_{LO2})$ . The LO signal is shifted in phase by  $90^\circ$ ,  $\sin(2\pi f_{LO2})$  to find the imaginary component of the signal.

The 2<sup>nd</sup> oscillator frequency is fixed to be equal to the 1<sup>st</sup> IF frequency,  $f_{LO2} = f_{IF1}$

$$f_{IF2} = f_{IF1} \pm f_{LO2} \rightarrow [0 \text{ Hz} \quad 2f_{IF1}] \quad (29)$$

Therefore, the output signal of this mixing stage has frequencies at baseband (0 Hz) and double the IF frequency, the latter of which are removed with a low pass filter. Gain and phase correction are also be applied after filtering. The outputs of this stage are analog in-phase quadrature (IQ) signals.

(Note a simplified version of the RTSA is pictured as heterodyne in Figure 15 above. In SH mode, the RTSA will translate frequency into another IF and perform baseband demodulation in the digital-domain not the analog-domain.)

As a result of multiple stages of filters the signal is said to be bandlimited, i.e. most of the harmonics are removed and the communication link is restricted to the bandwidth of the baseband message. Presenting the signals as IQ measurements is a handy way to retain the phase information of the signals. It also makes the subsequent calculations easier to perform, since complex numbers are stored and evaluated in Cartesian form on computers.

Next, the analog signals are transformed into digital signals with the analog to digital converter (ADC). The analog signal is sampled at 125 Msamples/sec. This stage prepares the data for the FFT analysis. The signals must be discrete, the number of samples must be a power of 2, and frequencies must represent data contained in (i.e. the baseband of) the input RF signal.

Depending on the RBW, the sampling frequency may be decreased after the ADC stage. This process is called decimation because the signal sample is reduced in size. The data is often processed by windowing to give a better estimate of the PSD. For windowing, the data is separated into overlapping segments and the FFT is performed on each “window.” The overlapping segments are then averaged to estimate the power present in each frequency bin. A common algorithm used to estimate the power is Welch’s method.

The program that controls the RTSA employs a built-in FFT from the NumPy module, which is in widespread use [44]. The FFT result for each frequency bin,  $V_k$ , are conveyed as power measurements by squaring the magnitude. Since the difference between each frequency bin is the RBW, the PSD results are commonly returned with units of  $\left[\frac{mW}{RBW}\right]$  or  $\left[\frac{dBm}{RBW}\right]$ :

$$PSD_k \left[ \frac{mW}{RBW} \right] = \frac{|V_k|^2}{Z} \rightarrow 20 \log_{10}(|V_k|) - 10 \log_{10}(Z) \left[ \frac{dBm}{RBW} \right] \quad (30)$$

In practice, RF equipment is calibrated to have an impedance match, 50  $\Omega$ . When each piece of equipment has the same impedance, the equivalent impedance on either the input or the

output of each device looks like a  $50\Omega$  load. This station implements  $50\Omega$  impedance. Impedance matching enables the maximum amount of power to be transferred from each piece of equipment to the other and limits the reflections that travel back from either port. The equipment for RF has a standard impedance match of  $50\Omega$ , however when converted from analog to digital the impedance is likely larger (around  $1\text{ k}\Omega$ ).

Now, the rest of the station equipment will be described in greater detail. At either a fixed or mobile station, the reference antenna is a Diamond D3000N Super Discone with a nominal gain of 2 dBi [45]. The D3000N is a wideband omnidirectional (in azimuth) antenna capable of receiving signals from 25 to 3000 MHz. The D3000N is mounted vertically at each location; therefore the antenna is most sensitive to signals that travel along the horizon.

An LNA is employed at both the fixed and mobile stations. An LNA improves the sensitivity of the measurements by amplifying the received signals while adding minimal noise. At a fixed location the RF Bay Inc. LNA-1520 amplifies the received signals by  $20.1 \pm 0.60$  dB [46]. In mobile locations, the COM Power PAM-103 amplifies the received signals by  $35.5 \pm 0.80$  dB [47]. The fixed location receives higher-powered signals that require a smaller gain to avoid saturation.

Depending on the location, either the LNA or RTSA-7500 spectrum analyzer is prone to saturation due to FM signals or 2-way hand held radios between 150 and 165 MHz. The FM radio station at Montana Tech, KMSM (103.9), is a particular nuisance; it is possible to demodulate and listen to the musical programming being transmitted on the station's 3<sup>rd</sup> harmonic. Since these bands are not of interest, a high pass filter is employed before the LNA. The HP 7162/174 S50 filter from Tin Lee Electronics provides minimum attenuation ( $-0.74 \pm$

0.52 dB) along the span of interest and attenuates signals below 164 MHz by at least 40 dB and up to 101 dB [48].

There are several power limiting measures employed to prevent damage to the front-end of the LNA and the RTSA-7500. The first, an L-com Coaxial Lighting Protector AL-NMNFB contains a gas-discharge tube that acts as a fuse [49]. When the gas burns, the energy is directed towards earth ground. The surge protector is connected to earth ground via the power breaker box located in the room. For this reason, it is only employed at the fixed Museum station. Furthermore, it is placed between the antenna and the filters.

The second power limiting measure is a modified FM Notch filter FLT201A/N from Stridsberg Engineering [50]. A 10 k $\Omega$  surface mount resistor was soldered between the center feedline and ground that is normally open. This “bleeder” resistor dissipates the static electricity that accumulates along the co-axial cable and antenna as they move. This modification moved the notch slightly; the filter attenuates the received signals by -35.5 dB and -32.5 dB at 88 MHz and 108 MHz respectively.

Third, the LNA acts as a power-limiting device. P1dB is a metric used to quantify the saturation point of the amplifier. It is assumed that the P1dB is near the maximum power output from the LNA. To locate the P1dB point, one needs to determine the slope of the transmitter when it operates linearly, then find the difference of 1 dB between the slope and the output gain measurements. If the P1dB of the LNA is greater than +10dBm, which is the maximum RF Input at the RTSA-7500, the appropriately-sized attenuator is put inline between the two.

Additional attenuators may be required if the signals present at a given location cause device saturation. External batteries power all equipment for the mobile station, while AC/DC power adapters power devices at locations with available power. DC blocks are placed before the



LNA and RTSA-7500 to absorb direct current that may flow along the co-axial cables. Table II summarizes the equipment characteristics employed at either the fixed or mobile station.

**Table II: Equipment Summary**

<b>Equipment</b>	<b>Setup</b>	<b>Company</b>	<b>Gain (174 – 1000 MHz)</b>	<b>Misc. Characteristics</b>
LNA-1520	Fixed	RF Bay Inc.	$20.1 \pm 0.599 \text{ dB}$	$P_{1dB} : +20.2 \text{ dBm}$ $NF : 1 \text{ dB}$ $range : 20$ $- 1500 \text{ MHz}$
Preamplifier PAM-103	Mobile	COM Power	$35.5 \pm 0.80 \text{ dB}$	$P_{1dB} : +4 \text{ dBm}$ $NF : < 6 \text{ dB}$ $range : 1$ $- 1000 \text{ MHz}$
RTSA-7500	Fixed / Mobile	Berkeley Nucleonic Corporation (BNC)	$0 \text{ dB (nominal)}$	IBW: 40 MHz (SH mode) $Max RF_{in} :$ $+10 \text{ dBm}$
Coaxial Lighting Protector AL-NMNF B	Fixed	L-Com	$-0.22 \pm 0.09 \text{ dB}$	$range : DC - 3 \text{ GHz}$ Terminal must be tied to ground
FM Notch Filter FLT201A/N	Fixed / Mobile	Stridsberg Engineering, LLC	$-1.01 \pm 0.85 \text{ dB}$	Modified with 10 k $\Omega$ resistor to ground 88 MHz : $-35.5 \text{ dB}$ 108 MHz : $-32.5 \text{ dB}$
High Pass Filter HP 7162/174 S50	Fixed / Mobile	Tin Lee Electronics	$-0.74 \pm 0.52 \text{ dB}$	$< 164 \text{ MHz} :$ $at least - 40 \text{ dB}$
Discone Antenna DN3000N	Fixed / Mobile	Diamond Antenna	$2 \text{ dBi (nominal)}$	$range : 25$ $- 3000 \text{ MHz}$

Shield boxes are employed to remove emissions generated by equipment. Active devices, in particular the spectrum analyzer and computer, must be shielded. The shield box employs both wire mesh and foam that attenuates the signals of the instruments placed inside.

Note that the harmonics that appear across the span: 250 MHz, 425 MHz 500 MHz, 600 MHz, 625 MHz 700 MHz, and 875 MHz in Figure 16 disappear when the equipment is shielded

in Figure 17. The persistent higher noise floor below 325 MHz is most likely caused by emissions from the mobile station laptop.

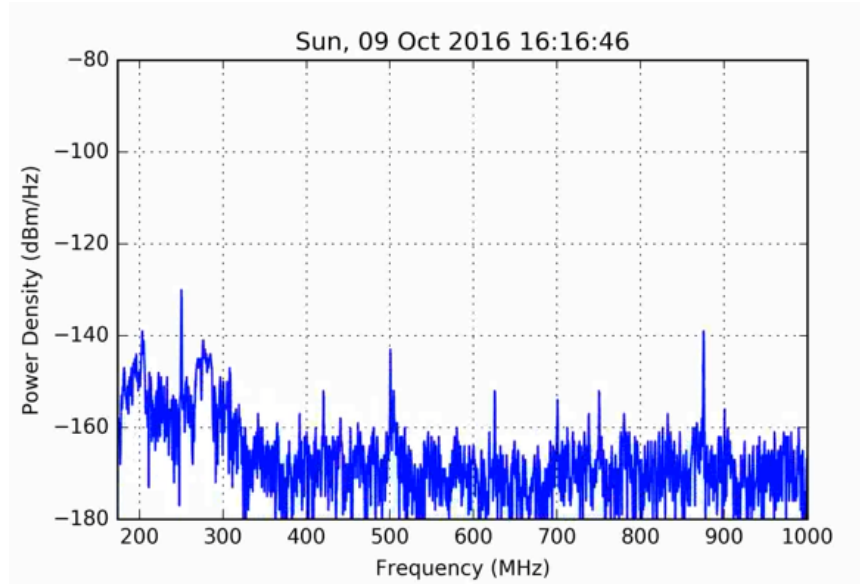


**Figure 16: PSD Measurement without Shielding**

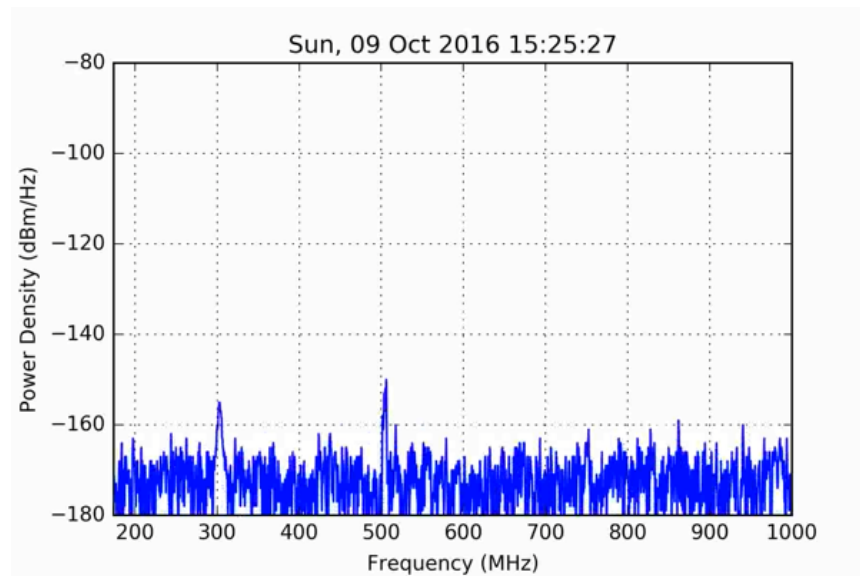


**Figure 17: PSD Measurement with Shielding**

For this thesis, noise measurement studies were also conducted. To minimize the strength of the RF signals received, a 20 dB attenuator was placed at the end of the equipment and PSD measurements were collected. The attenuator acts as a terminating load since it has  $50\Omega$

impedance match with the RF input to the spectrum analyzer. For the fixed station at Montana Tech, the antenna, co-axial cable and surge-protector were removed and replaced with a 20 dB attenuator. For the mobile station, only the antenna and co-axial cable were replaced with the 20 dB attenuator.

### 4.3. Locations

PSD measurements were taken at the following locations: Moose Lake Road near Philipsburg, Montana, and two locations in Butte, Montana: the Museum Building and The M, both on the Montana Tech campus. Figure 18 depicts the area surrounding the two locations. All maps were made with Google Earth Pro [51].

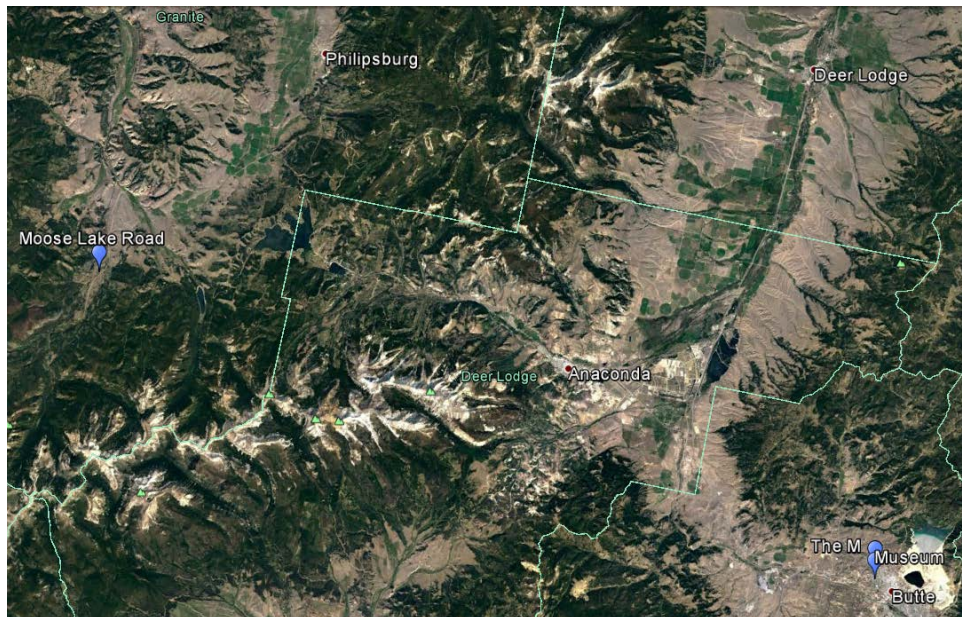


Figure 18: Map of Test Locations

The remote Moose Lake Road is 28 km southwest of Philipsburg, Montana, a rural town of population 800. This remote location has a height above mean sea-level (AMSL) of 1746 meters. The D3000N discone antenna height above ground level (AGL) was 3 meters. Figure 19 depicts the D3000N antenna mounted at Moose Lake Road.



**Figure 19: Discone Antenna at Moose Lake Road Location**

The campus of Montana Tech sits atop a hill, which overlooks the city of Butte (population 34,000). The D3000N discone antenna is located on the parapet of the Museum building, a 3½ story building, as pictured in Figure 20. At the Museum location, the height AMSL is 1762 meters, and the antenna is 17 meters high.

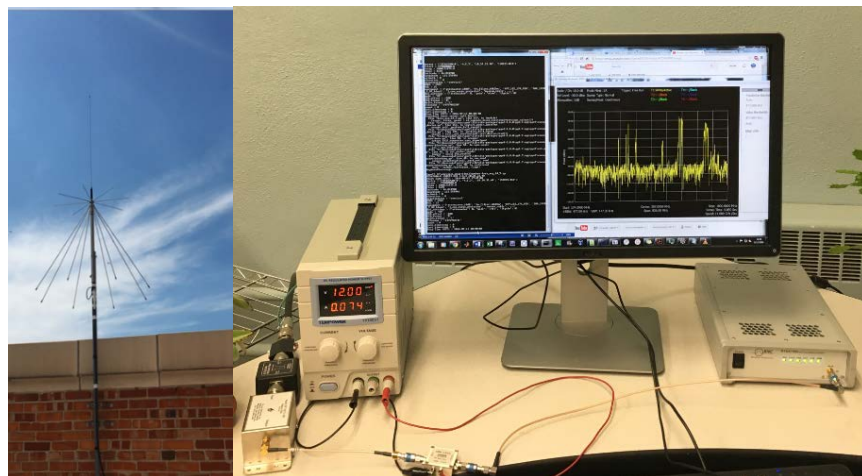


**Figure 20: Museum Spectrum Monitoring Station at Montana Tech**

Spectrum measurements were also taken on The M, which is located on Big Butte, situated above the main campus of Montana Tech. The M has an AMSL of 1901 meters, and the discone antenna is mounted on a tripod with an effective height of 2 meters. The two locations on the Montana Tech Campus have a distance of 988 meters between them.

#### **4.4. Procedure**

In order to provide long-term spectrum occupancy measurements, the station gathers data by automation. The spectrum analyzer takes 50 ms to sweep the span, however the overhead differs at each location. At the fixed station (Museum) the overhead results in 17 sweeps/second captured. At a mobile station (the M and Moose Lake), the overhead results in 15 sweeps/second. This difference is likely due to the MAC layer protocol of each Microsoft PC. As a consequence during a 24 hour period, the fixed station desktop stores 2.4 Gb per day, the mobile station laptop stores 2.3 Gb per day. To collect long-term measurements ThinkRF's API called pyRF API (v 2.8.0) was employed [52].

The operator must follow the test procedure to ensure the equipment has been set-up correctly and is operating normally. Figure 21 depicts the flow chart for the test procedure, which includes six steps: (1) Assemble Equipment, (2) Test Equipment Gain Interpolation, (3) Test Equipment Operation, (4) Set Location information in Header, (5) Record Spectrum Data, and (6) Disassemble Equipment.

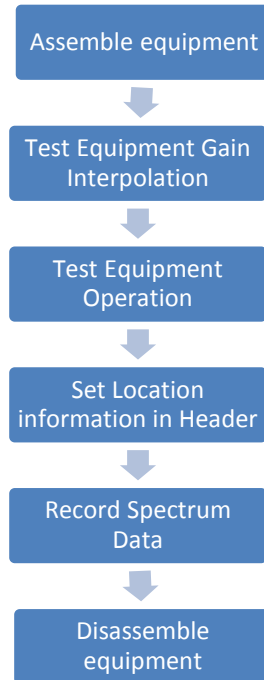


**Figure 21: Test Procedure Flow Chart**

The operator checks that the appropriate gain (\*.csv) file for each piece of equipment is in the working folder, and then tests the equipment gain interpolation. At various locations, the equipment setup may change because additional attenuators are required or a different LNA is in use.

Since the equipment is completely assembled and disassembled at each mobile location, the operation of the equipment is tested before any spectrum data is acquired and processed. A single tone of 430 MHz (plus its harmonics) is transmitted at a nominal output power level of -40 dBm by a TPI-1002-A signal generator [53]. The transmitting whip antenna (vertically mounted) is placed at a set pacing (1.0 meter) from the discone antenna; the gain of this antenna at 430 MHz is 3.00 dBi in azimuth [54]. The height of the whip antenna is 0.6 meters lower than the height of the discone antenna. This results in an FSPL of 25 dB.

$$P_{Rx,prediction} = P_{Tx} - FSPL + G_{Tx} = -40 \text{ dBm} - 25 \text{ dB} + 3 \text{ dBi} = -62 \text{ dBm} \quad (31)$$

After running the equipment gain interpolation, the Rx equipment gain at 430 MHz is determined then subtracted from the channel power as measured from 425 to 435 MHz:

$$P_{Rx,corrected} = P_{Rx,Measurement} - G_{Rx,equipment} \quad (32)$$

If the corrected Rx channel power measurement (Equation 32) is within 1 to 2 dB of the Rx channel power prediction (Equation 31) the equipment is working properly.

Before recording the spectrum data, the operator declares the location setting (latitude, longitude, altitude, and the orientation and height of the antenna) in the header. Lastly, personal electronic devices are either turned off or placed in the shield boxes.

Figure 22 depicts a flow chart of the programming script that controls 24/7 data collection. Normally, each day begins and ends at midnight coordinated universal time (UTC); however, the operator may set the stop time to be any period of time from the present, such as two hours or five minutes. Additionally, the operator may input a newline character into the command line to override the stop time and exit the program. The header file is the last file updated when the user exits the program or the stop time is exceeded. Binary files for the PSD measurements and the difference between timestamps are appended each time the RTSA device performs a sweep.

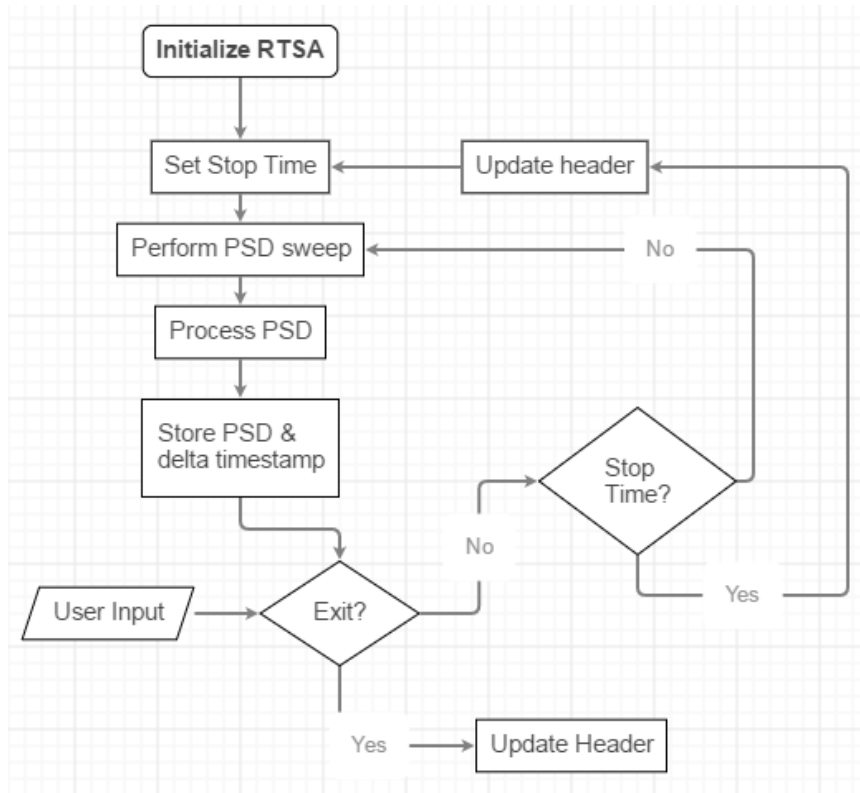


Figure 22: Data Acquisition Flow Chart

PyRF and its required dependencies are used to control the RTSA-7500 [53]. The device is initialized by connecting over IP and requesting sweep permission (see Figure 23):

```

# Initialize & Connect to Device
dut = WSA()
wsas_on_network = discover_wsa()
for wsa in wsas_on_network:
    print wsa["MODEL"], wsa["SERIAL"], wsa["FIRMWARE"], wsa["HOST"]
wsa=wsas_on_network[0]
ip=wsa["HOST"]
dut.connect(ip)
dut.request_read_perm()
sd = SweepDevice(dut)
  
```

Figure 23: RTSA Device Initialization in Python

The pyRF function used to perform a PSD sweep is called *capture\_power\_spectrum()*. This function returns PSD measurements for a range of frequencies by combining the FFT results for sections along the span. The operator requests a start and stop frequency, and an



RBW, all of which may be adjusted by the RTSA-7500. Since the resolution bandwidth is ~488 kHz and the sampling frequency 125 MHz, frequencies across the span are processed in sections with a sample size of 256.

$$N = 256 \approx \frac{f_s}{RBW} = \frac{125 \text{ MHz}}{488 \text{ kHz}} \quad (33)$$

Additionally, the device is set to operate in SH mode and both the internal gain amplifiers, attenuator, and IF filter gain are all set to 0 dB. Figure 24 depicts the sweep setting declarations:

```
# Sweep settings
settings = OrderedDict()
settings['START_FREQ']=174e6 # Hz
settings['STOP_FREQ']= 1e9 # Hz
settings['RBW']=500e3 #Hz
settings['dut_settings']={'gain': 'vlow','attenuator': 0, 'ifgain': 0} # dB
settings['mode']='SH'

# Initial Sweep - frequencies may be adjusted
fstart, fstop, init_power = sd.capture_power_spectrum(*settings.values())
```

**Figure 24: RTSA Sweep Settings and Initial Sweep**

A PSD sweep is assigned an epoch timestamp on arrival, however only the difference in milliseconds between timestamps is stored. Epoch time is a count-up of the seconds that have elapsed from 00h:00m:00s January 1<sup>st</sup>, 1970 Coordinated Universal Time (UTC). This method ensures that each timestamp is unique.

The frequency for each PSD measurement is not returned by the RTSA, only the start and stop frequencies for the whole span. The frequencies are approximated by assuming the step in frequency between bins is linear. A NumPy function called *linspace()* generates the frequency vector (see Figure 25). Its inputs are the start frequency, stop frequency and the number of frequency bins, which is found by finding the length of the PSD measurement.

```
# Generate Frequency Vector |
fbins=len(init_power)
f_vec=np.linspace(fstart, fstop,fbins) #Hz
```

Figure 25: Frequency Interpolation

Additionally, the RBW is determined from the start and stop frequency and the number of frequency bins:

$$RBW = \frac{f_{stop} - f_{start}}{\text{length}(PSD \text{ Sweep})} [Hz] \quad (34)$$

This RBW is at least 10x smaller than the target channel bandwidth, 5-MHz. This ratio helps ensure that spectrum events will be captured. While a lower RBW may have better resolution and lower noise floor, it is more likely that temporal events will be missed because of the slower sweep time.

Besides plotting, these frequency calculations are used to process the PSD sweep. To find the input power at the Rx,  $P_{Rx}$ , the gain or loss effects of the Rx equipment must be removed. Since the Rx equipment adds gain to the signals, the power of the signal at the Rx is determined by removing the gain. The PSD measurement is processed on a frequency bin-by-frequency bin basis, the frequency span of interest is used to interpolate the gain and losses due to each piece of equipment. This method normalizes the data, so that the PSD measurements from different equipment setups may be compared.

The NumPy function *interp()* is used to find a one-dimensional piecewise linear interpolation of the measured (or nominal) equipment gain and its associated frequency for the calculated frequency span of interest.

Gain measurements of all equipment (save the antenna and spectrum analyzer) were made on a HP 8753E RF Vector Network Analyzer [55]. Signals with known amplitudes and

frequencies are input into either port 1 or port 2, and the output may be measured on either port. When measuring gain, four types of measurements may be made: S11, S12, S21, and S22 (see Figure 26). The numbers refer to the port 1 or the port 2. S11 and S22 are measurements of the gain ratio that reflect back from a port 1 and port 2 respectively. S12 measures the gain ratio from the port 1 to port 2, S21 measures the gain from the port 2 to port 1.

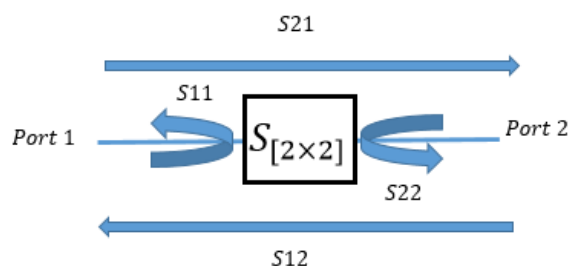


**Figure 26: Gain Measurements on Network Analyzer**

All S21 performed on the equipment were shown to be sufficiently flat along the frequency span from 174 to 1000 MHz. However, it should be noted that measurements become less sensitive as the frequency increases (see Figure 27 and Figure 28). This behavior is more apparent at the fixed station compared to the mobile station because of the added attenuators. (See Appendix B for the S21 of each piece of equipment).

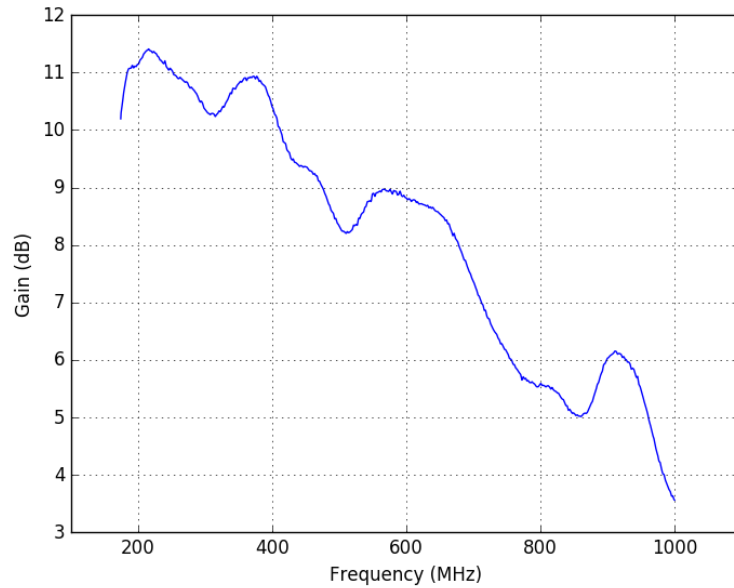


**Figure 27: Equipment Gain Interpolation for Fixed Station Equipment**

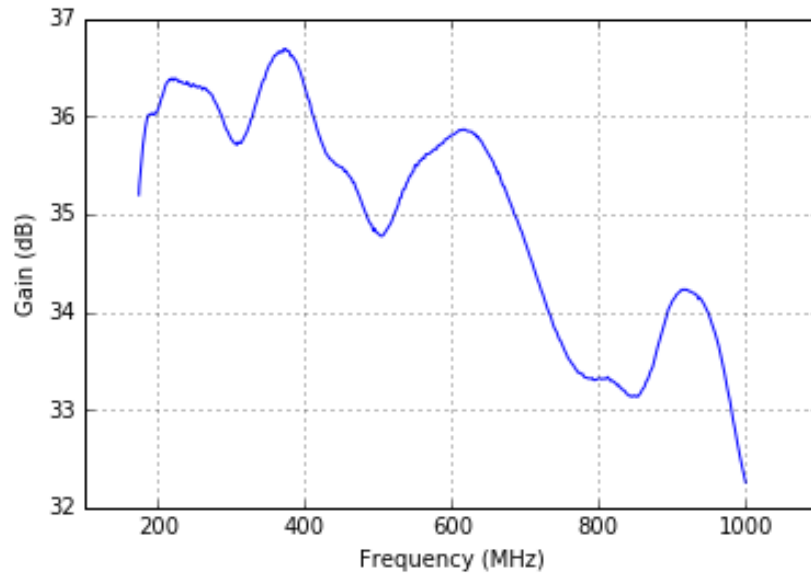


**Figure 28: Equipment Gain Interpolation for Mobile Station Equipment**

The frequency and gain values for each piece of equipment to be interpolated are stored as csv files, where the 1<sup>st</sup> line is the frequency in Hz and the 2<sup>nd</sup> line is the gain (or loss) in dB for each frequency (see Figure 29).

	A	B	C	D	E	BIL	BIM	BIN	BIO
1	30000	1904981	3779963	5654944	7529925	2.99E+09	3E+09	3E+09	3E+09
2	-76.718	-94.323	-83.08	-93.162	-94.914	-15.613	-15.02	-14.365	-13.817

Figure 29: Gain Measurements of HP Filter Loss

For the D3000N discone antenna only the nominal value is known for the frequency range (see Figure 30).

	A	B
1	2.50E+07	3.00E+09
2	2	2
3		

Figure 30: D3000N Antenna Nominal Gain

After the initial sweep, these S21 gain measurements are interpolated, and summed together in order to find the EIRP. The gain files are stored in the project folder and determined on run-time as pictured in Figure 31.

```
# Load Equipment Gain/Loss (dB)
path="wireless_prjs\\final"
equipment_gain=np.zeros(fbins)
directory = os.path.join("c:\\",path)
for file in os.listdir(directory):
    if file.endswith(".csv"):
        with open(file, 'r') as f:
            header['equipment'].append(f.name[:-4])
            # Read in frequency
            f_str=f.next()
            f_temp=[float(i) for i in f_str.split(',') if i]
            f_temp=np.reshape(f_temp, len(f_temp))
            # Read in Gain
            g_str=f.next()
            g_temp=[float(i) for i in g_str.split(',') if i]
            g_temp=np.reshape(g_temp, len(g_temp))
            # Interpolate
            gain=np.interp(f_vec, f_temp, g_temp)
            # Sum equipment gains
            equipment_gain+=gain
```

Figure 31: Equipment Gain Interpolation

Equation 34 demonstrates one additional normalization step. The PSD measurements are returned relative to the RBW. They are processed to convey each PSD measurement in units of  $\frac{dBm}{Hz}$  instead of  $\frac{dBm}{RBW}$ . Since division in linear is equivalent to subtraction in logarithmic, the RBW in dB is subtracted from the PSD measurement.

$$PSD(f) = PSD_{measured} - G_{ant} - G_{loss} - G_{LNA} - 10 \log_{10}(RBW) \quad (35)$$

Each PSD sweep is compressed by rounding the power spectral density float to the nearest integer. The data is further compressed by encoding. Most wireless PSD measurements range from  $-235 \frac{dBm}{Hz}$  to  $+20 \frac{dBm}{RBW}$ , this range requires at least 255 unique values or 8 bits. Recall that the theoretical limit for noise floor at 60° C is  $-174 \frac{dBm}{Hz}$ . Measurements made below  $-174 \frac{dBm}{Hz}$  occur because the amplitude of the measured signal approach is closer to 0. The integer is encoded into a character by applying an offset, so that coded measurement spans from 0 to 255. Equation 35 summarizes both steps:

$$PSD_{char} = int\left(\text{round}(PSD_{float})\right) + PSD_{offset} \quad (36)$$

Further (reversible) compression may be applied during post-processing with the 7zip utility. The effective compression for a PSD sweep from float to “7-zipped” character is 93%, therefore 2.4 Gb is compressed to 1.4 Gb, and 2.3 Gb is compressed to 1.2 Gb.

Figure 32 pictures an example header for a 24 hour recording. The header contains information about the location and device. The latitude, longitude (both of which are given in decimal degrees), azimuth and elevation of the antenna, and altitude of the location given relative

to sea-level (ASML) and ground (AGL) are set by the operator. The initial and last timestamps are given in epoch time in milliseconds, but the filename is epoch time in seconds.

```

device : ['RTSA7500-8', '4.5.3', '10.38.32.48', '150223-034']
fstart : 174000000.0
fstop : 1000171875.0
fbins : 1692
latitude : 46.010708
longitude : 112.556881
azimuth : 0
elevation : 0
polarization : vertical
AMSL : 1762
AGL : 15
equipment : ['attenuator_10dB', 'fm_filter_10kOhm',
'HP7_162_174_550', 'LNA_1520_2_DC_block',
'l_com_surge_protector', 'museum_cable', 'omni_D3000N']
dut_settings : {'attenuator': 0, 'gain': 'vlow', 'ifgain': 0}
mode : SH
PSD_offset : -200
PSD_format : B
delta_format : I
filename : 1473552000
count : 1480184
init_timestamp : 1473552000179
last_timestamp : 1473638400011

```

**Figure 32: Typical Header File**

For the desktop at the fixed station, the number of sweeps of 1.48 million is typical for a 24 hour recording. For the laptop used in the mobile station, the number of sweeps is 1.29 million. This count is necessary to access and the binary files for the PSD measurements and delta timestamps. Since the data is homogenous, the data can be quickly read and written using the Python module array [56] (see Figure 33). However, both the binary format and the number of binary must be known to access and index the array. This method does not load the data into memory, but creates a map for quick access.

```

cc=header['count']
raw_data=array.array(header['PSD_format'])
with open(os.path.join(path, PSD_file+'.bin'), 'rb') as f_p:
    raw_data.fromfile(f_p, header['fbins']*cc)

delta=array.array(header['delta_format'])
with open(os.path.join(path,delta_file+'.bin'), 'rb') as f_d:
    delta.fromfile(f_d, cc)

```

Figure 33: Accessing Binary Data Efficiently

## 4.5. Results

One of the achievements of this project was to present the data publicly in video form. The videos are hosted on the Montana Tech Wireless Lab YouTube page, [goo.gl/RI0t5u](https://www.youtube.com/channel/UC0Ywn5qi34CDN5IF8Gmrgg), (see Figure 34) [57]. A better sense of the data as a whole can be gained from the published videos for each location, specifically the Museum Building and the M at the Montana Tech campus in Butte, Montana and Moose Lake Road outside Philipsburg, Montana. Since the data sets are so large, it is instructive to see the PSD measurements at both locations over time.

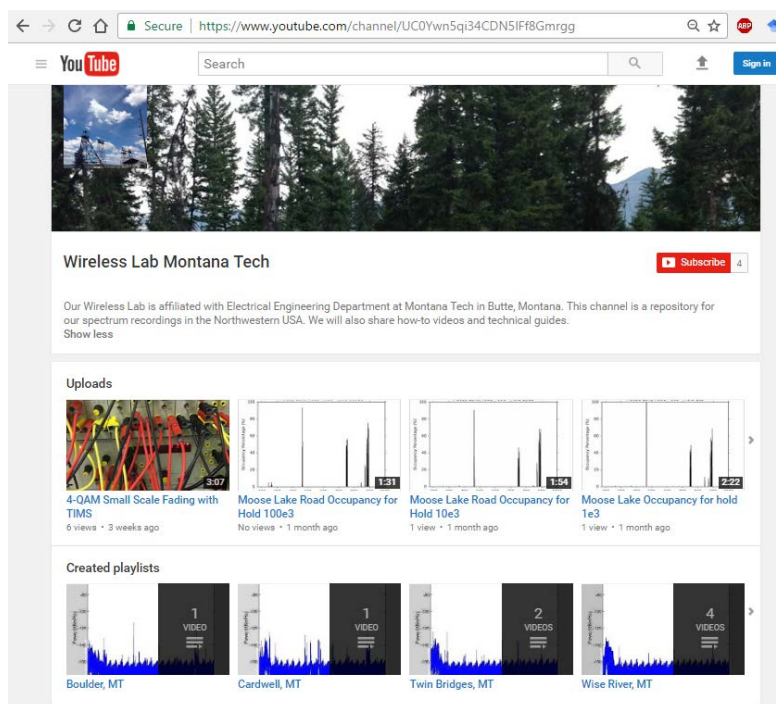
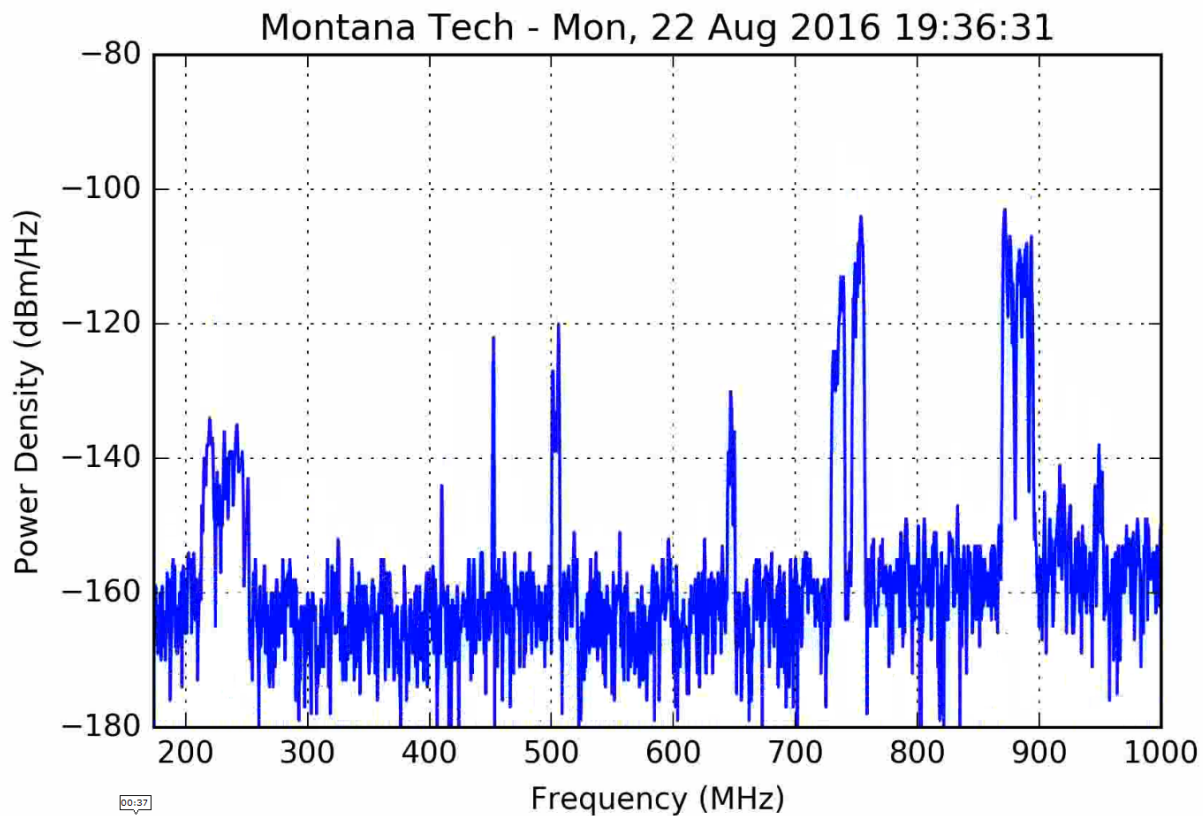


Figure 34: Montana Tech Wireless Lab YouTube Homepage



The measurements represent the power spectral density in  $\left[\frac{dBm}{Hz}\right]$  for 1692 frequency bins, which span from 174 MHz to 1000 MHz. The resolution bandwidth is 488 kHz. The data for the Montana Tech Museum was collected in August and September of 2016 and amounts to 32 Gb of data (not archived with 7zip utility). For data analysis this set was divided into a 19 by 1 million sweep data set, with labels 000 to 018. Figure 35 depicts a typical sweep captured at the Montana Tech Museum location.



**Figure 35: Typical Sweep for Montana Tech Museum Location**

Persistent signals at the Montana Tech Location include but are not limited to, the 70 cm Amateur Radio band at 450 MHz, TV Channels 19 from 500 to 506 MHz and Channel 43 from 644 to 650 MHz, LTE downlinks for AT&T from 729 to 746 MHz, Verizon from 746 to 756 MHz, and 2G/3G legacy system downlinks from 869 to 894 MHz.

In Figure 35 above, the radiated spurious emissions appear from 210 to 250 MHz. At the Montana Tech Museum Location, these radiated spurious emissions appear from 174 MHz to 550 MHz, and more predominantly below 350 MHz. The bandwidth is typically between 40-MHz to 100-MHz and appears for several sweeps that is approximately 150 ms. This activity also appears when PSD measurements are made with the Signal Hound BB60C Real-Time Spectrum Analyzer.

The data at the M was collected to observe if the radiated emission behavior differed further away from the buildings on the Montana Tech Campus. Data was gathered with equipment shielded and unshielded in September and October of 2016 and amounts to 729 MB of data (not archived with 7zip utility). Each set spans approximately three hours. These spurious emissions from 174 to 550 MHz can be viewed in both sets of measurements taken. A typical frame at the M with the equipment shielded can be seen in Fig 36, while Figure 37 depicts a typical frame where the equipment is not shielded.

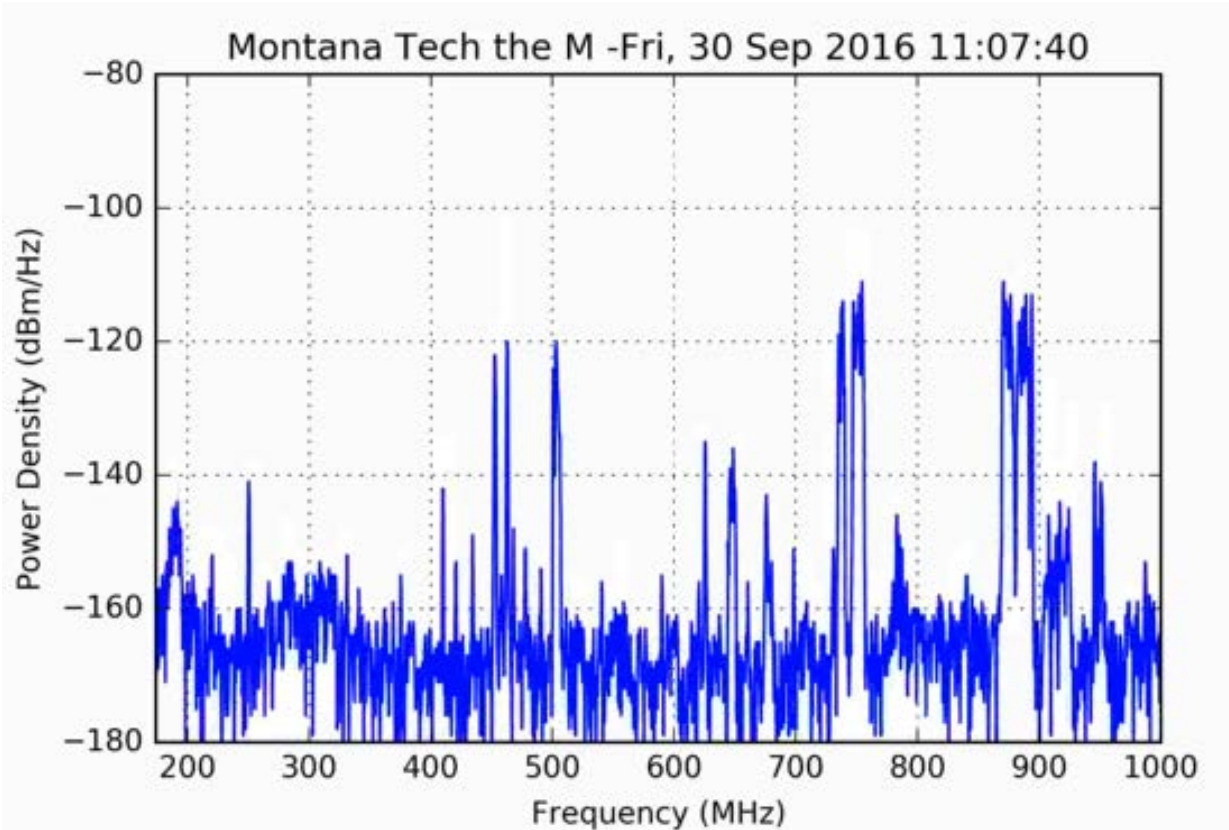


**Figure 36: Typical Frame Non-Shielded Equipment at The M**

Note that the activity from 275 to 325 MHz and 174 to 200 MHz are persistent in the non-shielded recording. Recall the higher noise floor was seen in data collected in remote areas when the equipment was not shielded. Therefore, these persistent wideband emissions (which results in a higher noise floor) are emissions from the mobile laptop.

When the equipment is shielded, the RTSA device harmonics are removed, as well as the persistent wideband emissions below 325 MHz. This results in a lower noise floor.

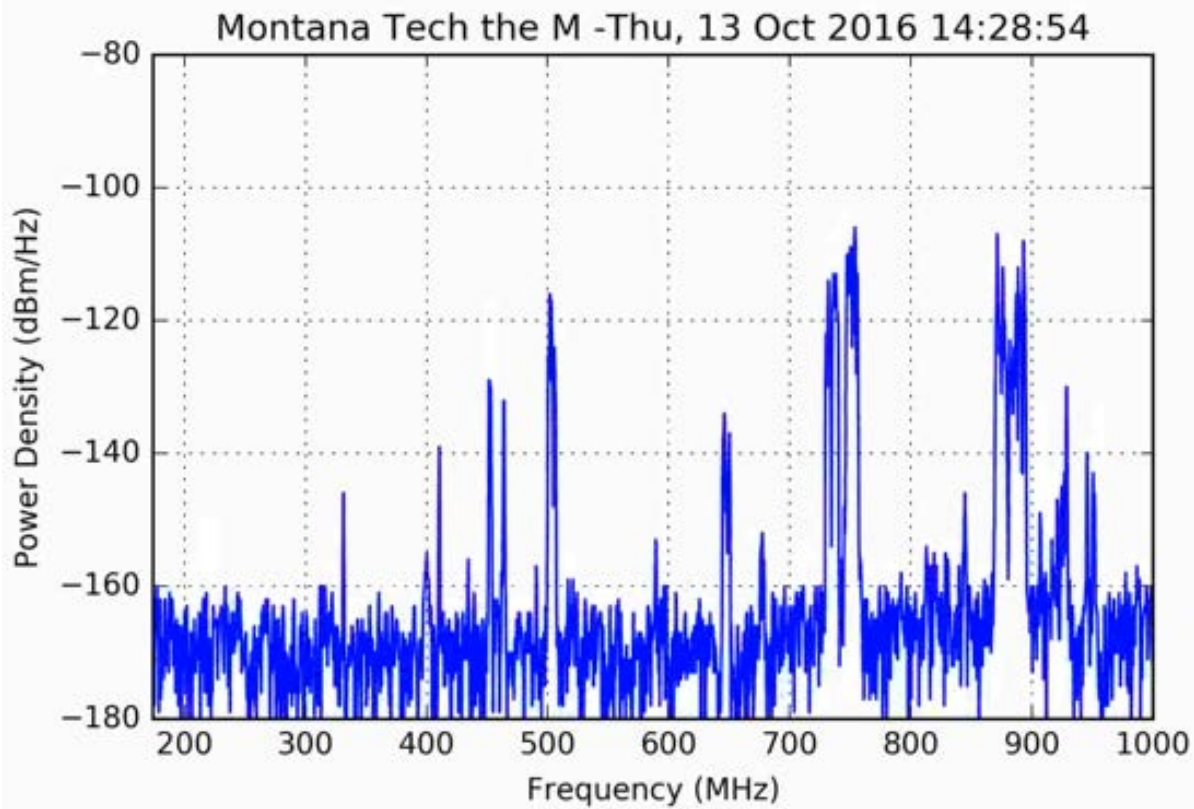
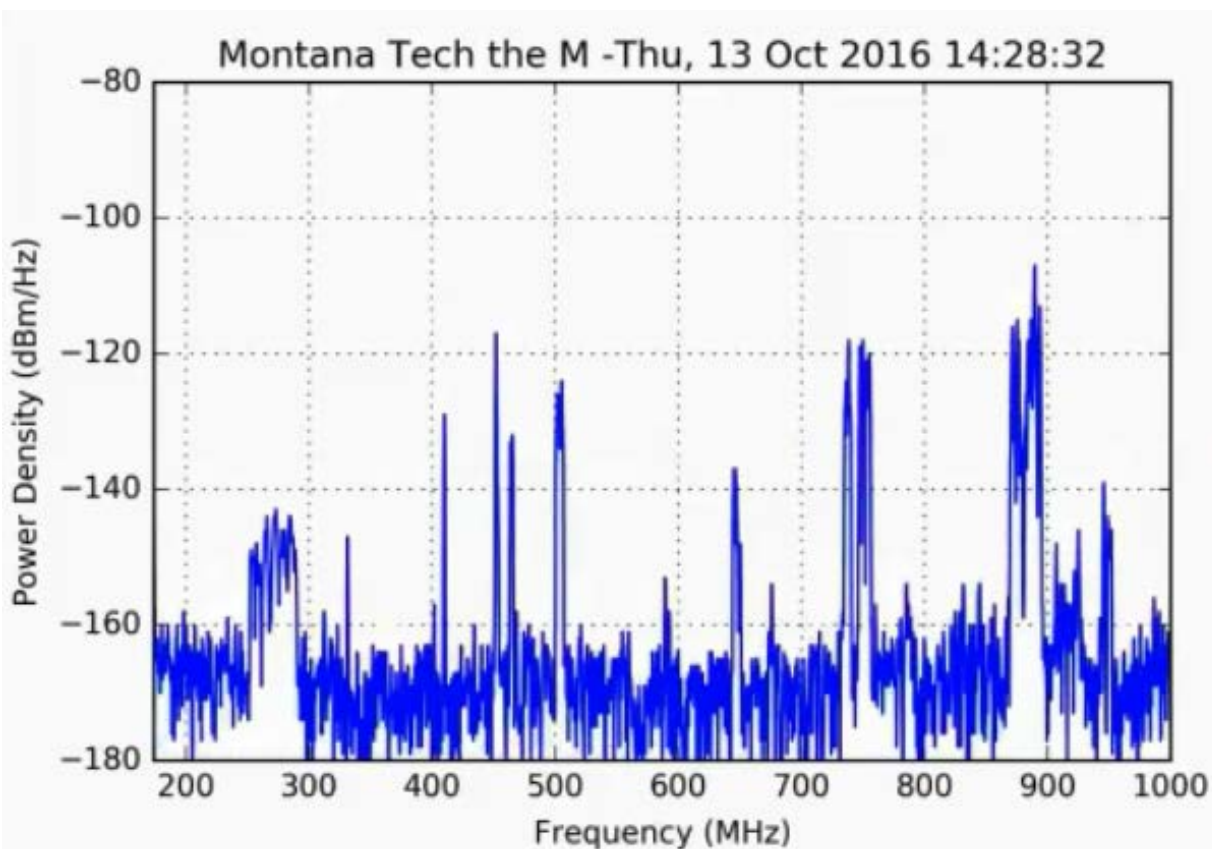


Figure 37: Typical Frame Shielded Equipment at The M

However, the momentary wideband spurious emissions also occur at the M even when the equipment is shielded, see Figure 38:



**Figure 38: The M Sweep with Spurious Emissions**

Initially, it was assumed that bands below 500 MHz were viable for testing a mobile broadband network. These pathological spurious emissions make these bands less valuable.

At the remote location, Moose Lake, the data was collected in November of 2016 for 2 weeks, which amounts to 29 Gb of data (not archived with 7zip utility). For data analysis, this set was divided into 17 by 1 million sweep data set, with labels 000 to 016. Figure 39 depicts a typical sweep captured by the RTSA:

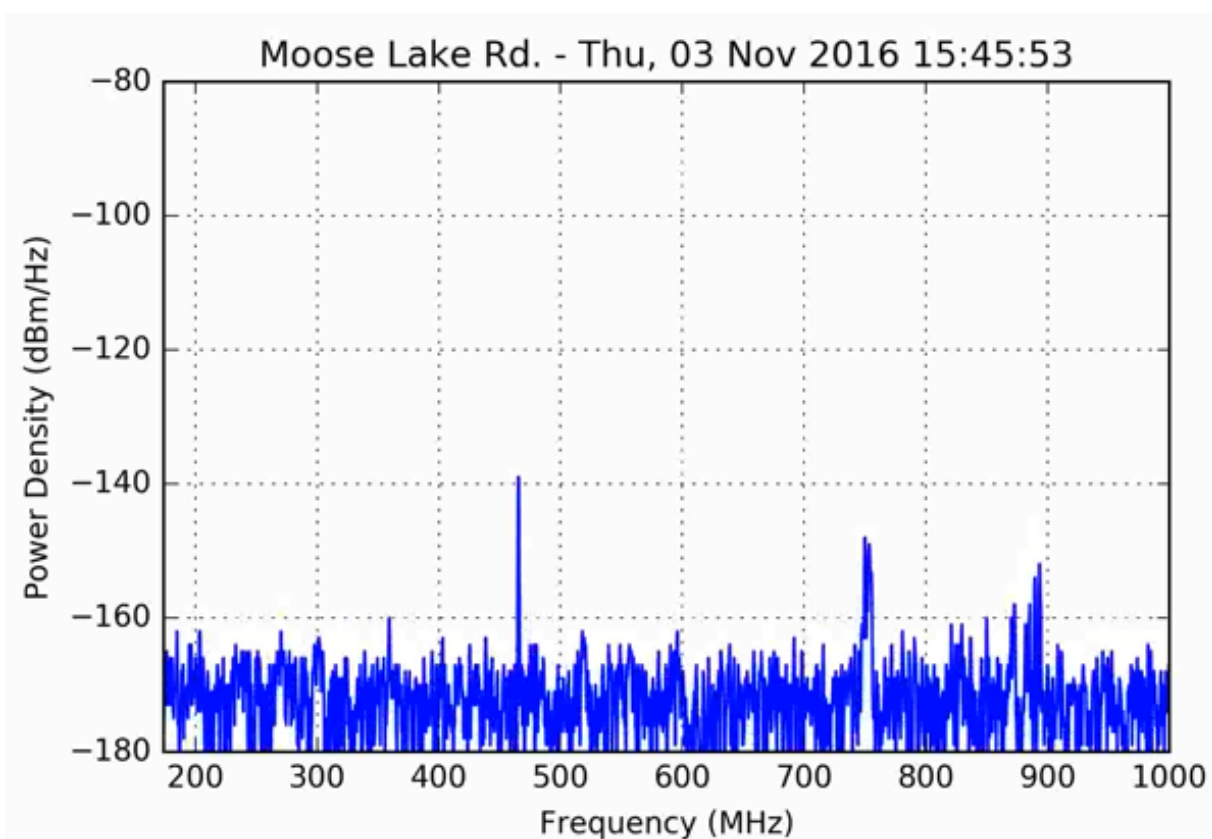


**Figure 39: Typical Frame at Moose Lake**

Persistent signals at the Moose Lake Road location include but are not limited to, a frequency-hopping repeater from 460 to 472 MHz that is licensed for Meteorological Satellites, LTE Downlinks for Verizon from 746 to 756 MHz, and 2G/3G legacy downlinks from 869 to 894 MHz.

The spurious emission behavior appears more infrequently and with smaller amplitude in the recordings taken at Moose Lake Road. In Figure 49 below, the momentary wideband spurious emissions appear from 174 to 200 MHz. The long-term magnitudes of these spurious emissions are more clearly seen when a number of sweeps are held and the maximum is found for the hold (see Figure 41 and 42 in Section 4.6 below).

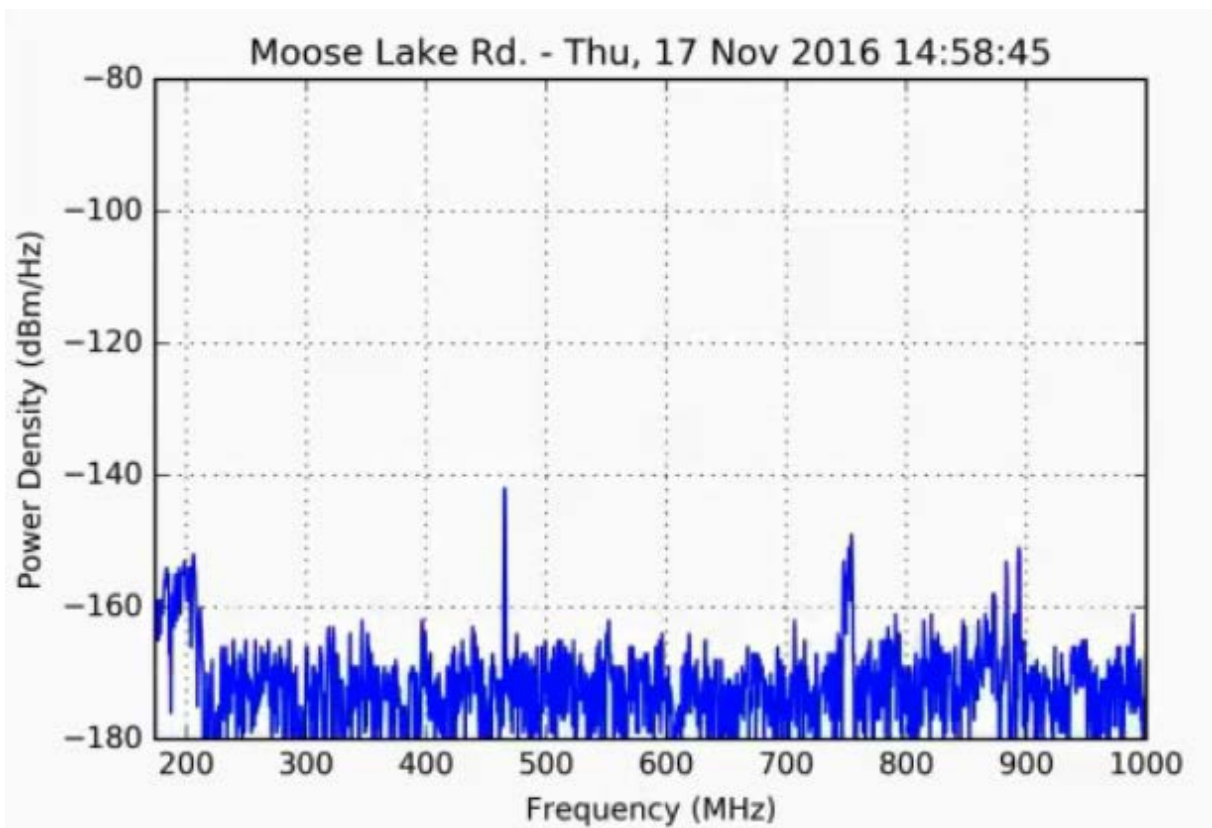


Figure 40: Frame with Spurious Emissions at Moose Lake

#### 4.6. Analysis

The spectrum for the Montana Tech Museum and Moose Lake Road locations were characterized with several metrics: maximums, means, occupancy percentage, and distribution. The analysis was either performed for each frequency bin or for each channel. Since the RBW is 488 kHz and a channel contains 12 frequency bins, each channel has a bandwidth of 5.88-MHz, which results in 141 channels. The maximum and mean over-the-air measurements and noise-only measurements of each frequency bin were presented for each location. Occupancy thresholds were found for each channel, and an occupancy percentage was found for each frequency bin. Distribution plots of noise-only measurements and over-the-air measurements were found for each channel.



Various holds were applied to the data, and the maximum and mean were found for each frequency bin over that time period. While the data at Moose Lake Road was collected continually for 2 weeks, the data collected at the Museum has time gaps. Table III approximates the time duration for each hold based on a sweep time of 15 sweeps/sec for the Museum Location, and 17 sweeps/sec for Moose Lake.

**Table III: Time Duration for Each Hold**

<b>Hold</b>	<b>Museum</b>	<b>Moose Lake</b>
Hold	Museum	Moose Lake
1e3	58 s	67 s
10e3	9 m 48 s	11 m 7 s
100e3	1 h 38 m 2 s	1 h 51 m 7s

Figure 41 depicts a typical hold comparison frame for the Museum location: the maximum and the mean in each frequency bin are found for various holds: 10, 1e3, 10e3, 100e3, and 1e6. For the Montana Tech locations, several of these momentary spurious emissions are captured every minute. At the remote location, Moose Lake (see Figure 42), these momentary spurious emissions are captured several times an hour or once every several hours.



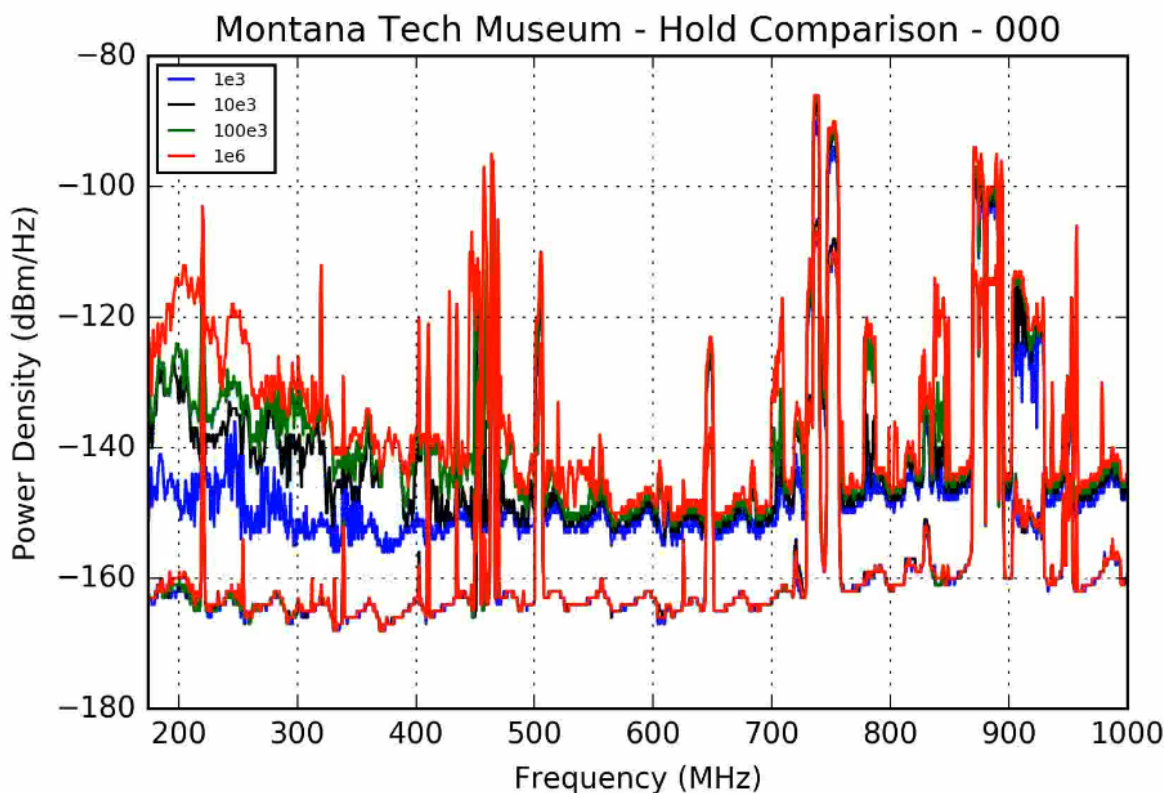


Figure 41: Montana Tech Museum Hold Comparison

Besides the persistent signals described earlier, other notable activity at the Montana Tech location occurred in the industrial, scientific and medical (ISM) radio band from 902 to 928 MHz. This band is used by low-powered unlicensed devices. This band is called the 33-cm band by Amateur Radio operators, who are licensed to use this band on a secondary basis. In this band, the devices appear to perform frequency-hopping to find an available channel. There is also activity from 942 to 955 MHz, which is allocated for fixed communications. In Butte, Montana this may be used by aural broadcast auxiliary stations in order to transmit from the studio to the broadcast transmitter.

Besides the 70 cm Amateur Radio in use from 450 to 455 MHz, the Amateur Radio 1.25 m band is also in use from 223 to 235 MHz. The signal at 220 MHz is located in a TV

“white space” and its magnitude varies dramatically. White spaces refer to frequencies allocated nationally for broadcasting service that are not used locally for broadcasting.

The spectrum from 225 to 450 MHz are designated for government use, both Federal and non-Federal. There appear to be various narrow band (less than 1-MHz) transmit signals. Some of these bands are shared with non-government entities, but the majority are exclusive for government use.

When the data is held for both locations, the uplink activity for LTE and 2G/3G can be seen more clearly. Verizon LTE uplink spans from 777 to 787 MHz, and 2G/3G uplink spans from 824 to 849 MHz. Only at the Museum location can AT&T uplink be viewed from 706 to 716 MHz.

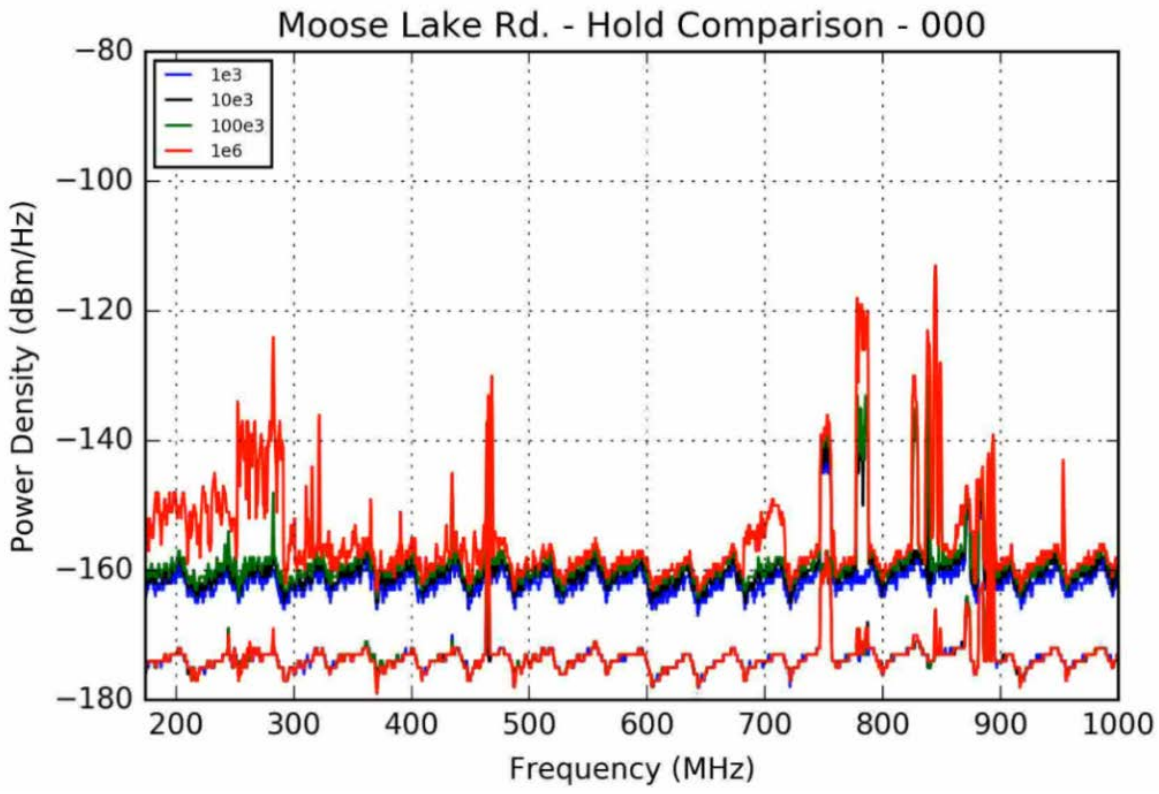


Figure 42: Moose Lake Road Hold Comparison

Both locations have activity in the 400 MHz band. The frequencies from 455 MHz to 470 MHz are licensed to Meteorological Satellite (either earth-to-satellite or satellite-to-earth).

The hold comparisons show behavior of the signal over different lengths of time. The persistence is hinted by the relationship between the average and the maximum: as the average of signal approaches its maximum, the signal becomes more persistent. However, the maximum hold does not give an indication as to how long the signal was at the maximum power level for that frequency bin.

Noise measurement studies were conducted for both equipment setups and environments by replacing the antenna with a terminating load. A single 1 million sweep data set was processed for each to find PSD as if the antenna were connected. Figure 43 depicts a typical frame for the hold comparison at Montana Tech (fixed) station setup. Figure 44 depicts a typical frame for the hold comparison with the Moose Lake (mobile) station setup.

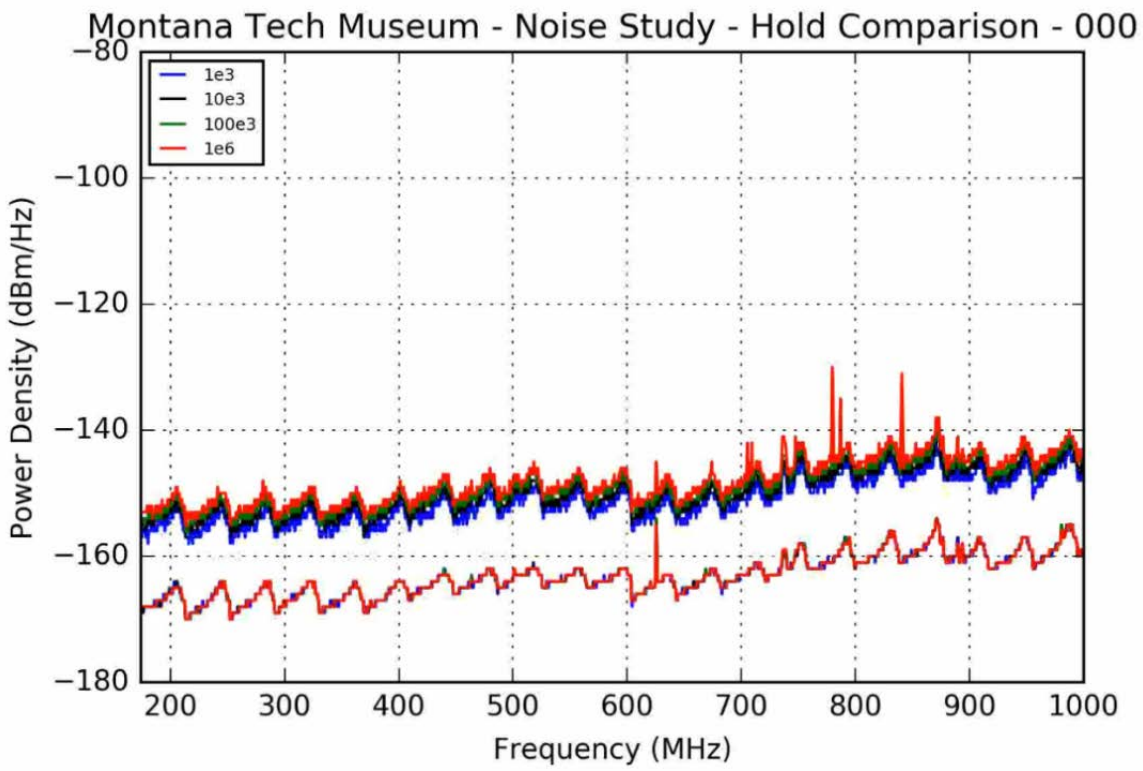
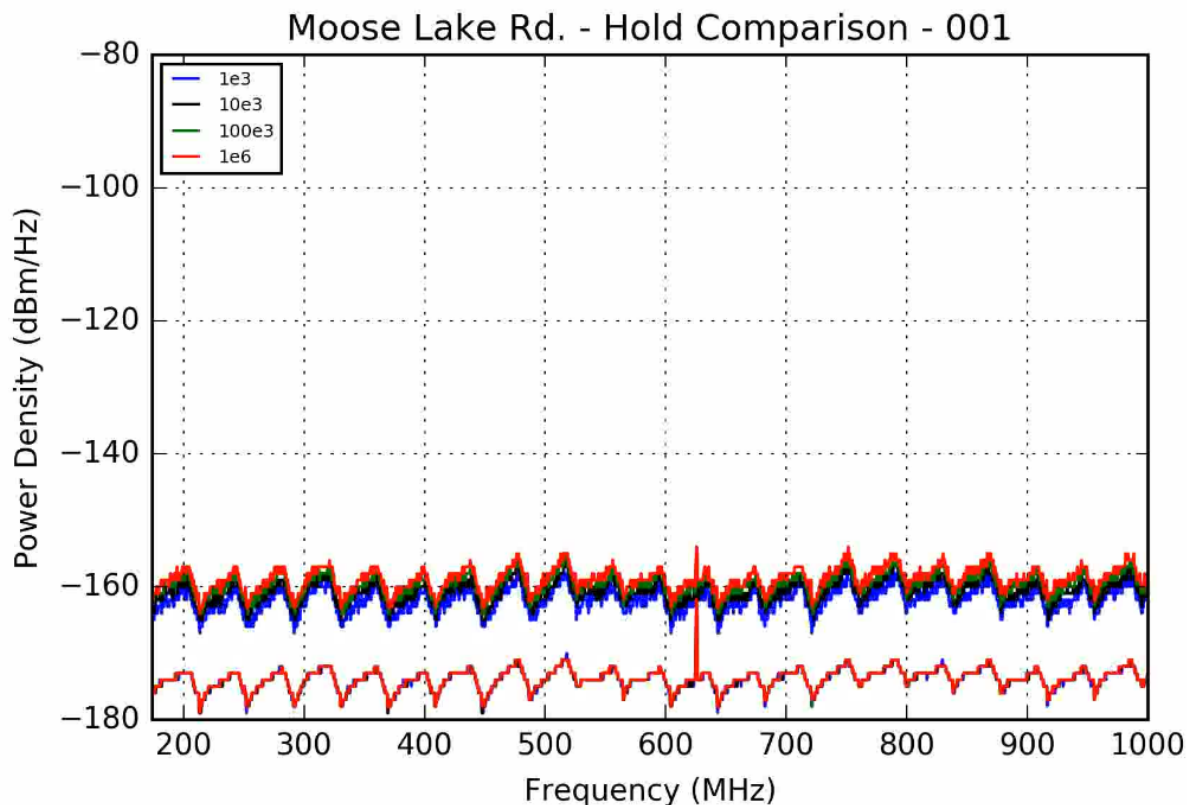


Figure 43: Noise Hold Comparison Analysis for Museum Setup

The harmonic for the RTSA can be clearly seen where it deviates from the average noise floor at 625 MHz. It also appears that cell phone emissions were also received across the 700 MHz band and 800 MHz band over the course of recording. Note that the 625 MHz harmonic is not detected in the Moose Lake hold measurements.



**Figure 44: Noise Hold Comparison Analysis for Moose Lake Setup**

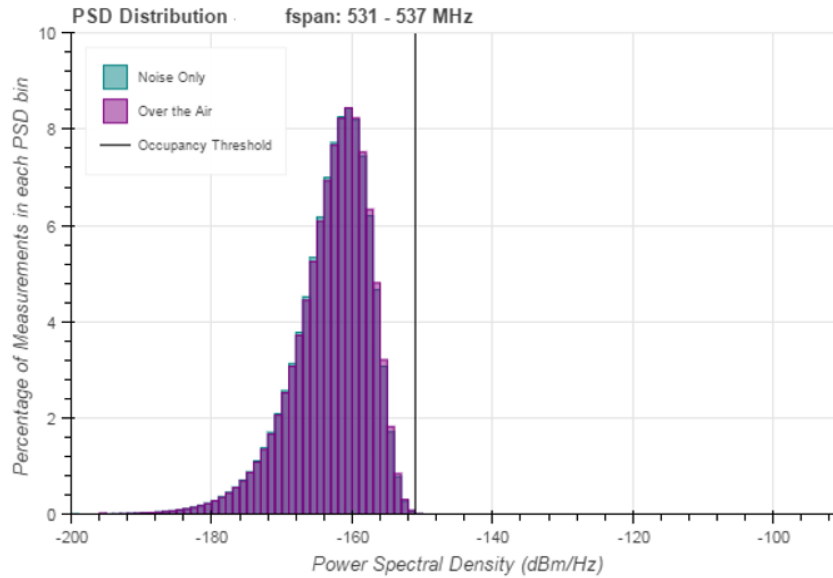
Note the shift in the average noise floor measurements between the noise studies. This is due to the difference in the equipment setups and environment. There are attenuators and an LNA with a smaller gain at the Museum location. Temperature may also be a factor, the Moose Lake noise data sets were both collected outside during the winter, while the Museum noise data sets were collected inside during the summer. In general, the equipment in the remote location is more sensitive, the average noise floor for the Moose Lake equipment and environment is -173 dBm/Hz, the average noise floor the Montana Tech Museum is -163 dBm/Hz.

These noise studies were used to determine the occupancy threshold of each channel for over-the-air (i.e. data collected with antenna) at both locations. The maximums for a hold of 10e3 were stored for each frequency bin, then the median of those values were found for each channel.

This method of determining the occupancy threshold was born out of convenience, since this data was already acquired for the hold comparison analysis. This method was found to be sufficient when the distribution for the noise and over the air measurements were plotted against each other. The thresholds were chosen to minimize false-positives, therefore the average occupancy for the noise measurements is 0.007%.

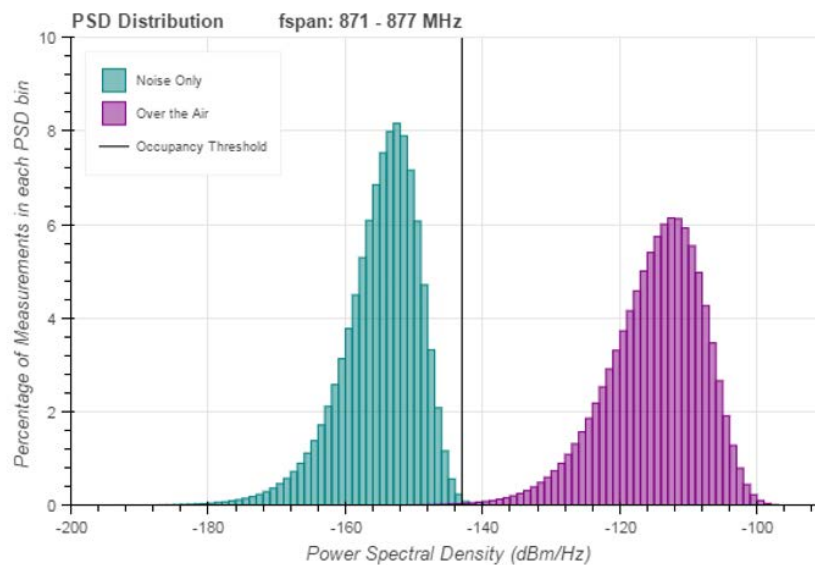
There are over-the-air measurements below the occupancy channel than are statistically different than noise-only measurement. As a consequence, it appears that false negatives are more likely to occur than false positives for certain channels. A more sophisticated occupancy test for any given measurement may be a fruitful path to consider but is currently out of the scope of this project.

These occupancy thresholds are plotted against the PSD distribution for the noise-only measurements and over-the-air measurement for each channel (note in the following analysis, each channel has its own number from 0 to 140). Figure 45 depicts a typical idle channel, in this case channel 61, which spans from 531 to 537 MHz. Here the noise-only measurements and over-the-air measurements appear to overlay. A large majority of channels at each location are equivalent to noise-only measurements.



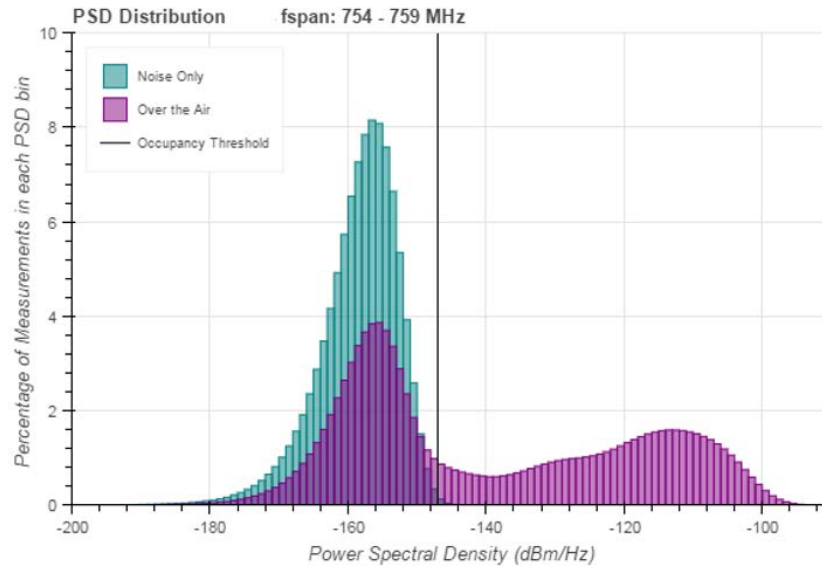
**Figure 45: Typical Idle Channel at Montana Tech**

Active channels will have different distributions, in some cases the over-the-air measurements follow a single distribution, and in others the distribution is multi-modal. Figure 46 depicts Channel 119, which spans from 871 to 877 MHz and contains the 2G/3G downlink. Most of the over-the-air measurements (99.80%) are completely above the occupancy threshold for this channel.



**Figure 46: Active Channel 2G/3G Downlink at Museum Location**

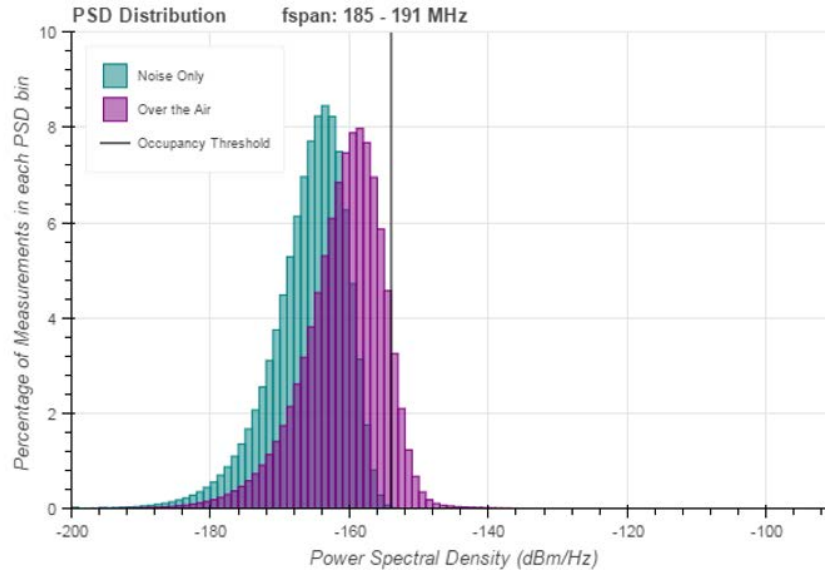
Figure 47 depicts channel 99, which spans from 754 to 759 MHz and contains a portion of the Verizon LTE downlink channel. Since the actual Verizon LTE channel (746 – 756 MHz) is divided between two channels, measurements equivalent to noise-level make up a substantial (greater than 51%) portion of the channel activity in channel 99.



**Figure 47: Active Channel with Noise, Verizon LTE Downlink, at Museum Location**

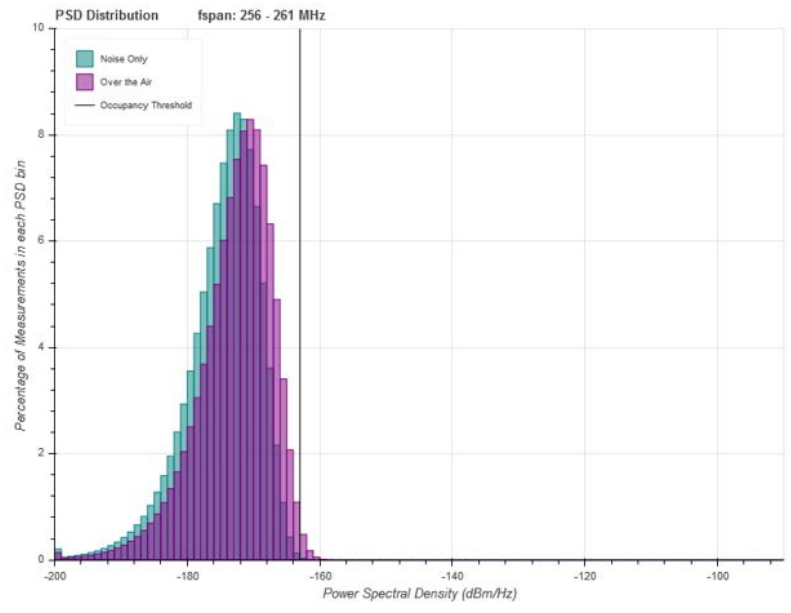
Channels that are dominated by temporary spurious emissions show a mean-shift upwards, and have longer tails on the right compared to the noise-only measurements. For the emission-dominated channels from 174 to 320 MHz at Montana Tech Museum, the mean are increased by +2 dB to +8 dB. Figure 48 depicts Channel 2 that has mean shift of 6.2 dB.





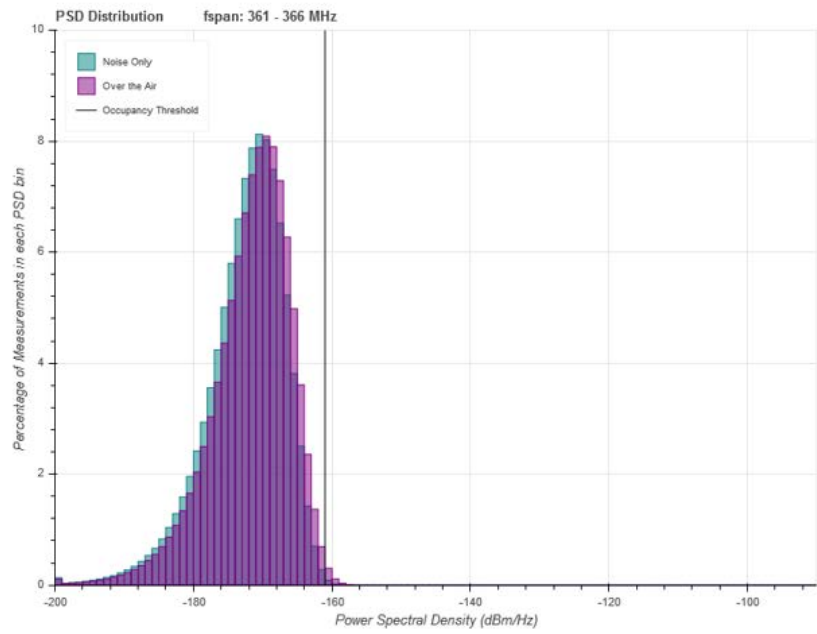
**Figure 48: Museum Location Typical Spurious Emissions Dominated Channel**

A noise measurement study was also conducted with the equipment employed at Moose Lake Road. The emission behavior occurs predominately around 260 MHz and 365 MHz, however the over-the-air measurements are similar to the noise-only measurements taken with the same equipment. Figure 49 depicts Channel 14 at the Moose Lake location that spans from 256.1 MHz to 261.5 MHz, and has a mean shift of 1.9 dB.



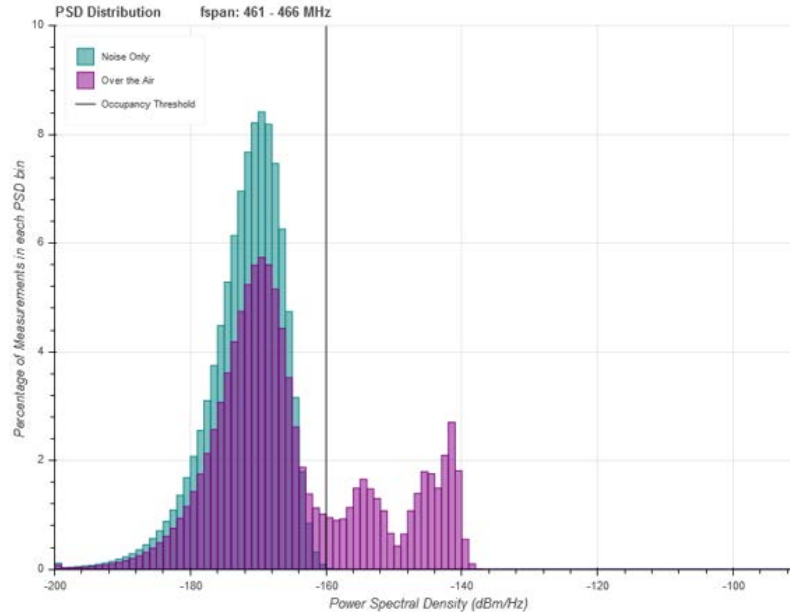
**Figure 49: Spurious Emissions Dominated Channel 14 at Moose Lake Road Location**

Figure 50 depicts Channel 32 at the Moose Lake location that spans from 361.6 MHz to 367.0 MHz, and has a mean shift 0.7 dB.



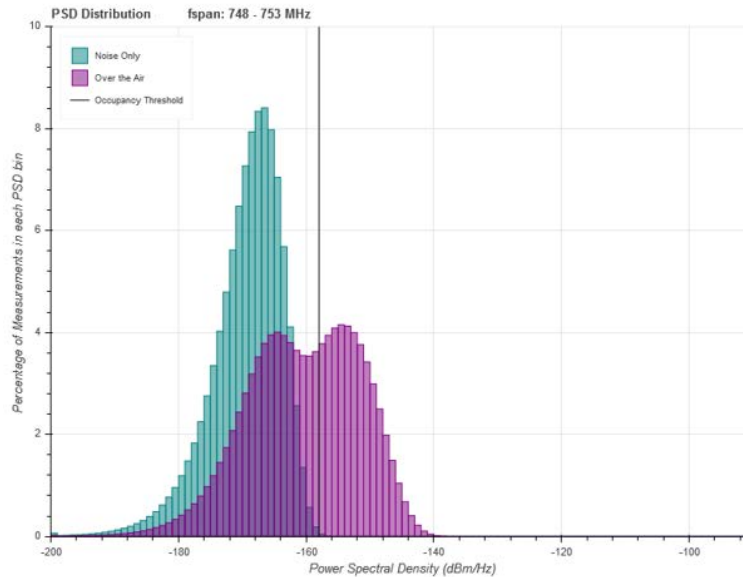
**Figure 50: Spurious Emissions Dominated Channel 32 at Moose Lake Road Location**

One of the few active channels, Channel 49, spans from 461.3 MHz to 466.7 MHz. This channel captures transmission from what appears to be a frequency-hopping transmitter. The distribution depicted in Figure 51 shows two distinct transmission levels at -154 dBm/Hz and -142 dBm/Hz.



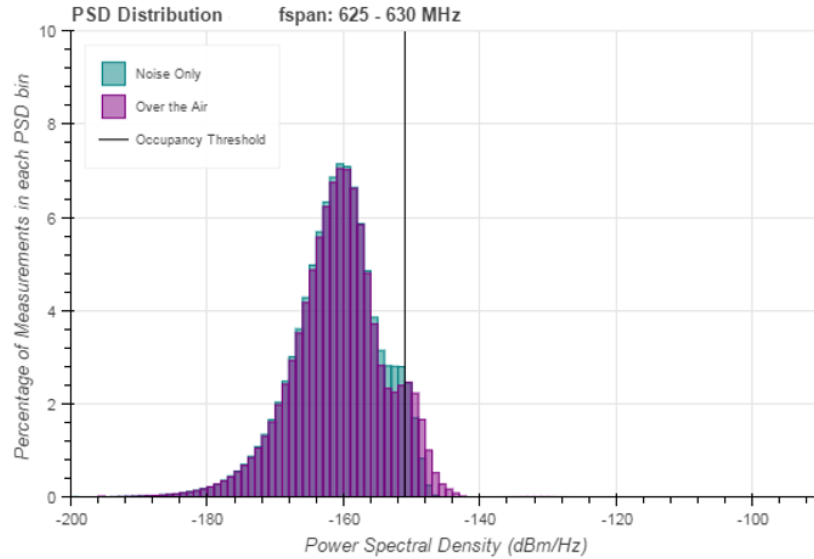
**Figure 51: Channel 43 at Moose Lake Road Location**

Figure 52 depicts Channel 98, a channel that may benefit from a more nuanced occupancy test, which approximates the likelihood that a signal below the occupancy threshold is active. The channel spans from 748.6 to 753.9 MHz and is licensed for LTE downlink communication for Verizon.



**Figure 52: Channel 98 at Moose Lake Road Location**

When the equipment is shielded from the antenna, the harmonic at 625 MHz disappears. However, during noise studies when the antenna is replaced by a terminating load the 625 harmonic reappears. At the Museum location, the equipment was not shielded (Figure 53). At Moose Lake Road the equipment is shielded (Figure 54). While various harmonics disappear when the equipment is shielded, the 625 MHz harmonic is internally generated. The harmonic reappears for the Moose Lake Road noise study because the equipment itself is acting like a resonant antenna at that frequency.



**Figure 53: Channel with RTSA 625 MHz Harmonic at Museum Location**

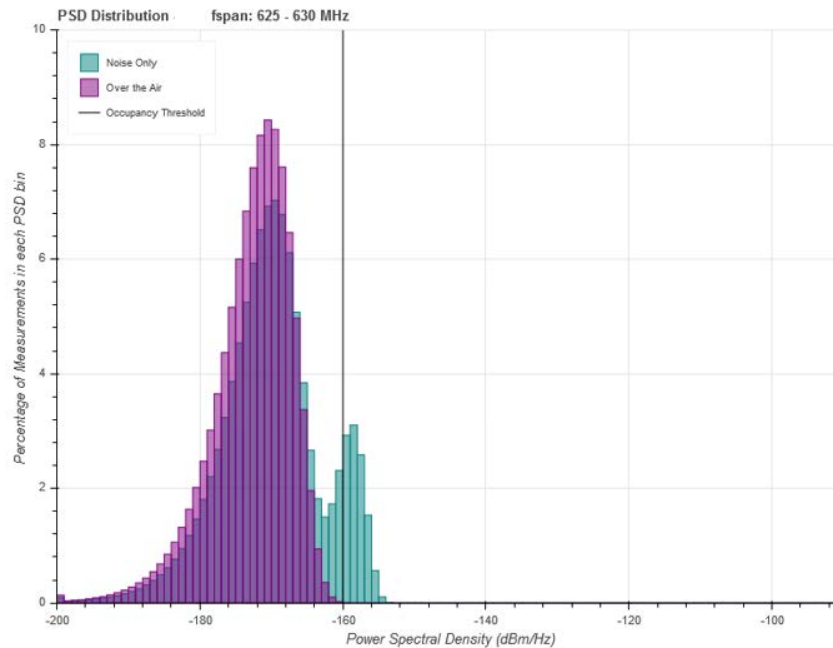


**Figure 54: Channel with RTSA 625 MHz Harmonic at Moose Lake Road Location**

Several metrics were used to determine whether a channel was occupied or un-occupied, see Table IV. These are the maximum PSD measurement made, the percent occupancy above a threshold and the mean shift for PSD measurements between the noise-only measurements and over-the-air measurements. The maximum PSD threshold of -116 dBm/Hz was chosen to capture

activity that did not meet the occupancy requirements or the mean shift requirements. When a channel has an occupancy percentage greater than or equal to 1%, the channel is deemed to be active. Lastly, when the mean shift is greater than or equal to +2 dB, the channel is deemed active.

**Table IV: Channel Occupancy Metrics**

Max PSD	% Occupancy	Mean Shift
$\geq -116 \frac{dBm}{Hz}$	$\geq 1\%$	$\geq +2 dB$

Communication channels that span greater than or fewer than 12 frequency bins, or are divided between frequency bins of two or more channels as designated by this work could be better characterized. For active channels, a more accurate approach would analyze only the frequency bins within the channel bandwidth. Since the purpose of this analysis is to identify channels that may be available for sharing, the less accurate method was sufficient. This method targets channels where the over-the-air measurements most closely resemble the noise-only measurements.

The occupancy percentage for each channel was determined by summing the number of over-the-air measurements above the occupancy threshold and dividing by the total number of measurements. The results are reported as percentages.

The occupancy is determined for the channel, if any frequency bin is above the channel threshold the sum is incremented:

$$\text{Percent Occupancy} = \frac{\text{sum}}{\# \text{ of sweeps}} \quad (37)$$

The mean shift for each channel was determined during post-processing. The PSD measurements for each frequency bin were converted to linear. The average RMS power is

determined by summing the linear channel power of each sweep, and finding the average. The linear average result is then converted to decibel:

$$P_{rms} = \frac{1}{n} \sum P_{Rx,linear}, n = \# \text{ of sweeps} \quad (38)$$

The difference was found between the RMS power of over-the-air measurement and the noise only measurements. A positive-shift occurs when the mean of the over-the-air measurements is greater than the mean of the noise-only measurements.

As a consequence of these three metrics, there are 71 Channels for the Museum location, and 14 channels for the Moose Lake Road location that are designated occupied. See Appendix C for a table of occupied channels at the Montana Tech Museum location and Table V for a occupied channels at the Moose Lake Road location. These tables are divided into bands that share the same spectrum allocation as found on SpectrumWiki.com [58]. The FCC TV channel database was used to identify TV broadcast transmissions in Montana [59].

Table V: Occupied Channels at Moose Lake Road Location

Name	Frequency Range (MHz)	Max PSD ( $\frac{dBm}{Hz}$ )	Percent Occupancy (%)	Mean shift (dB)	License	Transmission Type
49	461.3 – 466.7	-127	26.46	17	Land mobile	Meteorological Satellite
50	467.1 – 472.5	-114	0.01	-1		
97	742.7 – 748.1	-139	5.90	5	Fixed Land Mobile Broadcasting	Verizon LTE Downlink
98	748.6 – 753.9	-135	35.03	13		
99	754.4 – 759.8	-135	13.66	10		
103	777.9 – 783.2	-116	0.01	-1	Fixed Land Mobile Broadcasting	Verizon LTE Uplink
104	783.7 – 789.1	-116	0.01	-1		
111	824.8 – 830.1	-115	0.17	3	Fixed Land Mobile Broadcasting	Public Safety Radio Systems  2G/3G Uplink
113	842.4 – 847.7	-113	0.42	2		
118	865.8 – 871.2	-143	1.44	2	Fixed Land Mobile Broadcasting	2G/3G Downlink
119	871.7 – 877.1	-146	5.05	4		
120	877.5 – 882.9	-145	11.60	6		
121	883.4 – 888.8	-143	20.03	8		
122	889.3 – 894.6	-138	33.90	13		

To get a better estimation the occupancy percentage, the following analysis was completed for each frequency bin. A simple threshold test was performed: if the PSD is greater than the threshold the frequency bin is active (1), if less than or equal to the threshold the



frequency bin is idle (0). The occupancy threshold was determined on a channel-by-channel basis as described earlier.

To summarize the activity for the whole data set, the occupancy for each frequency bin was made for both locations. Figure 55 depicts the occupancy percentage for each frequency bin at the Montana Tech Museum location. Figure 56 depicts the occupancy percentage for each frequency bin at the Moose Lake Road location.

The Montana Tech Wireless Lab YouTube channel hosts videos where the occupancy is found for different holds: 100, 1e3, 10e3, 100e3 and 1e6. This gives a better idea of the occupancy over different time-periods.

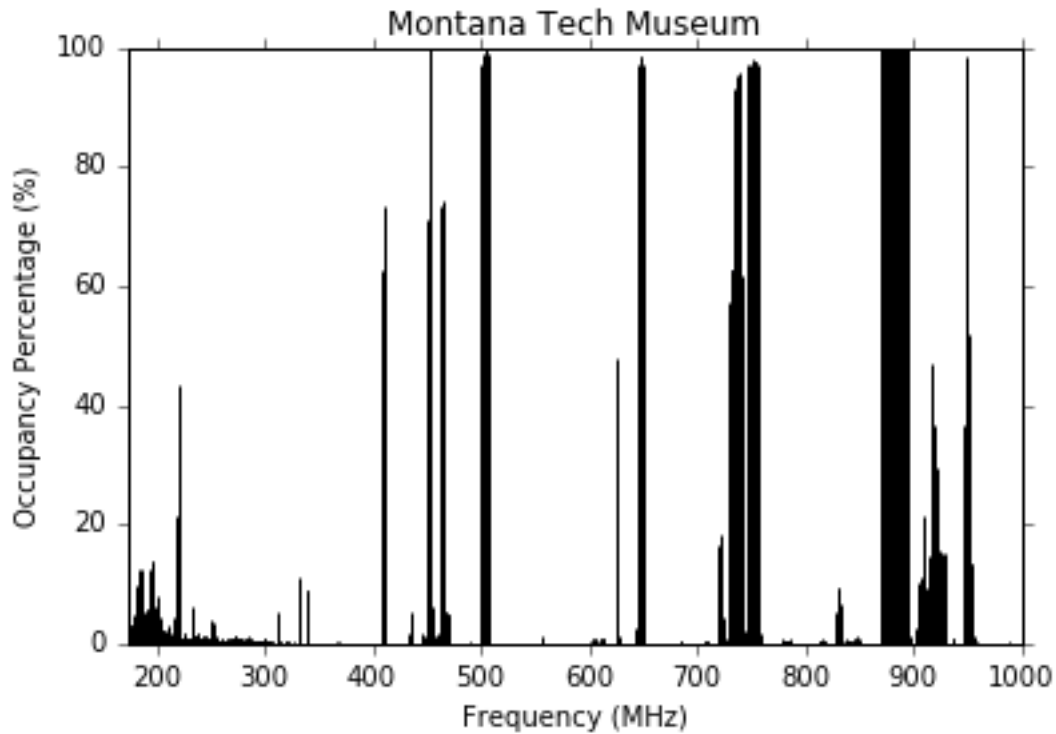
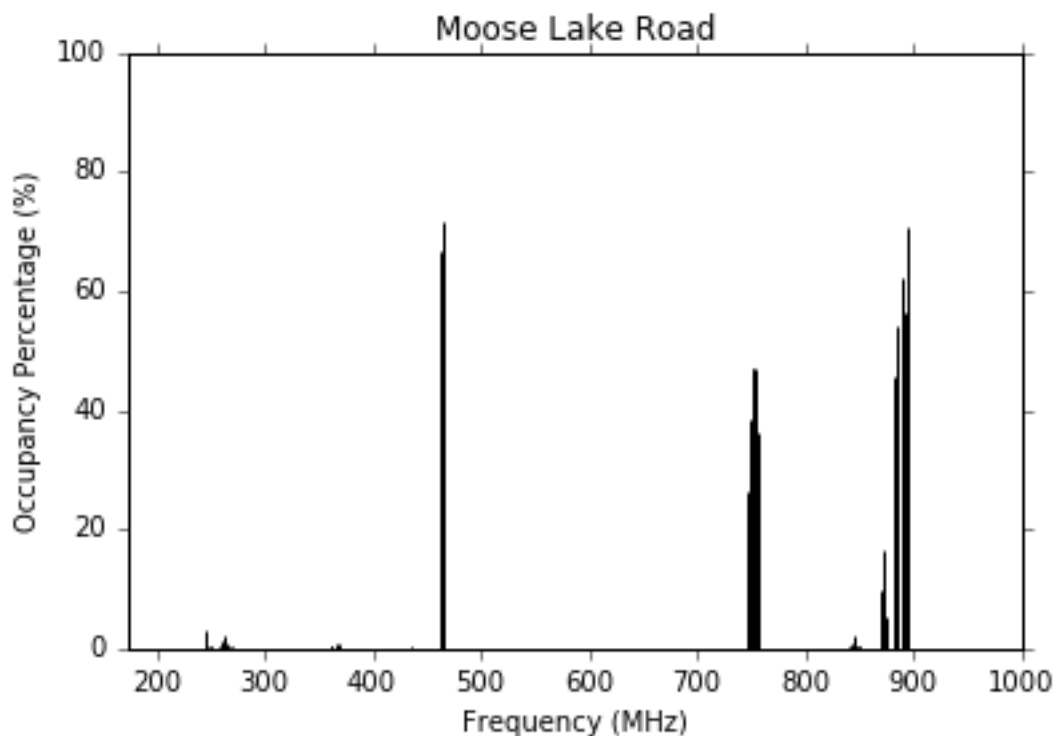


Figure 55: Museum Occupancy Plot for Each Frequency Bin



**Figure 56: Moose Lake Occupancy Plot for Each Frequency Bin**

At both locations there are many frequency bins below a given threshold. Recall there are 1692 frequency bins across the span. There are 1262 frequency bins at Tech Museum, and 1631 frequency bins at Moose Lake Road below 1% occupancy. There are 1476 frequency bins at the Museum location and 1645 at Moose Lake Road below 10% occupancy. Below 0.1% occupancy, there are 888 frequency bins at the Museum and 1564 at Moose Lake Road.

The spurious emissions dominated frequency bins clustered around 250 MHz, and 360 MHz have occupancy percentages that vary from 0.15% to 3.21% at Moose Lake Road. At the Montana Tech Museum location, the spurious emissions dominated channels from 174 to 300 MHz (except the 1.25-m Amateur Radio band) vary from 0.18% to 14.07%.

In general, downlinks for broadband mobile communication are easier to capture than uplinks, since the uplinks are time-slotted, spatially distributed, and power-controlled. A controller designates when a mobile user may transmit to a base station. The mobile users that

are transmitting directionally to the base station are distributed in various locations relative to the spectrum monitoring station. The mobile devices themselves are power-limited because of the battery and size restriction.

A comparison of wireless mobile communication channels is summarized in Table VI.

**Table VI: Mobile Communications at Museum and Moose Lake**

frequency	direction	LTE BAND	Max PSD (dBm/Hz)		Max Occupancy Percentage		Carrier
			Museum	Moose Lake	Museum	Moose Lake	
704 – 716	uplink	17 FDD	-102	-142	0.25	0.007	AT&T
734 – 746	downlink		-84	-135	95.93	0.16	
717 - 728	downlink unpaired	29 FDD	-119	-142	18.23	0.006	carrier aggregation
746 - 756	downlink	13 FDD	-89	-139	97.93	47.26	Verizon
777 – 787	uplink		-111	-116	0.79	0.03	
824 - 849	uplink	5 FDD	-97	-115	9.39	2.19	2G/3G
869 - 894	downlink		-93	-143	99.98	70.73	

The data does not demonstrate the quality of cellular coverage in the remote locations. From personal experience of the operator, there is no meaningful cellular coverage at the Moose Lake Road location, while cellular coverage at Montana Tech Museum is good.

Large portions (greater than 40 MHz) of spectrum at Montana Tech Museum location and Moose Lake Road location can be designated unoccupied most of the time. The frequencies from 350 to 409 MHz, from 508 to 555 MHz, from 557 to 625 MHz, from 651 to 718 MHz, and from 960 to 1000 MHz at Montana Tech have less than 1% occupancy. Moose Lake Road has an occupancy percentage less than 1% from 174 to 243 MHz, from 263 to 462 MHz, from 467 to 746 MHz, from 757 to 843 MHz, from 846 to 869 MHz, and from 896 to 1000 MHz.

While not all unoccupied channels are available for sharing, there are several occupied channels that may be available for sharing. In particular, the spurious emissions dominated channels from 174 MHz to 200 MHz. There are no TV stations transmitting from 510 to 550

MHz in the Butte-Silver Bow County where Montana Tech is located, or in Granite County where Moose Lake Road is located. While some of these channels are dominated by spurious emissions in Butte, they are relatively free of any transmission at Moose Lake Road. Even though the frequencies from 902 to 928 MHz are designated “occupied” at the Montana Tech locations and are allocated for unlicensed ISM use.

## 5. Propagation Modeling

The Wireless Lab at Montana Tech was granted an experimental license to operate at 20 W effective radiated power (ERP) station from 510 to 550 MHz. The Longley-Rice Path Loss model is implemented to predict the channel characteristics of this station, WK9XUC. The ITM algorithm will be described in detail. The irregular terrain input parameters of the model will be tested for mountainous terrain. This work tests the signal propagation of a cellular base station and TV stations operating in these bands and models the co-channel and adjacent channel interference between these stations. In these simulations, the transmit power on the WK9XUC station is adjusted to determine when the interference exceeds 5% EVM for receiver locations in western Montana.

### 5.1. Locations

Twenty-three UHF TV stations operating from 470 to 700 MHz within 242 km of Butte, Montana were located. The location of the transmitters, including WK9XUC and each TV station are pictured in Figure 57. Each TV station's location has a blue pin on the map. TV stations are referenced by their call sign, a unique name that starts with K. The WK9XUC station is located at the Museum Building at Montana Tech, and its location has a white bull's eye.

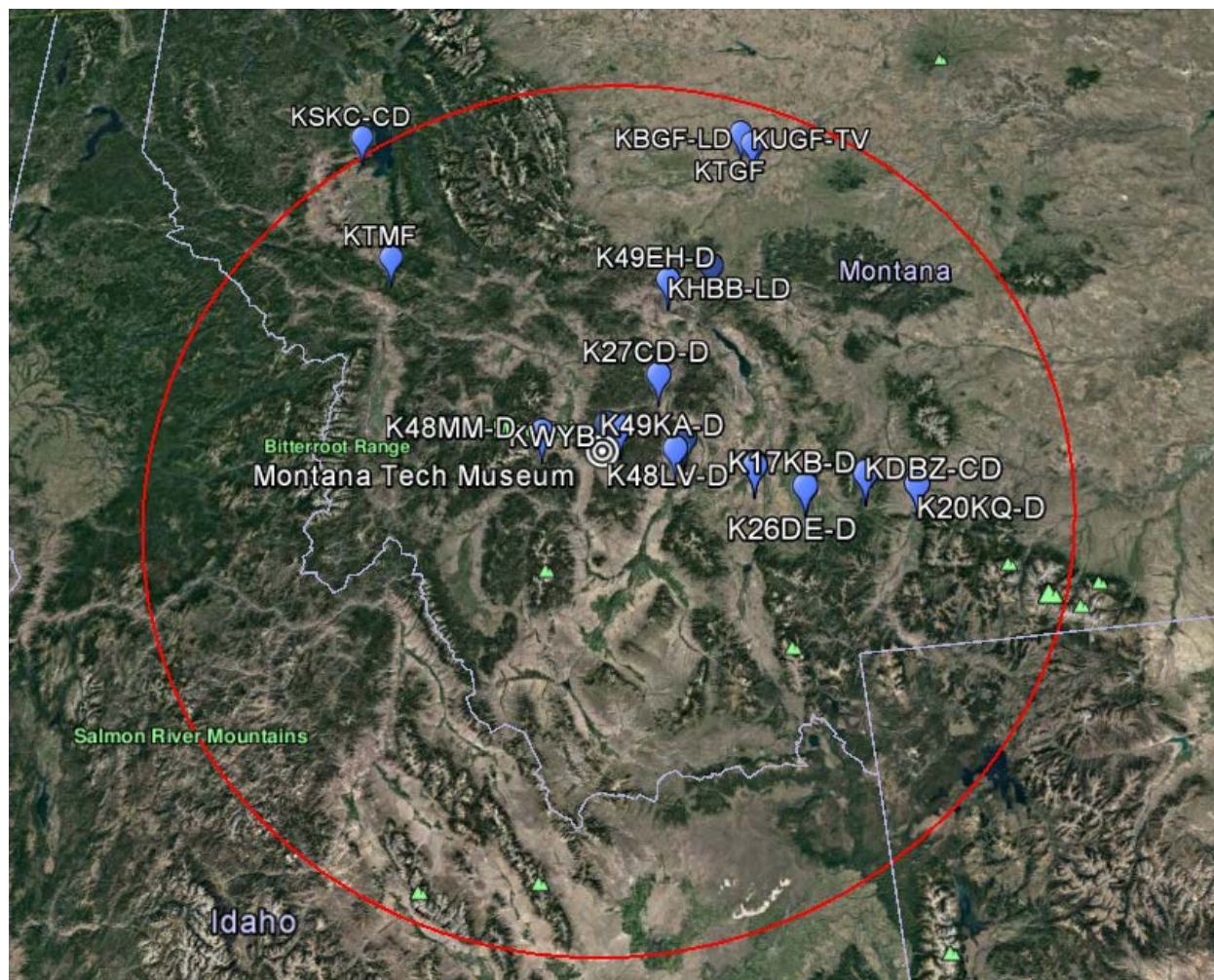


Figure 57: UHF TV Channels within 242 km of Tech Museum

A summary of the TV channel characteristics is given in Table VII. Several online databases were used to populate the table, including the FCC TV-query, fccdata.org and Rabbit Ears [60-61]. Several stations did not have consistent antenna heights or ERP listed, these are marked with an \*. The TV stations located in Butte, Montana are in **bold**.

These channels are 6-MHz wide, but only the center frequency is cited in the table. The distances are relative to the WK9XUC station in Butte, Montana.

TV station engineers commonly cite the transmit power in ERP instead of EIRP. The power is given in relation to a dipole antenna (dBd) instead of an isotropic antenna (dBi) and the gain of the transmit antenna is assumed to be maximum gain.

$$ERP = P_{Tx} + G_{Tx,max} (dBd) \quad (39)$$

The following equation is used to convert from ERP to EIRP. The difference is the gain of a dipole antenna in relation to an isotropic antenna.

$$EIRP = ERP + 2.15 dBi \quad (40)$$

**Table VII: Summary of TV UHF Channels**

Station	Location	Broadcaster	$f_c$ [MHz]	Distance [km]	ERP [kW]	Max. Antenna Gain [dBd]	Antenna height [m]
K17KB-D	Belgrade	Montana PBS	491	108.24	1.53	7.87	32.0
<b>KWYB</b>	<b>Butte</b>	<b>ABC, Fox</b>	<b>503</b>	<b>8.91</b>	<b>46.0/110.7*</b>	<b>16.82</b>	<b>86.3*</b>
KBGF-LD	Great Falls	NBC, CW	503	196.47	15	11.76	169.8*
K20KQ-D	Livingston	ABC, FOX	509	162.52	1.4	11.46	40.0*
KUGF-TV	Great Falls	Montana PBS	515	195.35	23.4	12.04	169.8*
KHBB-LD	Helena	ABC, Fox	515	93.85	5	10	38.0*
KTMF	Missoula	ABC, Fox	527	158.09	92.6	18.1	89.0*
K26DE-D	Bozeman	CBS, CW	545	108.24	4.51	14.14	24.4*
K27CD-D	Boulder	Montana PBS	551		0.372	10.93	15.0*
KSKC-CD	Ronan	PBS	551	235.22	6.6	14.22	151.8*
KWYB-LD	Bozeman	ABC, Fox	557	136.16	11.9	13.77	115.0*
KUHM-TV	Helena	Montana PBS	563	111.7	43.4	17.4	44.5*
K31KR-D	Three Forks	n/a	575	80.36	1	3.01	31.1*
<b>K39JC-D</b>	<b>Butte</b>	<b>GCN</b>	<b>623</b>	<b>2.60</b>	<b>0.625</b>	<b>10.18</b>	<b>37.0*</b>
K40HL-D	Whitehall	n/a	629	42.63	1.7	12.3	15.3*
KDBZ-D	Bozeman	NBC, Me-TV, Movies!	641	136.16	15	14.6	115*
<b>K43DU-D</b>	<b>Butte</b>	<b>Montana PBS</b>	<b>647</b>	<b>8.90</b>	<b>4.55</b>	<b>12.6</b>	<b>62.0*</b>
K44JW-D	Three Forks	n/a	653	80.35	1	3.01	31.1*
KTGF	Great Falls	Me-TV, JUCE, TBN	659	199.54	0.78	11.4	244.0*
K48LV-D	Three Forks	n/a	677	80.35	1	3.01	31.1*
K48MM-D	Deer Lodge	ABC, Fox	677	107.61	0.8	9.03	9.1*
K49KA-D	Whitehall	n/a	683	39.28	.338	10.52	39.0*
K49EH-D	Helena	Montana PBS	683	93.79	3.1	10.93	31.0

KWYB's license to operate at a lower power level is temporary due to damage to the transmitter equipment. When channel measurements were performed in August/September 2016 the antenna was transmitting at the lower power. This station is expected to be repaired in spring or summer of 2017. For measurement results, the transmit power is lower, EIRP of 79 dBm, for predictive results, both power levels will be presented. The higher transmit power is 83 dBm.

To predict the channel characteristics of this lab's station WK9XUC, SPLAT! was used to model the path loss to a grid of receiver sites in Butte and population centers within 50 km of Butte, specifically Anaconda, Deer Lodge, Boulder, Whitehall, Cardwell, and Divide. Figure 58 depicts the relative locations. Each population grid contained Rx sites spaced 1 km apart. All receiver locations in the population grid have a height of 6 meter. Furthermore, each grid was defined by a set of latitudes and longitudes: (N, E), (S, E), (S, W), and (N, W). The characteristics of each grid is summarized in Table VIII.

Since a large set of path loss predictions were required for this work and SPLAT! is used from the command line, various bash scripts were employed (see Appendix D for more details). The average path loss was found for WK9XUC operating at 500 MHz and 560 MHz. For most locations, the maximum difference was 3 dB and the average difference was 2 dB. The path loss is used to determine the received channel power for each Rx location on the grid. The SNR was determined for the TV stations, and the SINR was determined by adjusting the power level of WK9XUC.



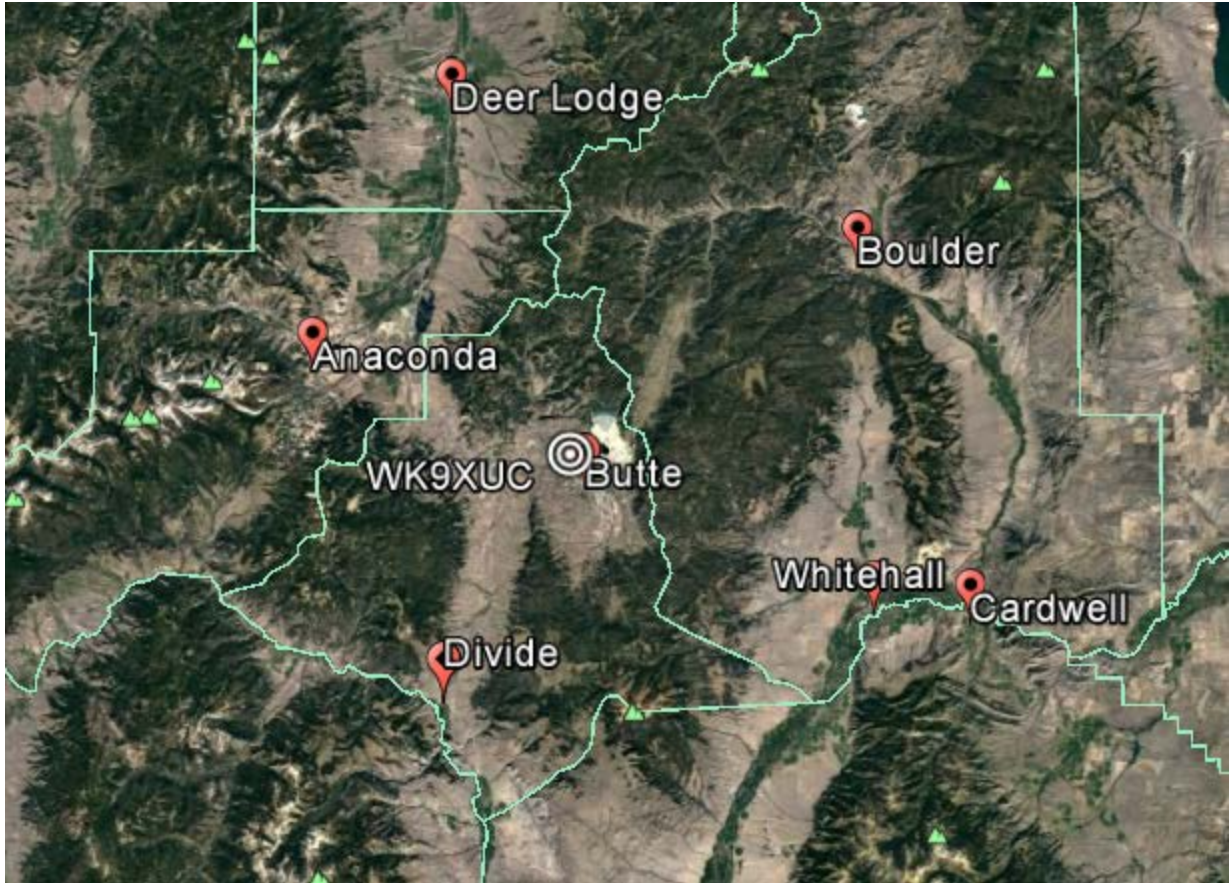


Figure 58: Map of Grid Locations

Table VIII: Population Grid Summary

Name	Population Center Coordinates	N	E	S	W	# of Rx locations
Anaconda	46.13°, -112.95°	46.18°	-112.78°	46.09°	-113.07°	288
Boulder	46.24°, -112.12°	46.25°	-112.06°	46.20°	-112.16°	63
Butte	46.00°, -112.53°	46.05°	-112.40°	45.90°	-112.75°	522
Deer Lodge	46.40°, -112.74°	46.45°	-112.68°	46.32°	-112.84°	224
Divide	45.75°, -112.75°	45.77°	-112.74°	45.71°	-112.79°	40
Whitehall	45.87°, -112.10°	45.89°	-111.97°	45.78°	-112.24°	378
Cardwell	45.86°, -111.95					

## 5.2. Methodology

ITM predicts the median path loss of radio signals from 20 MHz to 20 GHz. For a given point-to-point communication link, it will predict a propagation loss based on LOS path between the transmitter and receiver based on a user-defined terrain profile, elevation data and statistical

inputs. The input parameters were first calibrated by predicting the path loss from each TV station to the Rx at the Montana Tech Museum. Once calibrated, the predicted channel power is compared to measurement results taken at the Museum location. Finally, the path loss for each location on the population grid was predicted with SPLAT!. The path loss was used to predict the receive power for a local TV station and WK9XUC for each Rx.

### **5.2.1. Path Loss Parameters**

Currently, the Montana Tech Wireless Lab uses open source software called SPLAT! [62]. It is a C++ program run from the command-line on a Linux system. The main input parameters are the locations (latitude and longitude) and antenna heights of the transmitter and receiver, elevation data provided by NASA Shuttle Radio Topography Mission (SRTM) and irregular terrain parameters [63]. The SPLAT! program has two source files, `splat.cpp` and `itwom3.0.cpp`. The former displays and organizes the data returned by the latter, which is a hybrid of the ITM model and Irregular Terrain with Obstruction Model (ITWOM). ITWOM claims to model how obstructions along the terrain increase the attenuation. These obstructions are called “clutter” and have a hard-coded height and density. Since ITWOM sometimes returns unrealistic results, only ITM is used in this work [64].

SPLAT! employs 3D geometry to describe the distance, azimuth and elevation direction from one site to the other. The distance between the two sites is the shortest distance between their latitude and longitude coordinates on the Earth. As pictured in Figure 59, the earth is assumed to be a sphere.

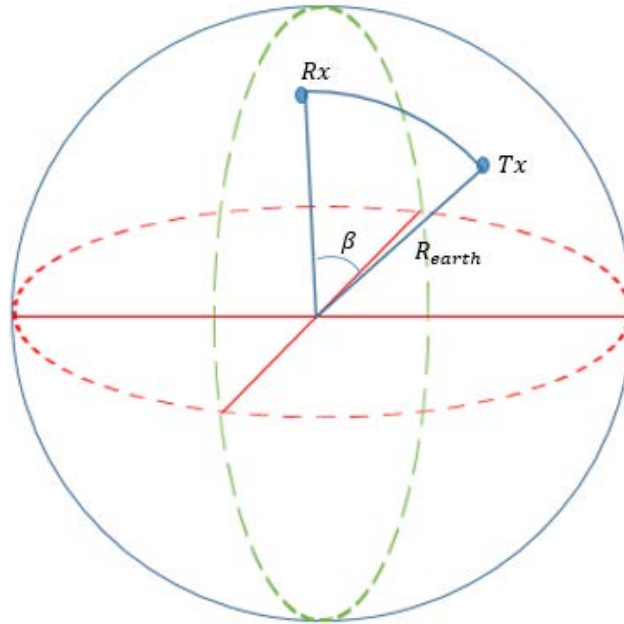


**Figure 59: Distance between Tx and Rx on Earth**

This distance is commonly called the great circle distance. For a set of geographical coordinates (in radians),  $(\varphi_{Tx}, \lambda_{Tx})$  and  $(\varphi_{Rx}, \lambda_{Rx})$ , this work employs the Haversine formula to calculate the great circle distance. The proof of this formula can be found at the site [65].

$$d_{great\ circle} = R_{earth} \beta = R_{earth} 2 \arctan\left(\frac{\sqrt{a}}{\sqrt{1-a}}\right) \quad (41)$$

where  $a$  is the square on the bisected cord between Rx and Tx:

$$a = \sin^2\left(\frac{\Delta\varphi}{2}\right) + \cos(\varphi_{Tx}) \cos(\varphi_{Rx}) \sin^2\left(\frac{\Delta\lambda}{2}\right) \quad (42)$$

where  $\varphi$  is degrees in latitude and  $\lambda$  is degrees in longitude. The earth is assumed to be a perfect sphere with a radius,  $R_{earth}$ , of 6371 km (~3,959 miles).

To calculate the azimuth angle from the Tx to the other Rx in reference to True North, the following formula is used [66]:

$$\theta = 2 \arctan \left( \frac{\sin(\Delta\lambda) \cos(\varphi_{Rx})}{\cos(\varphi_{Tx}) \sin(\varphi_{Rx}) - \cos(\varphi_{Tx}) \cos(\varphi_{Rx}) \cos(\Delta\lambda)} \right) \quad (43)$$

To return the result in degrees with a range  $0^\circ \leq \theta < 360^\circ$ , convert from radians to degrees, then add  $360^\circ$  to the result then divide by  $360^\circ$  and return the remainder. To find the azimuth of the Rx to the Tx, alternate the position of the variables. Or perform the following operation, add  $180^\circ$  to the azimuth of the receiver, then divide by  $360^\circ$ , and return the remainder. In Python, these operations take two lines as pictured in Figure 60:

```
theta_tx=(360+rad2deg(theta)) % 360
theta_rx=(180+theta_tx) % 360
```

**Figure 60: Python Azimuth Normalization**

These equations (Equations 41 – 43) were also used to verify SPLAT! and create the population grids.

All SRTM elevation files have a raster size of  $1^\circ$  in longitude and latitude but the spatial resolution varies. The spatial resolution or distance between each elevation sample depends on the latitude and whether the file is either SRTM3 or SRTM1. All elevations are given to the nearest meter. Figure 61 and Figure 62 depict the coverage area across the globe from SRTM1 and SRTM3 respectively [67, 68]. Path Loss analysis performed with SRTM1 is designated HD, and with SRTM3 non-HD.



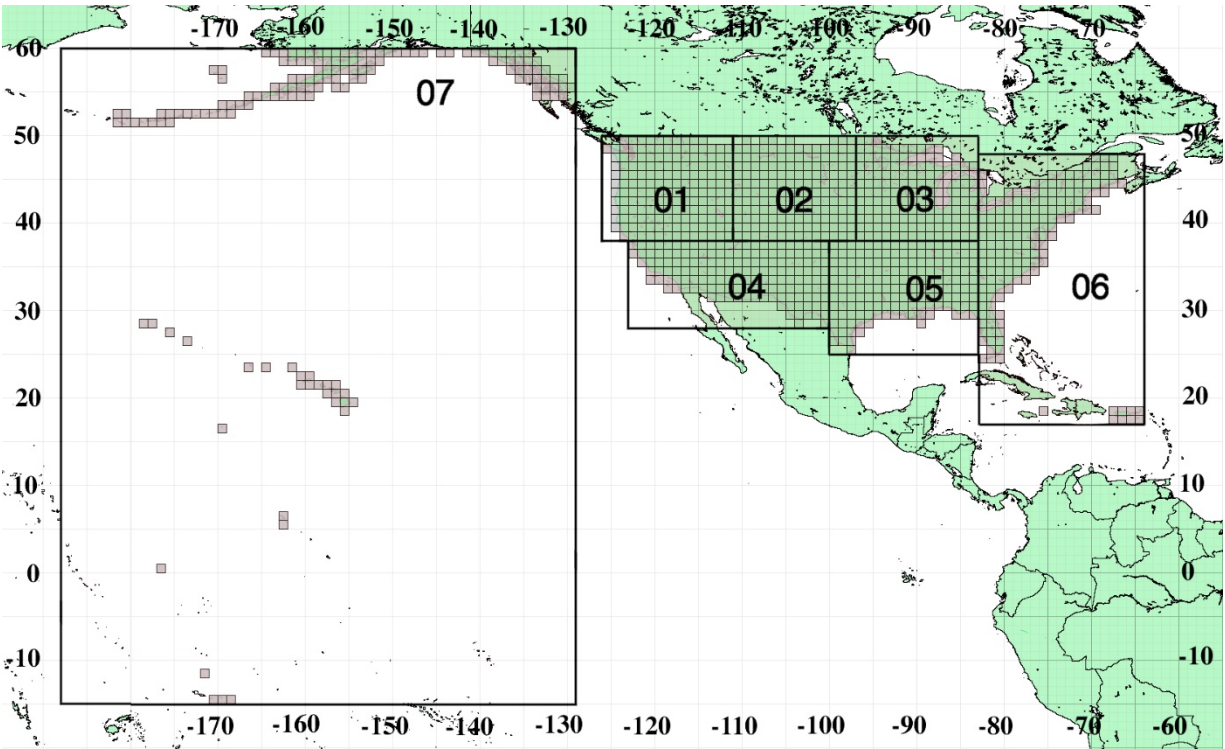


Figure 61: SRTM1 Coverage Area

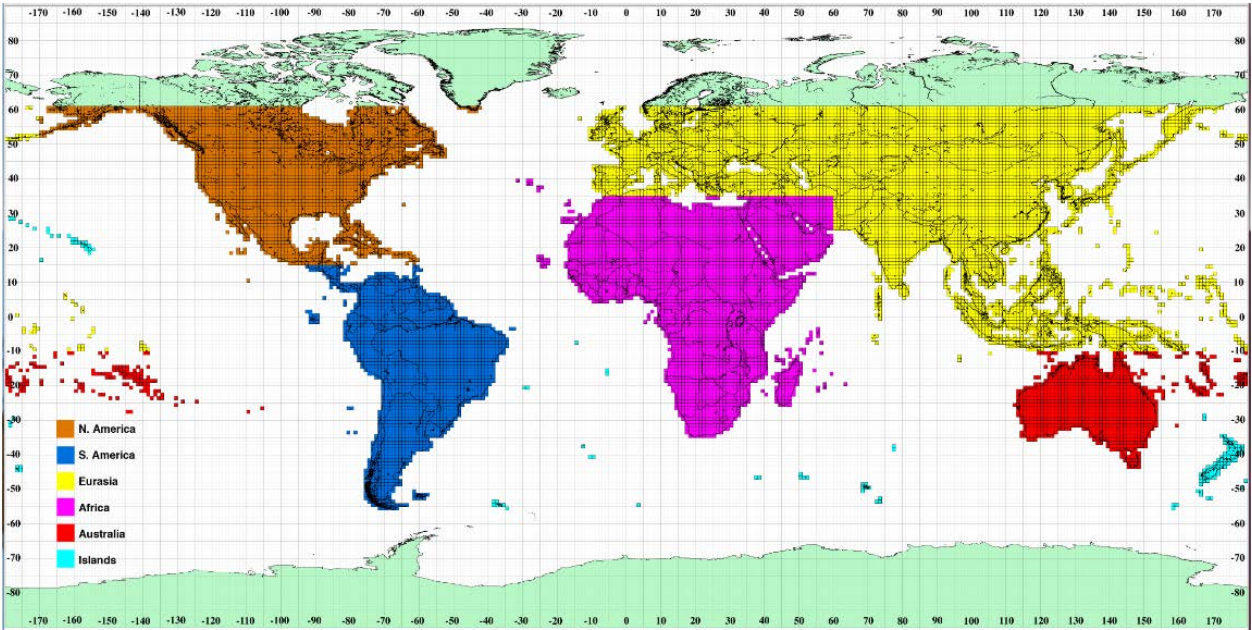


Figure 62: SRTM3 Coverage Area

On the SRTM site the files have an \*.hgt extension, and SPLAT! includes utilities to convert them from \*.hgt to \*.sdf: srtm2sdf for SRTM3 files, and srtm2sdf-hd for SRTM1 files.

While the distance in latitude remains fairly constant across the globe, the distance in longitude varies by cosine. This is because the earth is spherical in shape.

$$d_{longitude} = d_{latitude} \cos(x_{latitude}^{\circ}) \quad (44)$$

There are 60 arc-seconds in an arc-minute, and 60 arc-minutes in  $1^{\circ}$  longitude or latitude. For SRTM1 files there is one sample every 1 arc-second, for SRTM3 there is one sample every 3 arc-second. Therefore, the number of elevations samples for  $1^{\circ}$  in latitude or longitude for SRTM1 can be calculated:

$$\frac{1 \text{ sample}}{\text{arc} - \text{second}} \times 60 \frac{\text{arc} - \text{second}}{\text{arc} - \text{minute}} \times 60 \frac{\text{arc} - \text{minute}}{\text{degree}} = 3600 \frac{\text{samples}}{\text{degree}} \quad (45)$$

**Table IX: Approximate Resolution for Each Elevation SDF File in Montana**

Original File	Latitude (N/S) Distance	Longitude (E/W) Distance ( $45^{\circ}$ N)	Number of elevation samples in file
SRTM3	93 meters	66 meters	$1200^2$
SRTM1	31 meters	22 meters	$3600^2$

One can designate irregular terrain parameters for a given Tx station, or SPLAT! will generate the default parameters. Table X includes a summary of the default parameters and the chosen test parameters. Both the ERP and the frequency depend on the test station. The NTIA published a guide for using the ITM [69]. This document was helpful for calibrating the irregular terrain parameters.

A certain level of skepticism should be adopted when applying a general statistical model to a specific test scenario. This work will compare the default parameters and test parameters but it should be noted that both the Institute for Telecommunication Scientists (ITS) guide and John Magliacane (SPLAT! creator) recommend that the default parameters be used for the majority of

scenarios. These suggestions hint that the input parameters are not the defining feature of the model.

**Table X: SPLAT! Irregular Terrain Parameters**

Name	Symbol	Units	Control	Test 1	Test 2
Relative Permittivity (Earth Dielectric Constant )	$\epsilon_r$	dimensionless	15.000	4.000	4.000
Earth Conductivity	$\sigma$	Siemens/meter	0.005	0.001	0.001
Surface Refractivity (Atmospheric Bending Constant)	$N_s$	dimensionless	301.000	301.00	280.00
Frequency	$f_c$	MHz	Varies	Varies	Varies
Radio Climate	n/a	n/a	5	5	4
Polarization	n/a	n/a	1	1	1
Fraction of Situations	$z_s$	dimensionless	0.50	0.50	0.50
Fraction of Time	$z_T$	Dimensionless	0.50	0.50	0.50
Effective Radiated Power	$ERP$	Watts	Varies	Varies	Varies

Relative permittivity  $\epsilon_r$  and conductivity  $\sigma$  describe the impedance of a dielectric material. In the case of RF signals, the ground is a lossy material. As the signal travels along the earth, the ground will absorb and conduct charge in response to the changing electric field. Relative permittivity quantifies how easily this process occurs; it is the resistance of the medium to the changing electric field. Conductivity quantifies the material's ability to conduct electricity. Soil with moisture has a higher conductivity than soil with less moisture. Larger values in relative permittivity or conductivity cause the signal attenuation to increase.

Relative permittivity and conductivity are used to determine the complex permittivity,  $Z_g$ , which changes depending on the signal polarization:

$$Z_g = \begin{cases} \sqrt{\epsilon'_r - 1} & \text{horizontal polarization} \\ \frac{\sqrt{\epsilon'_r - 1}}{\epsilon'_r} & \text{vertical polarization} \end{cases} \quad (46)$$

where, the complex relative permittivity,  $\epsilon'_r$ , is given with the following equation:

$$\epsilon'_r = \epsilon_r + i \frac{Z_0 \sigma}{k} \quad (47)$$

where,  $Z_0$  is the impedance of free-space, and  $k$  is the wave number,  $Z_0 = 376.62 \Omega$ ,  $k = \frac{2\pi}{\lambda}$  and  $\lambda$  is the wavelength.

For testing, the polarization is set to vertical because the antenna at Montana Tech is mounted vertically and this model assumes that both the Tx and Rx antennas have the same polarization. Polarization refers to the orientation of the signal (electromagnetic wave) as it propagates across the ground: the electric field of a vertically polarized antenna is perpendicular to the earth, whereas the electric field of a horizontally polarized antenna is parallel.

The NTIA guide includes a table that pairs relative permittivity,  $\epsilon_r$  and conductivity,  $\sigma$ . The data is summarized in Table XI. The amount of water in the soil appears to be the significant feature, since the Montana soil is relatively rocky, and the soil is arid in summer months. The “poor ground” parameters were chosen for testing. However, it should be noted that the authors recommend using the “average ground” constants for most scenarios.

**Table XI: Suggested Values for Electrical Ground Constants**

Descriptor	Relative permittivity, $\epsilon_r$	Earth conductivity, $\sigma$ ( $\frac{\text{siemens}}{m}$ )
Average ground	15	0.005
Poor ground	4	0.001
Good ground	25	0.020
Fresh water	81	0.010
Sea water	81	5.0

Another input is the minimum monthly mean for surface refractivity ( $N_s$ ), which is determined statistically for different climates. As a signal passes through the atmosphere, its path will bend according to temperature, pressure, and humidity of the air. Even though technically



refractivity is a characterization of the atmosphere, historically it's been associated with surface elevation and a radio climate, of which there are seven (see Table XII) [69].

**Table XII: Radio Climates and Suggested Values**

Number	Name (example)	Surface Refractivity $N_s$
1	Equatorial (Congo)	360
2	Continental Subtropical (Sudan)	320
3	Maritime Subtropical (West Coast of Africa)	370
4	Desert (Sahara)	280
5	Continental Temperate	301
6	Maritime Temperate, over land (United Kingdom and continental west coasts)	320
7	Maritime Temperate, over sea	350

Conventionally, the units of surface refractivity,  $N_s$  is given as N-units. However, it is better understood as a dimensionless value, which is used to determine the refractive index,  $n$  of an electromagnetic wave as it propagates through a medium. In optics, the medium changes the phase velocity of light that causes it to bend according to its wavelength. Any refractive index is relative to 1, which is refractive index of light in a vacuum:

$$n = 1 + N_s \times 10^{-6} \quad (48)$$

Since RF signals are also electromagnetic waves, the same theory is applied. The values of surface refractivity are meant to model the moisture, pressure and temperature of the atmosphere. The International Telecommunication Union (ITU) publishes a recommendation on how to determine the surface refractivity of radio waves for various climates [70]. Long-term measurements were conducted to determine the surface refractivity at a given elevation above sea-level,  $h$  (km). Their model determines the surface refractivity,  $N_s$  to a global mean of surface refractivity,  $N_0$  of 315, and a height,  $h_0$  of 7.35 km.

$$N_s = N_0 e^{-h/h_0} \tag{49}$$

ITM uses an older version of the recommendation, where  $N_0$  varied from 290 to 390 for various climates, and  $h_0$  was 9.46 km [71]. It's important to note that there appears to be either a bug in the code or error in the documentation. The documentation describes the input as surface refractivity  $N_s$  but the SPLAT! code treats the input as  $N_0$  in order to calculate surface refractivity,  $N_s$ . This is important to note because it means that in some point-to-point analysis mode, parameters are treated as out-of-bounds when they fall within the guidelines.

This surface refractivity is experimentally measured at different frequencies and is summarized with contour maps for different regions in the world (see Figure 63 and Figure 64) [73, 74].

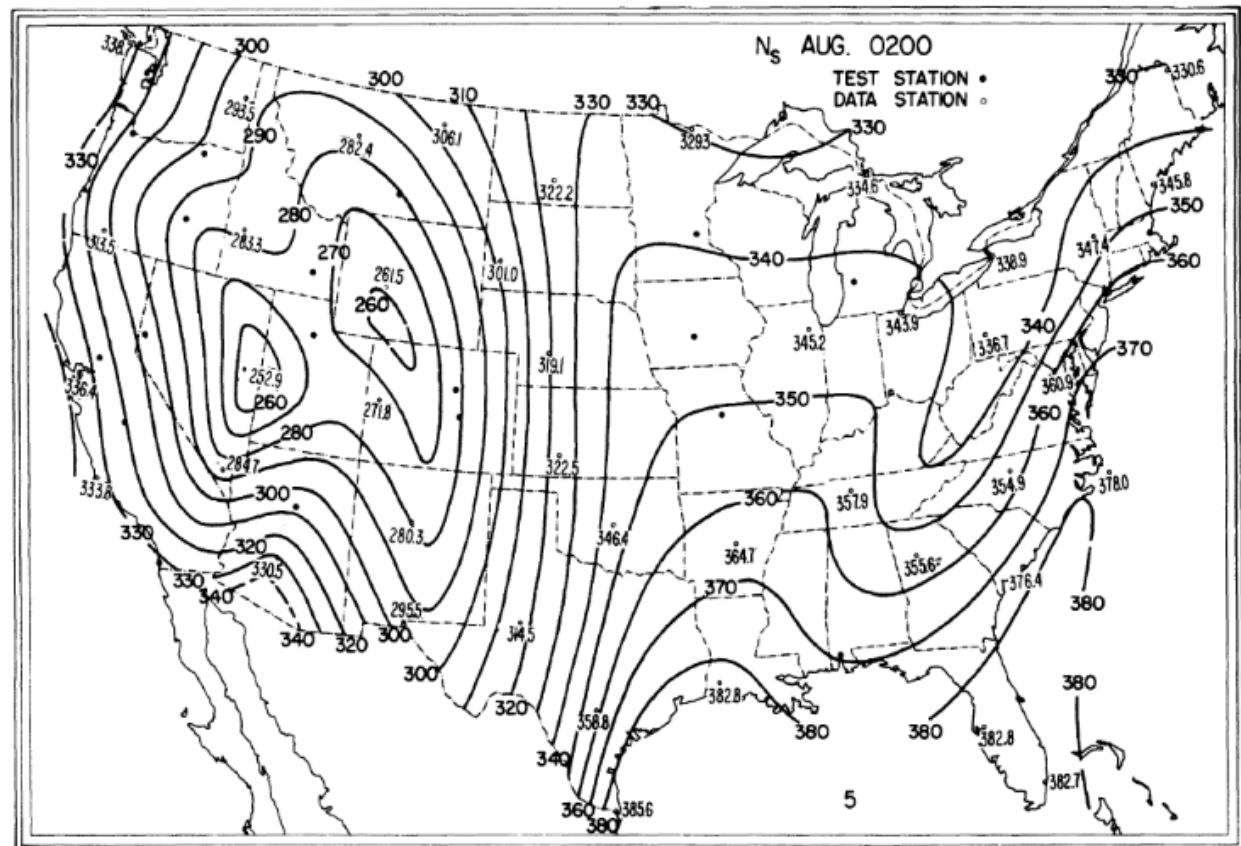


Figure 63: Surface Refractivity,  $N_s$  Mean August

Mean values of the measurement were also taken in February:

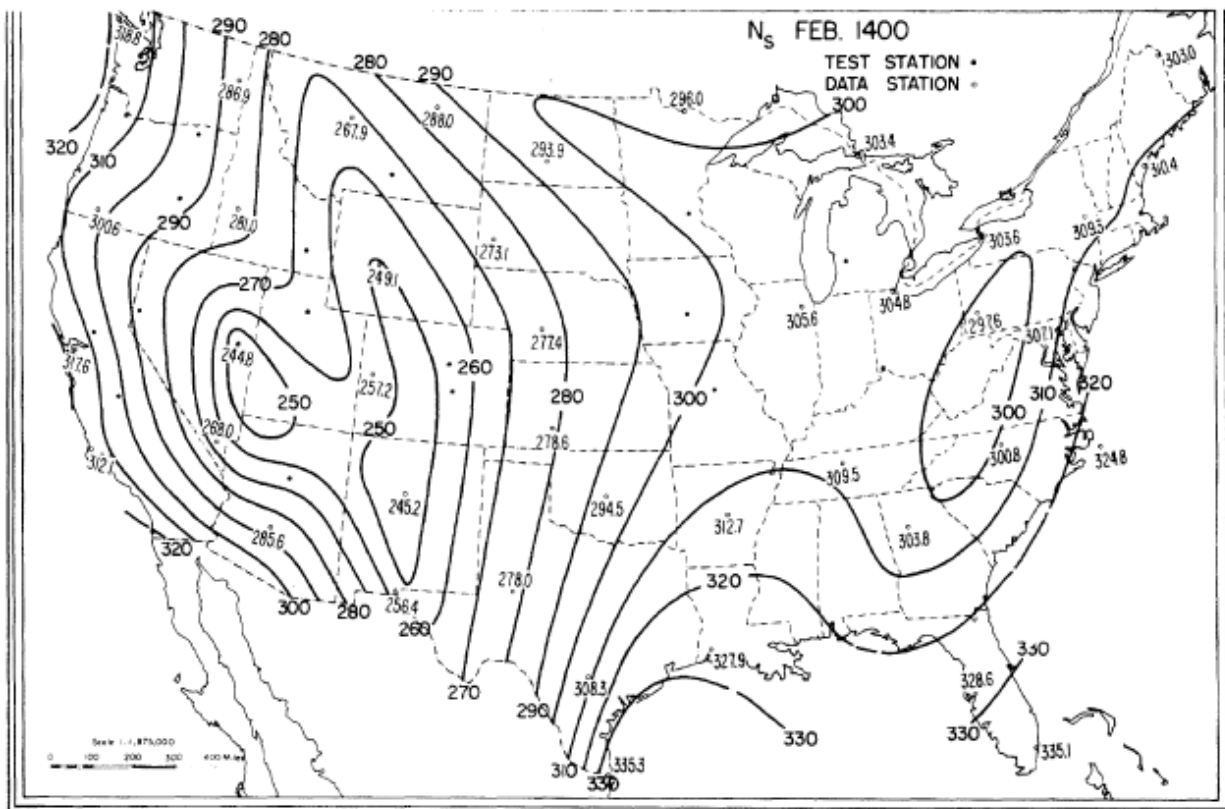


Figure 64: Surface Refractivity,  $N_s$  Mean February

The annual mean varies from 240 to 300 for semi-arid mountainous areas (Denver, Colorado; Colorado Springs, Colorado; Grand Junction, Colorado; Billings, Montana; Great Falls, Montana; Lander, Wyoming,) [72]. Since the PSD measurements were taken in summer months (July- August), the “semi-arid” parameters were chosen for testing. These parameters appear to be “coupled” so as to keep them consistent, and the Relative Permittivity, Earth Conductivity, Surface Refractivity and Radio Climate were chosen to match for Test 2 parameters. Test 1 parameters coupled only Relative Permittivity and Ground Conductivity. Table XIII summarizes the test parameters.

**Table XIII: SPLAT! Test Input Parameters**

Name	Control	Test 1	Test 2
Relative Permittivity, $\epsilon_r$	15.000	4.000	4.000
Ground Conductivity, $\sigma$	0.005	0.001	0.001
Surface Refractivity, $N_s$	301.000	301.00	280.00
Carrier Signal, $f_c$	Varies	Varies	Varies
Radio Climate	5	5	4
Polarization	1	1	1
Fraction of Situations, $z_s$	0.50	0.50	0.50
Fraction of time, $z_T$	0.50	0.50	0.50
<i>ERP</i>	Varies	Varies	Varies

The two statistical inputs are fraction of time,  $q_T$ , and fraction of situations,  $q_s$ . Fraction of time is considered to be a level of reliability, fraction of situations is considered to be a level of certainty. This criteria is denoted as  $F(z_t, z_l)$ . There is an additional statistical input, hard-coded into the SPLAT! program, which is called fraction of locations. In point-to-area mode the fraction of locations is hard-coded at  $q_L = 0.5$ . This work only implements point-to-point analysis.

### 5.2.2. ITM Algorithm

In order to discuss the statistical parameters, fraction of situations,  $z_s$  and fraction of time,  $z_T$  it is necessary to discuss the ITM algorithm. The model bases its path loss prediction on the energy scattered or deflected from the first obstruction along the path. The point-to-point analysis restricts the path to one azimuthal direction, and one elevation direction. The basic assumption is that this path is the ‘dominant’ one; the signal will propagate directly (LOS), diffract along the obstruction(s), or scatter due to the troposphere.

The ITM path loss equation is the combination of the free-space path loss, the attenuation due to terrain,  $A_{\text{ref}}$  and the quantile attenuation,  $A_q$  due to statistical variation over time.

$$P_{loss} = FSPL + A_{ref} + A_q \quad (50)$$

A profile of the elevations is created from the transmitter site and the receiver site. The path is scanned from obstacles by comparing the elevation angles of the LOS path to elevation angle to each point along the path. If the elevation angle to the points is greater than the elevation to the LOS path, there is an obstruction. Figure 65 depicts a double horizon path between the Tx and the Rx.

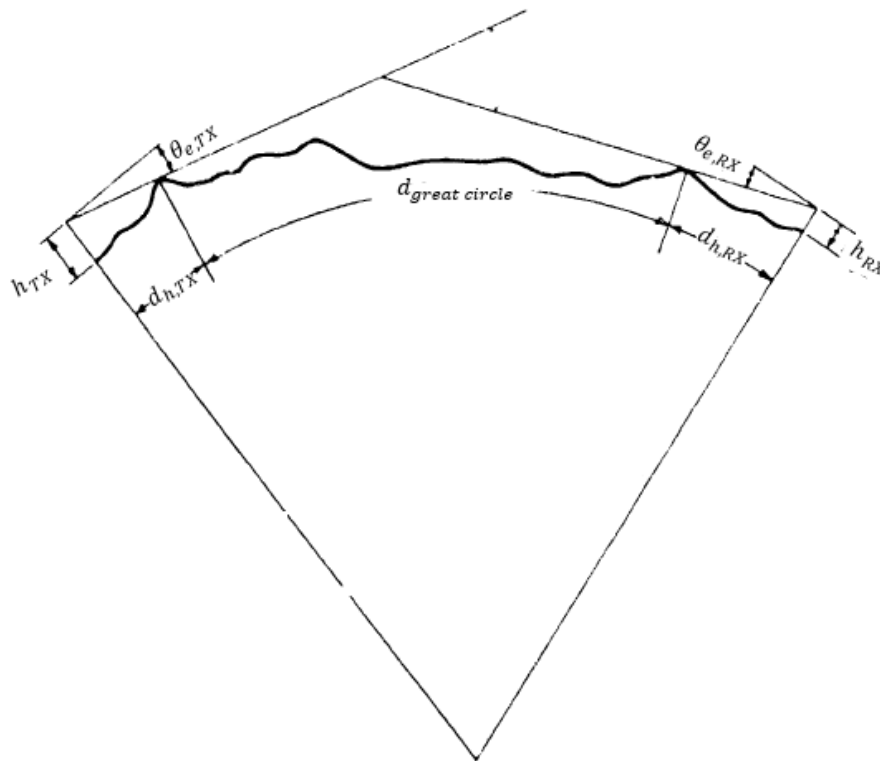


**Figure 65: Geometry of Double Horizon Path**

If the first obstruction along the path is the same for the Tx and Rx, they share the same horizon, then path is designated single horizon.

The free-space path loss is a function of the frequency and distance between the two sites. The great-circle distance is the shortest distance between two sites according to their latitude and longitude coordinates on the surface of earth.

$$FSPL = 20 \log_{10} \left( \frac{\lambda}{2\pi d} \right), d = d_{great\ circle} \quad (51)$$

Each propagation mode has its own  $A_{ref}$  calculation. ITM has three modes depending on the distance and obstruction(s) between the two sites. The aim of this model is to create a continuous path loss function as the distance between the receiver and transmitter increases.

Figure 66 depicts the reference attenuation,  $A_{ref}$  as it transitions from each propagation mode. The code will use  $max()$  or  $min()$  functions to keep a calculation within the desired range. Each mode has its own curve that it is fitting.

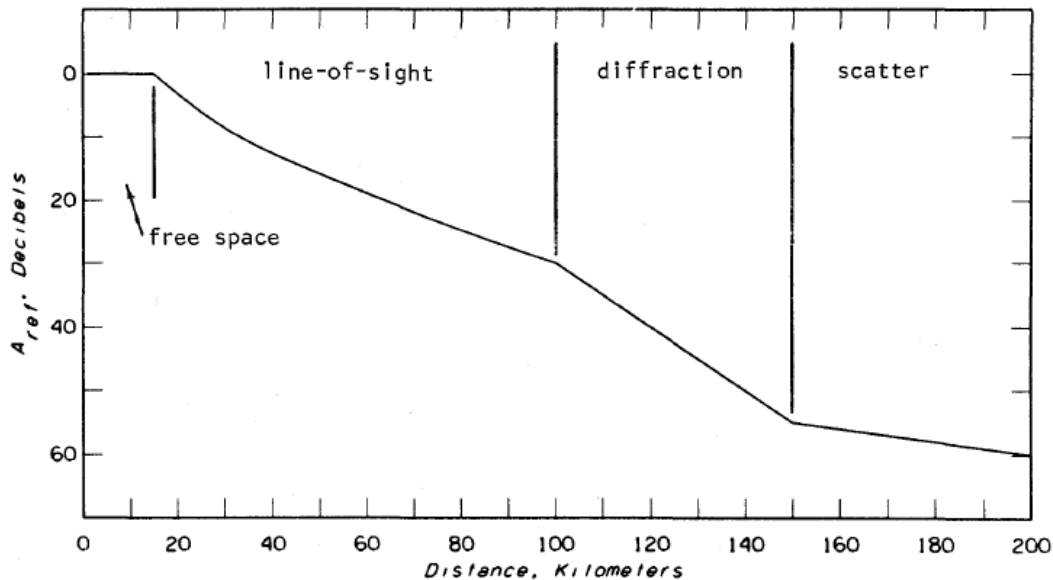


Figure 66: Typical Reference Attenuation

$$A_{ref} = \begin{cases} A_{LOS} & d \leq d_{LS} \\ A_{diffraction} & d_{LS} \leq d \leq d_x \\ A_{scatter} & d_x \leq d \end{cases} \quad (52)$$

ITM algorithm switches mode from LOS to diffraction if the distance between the two sites is greater than the sum of LOS horizons for each site.

$$d_{LS} = d_{horizon,TX} + d_{horizon,RX} \quad (53)$$

The threshold distance,  $d_x$  between the diffraction and troposcatter mode varies depending on the input parameters. For point-to-point test scenarios tested in mountainous terrain the distance threshold for troposcatter mode,  $d_x$ , is approximately 160 km, as determined from predictions in Table XVII on page 111.

Each antenna has its own distance to the horizon, which depends on the antenna height and the radius of the earth. The antenna height,  $h$ , is greatly exaggerated in Figure 67 [73].

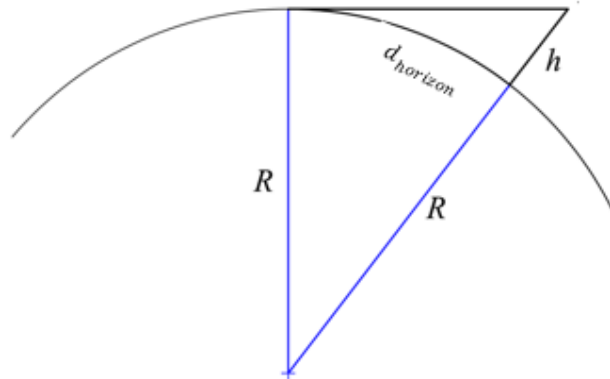


Figure 67: Horizon Distance

The greater the antenna height the greater horizon distance. When the LOS path hits an obstacle (i.e. the horizon), the attenuation increases because wave diffracts. The horizon distance is calculated using the following equation:

$$d_h = d_{horizon}[km] = \sqrt{\frac{2h_{antenna}[m]}{\gamma_e[km^{-1}]}} \quad (54)$$

where,  $\gamma_e$  is the curvature of the earth for a given atmosphere refractivity [71]. Note the horizon will change if there is an obstruction that occurs before the possible horizon.

To model the bending of the signal path as it passes through the Earth's atmosphere, the radius of the earth changes due to the surface refractivity,  $N_s$  [71]. This in turn changes the horizon distance.

$$\gamma_e = \gamma_a \left( 1 - 0.04665e^{\frac{N_s}{N_1}} \right) \quad (55)$$

where,  $\gamma_a$  is the inverse of the earth's radius (6,353 km). The inverse is scaled by  $1 \times 10^6$ , which results in  $157 \frac{N-units}{km}$ .  $N_1$  is some empirical constant, 179.3  $N - units$ .

There are many calculations in the algorithm and furthermore in the SPLAT! program that include hard-coded constants, for example  $N_1$  and 0.04655. While they may represent an unknown "theoretical" constant, it is unclear from the documentation. Other such unique values occur commonly in the code, they would preferably be replaced by named constants. This is the greatest barrier to understanding this specific empirical model. Since these formulas are designed to fit empirical measurements, it appears as though any given constant is chosen when it fits the measurements "best" for various scenarios.

The diffraction is assumed to be rounded-earth diffraction or knife-edge. The calculation for each type calculation is weighted differently based on empirical measurements [71]. Knife-edge occurs only when the elevation angle is steep and the obstacle is close to the station.

Troposcatter occurs when the signal reflects off the first layer of the atmosphere, the troposphere.



Other distance calculations include an immediate terrain distance,  $d_L$ , one for each station,  $d_{L,TX}$  and  $d_{L,RX}$  [71]. These distances define a range of interest between the Rx and Tx and the irregularity terrain parameter,  $\Delta h$ :

$$d_L = \min(15 h_{antenna}, 0.1 d_{horizon}) \quad (56)$$

Only the elevations along the path between these distances are used to determine the effective antenna heights [71]. These are fitted with a least square line and the elevations on the fitted line for the  $d_L$  of each station,  $h_{fit} = F(d_L)$ :

$$h_e = h_{effective} = h_{elevation} + (h_{elevation} - \min(h_{elevation}, h_{fit})) \quad (57)$$

Essentially, if the antenna is higher than the terrain along the path, the effective antenna height is raised. Otherwise, it is kept the same.

The elevation heights along the path between the Rx and Tx are used to determine the terrain irregularity parameter,  $\Delta h$ . At most twenty-five elevation heights between  $d_{L,RX}$  and  $d_{L,TX}$  are collected and fitted with a straight line. From this set, the inner-quartile of the elevations are found,  $\Delta h(d)$ . Then formula is applied to find the irregular terrain parameter:

$$\Delta h = \frac{\Delta h(d)}{\left(1 - 0.8 e^{-\min\left(20, \frac{d}{D} \times 10^4\right)}\right)} \quad (58)$$

where,  $D = d_{great\ circle} - (d_{L,TX} + d_{L,RX})$  and  $d_L$  is the immediate terrain distance for each antenna (see Equation 55) [71]. Lastly, the elevation angles from the Tx or Rx to the horizon is determined:

$$\theta_e = \theta_{elevation} = \frac{0.65 \Delta h \left( \frac{d_{LS}}{d_L} - 1 \right) - 2h_e}{d_{LS}} \quad (59)$$

where  $d_{LS}$  is the sum of the horizon distances for the Tx and Rx antenna, see Equation 52 [71].

To better understand the model, the curves for the reference attenuation,  $A_{ref}$ , when the irregular terrain parameter changes are presented in Figure 68. Each curve represents a distance between each Tx and Rx station. This is a test-case found in the ITS guide for the reference attenuation,  $A_{ref}$  as the irregular terrain parameter varies when  $f_c = 150 \text{ MHz}$ ,  $h_{TX} = 30 \text{ m}$  and  $h_{RX} = 2 \text{ m}$  [69]. Each curve represents a different distance:

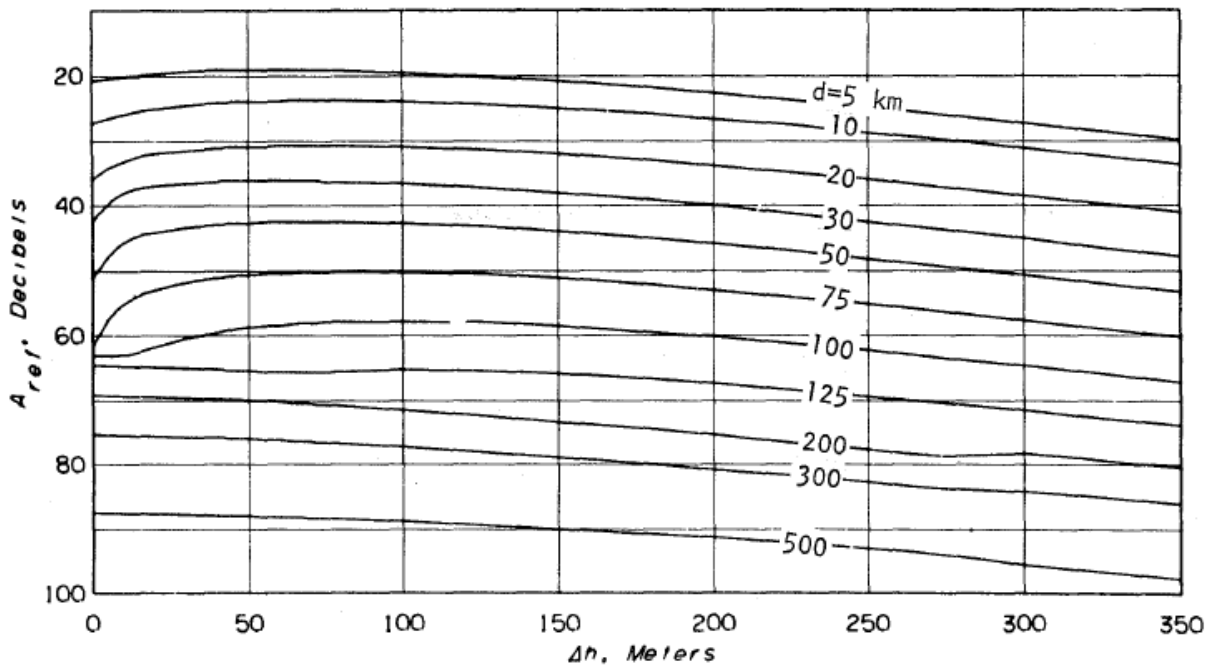


Figure 68: Reference Attenuation Test Case

The attenuation increases as the irregular terrain parameter increases, the same is true for the distance between the transmitter and receiver.

Here are the values of irregular terrain parameter for different types of terrain [69].

Average terrain has an irregular terrain parameter,  $\Delta h = 90 \text{ m}$ :

**Table XIV: Irregular Terrain Parameter for Various Terrains**

Terrain	$\Delta h$ (m)
Flat	0
Plains	30
Hills	90
Mountain	200
Rugged Mountains	500

Each propagation mode: LOS, diffraction and troposcatter, has its own formula that is summarized in the in the paper [71]. Many of these calculations include constants and relationships that were found empirically (as has already been seen).

Any deviation from the reference attenuation,  $A_{ref}$  is handled by the quantile attenuation,  $A_q$ . The quantile attenuation,  $A_q$  is determined by the statistical inputs. It is assumed that there is variation of the measurements over time, in confidence (called situation) and by location:

$$A_q = A(q_T, q_S, q_L) \quad (60)$$

The quantile attenuation,  $A_q$ , result in point-to-point mode is interpreted as follows:

“With probability (or confidence)  $q_S$  the attenuation will not exceed  $A_q$  for at least  $q_T$  of the time.” [71]

These fractions are scaled by the inverse of the complementary normal distribution function. In area prediction mode the  $A_q$  result is to be interpreted as follows:

“In  $q_S$  of the situations there will be at least  $q_L$  locations where the attenuation does not exceed  $A_q$  for at least  $q_T$  of the time.” [71]

It’s difficult to interpret the results since,  $A_q$  is not returned by the program, therefore the parameters are set to 0.5 for each quantile to find the median attenuation. This quantile attenuation attempts to quantify the distribution of the measurements.

To better clarify quantile attenuation,  $A_q$ , the ITS guide includes a channel test case of measurements and predictions as pictured in Figure 69 [69]. This should give an idea of the accuracy, as it appears that by altering the fractions, one may get around 20 dB difference in attenuation. These quantile deviations are due to channel fading, which can be seasonal, but is primarily due to multipath propagation.

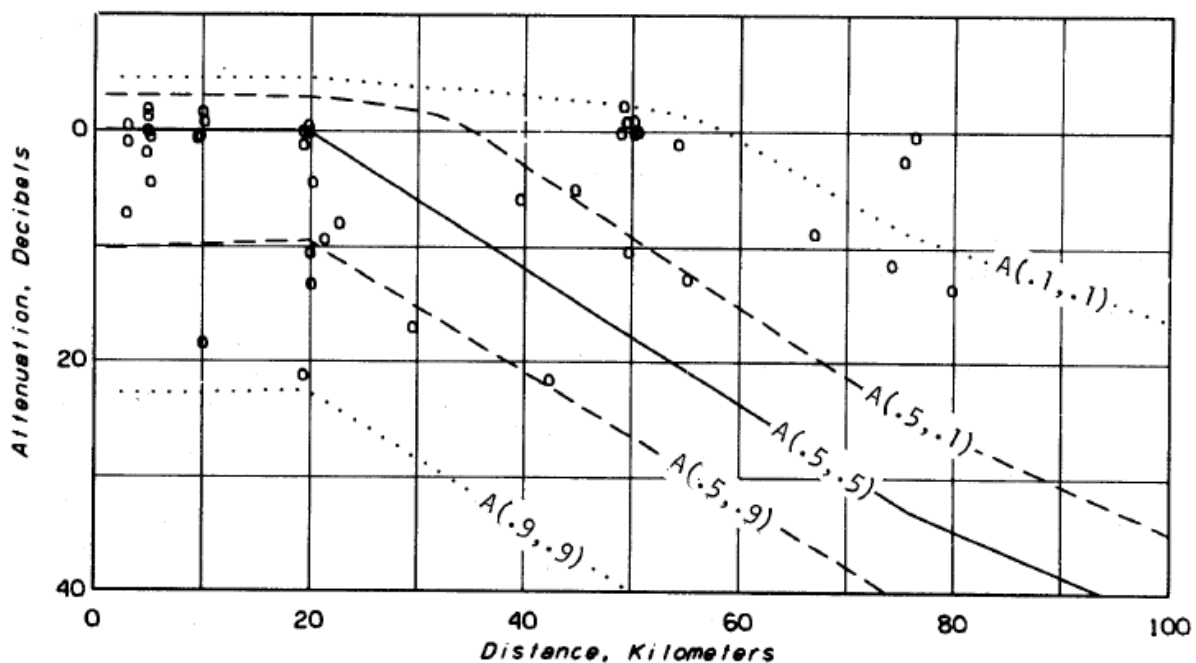


Figure 69: Test Case for Quantile Attenuation

Each fraction is scaled by the inverse of the complementary normal distribution function,

$$Q(z) = \frac{1}{\sqrt{2\pi}} \int_z^{\infty} e^{-\frac{u^2}{2}} du \rightarrow z = Q^{-1}(q) \quad (61)$$

Each quantile is scaled to be a deviate,  $z$ :

$$z_T = z(q_T) = Q^{-1}(q_T), \quad z_L = z(q_L) = Q^{-1}(q_L), \quad z_S = z(q_S) = Q^{-1}(q_S) \quad (62)$$

Each deviate is used to determine the additional attenuation:

$$A_q = \begin{cases} A' & \text{if } A' \geq 0 \\ A' \frac{(29 - A')}{(29 - 10A')} & \text{otherwise} \end{cases} \quad (63)$$

where,

$$A' = A_{ref} - A_{median} - Y_T - Y_L - Y_S \quad (63)$$

The median attenuation,  $A_{median}$  is determined by climate, and an obscure value called the effective distance that is determined from the antenna height and wave number. Both time and location deviations,  $Y_T$  and  $Y_L$  are determined by  $z_T$  and  $z_L$  respectively. However, the situation deviation is determined by all three:  $z_T$ ,  $z_L$ , and  $z_S$ . The weights and variables appear to have been chosen to fit the lines on Figure 69.

### 5.2.3. Propagation Mode Case Studies

For reference, LOS, diffraction dominant, and troposcatter dominant views of the elevation and path loss predictions will be provided for ITM HD files (generated from SRTM1 elevation profiles). For each path, the Rx is the antenna located on the Museum Building at Montana Tech. The TV characteristics are summarized in Table XV.

**Table XV: Propagation Mode Case Studies**

Call Sign	City	Distance (km)	Propagation mode
K43DU-D	Butte	8.90	LOS
K49KA-D	Whitehall	39.28	Diffraction
KTMF	Missoula	158.09	Troposcatter

The LOS path is from a transmitter located on the East Ridge, K43DU-D. Figure 70 depicts the elevation profile between the Rx and the Tx. Figure 71 depicts the path loss between the Tx and Rx. Note that the distance between is in meters, however 0 km is the Rx in the former and 0 km is the Tx in the latter.

The discontinuity occurs at the Berkeley Pit (~5.75 km from the Rx), where the ground elevation decreases. This increases the path loss by approximately 70 dB. The other variation occurs at the steepest slant between 6 and 8 km from the Rx (1.5 km from the Tx). The author suspects that this illustrates the two-types of diffraction, knife-edge and rounded-earth. It appears that the attenuation due to knife-edge diffraction is less dramatic.

For a visual aid, SPLAT! adds a First Fresnel zone and 60% of the First Fresnel zone to the LOS path. The Fresnel zone is an ellipse created about the LOS path, if an obstruction occurs within the First Fresnel zone, the signal is said to be greatly attenuated.

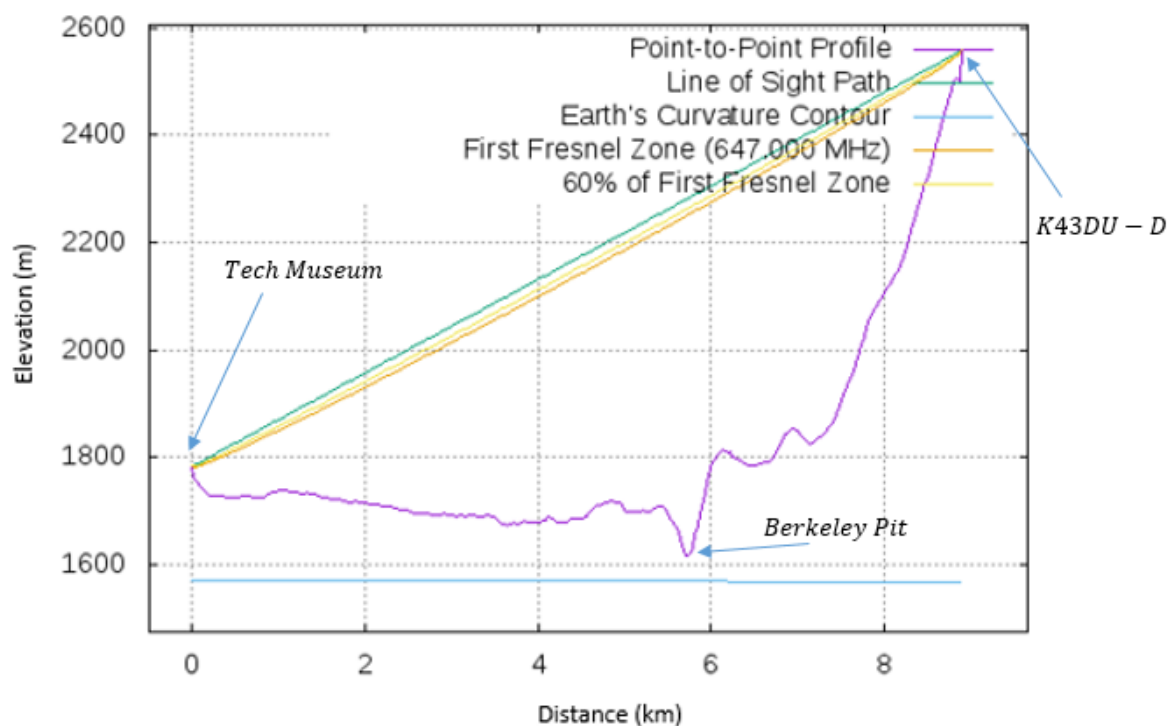
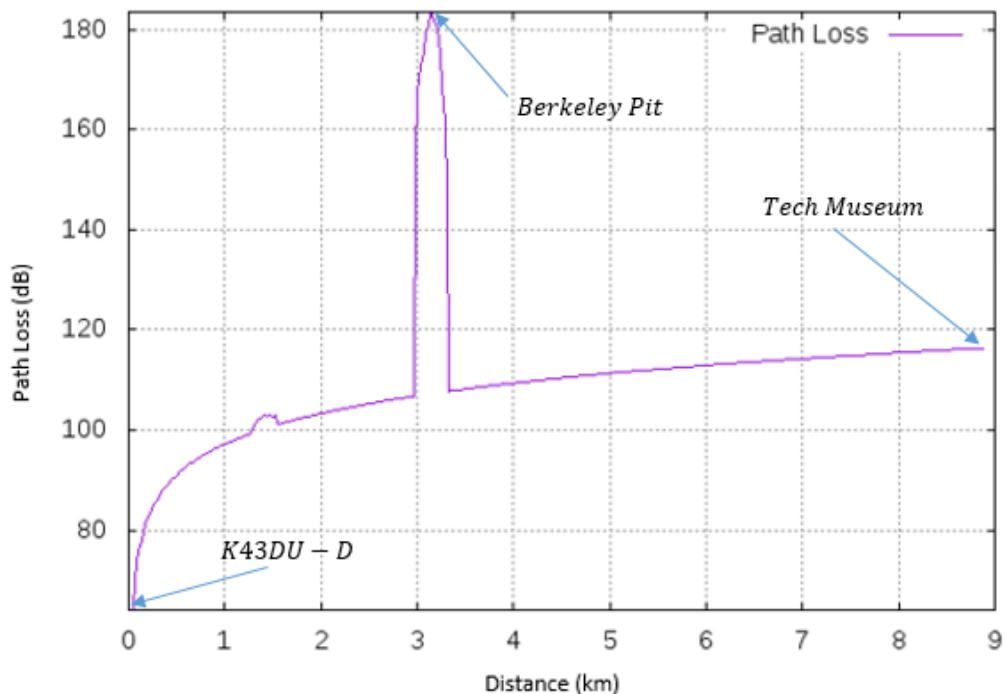


Figure 70: LOS Terrain Profile from Tech-Museum to K43DU-D



**Figure 71: LOS Path Loss from K43DU-D to Montana Tech Museum**

The Tx (K49KA-D), of the diffraction dominant path is located in Whitehall, Montana. The continental divide separates the Rx and Tx. Figure 72 depicts the terrain profile, Figure 73 depicts the path loss. As the signal traverses the terrain from the Tx to the Peak 1, the propagation mode goes from LOS to diffraction dominant. Once the signal hits the tallest peak, Peak 1, the mode switches to diffraction dominant and the path loss increases more than 60 dB. After Peak 2, the attenuation increases by another 20 dB.

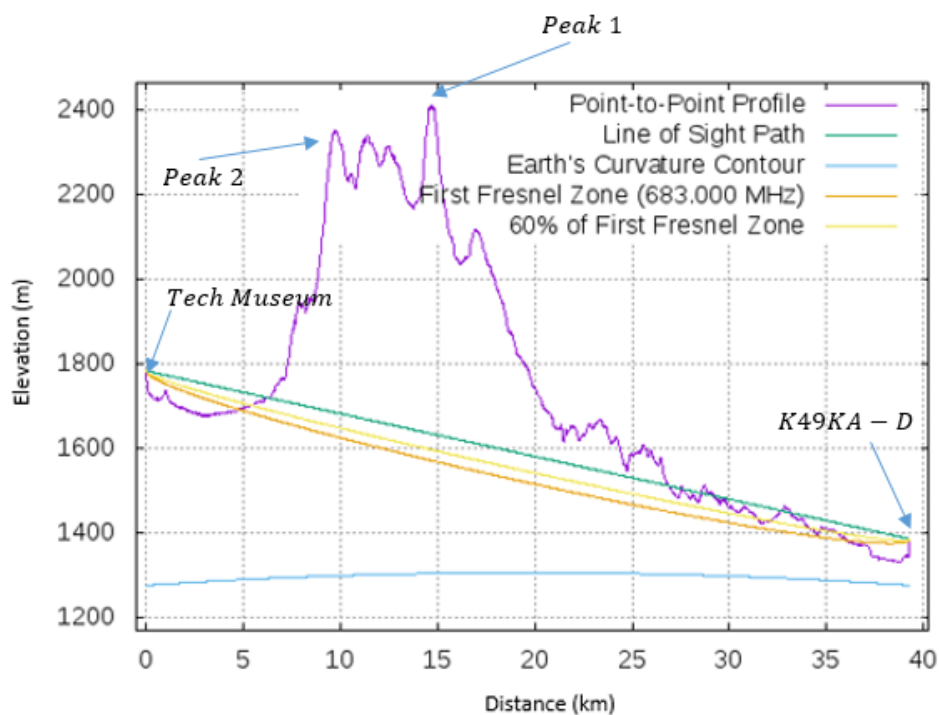


Figure 72: Diffraction Dominant Terrain Profile from Montana Tech Museum to K49KA-D

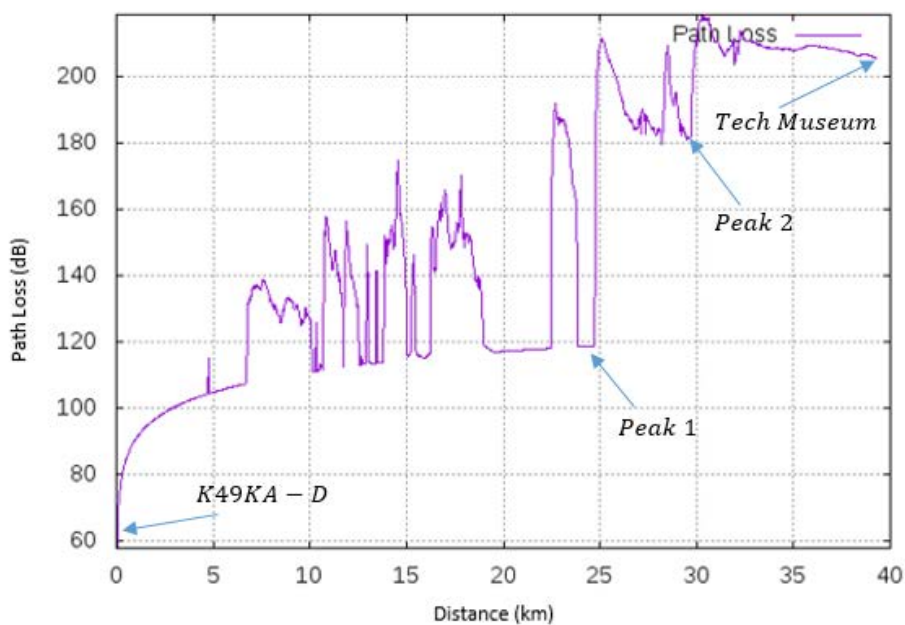
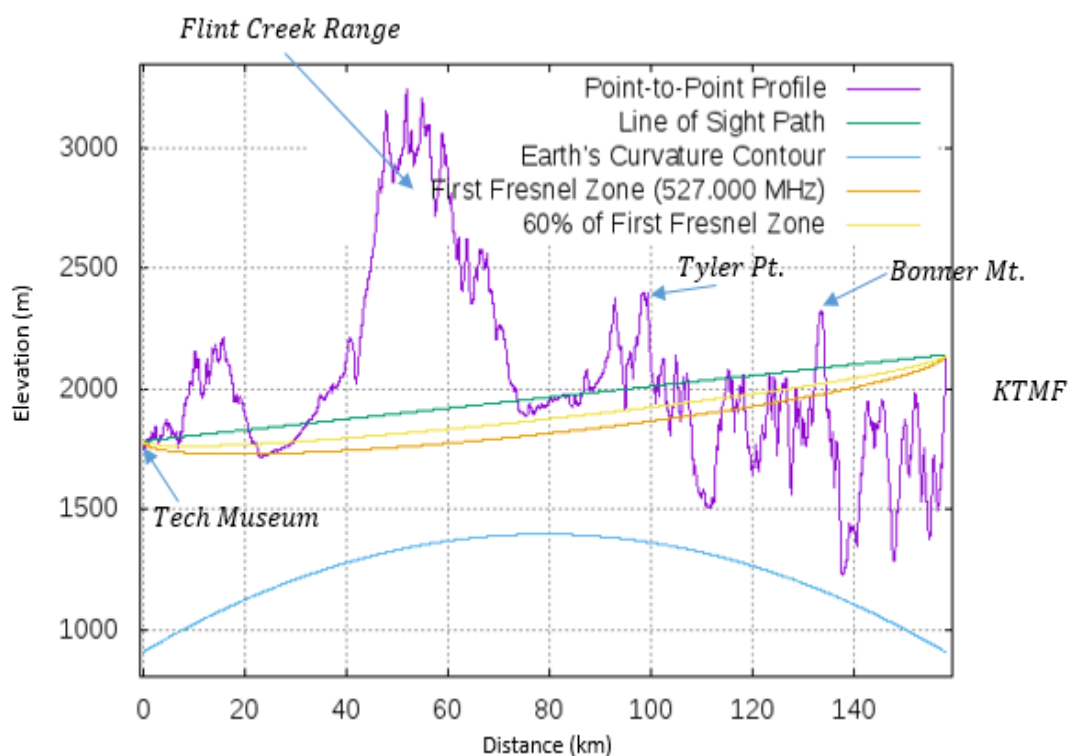


Figure 73: SPLAT! Diffraction Dominant Path Loss from K49KA-D to Montana Tech Museum



This troposcatter dominant path spans 158.09 km from the Rx to the Tx, KTMF near Missoula, Montana. The tall peaks in Figure 74 are the mountains southwest of Deer Lodge, Flint Creek Range. Figure 75 depicts the path loss from KTMF to Montana Tech Museum.



**Figure 74: SPLAT! Troposcatter Dominant Terrain Profile from Montana Tech Museum to KTMF**

The various curves that the path loss is made to fit appear as the elevations increase and decrease about the various peaks. The propagated mode for Bonner Mountain and the peaks of the Flint Creek Range are LOS. The propagation mode switches from LOS to diffraction-dominant mode as it traces the peaks. The propagation mode at Tyler Point is diffraction-dominant, until it switches to troposcatter around 150 km from the Tx.

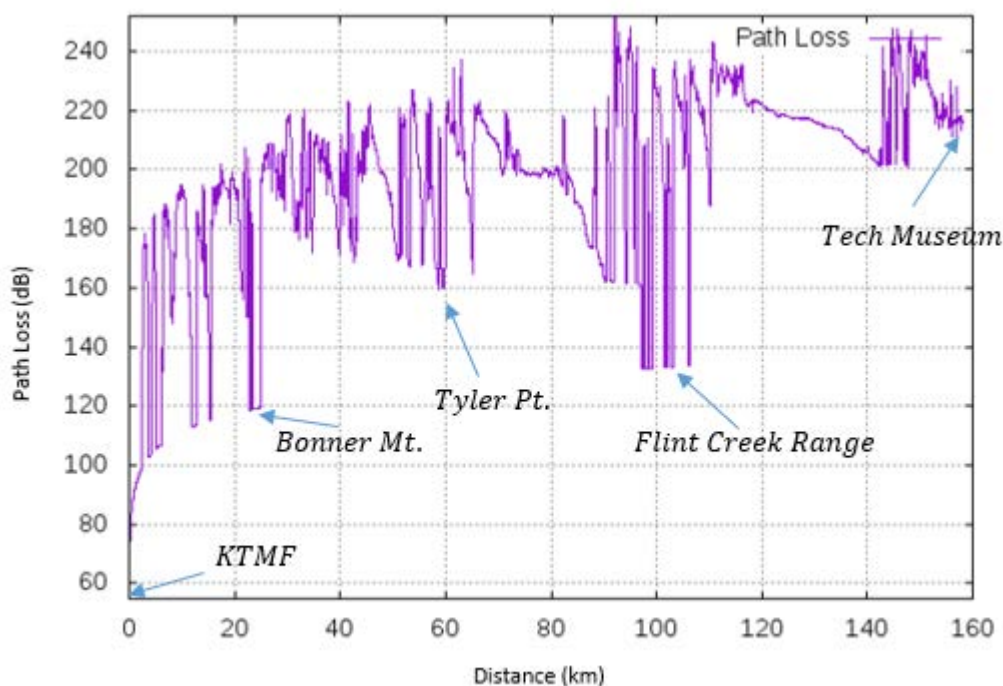


**Figure 75: SPLAT! Troposcatter Dominant Terrain Profile from KTMF to Montana Tech Museum**

### 5.3. Results

#### 5.3.1. SPLAT! Irregular Terrain Parameter Calibration

The path loss results are summarized in Table XVI for each input parameter set. For the majority of locations, the path loss results for each input parameter set are consistent with each other. However, there are several notable exceptions.

The TV stations with difference greater than 2 dB are KBGF-LD, K20KQ-D, KUGF-TV, KSKC-CD, and KTGF. K20KQ appears to be an edge case between diffraction-dominant and troposcatter-dominant, which may explain the large difference (14 - 15 dB) between ITM HD control parameters and the other path loss predictions. The mode of propagation for the rest of these TV stations is troposcatter-dominant. Signals that propagate in troposcatter-dominant mode appear to be more influenced by the irregular terrain parameters, these are also most difficult to verify.

Table XVI: Path Loss Predictions

Station	Distance (km)	Predicted Path Loss (dB)					
		ITM HD			ITM non-HD		
		Control	Test1	Test 2	Control	Test	Test 2
K17KB-D	108.24	200.52	200.61	201.62	201.2	201.29	202.1
KWYB	8.91	105.43	105.43	105.46	105.39	105.39	105.42
KBGF-LD	196.47	216.02	216.12	222.44	217.48	217.59	224.42
K20KQ-D	162.52	205.3	205.4	220.47	219.18	219.27	220.95
KUGF-TV	195.35	217.16	217.26	223.79	217.35	217.47	224.66
KHBB-LD	93.85	204.81	204.91	205.94	207.5	207.6	208.65
KTMF	158.09	204.11	204.18	206.18	203.79	203.87	205.98
K26DE-D	108.24	201.66	201.74	202.54	202.12	202.2	203.03
K27CD-D	41.61	197.81	197.91	198.72	198.16	198.26	199.08
KSKC-CD	235.22	223.16	223.26	229.43	225.34	225.45	231.93
KWYB-LD	136.16	203.46	203.55	204.69	204.51	204.61	205.76
KUHM-TV	111.7	197.87	197.93	198.98	200.61	200.68	201.73
K31KR-D	80.36	195.17	195.25	196.14	195.83	195.91	196.77
K39JC-D	2.60	96.52	96.52	96.53	96.35	96.35	96.36
K40HL-D	42.63	187.79	187.62	188.25	188.13	187.96	188.59
KDBZ-D	136.16	206.37	206.46	207.57	207.37	207.47	208.59
K43DU-D	8.90	107.62	107.62	107.64	107.58	107.58	107.6
K44JW-D	80.35	198.8	198.88	199.73	200.08	200.16	200.98
KTGF	199.54	226.46	226.58	231.96	226.01	226.12	231.62
K48LV-D	80.35	199.77	199.85	200.69	201.03	201.11	201.93
K48MM-D	107.61	164.34	164.38	165.17	165.53	165.57	166.38
K49KA-D	39.28	202.28	202.37	203.01	202.54	202.64	203.29
K49EH-D	93.79	211.46	211.56	212.57	211.81	211.91	212.92

Test 1 and the default parameters return similar results, within a 1 dB of each other; therefore, the relative permittivity,  $\epsilon_r$  and ground conductivity,  $\sigma$  appear to have little effect on the algorithm. Test 2 input parameters appear to have an effect when the propagation mode is

troposcatter-dominant; other LOS and diffraction-dominant path loss results are within 2 dB of the other predictions.

The propagation mode for each station and test parameter is summarized in Table XVII. The difference in path loss between each mode is instructive, since it gives a general sense of propagation in a mountainous terrain. For the default parameters and HD, i.e. SRTM1 elevation files, the troposcatter dominant propagation have path loss predictions that range from 150 to 235 dB. The diffraction dominant range is from 164 dB to 204 dB. The LOS path loss predictions vary from 96 to 107 dB.

The discontinuity between LOS and diffraction mode is most drastic. Once the mode of propagation is no longer LOS, the path loss increases by at least 50 dB, which means that the signal is 100,000 times smaller. The difference can be as much as 80 dB, which is 100 million times smaller. It can even be 100 dB, which is 10 billion times smaller. These trends may be seen in the reference figures (Figs. 70 to 75) where the path loss across the distance from the TV station to the Montana Tech Museum is shown.

For both sets of input parameters, Control and Test, there is little difference between ITM HD and ITM non-HD. K20KQ is an exception for reasons discussed previously. In order to save computation time, it appears as though it is acceptable to substitute ITM non-HD for ITM HD.

The path loss prediction for the population grids implemented ITM non-HD elevation files:

Table XVII: Input Parameters Propagation Type

Station	Distance (km)	Predicted Path Loss (dB)					
		ITM HD			ITM non-HD		
		Control	Test1	Test 2	Control	Test	Test 2
K17KB-D	108.24	Double Horizon, Diffraction Dominant					
KWYB	8.91	Line-Of-Sight Mode					
KBGF-LD	196.47	Double Horizon, Troposcatter Dominant					
K20KQ-D	162.52	Double Horizon, Diffraction Dominant		Double Horizon, Troposcatter Dominant			
KUGF-TV	195.35	Double Horizon, Troposcatter Dominant					
KHBB-LD	93.85	Double Horizon, Diffraction Dominant					
KTMF	158.09	Double Horizon, Troposcatter Dominant					
K26DE-D	108.24	Double Horizon, Diffraction Dominant					
K27CD-D	41.61	Double Horizon, Diffraction Dominant					
KSKC-CD	235.22	Double Horizon, Troposcatter Dominant					
KWYB-LD	136.16	Double Horizon, Diffraction Dominant			Single Horizon, Diffraction Dominant		
KUHM-TV	111.7	Double Horizon, Diffraction Dominant					
K31KR-D	80.36	Single Horizon, Diffraction Dominant					
K39JC-D	2.60	Line-Of-Sight Mode					
K40HL-D	42.63	Single Horizon, Diffraction Dominant					
KDBZ-D	136.16	Double Horizon, Diffraction Dominant			Single Horizon, Diffraction Dominant		
K43DU-D	8.90	Line-Of-Sight Mode					
K44JW-D	80.35	Single Horizon, Diffraction Dominant					
KTGF	199.54	Double Horizon, Troposcatter Dominant					
K48LV-D	80.35	Single Horizon, Diffraction Dominant					
K48MM-D	107.61	Double Horizon, Diffraction Dominant					
K49KA-D	39.28	Double Horizon, Diffraction Dominant					
K49EH-D	93.79	Double Horizon, Diffraction Dominant					

Lastly, the warning codes will be discussed; their descriptions are pictured in Figure 76.

```

errnum: 0- No Error.
1- Warning: Some parameters are nearly out of range.
           Results should be used with caution.
2- Note: Default parameters have been substituted for
           impossible ones.
3- Warning: A combination of parameters is out of range.
           Results are probably invalid.
4- Warning: Some parameters are out of range.
           Results are probably invalid.

```

**Figure 76: SPLAT! ITM Computation Warnings**

The two warning that are returned are numbered 3 and 4. A warning with a lower value will be overwritten by a warning with a larger value. The warning code are listed in Table XVIII.

When the Surface Refractivity,  $N_s$  is below 301 N-units, SPLAT! returns a warning of 4. It appears as though K27CD-D, K40HL-D, K49KA-D and K49EH-D all return warnings because of  $N_s$  parameter calculation. When the calculations are checked by hand, it does not appear as though it is the  $N_s$  directly or even the inverse of the relative earth radius,  $\gamma_e$ , so it's likely that all warning 4 are due to a bug.

The warning number 3 is due to either the grazing angle, the relative size of the immediate antenna distance,  $d_L$ , or the sum of the horizon distances,  $d_{LS}$ . The limit on the sum of horizon distance is 10,000 km, therefore, the warning 3 is likely due to the grazing angle or the immediate antenna distance.

Table XVIII: Input Parameters Warning Code

Station	Distance (km)	Predicted Path Loss (dB)					
		ITM HD			ITM non-HD		
		Control	Test1	Test 2	Control	Test	Test 2
K17KB-D	108.24	0	0	4	0	0	4
KWYB	8.91	0	0	4	0	0	4
KBGF-LD	196.47	0	0	4	0	0	4
K20KQ-D	162.52	0	0	4	0	0	4
KUGF-TV	195.35	0	0	4	0	0	4
KHBB-LD	93.85	3	3	4	3	3	4
KTMF	158.09	0	0	4	0	0	4
K26DE-D	108.24	0	0	4	0	0	4
K27CD-D	41.61	4	4	4	4	4	4
KSKC-CD	235.22	3	3	4	0	0	4
KWYB-LD	136.16	0	0	4	0	0	4
KUHM-TV	111.7	0	0	4	0	0	4
K31KR-D	80.36	0	0	4	0	0	4
K39JC-D	2.60	0	0	4	0	0	4
K40HL-D	42.63	4	4	4	4	4	4
KDBZ-D	136.16	0	0	4	0	0	4
K43DU-D	8.90	0	0	4	0	0	4
K44JW-D	80.35	0	0	4	0	0	4
KTGF	199.54	3	3	4	3	3	4
K48LV-D	80.35	0	0	4	0	0	4
K48MM-D	107.61	3	3	4	3	3	4
K49KA-D	39.28	4	4	4	4	4	4
K49EH-D	93.79	4	4	4	4	4	4

KSKC returns a warning 3 for ITM HD, but not ITM non-HD, but the difference between the two predictions is less than 1 dB. These warnings are mostly likely caused by the position of

the antenna to the 1<sup>st</sup> obstruction, since the input parameters are within the guidelines and the terrain is the only parameter that varies.

The terrain profile of K48MM-D, located near Anaconda, MT is pictured in Figure 77. Note the 1<sup>st</sup> obstruction from the TV station is within 5 km. The scenario is similar with KSKC and KTGF.

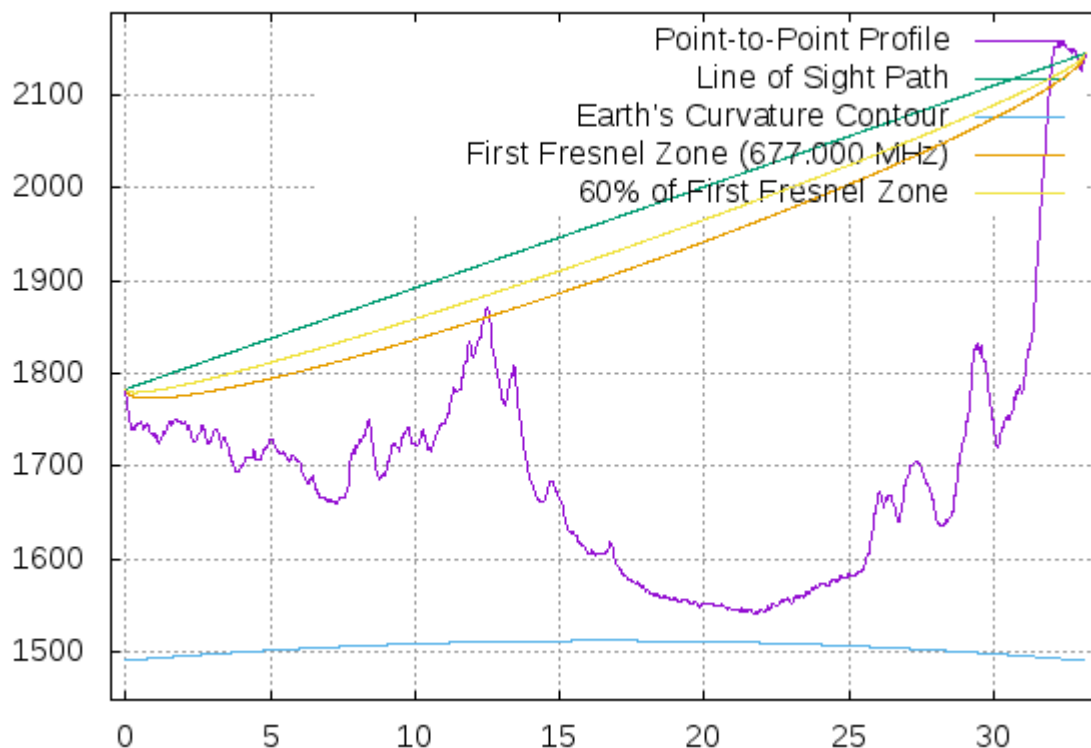


**Figure 77: K48MM-D Terrain Profile**

In order to heed the advice of the creators of the ITM algorithm and SPLAT!, only the default parameters and ITM non-HD will be used for the rest of this work. For most of these test cases the input parameters have little effect. The propagation mode, which is determined by the distance between each antenna and the distance to the horizon (1<sup>st</sup> obstruction) has the largest effect.



### 5.3.2. ITM Predictions Compared to Measurements

These path loss predictions for each channel are compared to the measurement results in several ways. In order to compare the predicted channel power,  $P_{Rx,itm}$ , the PSD measurement results must be analyzed. First the channel power for each sweep is determined. This is found by converting the PSD measurement from units of  $\frac{dBm}{HZ}$  to units of  $\frac{dBm}{RBW}$ .

$$PSD \left[ \frac{dBm}{RBW} \right] = PSD \left[ \frac{dBm}{HZ} \right] + 10 \log_{10}(RBW) \quad (64)$$

Then the PSD measurements for each frequency bin in the channel are converted to linear values (voltage or power) and summed. The result is then converted back to decibel.

$$P_{rx} = P_{channel}[mW] = \sum PSD_{linear}(f) \left[ \frac{mW}{RBW} \right] \rightarrow P_{rx}[dBm] = 10 \log_{10} P_{rx}[mW] \quad (65)$$

The average RMS power is determined by summing the linear channel power of each sweep and finding the mean. The linear average result is then converted to decibel. The average RMS channel power is also found for the noise-only measurements. If the channel power is below the noise level, it can be assumed that the signal was not measured.

Since the data set is large and the actual maximum power values that occur infrequently may skew the data, the peak power is found only after “smoothing” the data. A moving window (of 10 samples) is applied to each frequency bin in the channel, and the widowed RMS voltage for each frequency bin in the channel is found for the whole data set. A computationally fast way to complete this task is to convolve the voltage of each frequency bin with a window, which is  $n$  samples long and each value is  $\frac{1}{n}$  as pictured in Figure 78 below:

```
def window_rms(v_lin, window_size):
    p_lin = np.power(v_lin,2)
    window = np.ones(window_size)/float(window_size)
    return np.sqrt(np.convolve(p_lin, window, 'valid'))
```

**Figure 78: RMS Smoothing of Channel Power**

After windowing the smooth power values for each frequency bin in the channel, they are summed to find the channel power. Then maximum channel power is found for the whole data set. The Peak to Average Power Ratio (PAPR) is the ratio of this “smoothed” Peak Power to the average RMS channel power:

$$PAPR = \frac{P_{peak}}{P_{rms}} \quad (66)$$

The channel power results are summarized in Table XIX. The average channel power of K43DU-D is within 7 dB of the predicted channel power. KWYB is 16 dB difference, this difference may be due to the fact that Tx is not fully operational even at the lower power level. Recall that this KWYB will be tested at two power levels, 110.7 kW and 46 kW. Furthermore, the trees in front of the Museum building may add some attenuation.

The “smoothed” maximum power values are closer to the prediction than the average power values. This windowing is a type of averaging, when the window size is increased the smooth values approached the averaged values.

Table XIX: Channel Power at Montana Tech Museum

Station	Predicted [dBm]		Measured				
	ITM HD Default	ITM non- HD Default	Ave. Noise Channel Power [dBm]	Occupancy	$P_{rms}$ [dBm]	Smooth $P_{peak}$ [dBm]	PAPR
K17KB-D	-138	-139	-80				
KWYB	-33	-33	-75	99.98%	-49	-34	15
KBGF-LD	-144	-145	-75				
K20KQ-D	-168	-182	-77				
KUGF-TV	-141	-142	-75				
KHBB-LD	-138	-140	-75				
KTMF	-127	-126	-78				
K26DE-D	-133	-134	-77				
K27CD-D	-144	-144	-76				
KSKC-CD	-159	-161	-76				
KWYB-LD	-131	-132	-75				
KUHM-TV	-131	-134	-77				
K31KR-D	-133	-134	-79				
K39JC-D	-39	-39	-78	63.37%	-78	-40	38
K40HL-D	-129	-129	-77				
KDBZ-D	-133	-134	-79				
K43DU-D	-48	-48	-82	100.00%	-55	-52	3
K44JW-D	-137	-138	-80				
KTGF	-167	-167	-80				
K48LV-D	-138	-139	-75				
K48MM-D	-133	-134	-75				
K49KA-D	-147	-147	-80				
K49EH-D	-145	-145	-80				

Only signals that are LOS are able to be received by antenna at the Montana Tech Museum building. According to SPLAT!, the stations as close as Whitehall (around ~40 km distance from Butte), K40HL-D and K49KA, and Anaconda, K48MM-D are essentially blocked by the mountainous terrain. The attenuation increases dramatically when the signal propagates as diffraction dominant. Any signal that propagates in troposcatter-dominant mode would be difficult to verify, since it would require sensitivity at the receiver well below the noise floor.

It should be noted that the harmonic signal at 625 MHz is located in K39JC-D channel. It is likely that K39JC-D transmitter is licensed but not operational or operates only occasionally.

These predicted channel characteristics are positive from an interference point-of-view. The transmitters that are co-channel and separated by any mountainous terrain are less likely to interfere with each other. However, from a propagation point of view, a cellular network in mountainous terrain would require a higher number of base stations than a cellular network in flat terrain.

### **5.3.3. Interference Simulations**

The path loss predictions were used to predict co-channel and adjacent channel interference. Montana Tech was granted an experimental license to transmit from 510 to 550 MHz at ERP 20 W as station, WK9XUC. The SPLAT! ITM non-HD with default parameters was used to predict path loss for each city grid from WK9XUC and from any TV station nearby that transmits in the 500 MHz band. The path loss predictions were used to predict the receive power of the TV station (desired signal) and the receive power of the WK9XUC (interference signal).

Once these figures are calculated, the EVM for each location is determined. A baseline EVM was determined for the TV station and the EIRP of each Rx site on the grid. The baseline error is due only to noise. Assuming that a TV receiver system is designed to handle a maximum EVM of 5%, then any location on the grid where the noise error causes the EVM to exceed 5% is considered to be in a poor receiver location. As a result, any additional interference from WKXUC is inconsequential.

Only TV stations that operate from 470 to 560 MHz and are expected to be received at any grid location will be included in this analysis. There are two TV channels that fit these criteria, KQYB in Butte and K27CD-D in Boulder.

Contours are made with Matplotlib functions, *griddata()* from the mlab module and *contourf()* [74]. The python script may be seen in Figure 79. First the Rx coordinates and the EVM are mapped to a grid with *griddata()*. The interpolation of the EVM between Rx points is called natural neighbor, based on the Delaunay triangulation [75]. This method creates triangles between the longitude and latitude points, loni and lati, then places weights on the gridded EVM. Note to operate the features of the Matplotlib toolkit, Natgrid must be installed [76].

*contourf()* fills in the contours for each contour level based on the number of levels as defined by the user. Here the color bar has an upper limit of 5% and lower limit of 0%. Anything above 5% will have same color, anything below 0% will be left blank, since only the upper limit 'max' end is extended.

```

# define grid
delta_d=0.0100
loni=linspace(W,E,num_sites*2)
lati=linspace(S,N,num_sites*2)

# EVM SNR *****
plt.figure(figsize=(8.0, 5.0))
grid_EVM=griddata(Rx_x,R_xy,EVM,loni,lati,interp='nn')

EVM_max=0.05
EVM_ulim=EVM_max*100
EVM_llim=0
extend='max'
levels=np.linspace(EVM_llim,EVM_ulim,(EVM_ulim-EVM_llim)*10+1)

CS=plt.contourf(loni,lati,grid_EVM,
                vmax=EVM_ulim,vmin=EVM_llim,extend=extend,levels=levels)
clb=plt.colorbar()

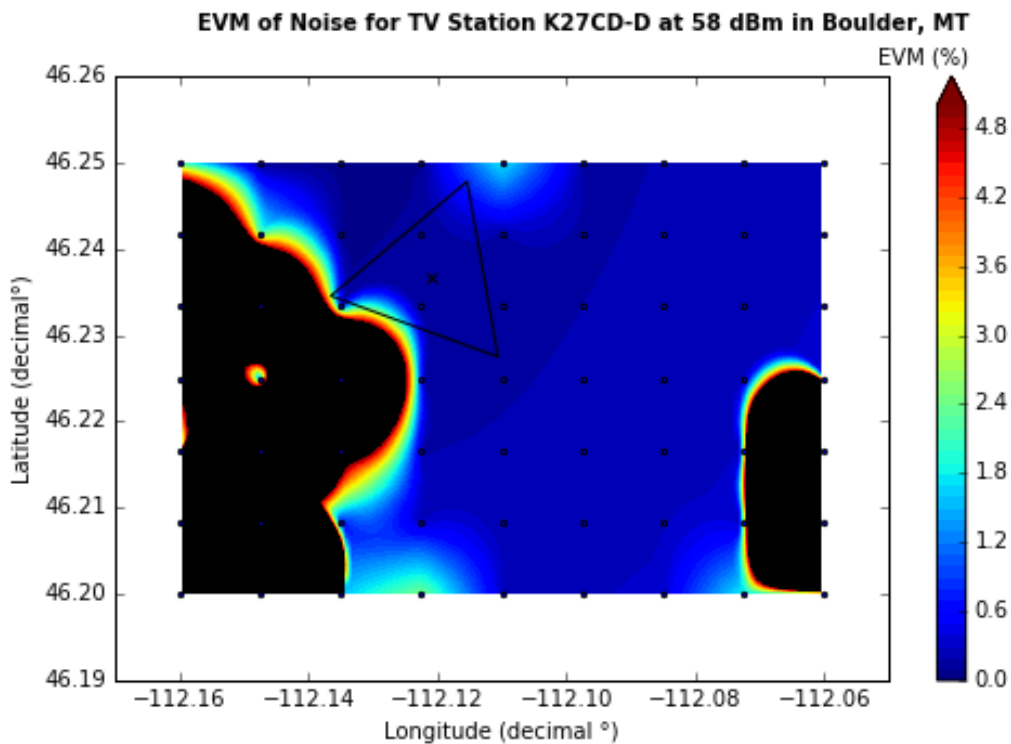
plt.scatter(Rx_x,Rx_y,marker='o',s=5,zorder=10)

```

**Figure 79: Matplotlib Contour Script**

The power of WK9XUC was then adjusted from 45 dBm (or 20 W ERP) to 135 dBm and the EVM due to the noise and interference was calculated. The acceptable co-channel power was found for each grid, which is that no populated and non-poor Rx location exceeds 5% EVM due to WK9XUC interference. Adjacent channel is similar except the power level of WK9XUC is lowered from 45 dBm to -15 dBm until no populated Rx location exceeds 5% EVM due to WK9XUC interference.

The poor receiver locations are marked black in each of the following pictures. The baseline EVM due only to noise is pictured in Figure 80 for K27CD-D operating in Boulder, Montana. The triangle surrounds the populations center that is marked with an x. Note that the brick red color that represent 5% EVM cannot be seen in this baseline EVM figure.



Now the power level of WK9XUC is increased until any location inside the village perimeter is 5% EVM. This threshold exceeded between 110 and 115 dBm, which is equivalent to 100 MW and 316 MW. Note the transition inside the city triangle perimeter as the brick red color appears in Figure 81 from Figure 82.

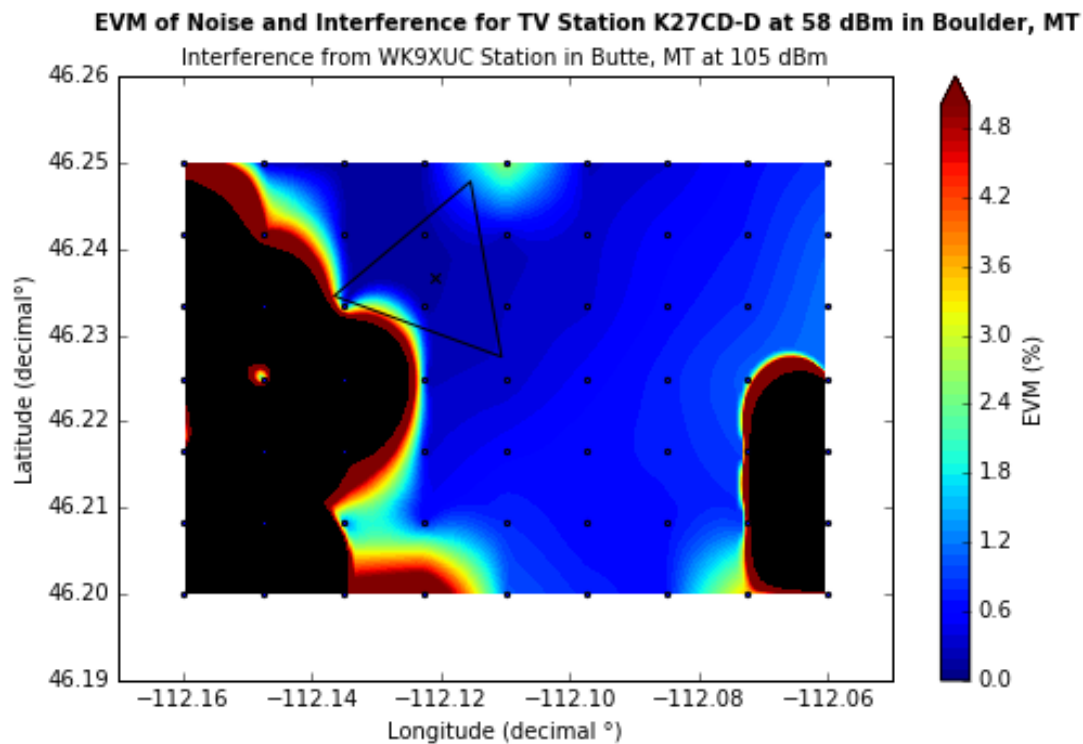


**Figure 81: EVM due Noise and Interference below 5% threshold in Boulder, MT**

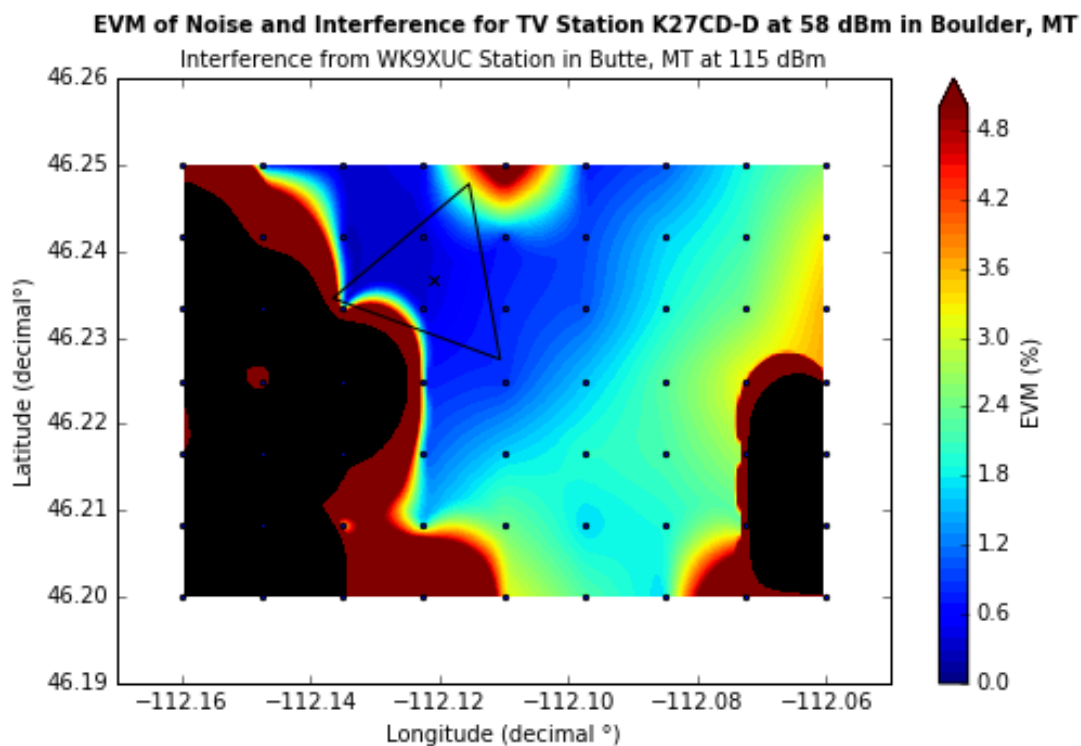


**Figure 82: EVM due Noise and Interference above 5% threshold in Boulder, MT**



When KWYB is operating at full power, it does not reach Boulder, Montana, therefore all Rx site are poor (blacked out). This is due to terrain, but also a null in the antenna's directivity is pointed towards Boulder.

Figure 83 and Figure 84 depict the baseline for KWYB in Anaconda, operating at 79 dBm and 83 dBm respectively. KWYB does transmit to some locations in Anaconda, but it's blocked out for most of the sites inside the perimeter of the town. It appears that another station K48MM-D provides TV channels ABC/Fox to Anaconda.

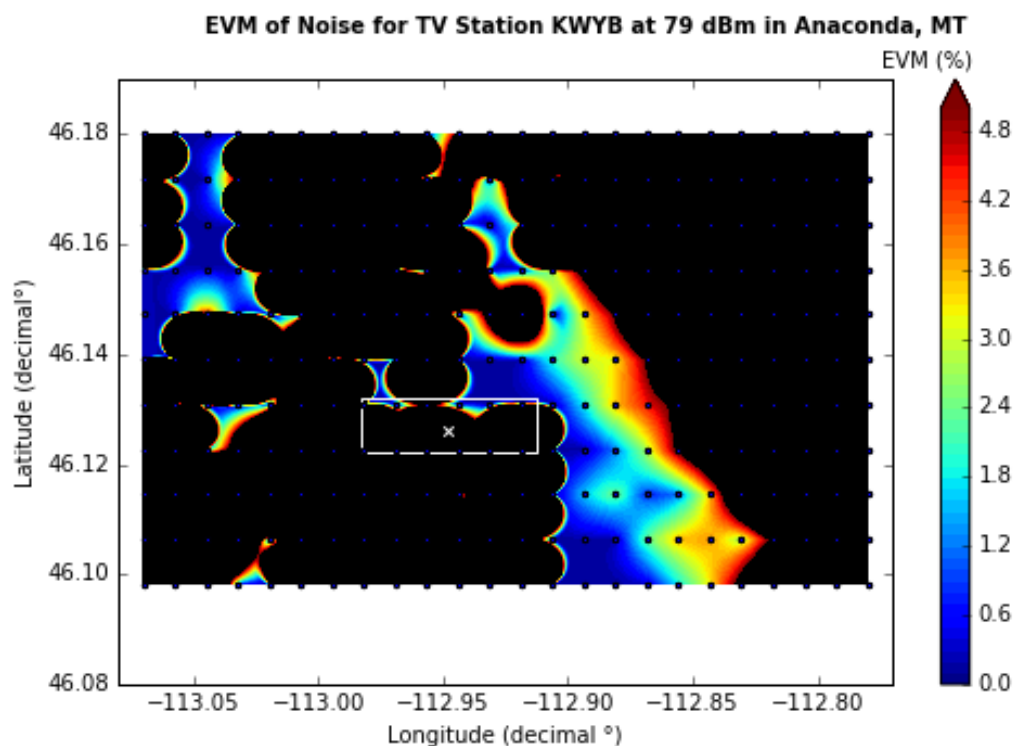


**Figure 83: EVM Baseline for KWYB at 79 dBm in Anaconda, MT**

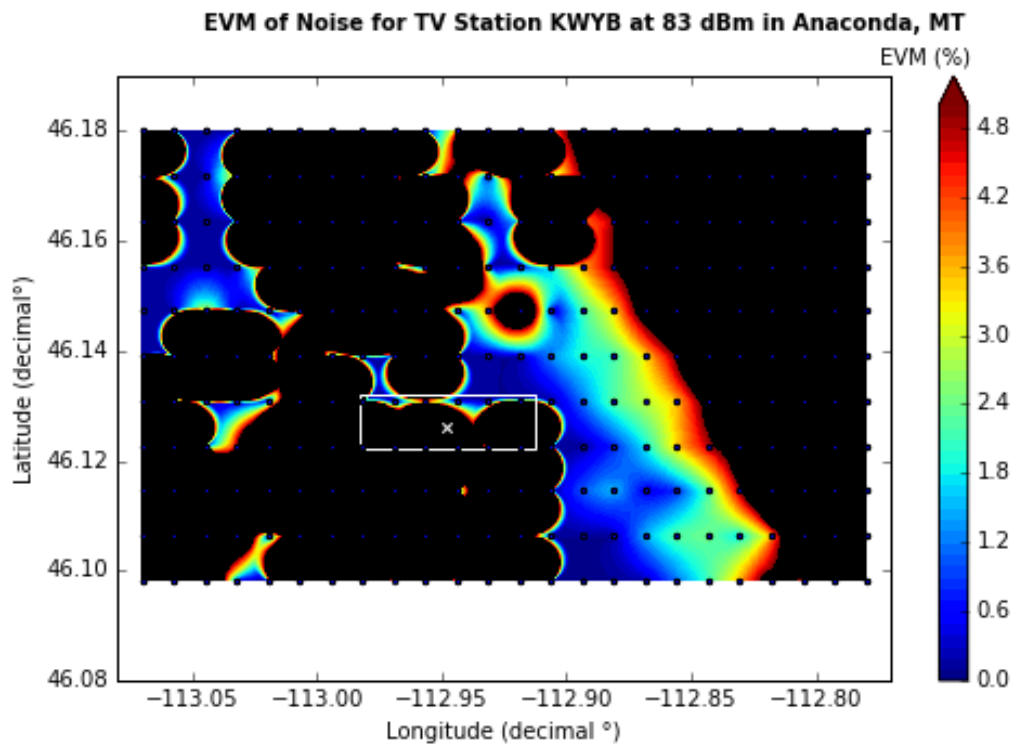


**Figure 84: EVM Baseline for KWYB at 83 dBm in Anaconda, MT**

When KWYB is operating at both power levels, the EVM threshold is exceeded by WK9XUC when it operates around 75 dBm as pictured in Figure 85 and 86.

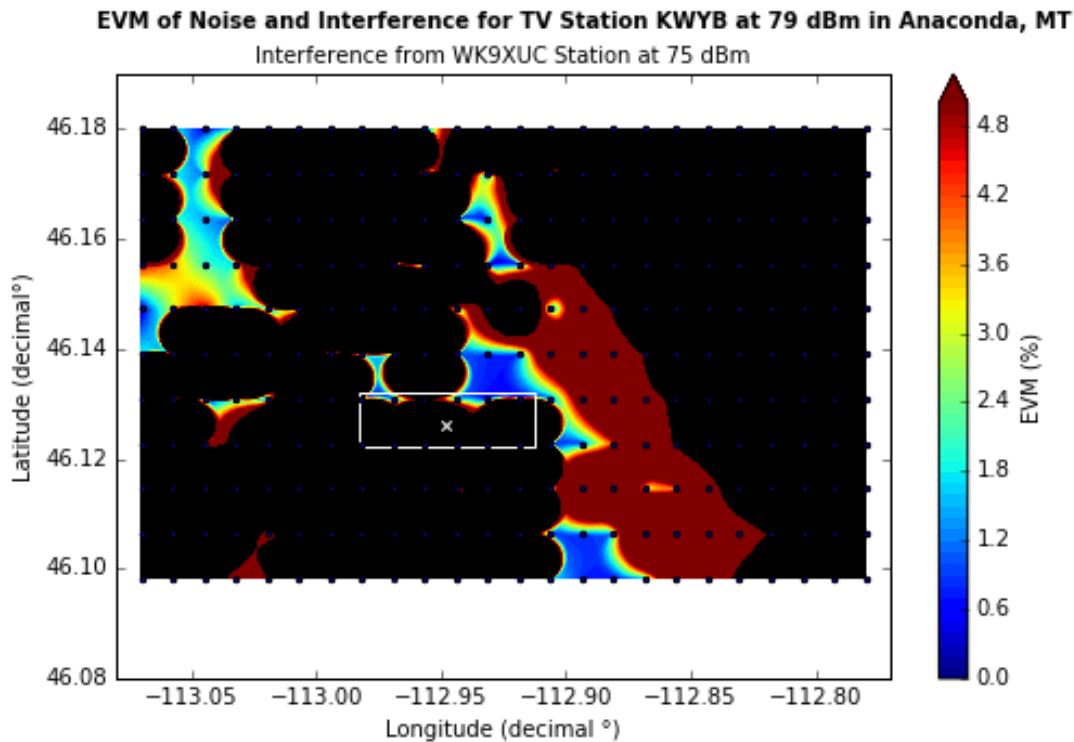


Figure 85: EVM due Noise and Interference for KYWB at 79 dBm in Anaconda, MT

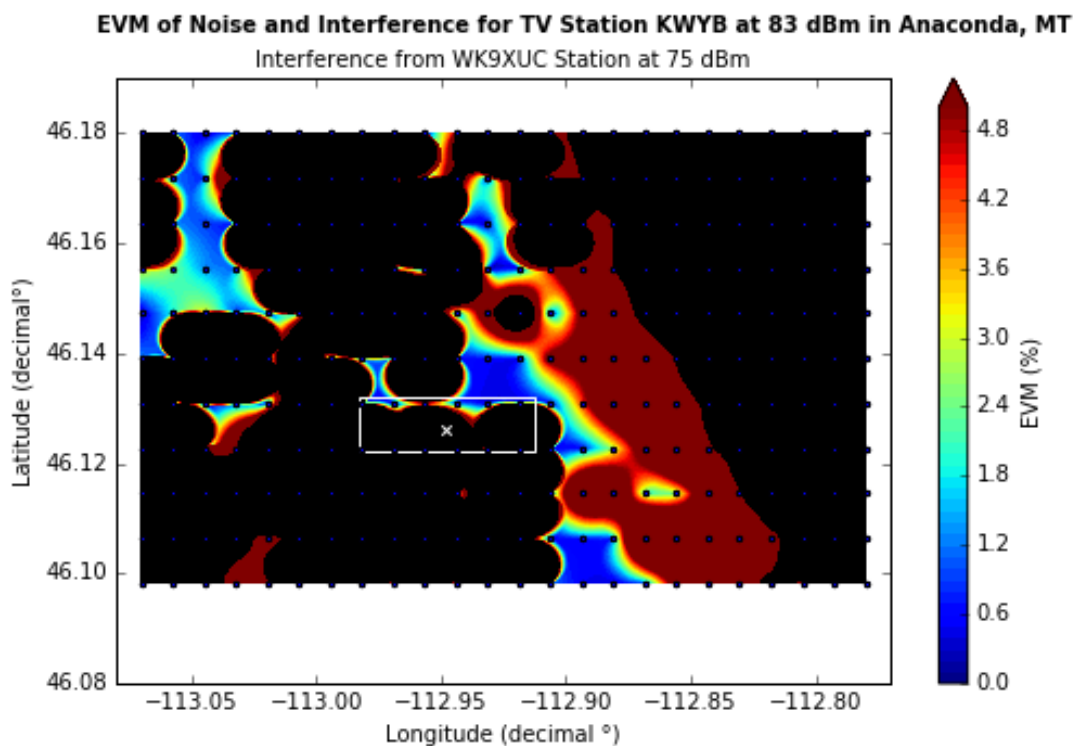
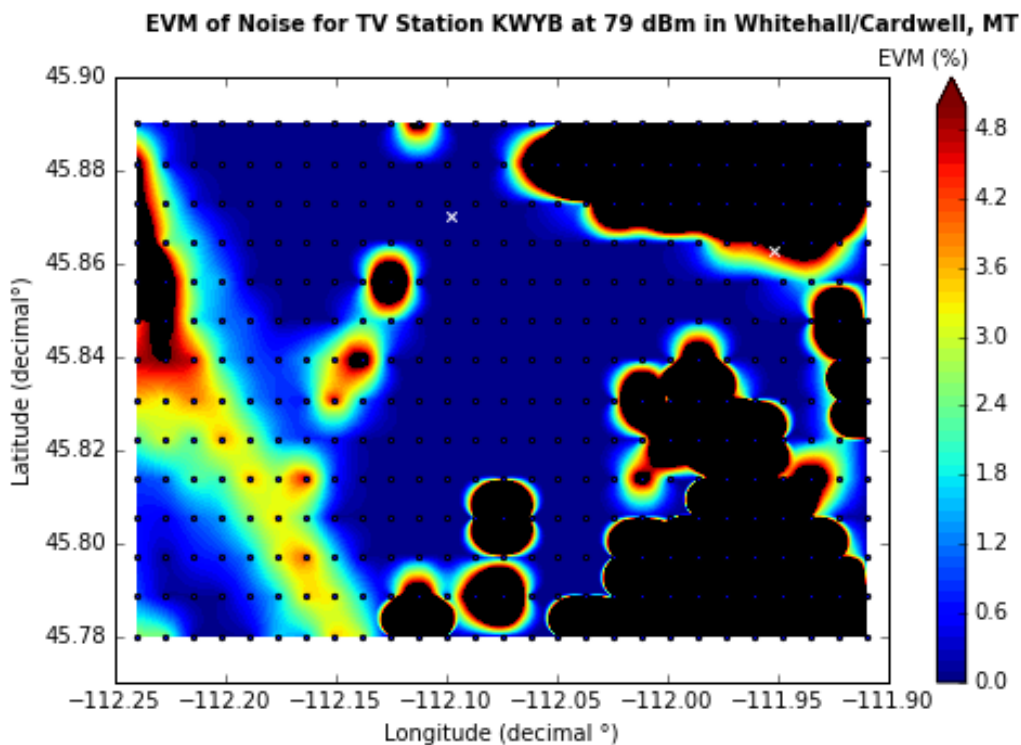


Figure 86: EVM due Noise and Interference for KYWB at 83 dBm in Anaconda, MT

Whitehall and Cardwell are included in the same map. The area is sparsely populated across the valley, and therefore no population perimeters are included. At the lower power level of KWYB, most of Cardwell (the town) already has poor reception as pictured in Figure 87:



**Figure 87: EVM Baseline for KWYB at 79 dBm in Whitehall/Cardwell, MT**

KWYB as a higher power level is pictured in Figure 88. Cardwell and the surrounding area is the limiting factor with respect to the EVM as WKXUC power is adjusted.

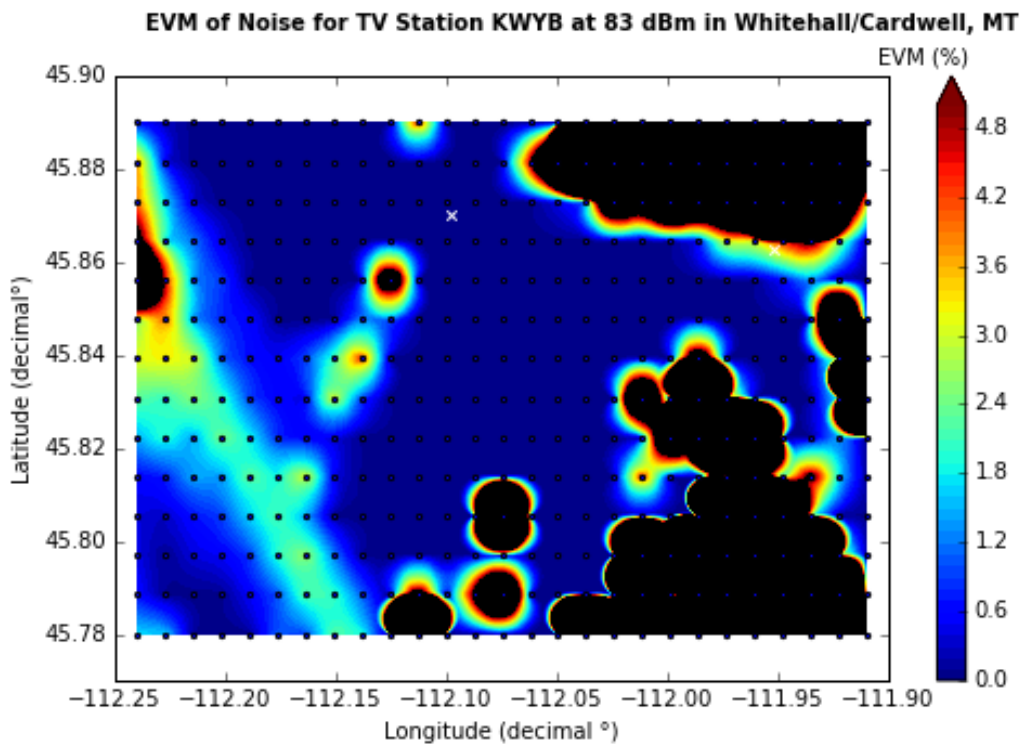


**Figure 88: EVM Baseline for KWYB at 79 dBm in Whitehall/Cardwell, MT**

The EVM exceeds 5% when WKXUC is operating around 95 dBm for both power levels of KWYB as pictured in Figure 89 and Figure 90:

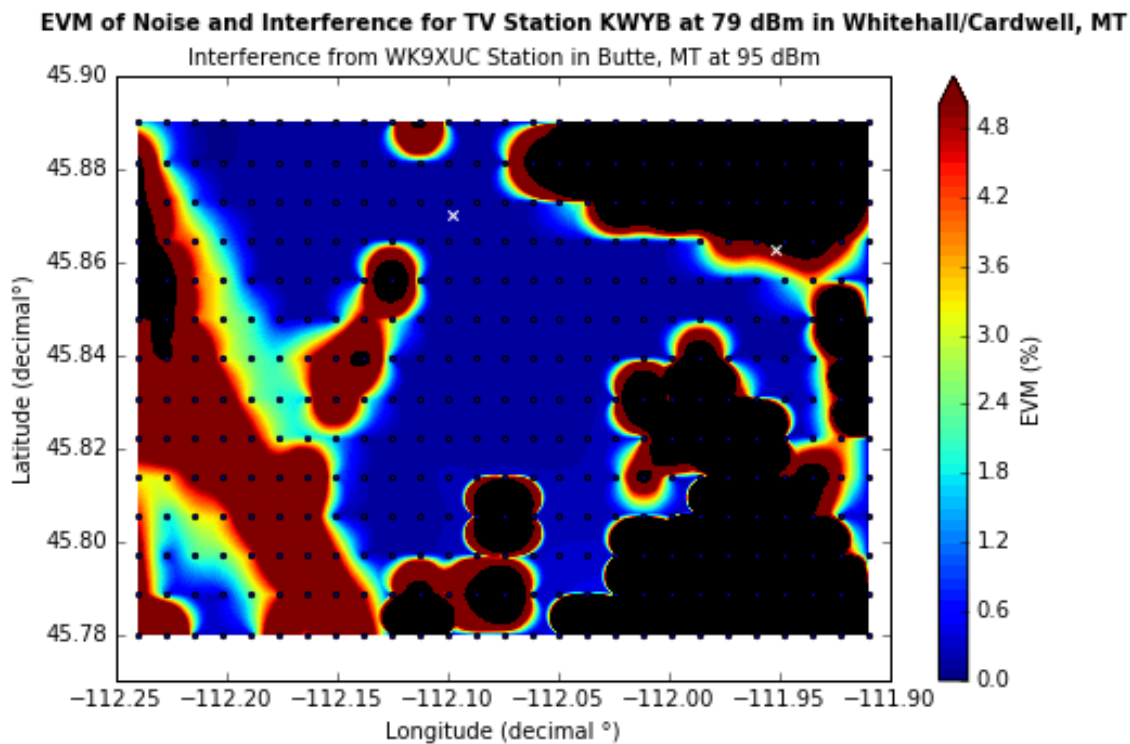


Figure 89: EVM due Noise and Interference for KWYB at 79 dBm in Whitehall/Cardwell, MT

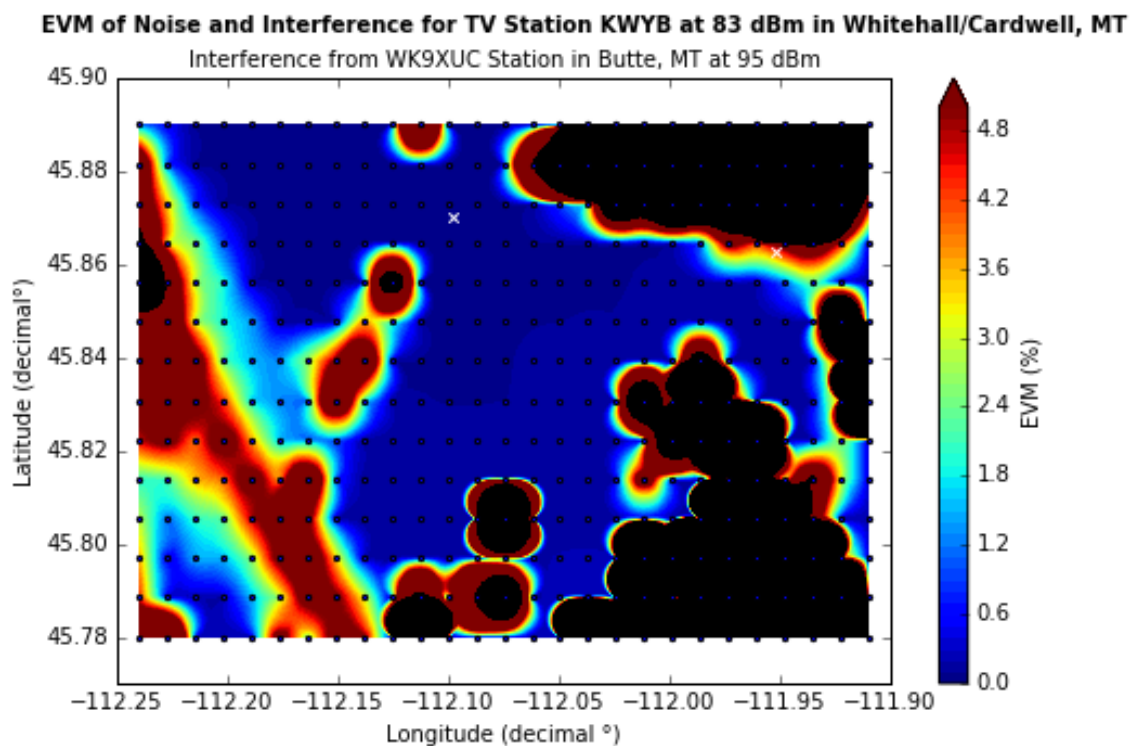
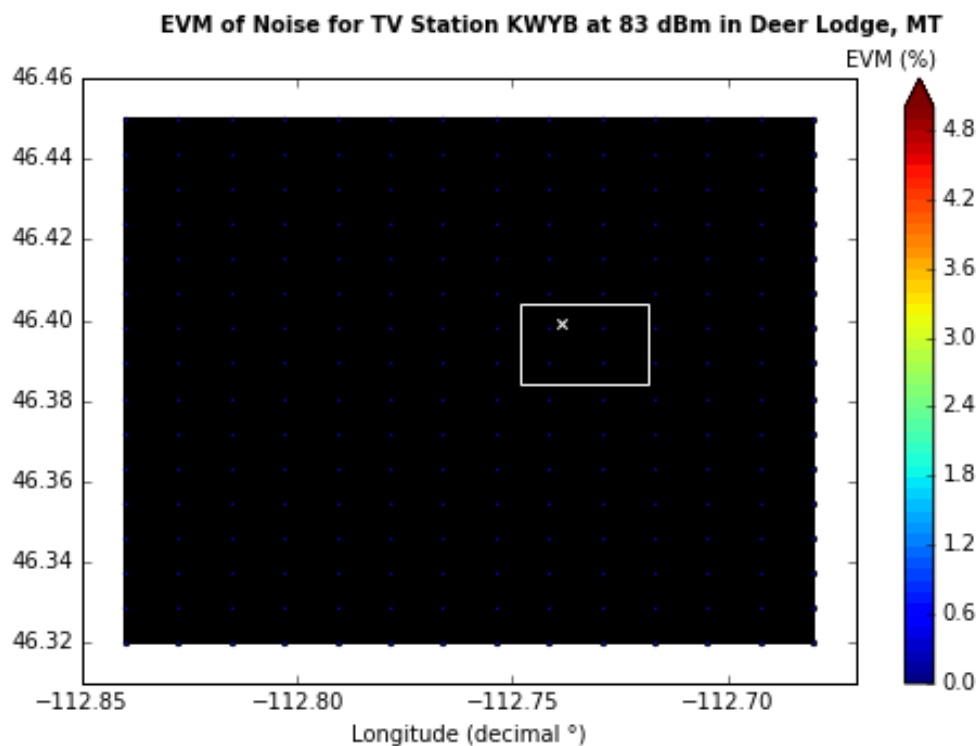
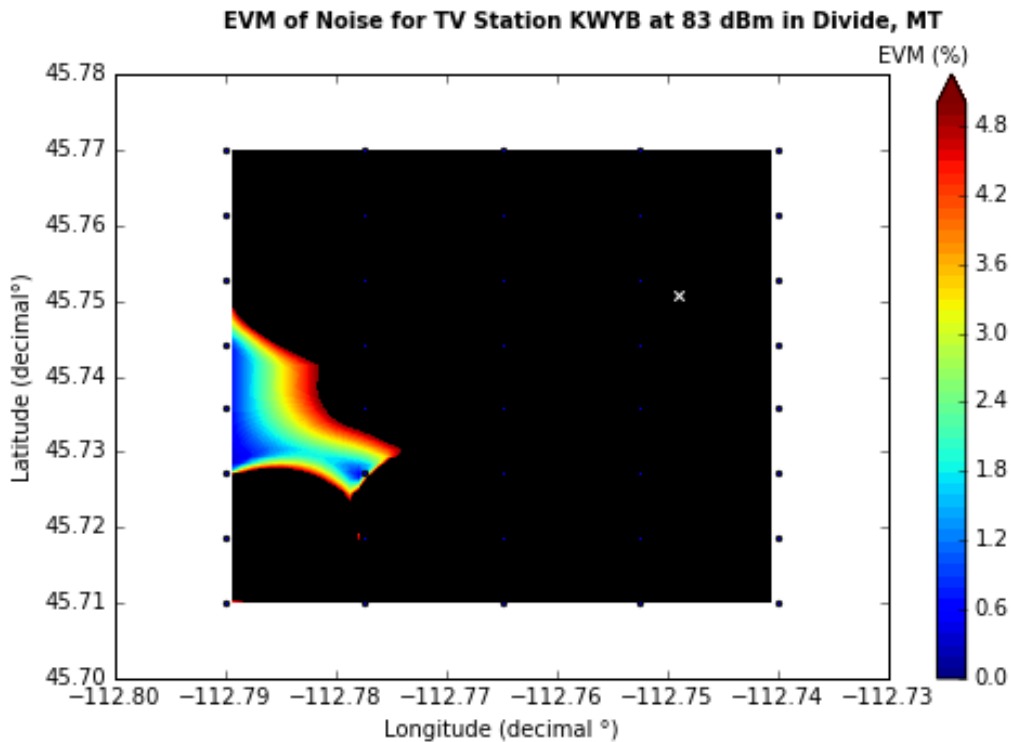


Figure 90: EVM due Noise and Interference for KWYB at 83 dBm in Whitehall/Cardwell, MT

The rest of the locations, Deer Lodge and Divide, have poor reception areas in all locations at the higher power level for KWYB as pictured in Figure 91 and Figure 92:



**Figure 91: EVM Baseline for KWYB at 83 dBm in Deer Lodge MT**



**Figure 92: EVM Baseline for KWYB at 83 dBm in Divide MT**

In Butte, the adjacent channel interference is determined by adjusting the power level until the areas surrounding Montana Tech Museum have an EVM of <5%. The baseline in this case is WK9XUC operating at 20 W ERP (45 dBm) as pictured in Figure 93 and Figure 94, for both power levels of KWYB. The blue triangle is the location of WK9XUC and the purple triangle is the location of KWYB on the continental divide:



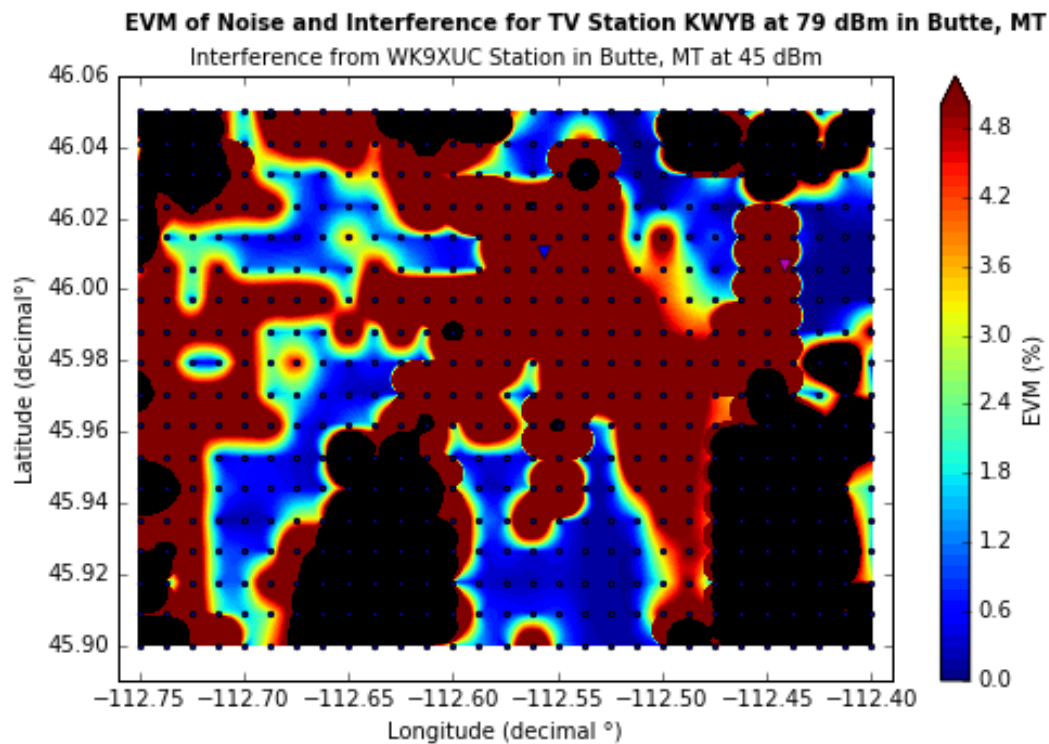


Figure 93: EVM Baseline for KWYB at 79 dBm in Butte, MT

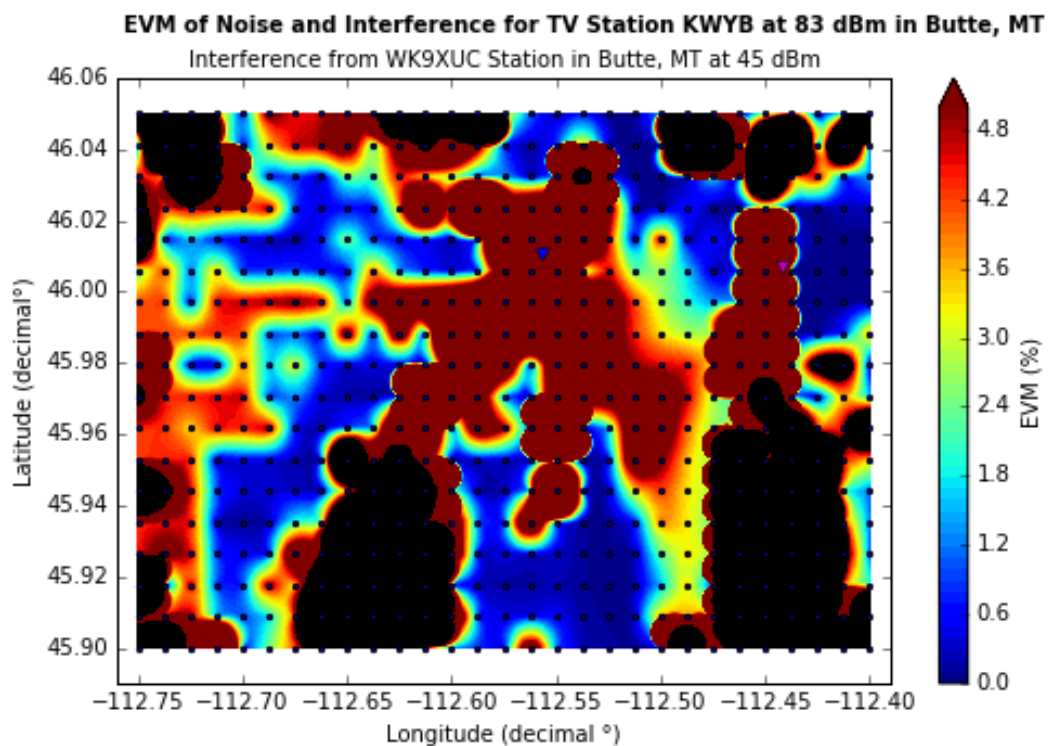
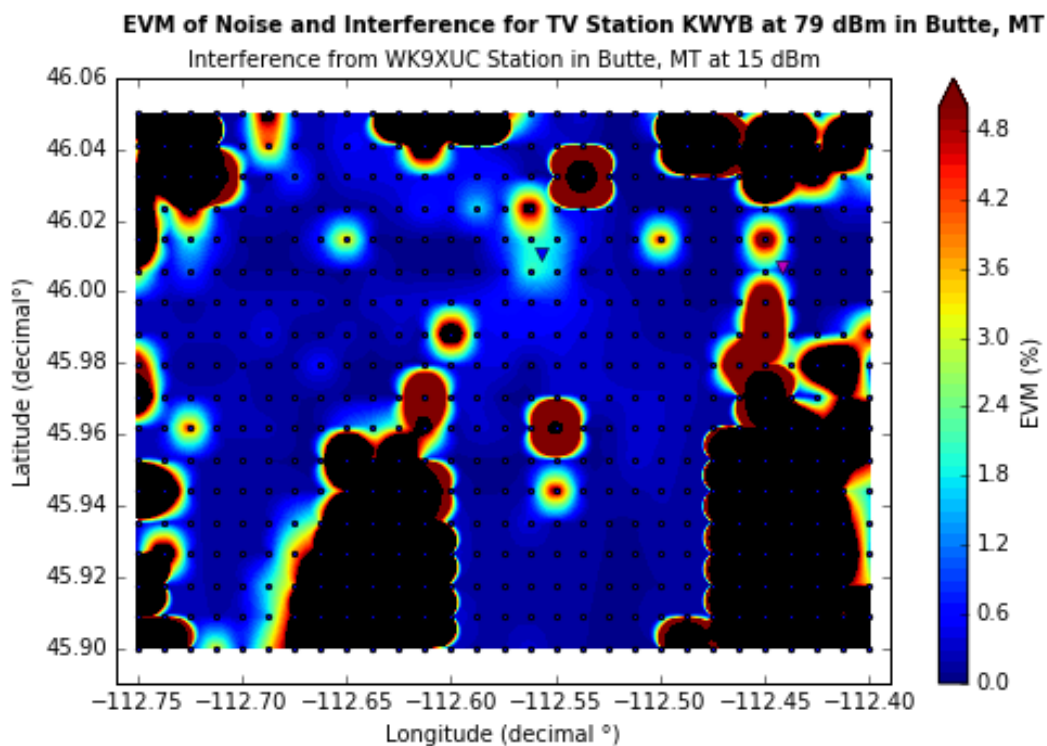
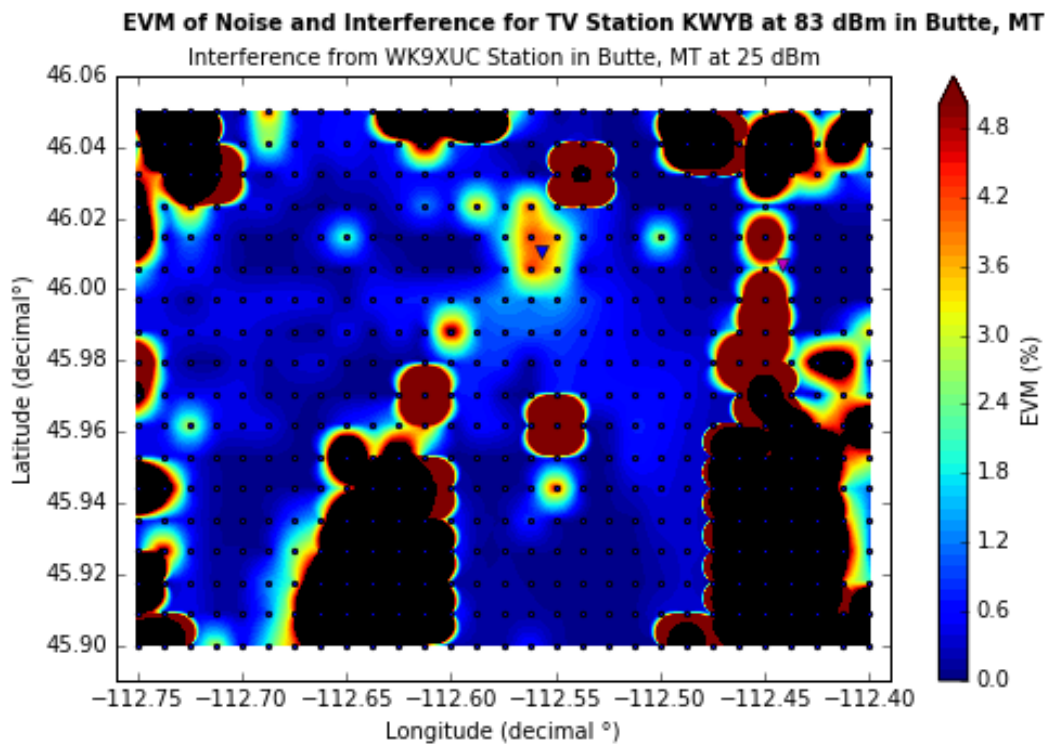


Figure 94: EVM Baseline for KWYB at 83 dBm in Butte, MT

The areas surrounding WK9XUC reach 5% at a power level near 15 dBm for the lower power level of KWYB, and near 25 dBm for the higher power level of KWYB as pictured in Figure 95 and Figure 96:



**Figure 95: EVM due Noise and Interference for KWYB at 79 dBm in Butte, MT**



**Figure 96: EVM due Noise and Interference for KWYB at 83 dBm in Butte, MT**

The simulations were run again to find when WK9XUC exceeded the maximum EVM in non-poor Rx locations to the nearest dB. The results of the EVM due to noise and interference from WK9XUC are summarized in Table XX:

Table XX: Summary of Channel Interference when EVM exceeds 5%

Location	Desired Station	Channel Frequency [MHz]	$P_{signal}$ [dBm]	WK9XUC $P_{interference}$ [dBm]	With 10 dB safety margin
Anaconda	KWYB	500 – 506	79	71	61
			83	75	65
Boulder	K27CD-D	548 – 554	45	111	101
	KWYB	500 – 506	79	no limit	no limit
			83	no limit	no limit
Butte	KWYB	500 – 506	79	23	13
			83	27	17
Deer Lodge	KWYB	500 – 506	79	no limit	no limit
			83	no limit	no limit
Divide	KWYB	500 – 506	79	no limit	no limit
			83	no limit	no limit
Whitehall	KWYB	500 – 506	79	89	79
			83	94	85

In order to operate at Montana Tech at 45 dBm or higher, and given a safety margin of 10 dB, the adjacent channel power must not exceed 13 dBm when KWYB is operating at 79 dBm, and 17 dBm when KWYB is operating at 83 dBm. When WK9XUC is operating from 510 to 560 MHz, WK9XUC must not exceed 101 dBm in order to not interfere with K27CD-D in Boulder, Montana.

Since it is doubtful that WK9XUC will operate anywhere near 100 MW, it will be assumed that 1000 W (60 dBm) is the upper limit of EIRP. The difference between the adjacent channel power and the channel power is the adjacent channel power ratio (ACPR). Comparing the adjacent channel power of 17 dBm to the channel power of 60 dBm gives an ACPR of

-43 dBc (the c stands for carrier). This figure is typical and manageable for current LTE and WLAN systems.

The propagation of WK9XCU is shown in Figure 97 when the station operates at 20 W ERP in and around Butte, Montana. Note for a large area of the locations around Butte, the signal and the noise have the same power level,  $SNR = 0 \text{ dB}$ . In Figure 98 the power level is adjusted to 1927 W, even then the signal does not propagate above the noise floor beyond the continental divide located on the east (right) side of the map.

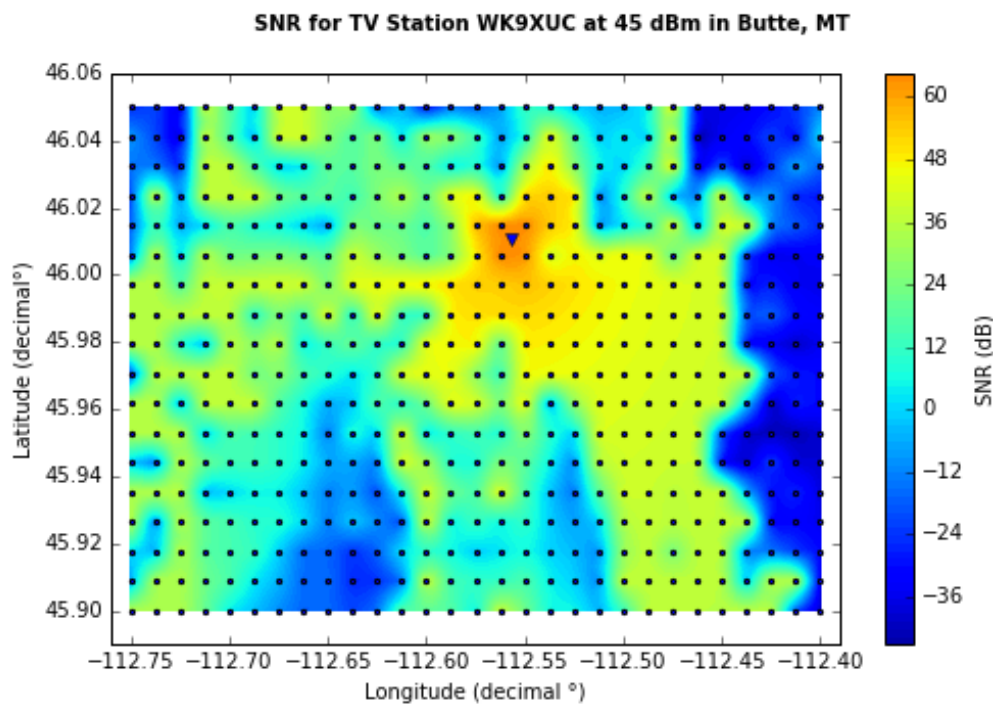


**Figure 97: Signal to Noise Ratio of WK9XUC Operating at 20 W ERP in Butte, Montana**

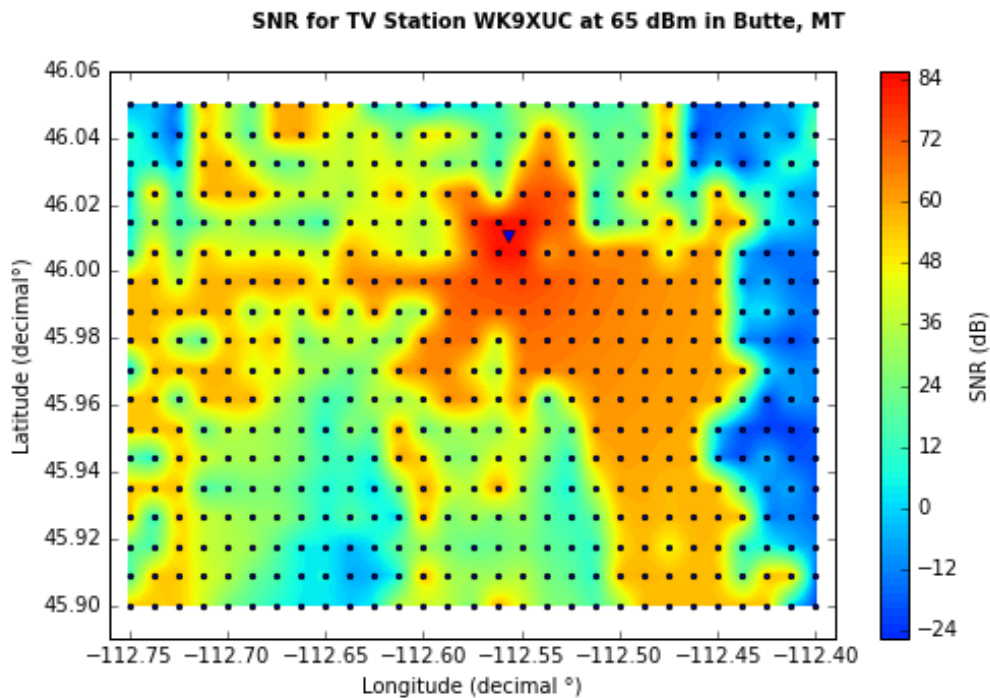


**Figure 98: Signal to Noise Ratio of WK9XUC Operating at 2 kW ERP in Butte, Montana**

WK9XUC is a noise-limited system even when it operates at 1000 W EIRP. Furthermore, this station will not interfere by co-channel when it operates at 1000 W.

## 6. Conclusion

In many respects, this work demonstrates that there is an abundance of completely underutilized spectrum available to provide mobile broadband communications in rural and remote area located in western Montana. By monitoring the spectrum from 174 to 1000 MHz at two locations, specifically at Montana Tech in Butte, Montana and a Moose Lake Road near Philipsburg, Montana for a minimum of 2 weeks, spectrum use can be quantified. This work characterizes the spectrum use across the span of interest by targeting 5-MHz channels. Each channel is characterized by occupancy percentage, mean shift and maximum power.

There are many channels available for sharing across the span from 174 to 1000 MHz, including but not limited to the spurious emissions dominated channels from 174 to 200 MHz, channels from 510 to 550 MHz and the ISM band from 902 to 928 MHz. However, the 500 MHz band is likely the best candidate for testing a rural broadband communications system. This is because of the interference from spurious emission below 500 MHz and the interference, which will likely occur, in the ISM band.

To design a rural broadband mobile communication system that optimizes coverage over capacity in mountainous terrain, this work models a cellular base station that operates in Butte, Montana. The Wireless Lab at Montana Tech was granted an experimental license to operate a 20 W ERP station, WK9XUC, in the 500 MHz band. The ITM was implemented to study the propagation and various interference scenarios of this station, WK9XUC, with other TV stations. This work demonstrates that cellular base station operating from 20 W to 1000 W in the 500 MHz band is viable from an interference point of view. Furthermore, WK9XUC is noise-limited because the mountainous terrain block signals at given height, power and location.

## References Cited

- [1] M. Allevan. (2016, July 14). *FCC OKs sweeping Spectrum Frontiers rules to open up nearly 11 GHz of spectrum* [Online]. Available: <http://www.fiercewireless.com/tech/fcc-oks-sweeping-spectrum-frontiers-rules-to-open-up-nearly-11-ghz-spectrum>
- [2] 5G [Online]. Available: <https://en.wikipedia.org/wiki/5G>
- [3] S. Segan. (2015, June 15). *3G v. 4G speeds* [Online]. Available: <http://www.pcmag.com/article/345123/fastest-mobile-networks-2016/4>
- [4] A. M. Kovacs. (2014, May 1). *Regulation in financial translation: Will the incentive auction increase mobile-broadband competition in rural America?* [Online]. Available: <http://cbpp.georgetown.edu/publications/will-incentive-auction-increase-mobile-broadband-competition-rural-america>
- [5] Spectrum Wiki. *Standard LTE bands* [Online]. Available: <http://www.spectrumwiki.com/Index.aspx>
- [6] Federal Communications Commission. (2014, May 15). *Staff summary of incentive auction report and order* [Online]. Available: <https://www.fcc.gov/document/staff-summary-incentive-auction-report-and-order>
- [7] J. Engebretson. (2015, July 16). *FCC adopts rural carrier bidding credit for 600 MHz auction, delays other key issues* [Online]. Available: <http://www.telecompetitor.com/fcc-adopts-rural-carrier-bidding-credit-for-600-mhz-auction-delays-other-key-issues/>
- [8] D. Meyer. (2016, October 19). *FCC 600 MHz auction stage 2 ends after 1 round; On to stage 3* [Online]. Available: <http://www.rcrwireless.com/20161019/policy/fcc-600-mhz-auction-stage-2-ends-1-round-stage-3-tag2>



- [9] M. Cotton et al., "An overview of the NTIA/NIST spectrum monitoring pilot program," *IEEE Wireless Communications and Networking Conf. Workshops (WCNCW)*, New Orleans, LA, 2015, pp. 217-222. doi: 10.1109/WCNCW.2015.7122557
- [10] Shared Spectrum Company. *Spectrum reports* [Online]. Available: <http://www.sharespectrum.com/papers/spectrum-reports/>
- [11] R. Aguilar-Gonzalez, M. Cardenas-Juarez, U. Pineda-Rico and E. Stevens-Navarro, "Spectrum Occupancy Measurements below 1 GHz in the City of San Luis Potosi, Mexico," *IEEE 78th Vehicular Technology Conf. (VTC)*, Las Vegas, NV, 2013, pp. 1-5. doi: 10.1109/VTCFall.2013.6692420
- [12] D. A. Roberson, C. S. Hood, J. L. LoCicero and J. T. MacDonald, "Spectral Occupancy and Interference Studies in support of Cognitive Radio Technology Deployment," *1st IEEE Workshop Networking Technologies for Software Defined Radio Networks*, Reston, VA, USA, 2006, pp. 26-35. doi: 10.1109/SDR.2006.4286323
- [13] N. Faruk et al, "Large scale spectrum survey in rural and urban environments within the 50 MHz-6 GHz bands," *Measurement*, vol. 91, pp. 228-238, Sept. 2016.
- [14] E. Wiles, B. Hill, F. A. da Silva and K. Negus, "Measurement and analysis of spectrum occupancy from 140 to 1000 MHz in rural western Montana," *10th European Conf. Antennas and Propagation (EuCAP)*, Davos, CH, 2016, pp. 1-4. doi: 10.1109/EuCAP.2016.7481328
- [15] V. Valenta et al, "Survey on spectrum utilization in Europe: Measurements, analyses and observations," *Proc. 5th Int. Conf. Cognitive Radio Oriented Wireless Networks and Communications*, Cannes, FR, 2010, pp. 1-5. doi: 10.4108/ICST.CROWNCOM2010.9220

- [16] S. D. Barnes, P. R. Botha, and B. T. Maharaj. "Spectral occupation of TV broadcast bands: Measurement and analysis," *Measurement*, vol. 93, pp. 272-277, Nov. 2016. doi: 10.1016/j.measurement.2016.07.020
- [17] K. A. Qaraqe et al, "Measurement and analysis of wideband spectrum utilization in indoor and outdoor environments," *12<sup>th</sup> Int. Conf. Communications Technologies (ICCT)*, Nanjing, CN, 2010. Available: [http://people.qatar.tamu.edu/khalid.qaraqe/KQPublications/icct10\\_v5.pdf](http://people.qatar.tamu.edu/khalid.qaraqe/KQPublications/icct10_v5.pdf)
- [18] M. Lopez-Benitez, A. Umbert and F. Casadevall, "Evaluation of Spectrum Occupancy in Spain for Cognitive Radio Applications," *IEEE 69th Vehicular Technology Conf. (VTC)*, Barcelona, ES, 2009, pp. 1-5. doi: 10.1109/VETECS.2009.5073544
- [19] R. Schiphorst and C. H. Slump, "Evaluation of Spectrum Occupancy in Amsterdam Using Mobile Monitoring Vehicles," *IEEE 71st Vehicular Technology Conf. (VTC)*, Taipei, TW, 2010, pp. 1-5. doi: 10.1109/VETECS.2010.5494056
- [20] L. Mendes, L. Gonçalves and A. Gameiro, "GSM downlink spectrum occupancy modeling," *IEEE 22nd Int. Symp. Personal, Indoor and Mobile Radio Communications*, Toronto, ON, 2011, pp. 546-550. doi: 10.1109/PIMRC.2011.6140021
- [21] S. Jayavalan, et al, "Measurements and analysis of spectrum occupancy in the cellular and TV bands," *Lecture Notes on Software Engineering*, vol. 2, no. 2, pp. 133-138, May 2014. doi: 10.7763/LNSE.2014.V2.110
- [22] M. H. Islam et al., "Spectrum survey in Singapore: Occupancy measurements and analyses," *3rd Int. Conf. Cognitive Radio Oriented Wireless Networks and Communications (CROWNCOM)*, Singapore, 2008, pp. 1-7. doi: 10.1109/CROWNCOM.2008.4562457

- [23] A. Marțian, C. Vlădeanu, I. Marcu, and I Marghescu, "Evaluation of spectrum occupancy in an urban environment in a cognitive radio context," *International Journal on Advances in Telecommunications*, vol. 3, no. 3, pp. 172-181, 2010.
- [24] S. W. Ellingson, "Spectral occupancy at VHF: implications for frequency-agile cognitive radios," IEEE 62nd Vehicular Technology Conference (VTC), 2005, Dallas, TX, USA, pp. 1379-1382. doi: 10.1109/VETECONF.2005.1558153
- [25] R. Attard et al., "A high-performance tiered storage system for a global spectrum observatory network," *9th International Conference on Cognitive Radio Oriented Wireless Networks and Communications (CROWNCOM)*, Oulu, FI, 2014, pp. 466-473. doi: 10.4108/icst.crowncom.2014.255740
- [26] R. Urban, T. Korinek, and P. Pechac, "Broadband spectrum survey measurements for cognitive radio applications," *Radioengineering*, vol. 21, no. 4, pp. 1101-1109, 2012. doi: 10.13164/re.2012.1101
- [27] S. Yin, D. Chen, Q. Zhang, M. Liu and S. Li, "Mining spectrum usage data: A large-scale spectrum measurement study," *IEEE Transactions on Mobile Computing*, vol. 11, no. 6, pp. 1033-1046, June 2012. doi: 10.1109/TMC.2011.128
- [28] A. Petrin and P. G. Steffes, "Analysis and comparison of spectrum measurements performed in urban and rural areas to determine the total amount of spectrum usage," *Proc. Int. Symp. Advanced Radio Technologies (ISART)*, Boulder, CO, USA, 2005, pp. 9-12. Available: <https://www.its.bldrdoc.gov/publications/05-418.aspx>
- [29] C. A. Hammerschmidt, Heather E. Ottke, J. Randy Hoffman "Broadband spectrum survey in the Denver area," NTIA, Washington, DC, Rep. *TR-13-496*, 2013. Available: <https://www.its.bldrdoc.gov/publications/2735.aspx>

[30] C. A. Hammerschmidt, "Broadband spectrum survey in the San Diego, California, area," NTIA, Washington, DC, Rep. *TR-14-498*, 2014. Available:

<https://www.its.bldrdoc.gov/publications/2741.aspx>

[31] C. A. Hammerschmidt "Broadband spectrum survey in the Chicago, Illinois, area," NTIA, Washington, DC, Rep. *TR-14-502*, 2014. Available:

<https://www.its.bldrdoc.gov/publications/2756.aspx>

[32] R. Bacchus, T. Taher, K. Zdunek and D. Roberson, "Spectrum utilization study in support of dynamic spectrum access for public safety," *IEEE Symp. New Frontiers Dynamic Spectrum (DySPAN)*, Singapore, 2010, pp. 1-11. doi: 10.1109/DYSPAN.2010.5457871

[33] R. I. C. Chiang, G. B. Rowe and K. W. Sowerby, "A quantitative analysis of spectral occupancy measurements for cognitive radio," *IEEE 65th Vehicular Technology Conference (VCT)*, Dublin, IE, 2007, pp. 3016-3020. doi: 10.1109/VETECS.2007.618

[34] M. Mehdawi, N. Riley, K. Paulson, A. Fanan, and M. Ammar, "Spectrum occupancy survey in HULL-UK for cognitive radio applications: measurement & analysis," *International Journal of Scientific & Technology Research*, vol. 2, no. 4, pp. 231-236, Apr. 2013. Available:

<http://www.ijstr.org/final-print/apr2013/Spectrum-Occupancy-Survey-In-Hull-uk-For-Cognitive-Radio-Applications-Measurement-&-Analysis.pdf>

[35] M. Wellens, J. Wu and P. Mahonen, "Evaluation of spectrum occupancy in indoor and outdoor scenario in the context of cognitive radio," *2nd Int. Conf. Cognitive Radio Oriented Wireless Networks and Communications*, Orlando, FL, USA, 2007, pp. 420-427. doi:

10.1109/CROWNCOM.2007.4549835

[36] T. Harrold, R. Cepeda and M. Beach, "Long-term measurements of spectrum occupancy characteristics," *IEEE Int. Symp. Dynamic Spectrum Access Networks (DySPAN)*, Aachen, DE, 2011, pp. 83-89. doi: 10.1109/DYSPAN.2011.5936272

[37] OpenSignal. *OpenSignal app* [Online]. Available: <https://opensignal.com/>

[38] OpenSignal. *The state of LTE* [Online]. (2016, February). Available: <https://opensignal.com/reports/2016/02/state-of-lte-q4-2015/>

[39] OpenSignal. *Compare mobile networks near you* [Online]. (2017, May). Available: <https://opensignal.com/coverage-maps/>

[40] A. G. Longley and P. L. Rice, "Prediction of tropospheric radio transmission loss over irregular terrain. A computer method-1968," ITS, Boulder, CO, Rep. *ITS-67*, 1968. Available: <https://www.its.bldrdoc.gov/publications/download/ERL%2079-ITS%2067.pdf>

[41] Borb – Wikimedia Commons. *Inverse square law* [Image]. Available: <https://commons.wikimedia.org/w/index.php?curid=3816716>

[42] Agilent Technologies. *Spectrum analysis basics* [Online]. Available: <http://cp.literature.agilent.com/litweb/pdf/5952-0292.pdf>

[43] Berkeley Nucleonics Corp. *RTSA7500 programmer's manual (v3.6.2)* [Online]. Available: [http://www.berkeleynucleonics.com/sites/berkeleynucleonics/files/products/manuals/model7500\\_programmersmanual\\_ver3\\_6\\_2.pdf](http://www.berkeleynucleonics.com/sites/berkeleynucleonics/files/products/manuals/model7500_programmersmanual_ver3_6_2.pdf)

[44] SciPy.org. *NumPy Manual v1.12: Discrete Fourier Transform* [Online]. Available: <https://docs.scipy.org/doc/numpy/reference/routines.fft.html>

[45] Diamond Antenna. *D3000N Super Discone Antenna* [Online]. Available: <http://www.diamondantenna.net/d3000n.html>

- [46] RF Bay, Inc. *LNA-1520* [Online]. Available: [http://rfbayinc.com/products\\_pdf/product\\_91.pdf](http://rfbayinc.com/products_pdf/product_91.pdf)
- [47] COM-Power Corporation. *PAM-103* [Online]. Available: <http://www.com-power.com/datasheets/PAM-103.pdf>
- [48] Tin Lee Electronics. *Welcome to Tin Lee Electronics Ltd.* [Online]. Available: <http://www.tinlee.com/index.php>
- [49] L-com. *N-Male to N-Female Bulkhead 0-3 GHz Coaxial Lightning Protector* [Online]. Available: [http://www.l-com.com/multimedia/datasheets/DS\\_AL-NMNFB-\\_PDF](http://www.l-com.com/multimedia/datasheets/DS_AL-NMNFB-_PDF)
- [50] Stridsberg Engineering, LLC. *FLT201A specifications* [Online]. Available: <http://www.stridsberg.com/prod02.htm>
- [51] Google Earth Pro. (2016). *Map data: Landsat / Copernicus* [Image].
- [52] PyRF. *PyRF documentation* [Online]. Available: <https://pyrf.readthedocs.io/en/latest/>
- [53] R. Yarbough. *TPI-1002-A Signal Generator* [Online]. Available: <http://www.rf-consultant.com/tpi-1002-a-signal-generator/>
- [54] Reuex Industrial Co., Ltd. (Nagoya Antenna). *Handheld Antenna NA-771, 144/430 MHz* [Online]. Available: <http://www.nagoya.com.tw/en/2-2277-66883/product/NA-771-id384799.html>
- [55] Keysight Technologies. *8753E RF Network Analyzer, 30 kHz to 3 or 6 GHz* [Online]. Available: <http://www.keysight.com/en/pd-1000002294%3Aeps%3Apro-pn-8753E/rf-network-analyzer-30-khz-to-3-or-6-ghz?cc=US&lc=eng>
- [56] The Python Standard Library. 8.6. *array* — *Efficient arrays of numeric values* [Online]. Available: <https://docs.python.org/2/library/array.html>

- [57] Wireless Lab Montana Tech. *YouTube Channel* [Online]. Available: <https://www.youtube.com/channel/UC0Ywn5qi34CDN5IFf8Gmrgg>
- [58] MMX Technology, LCC. *Spectrum Wiki* [Online]. Available: <http://www.spectrumwiki.com/Index.aspx>
- [59] Federal Communications Commission. (2017, March 26). *TV Query of stations located within 141 km of Butte, MT* [Online]. Available: <https://transition.fcc.gov/fcc-bin/tvq?state=MT&call=&arn=&city=&chan=&cha2=69&serv=&type=0&facid=&asrn=&list=1&dist=&dlat2=&mlat2=&slat2=&dlon2=&mlon2=&slon2=&size=9>
- [60] REC Networks. *FCCdata.org* [Online]. Available: <https://fccdata.org/>
- [61] SatelliteGuys. *RabbitEars* [Online]. Available: <http://www.rabbitears.info/>
- [62] J. Maglicane. *SPLAT! A terrestrial RF path analysis application for LINUX/UNIX* [Online]. Available: <http://www.qsl.net/kd2bd/splat.html>
- [63] USGS. *SRTM database* [Online]. Available: <https://dds.cr.usgs.gov/srtm/>
- [64] S. Kasampalis et al, “Comparison of Longley-Rice, ITM and ITWOM propagation models for DTV and FM broadcasting,” *16th Int. Symp. Wireless Personal Multimedia Communications (WPMC)*, Atlantic City, NJ, USA, 2013, pp. 1-6. Available: <http://ieeexplore.ieee.org/document/6618611/>
- [65] The Math Forum at NCTM. (1999, April 20). *Deriving the Haversine formula* [Online]. Available: <http://mathforum.org/library/drmath/view/51879.html>
- [66] A. McGovern. *Geographic distance and azimuth calculations* [Online]. Available: <http://www.codeguru.com/cpp/cpp/algorithms/article.php/c5115/Geographic-Distance-and-Azimuth-Calculations.htm>

[67] USGS. *Region definition* [Image]. Available:

[https://dds.cr.usgs.gov/srtm/version2\\_1/SRTM1/Region\\_definition.jpg](https://dds.cr.usgs.gov/srtm/version2_1/SRTM1/Region_definition.jpg)

[68] USGS. *Continent definition* [Image]. Available:

[https://dds.cr.usgs.gov/srtm/version2\\_1/Documentation/Continent\\_def.gif](https://dds.cr.usgs.gov/srtm/version2_1/Documentation/Continent_def.gif)

[69] G. A. Hufford, A. G. Longley, W. A. & Kissick, “A guide to the use of the ITS irregular terrain model in the area prediction mode,” NTIA, Washington, DC, Rep. 82-100, 1982.

Available: [https://www.ntia.doc.gov/files/ntia/publications/ntia\\_82-100\\_20121129145031\\_555510.pdf](https://www.ntia.doc.gov/files/ntia/publications/ntia_82-100_20121129145031_555510.pdf)

[70] ITU Radiocommunication Sector, “The radio refractive index: its formula and refractivity data,” ITU, Geneva, CH, 2015. Available: [https://www.itu.int/dms\\_pubrec/itu-r/rec/p/R-REC-P.453-11-201507-S!!PDF-E.pdf](https://www.itu.int/dms_pubrec/itu-r/rec/p/R-REC-P.453-11-201507-S!!PDF-E.pdf)

[71] G. A. Hufford, “The ITS irregular terrain model, version 1.2.2 – The algorithm,” NTIA, Boulder, CO, 1984. Available: [https://www.its.blrdoc.gov/media/50676/itm\\_alg.pdf](https://www.its.blrdoc.gov/media/50676/itm_alg.pdf)

[72] B. R. Bean, J. D. Horn and A. M. Ozanich, *NBS Monograph 22: Climatic charts and data of the radio refractive index for the United States and the World*. Washington, DC: U.S. Government Printing Office, 1960. Available:

<http://digicoll.manoa.hawaii.edu/techreports/PDF/NBS22.pdf>

[73] JeffConrad – Wikimedia Commons. *Geometric distance to horizon* [Image].

Available: <https://commons.wikimedia.org/w/index.php?curid=14958770>

[74] J. D. Hunter, “Matplotlib: A 2D graphics environment,” *Computing in Science & Engineering*, vol. 9, no. 3, pp. 90-95, 2007. doi: 10.1109/MCSE.2007.55

[75] *Delaunay triangulation* [Online]. Available:

[https://en.wikipedia.org/wiki/Delaunay\\_triangulation](https://en.wikipedia.org/wiki/Delaunay_triangulation)



[76] J. Whitaker. (2010, July 30). *NCAR natgrid library* [Online]. Available:  
<https://github.com/matplotlib/natgrid>

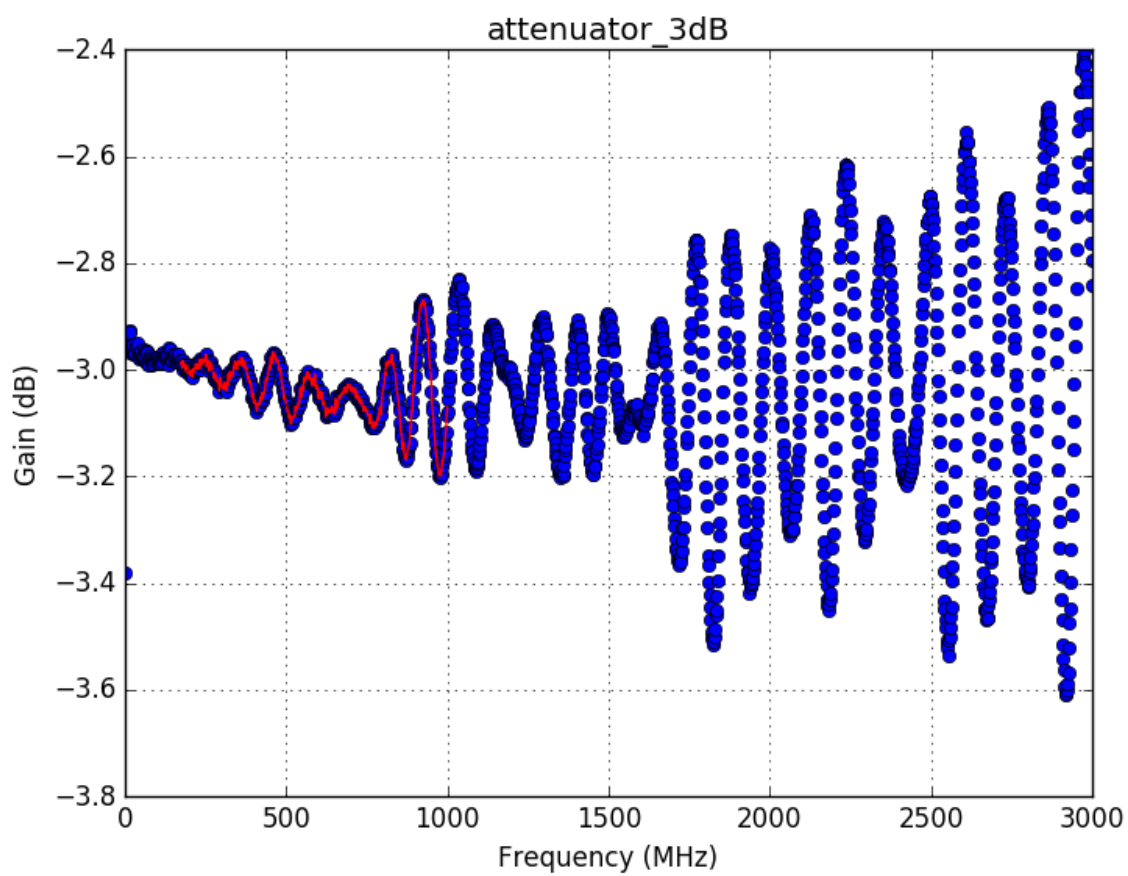
## Appendix A: Summary of Spectrum Monitoring Studies

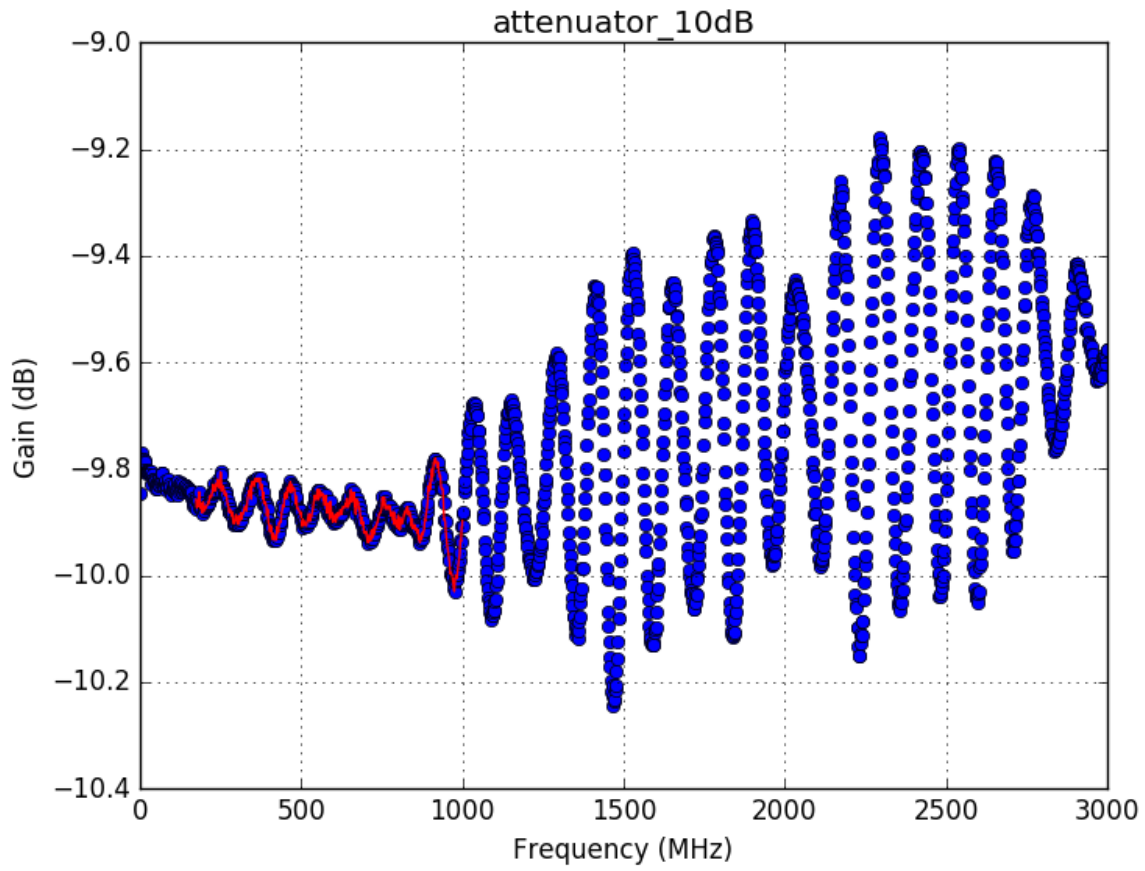
Table XXI: Summary of Spectrum Monitoring Studies

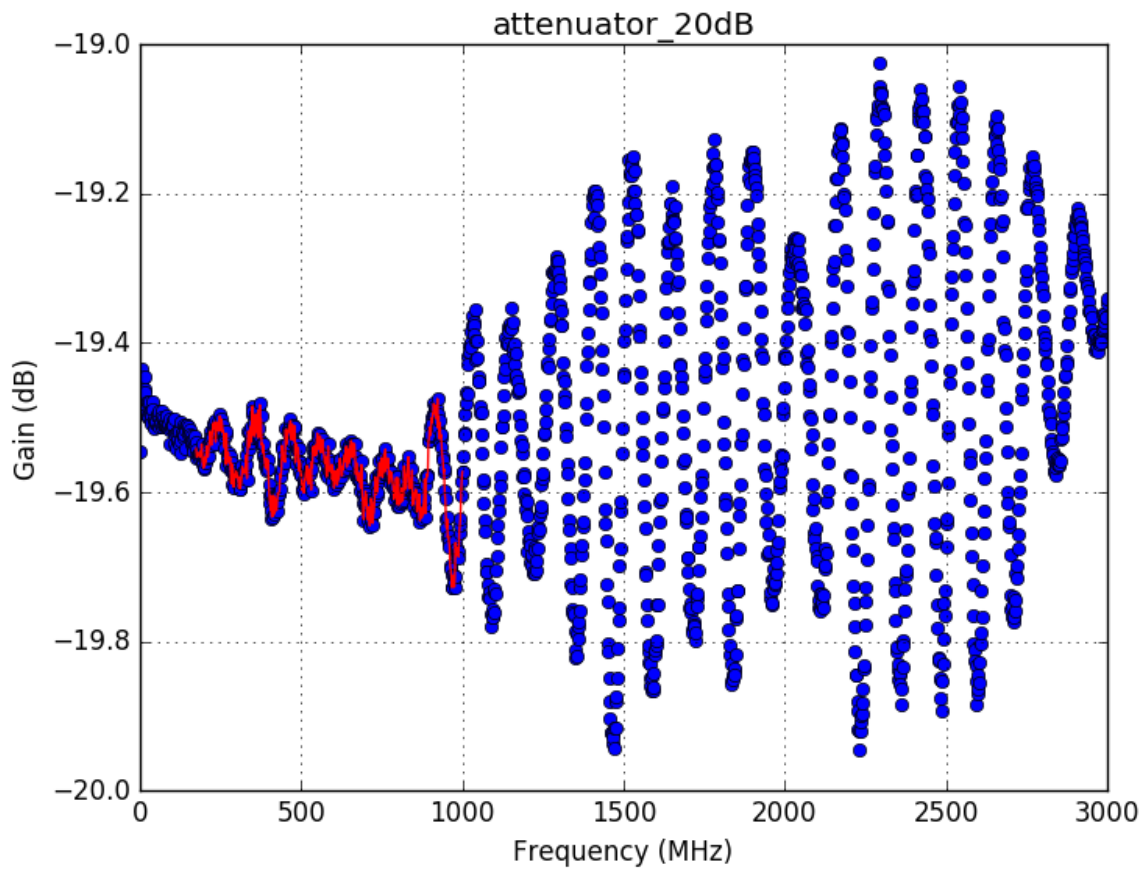
Work Cited	Location	# of Locations	Duration	Frequency Span [MHz]	RBW [kHz]	Designation
10	Virginia, USA Limestone, ME USA Dublin, Ireland Chicago, IL USA New York City, NY USA	10	1-3 days	30 – 3000 100 – 3000 30 - 2000	n/a 30 10,000 10	urban, rural
11	San Luis Potosi, Mexico	1	7.5 hours	30 – 910	1000	urban
12	Chicago, IL USA New York City, NY USA	2	2 days	30 – 3000	n/a	urban
13	Kwara, Nigeria	16	1 day	50 – 6000	n/a	urban, rural
14	Montana, USA Seattle, WA USA	13	10 mins.	140 – 1000	8	rural, urban
15	Brno, Czech Republic Paris, France	3	6 days	100 – 3000 400 – 6000 100 – 3000	3 55 55	urban, suburban,
16	Pretoria, South Africa	6	1 hour	174 – 254 470 – 854	500	urban
17	Doha, Qatar	1	3 days	700 – 3000	300	urban
18	Barcelona, Spain	1	2 days	75 – 3000	10	urban
19	Amsterdam, Netherlands	300	1 day	100 – 500	1330	urban
20	Aveiro, Portugal	1	4 days	930 – 960 1850 – 1880	100	suburban
21	Selangor, Malaysia	1	1 day	174 – 230 470 - 798 880 – 960 1710 – 1880 1885 – 2200	n/a	urban
22	Singapore	1	1 day	80 – 5850	150	urban
23	Bucharest, Romania	1	n/a	25 – 3400	300	urban
24	Columbus, OH USA	1	5 mins.	30 – 300	30	urban
25	Blacksburg, VA USA Chicago, IL USA Turku, Finland	5	1 day	30 – 130 130 – 800 650 – 1200 1200 – 3000 3000 - 6000	78 39 39 39 78	urban, suburban,
26	Czech Republic	5	Up to 4 hours Several days	700 – 2700 300 – 7000	12.5 1.25	rural, urban, suburban

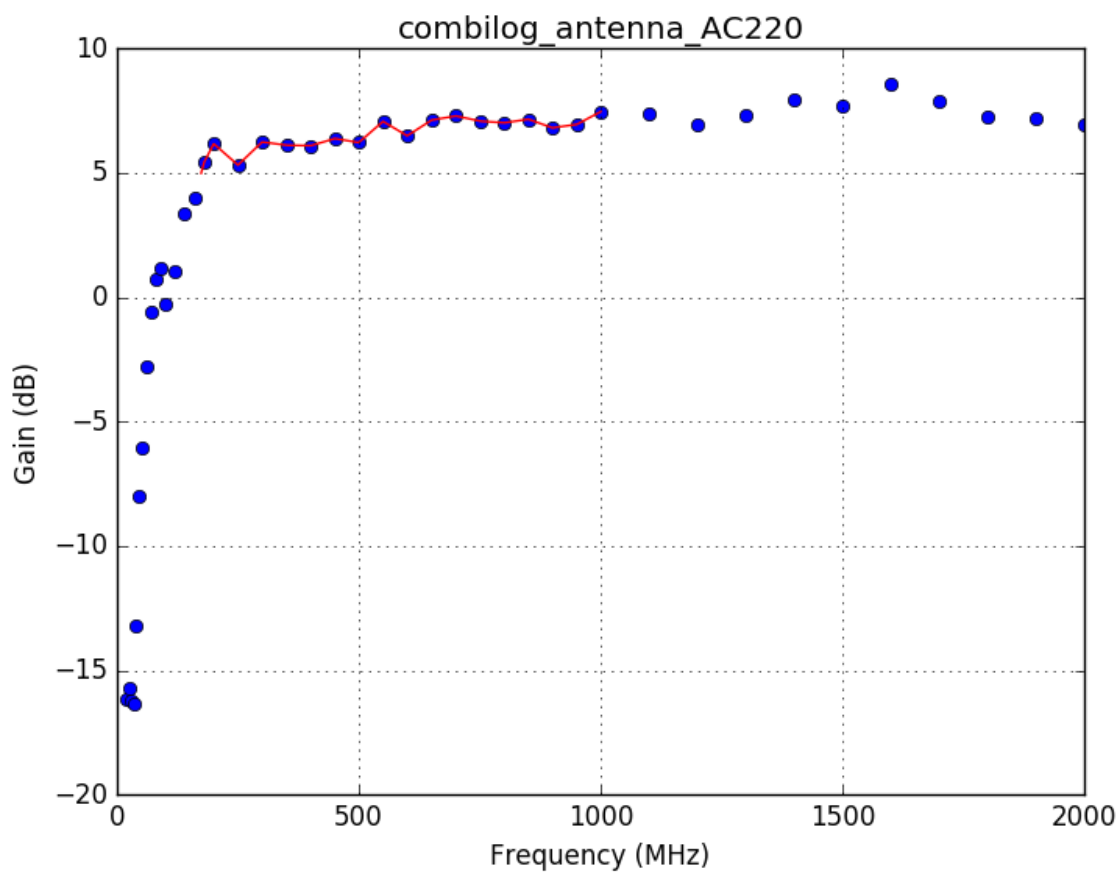
27	Guangdong, China	4	1 day	20 – 3000	200	urban, suburban
28	Atlanta, GA USA North Carolina USA	3	Several hours	400 – 7200	10	urban, suburban, rural
29	Denver, CO USA Boulder, CO USA	2	3 weeks	108 – 10,000	varies	urban
30	Chicago, IL USA	1	2 weeks	108 – 10,000	varies	urban
31	San Diego, CA USA	1	2 weeks	108 – 10,000	varies	urban
32	Chicago, IL USA	1	2007 – present 5 days	30 – 6000 150 – 174 450 – 471 820 – 869 4940 – 4990	10, 30 3, 10	urban
33	Auckland, New Zealand	2	12 weeks	806 – 2750	15 20 250	urban
34	Hull, United Kingdom	1	12 days	180 - 2700	30	urban
35	Aachen, Germany	2	7 days	20 – 6000	200	urban
36	Bristol, United Kingdom	1	6 months	300 - 4900	300	urban
This work	Montana, USA	2	2 weeks	174 – 1000	488	Rural

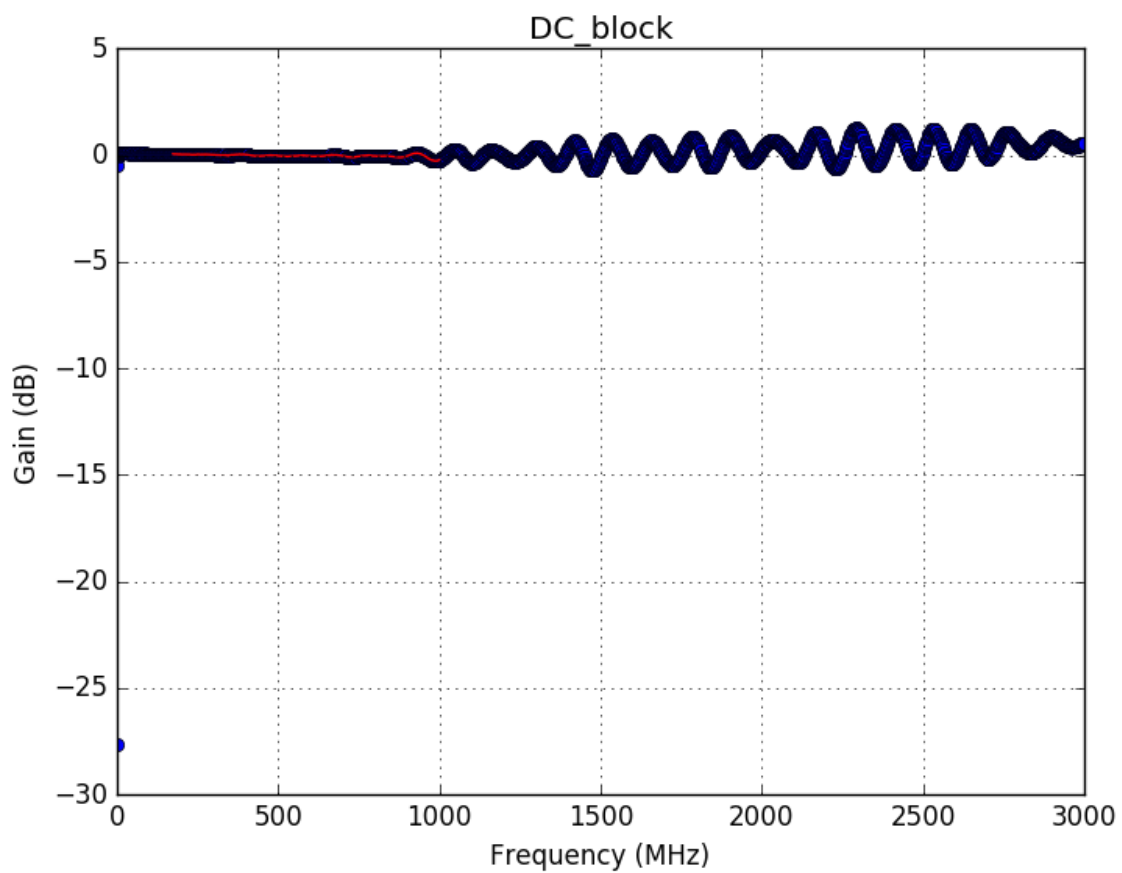
## Appendix B: S21 Measurements



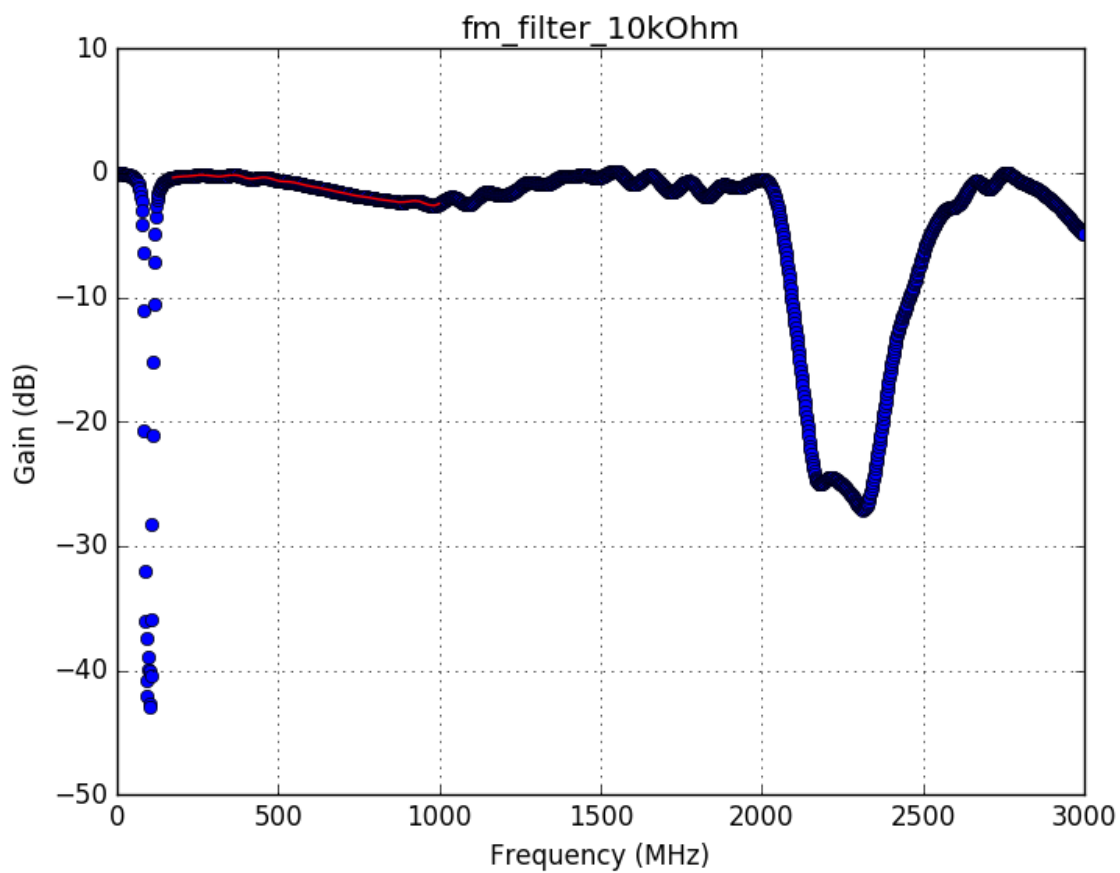


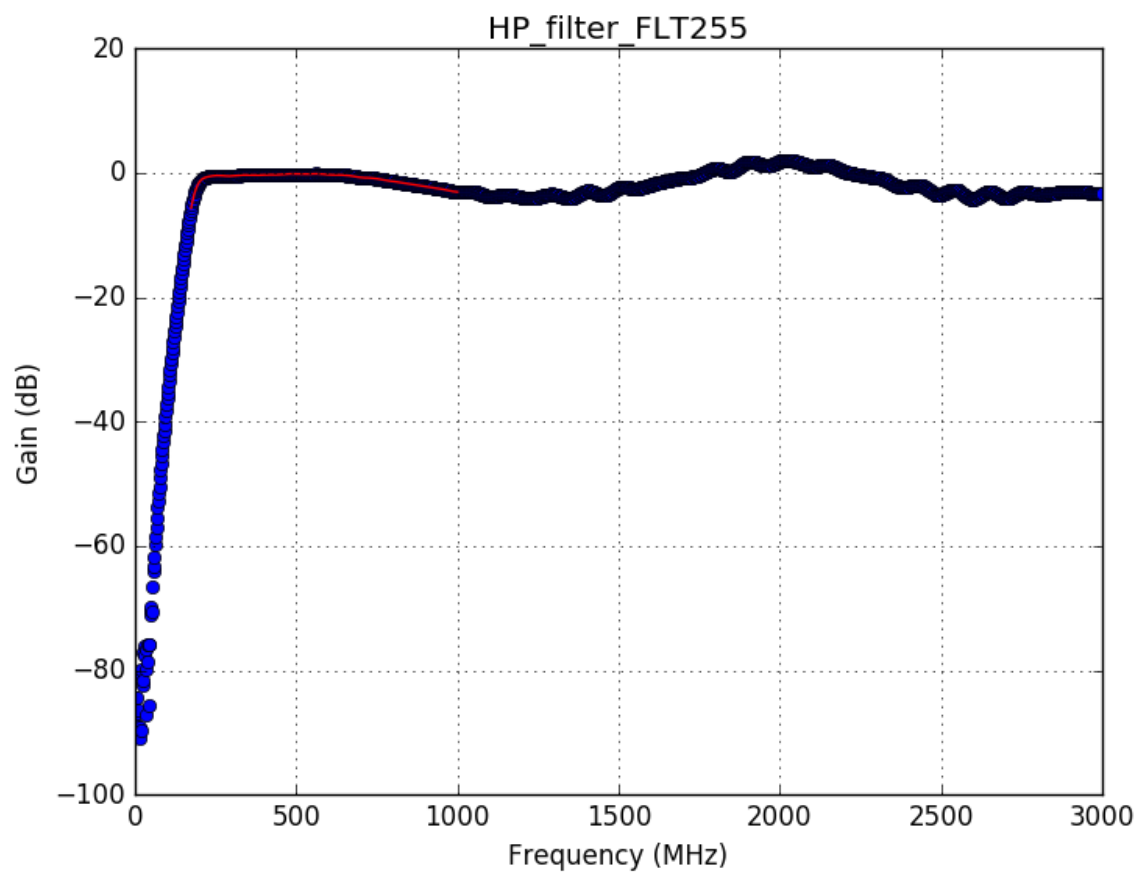


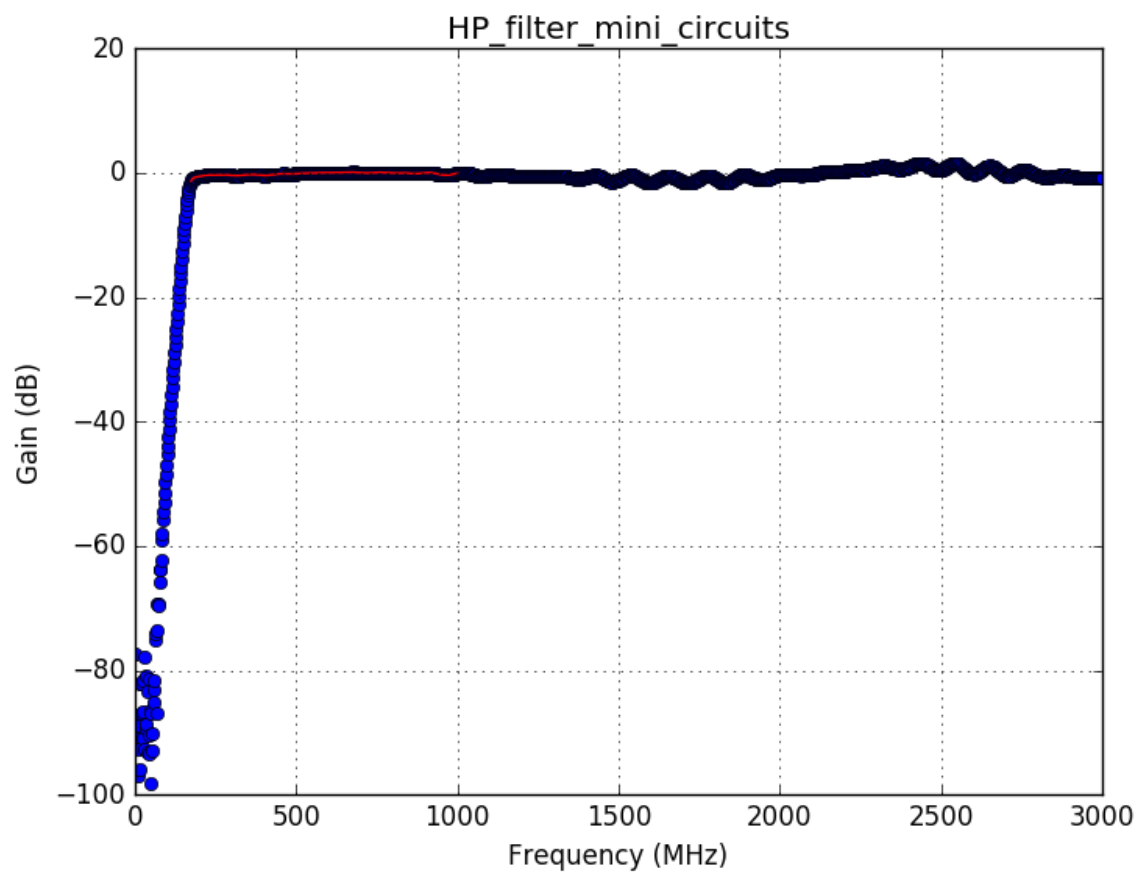


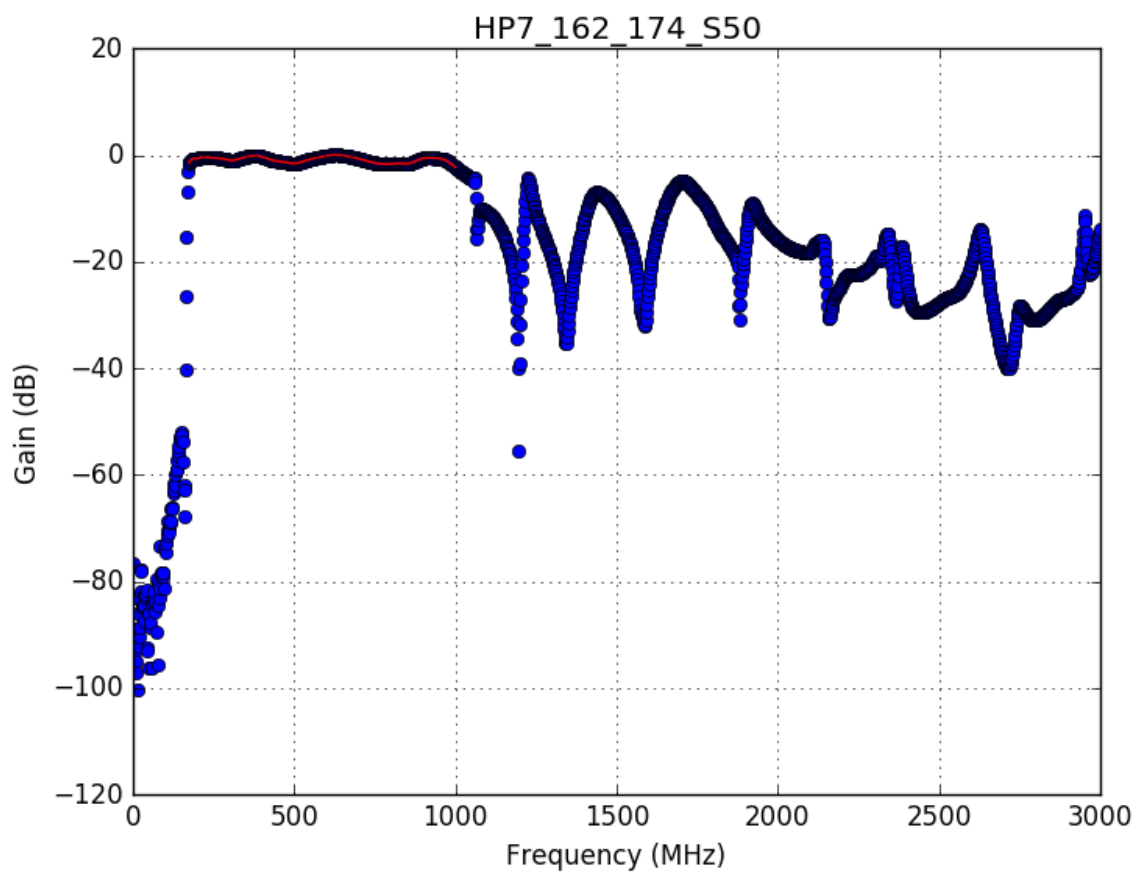


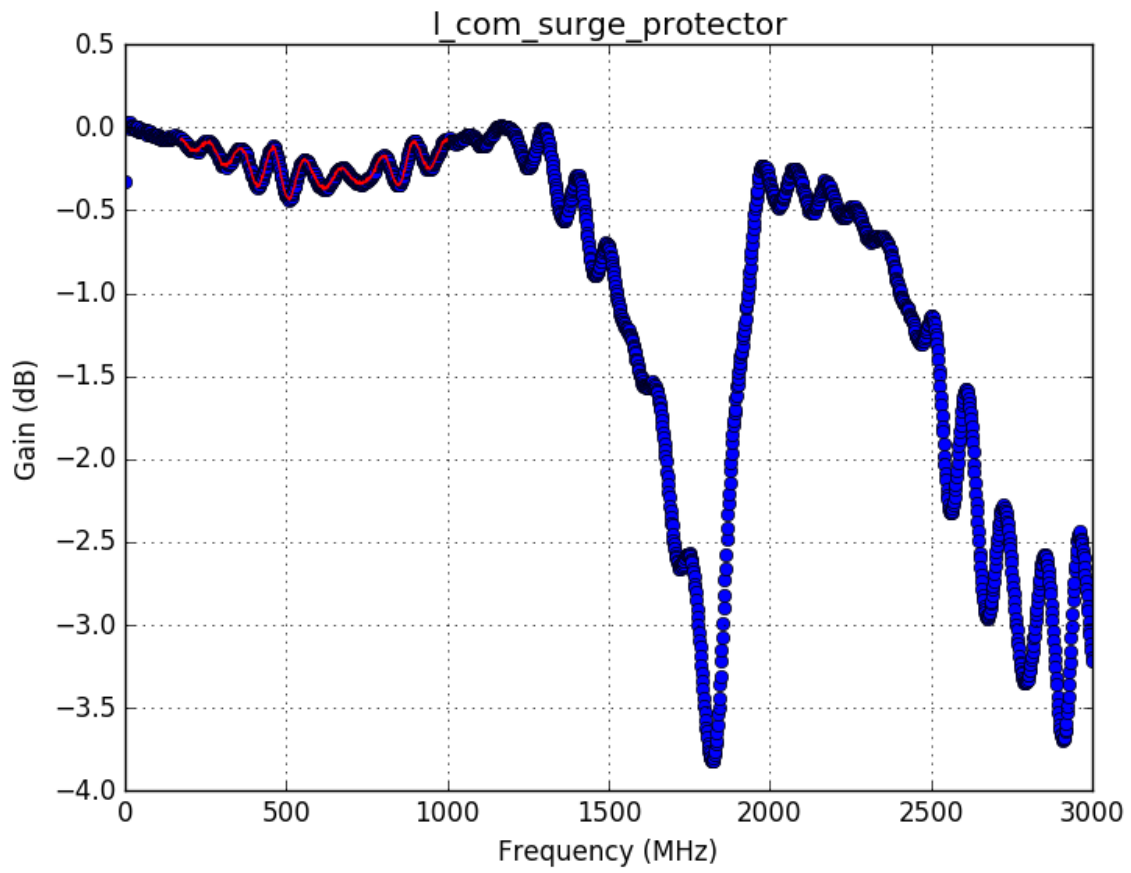


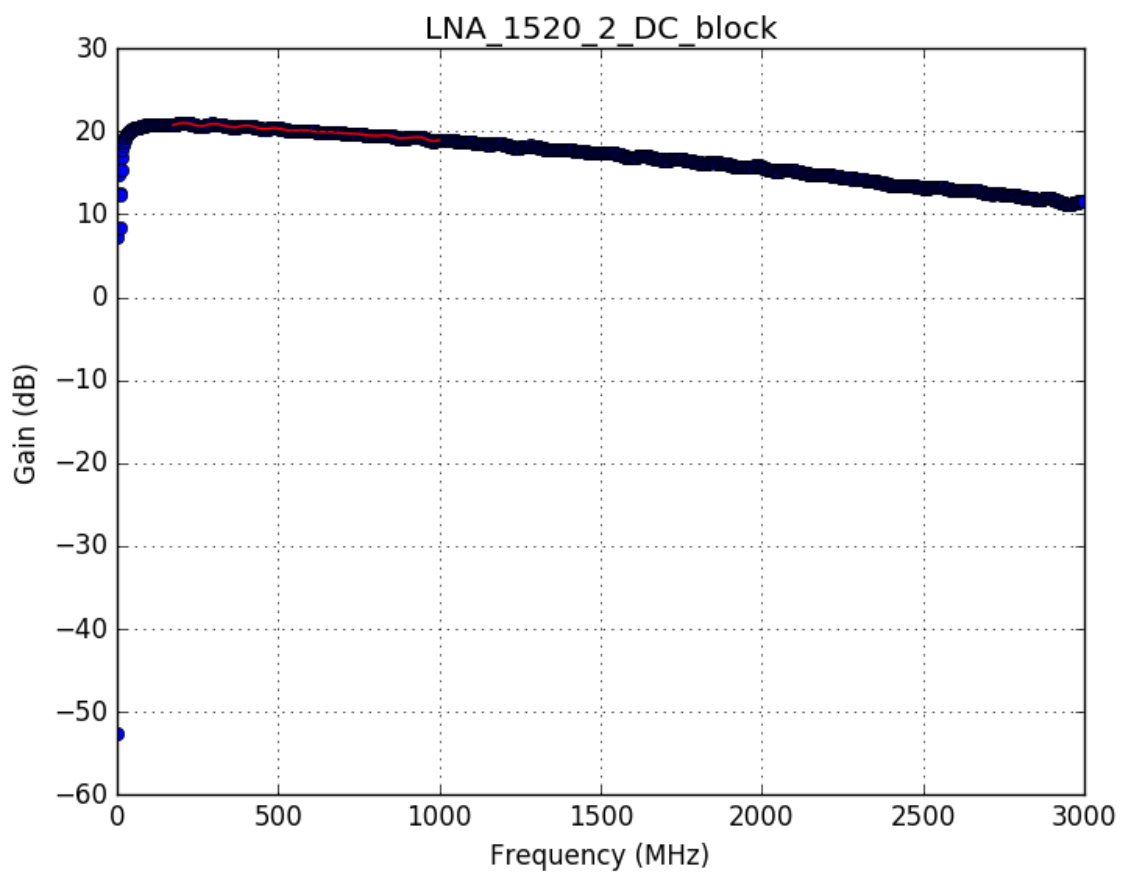


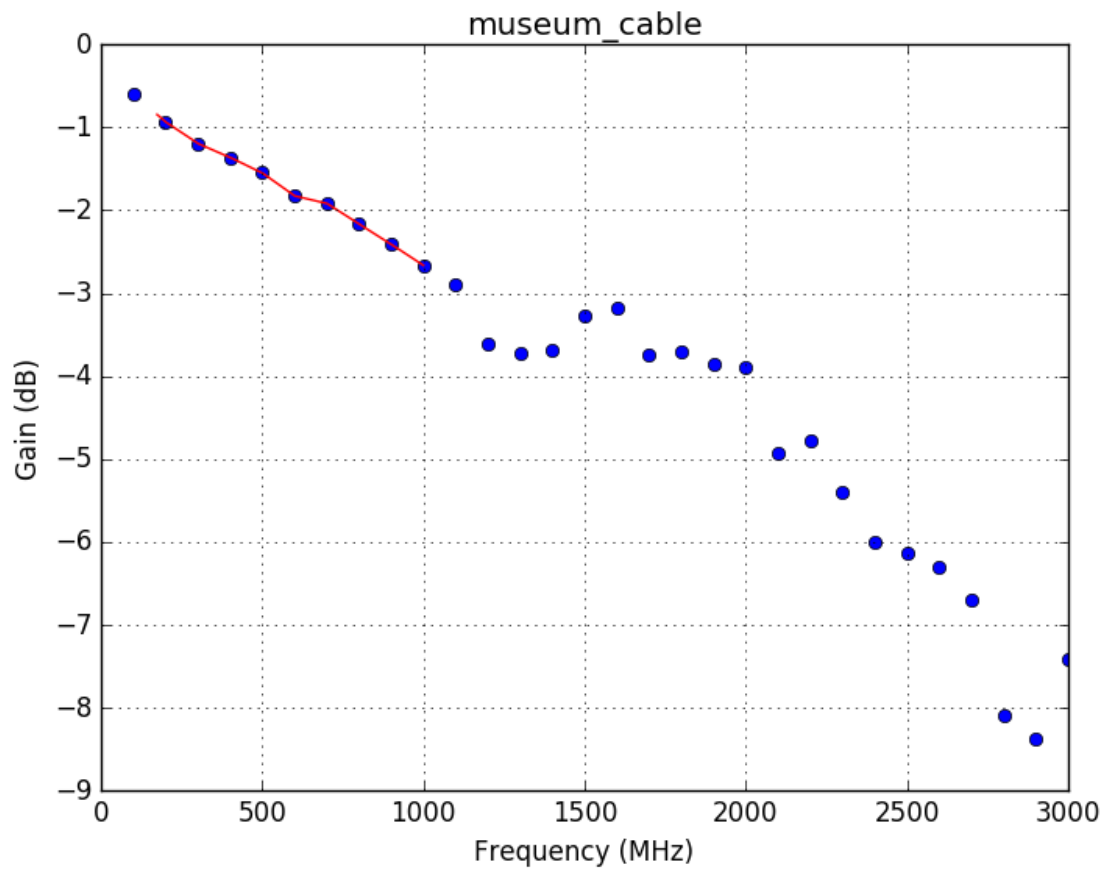


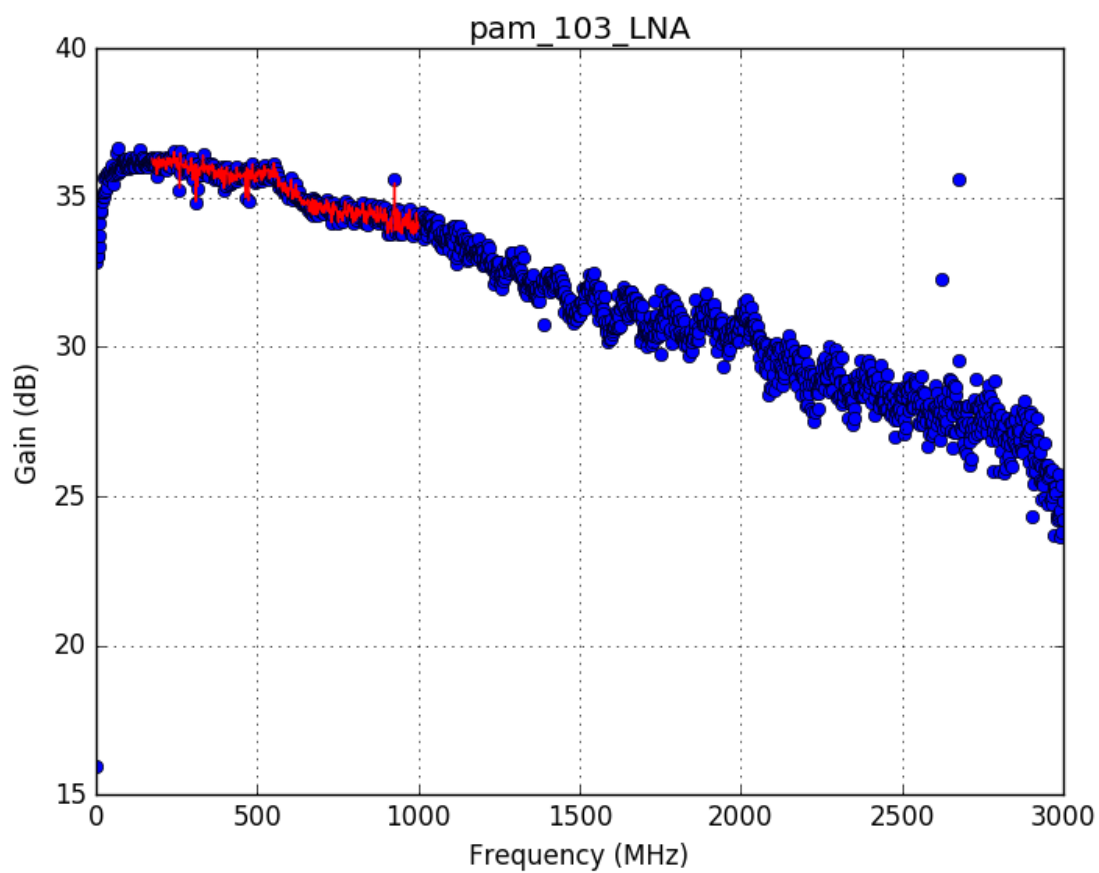














## Appendix C: Occupied Channels at Montana Tech Museum Location

Table XXII: Occupied Channels at Montana Tech Museum Location

Name	Frequency Range (MHz)	Max PSD ( $\frac{dBm}{Hz}$ )	Percent Occupancy (%)	Mean shift (dB)	Spectrum Allocation	Description
0	174.0 – 179.4	-101	3.49	8	Broadcasting	Spurious Emissions dominated channels
1	179.9 – 185.2	-114	8.73	7		
2	185.7 – 191.1	-115	5.02	6		
3	191.9 – 197.0	-108	9.49	7		
4	197.5 – 202.8	-111	5.04	6		
5	203.3 – 208.7	-109	2.03	5		
6	209.2 – 214.6	-112	1.77	5		
7	215.0 – 220.4	-103	11.01	31		
8	220.9 – 226.3	-115	2.03	13	Fixed Land Mobile	Amateur Radio 1.25 band
9	226.8 – 232.1	-118	0.85	4	Fixed Mobile	Spurious Emissions Dominated channels
10	232.6 – 238.0	-118	2.26	4		
11	238.5 – 243.7	-117	0.95	3		
12	244.4 – 249.7	-115	0.81	3		
13	250.2 – 255.6	-116	1.64	4		
14	256.1 – 261.5	-120	0.58	3		
15	261.9 – 267.3	-124	0.66	3		
16	267.8 – 273.2	-124	0.93	3		
17	273.7 – 279.0	-123	0.79	3		
18	279.5 – 284.9	-122	0.68	2		
19	285.4 – 290.8	-124	0.56	3		
20	291.3 – 296.6	-118	0.36	3		
21	297.1 – 302.5	-122	0.53	3		

23	308.8 – 314.2	–125	0.77	2		
24	314.7 – 320.1	–110	0.20	2		
26	326.4 – 331.8	–126	1.13	2		
28	338.2 – 343.5	–132	2.37	10		
40	408.5 – 413.9	–120	19.20	24	Fixed Mobile	Radio Astronomy
43	426.1 – 431.5	–111	0.04	0	Amateur	Amateur Radio
44	432.0 – 437.3	–105	0.78	9	Radiolocation	70 cm band
45	437.8 – 443.2	–104	0.01	0		
46	443.7 – 449.1	–107	0.33	2		
47	449.6 – 454.9	–106	46.94	29		
48	455.4 – 460.8	–89	0.72	17	Land Mobile	
49	461.3 – 466.7	–93	39.52	42		
50	467.1 – 472.5	–95	2.28	30		
55	496.5 – 501.8	–112	31.54	23	Fixed Land Mobile Broadcasting	TV Broadcast Channel 19
56	502.3 – 507.7	–110	81.35	32		
76	619.6 – 625.0	–114	0.19	8	Fixed Land Mobile Broadcasting	RTSA Harmonic
77	625.4 – 630.8	–111	6.10	4		
80	643.0 – 648.4	–122	71.77	25	Fixed Land Mobile Broadcasting	TV Broadcast Channel 43
81	648.9 – 654.3	–123	34.36	20		
89	695.8 – 701.2	–107	0.05	0	Fixed Land Mobile Broadcasting	AT&T LTE Uplink
90	701.7 – 707.0	–102	0.16	1		
91	707.5 – 712.9	–107	0.13	1		
93	719.2 – 724.6	–119	7.76	5	Fixed Land Mobile Broadcasting	LTE band 29 unpaired downlink
94	725.1 – 730.5	–113	13.64	19		(carrier aggregation)

95	731.0 – 736.3	–84	73.71	49	Fixed Land Mobile Broadcasting	AT&T LTE
96	736.8 – 742.2	–84	71.71	52		Downlink
97	742.7 – 748.1	–89	36.19	42		
97	742.7 – 748.1	–89	36.19	42	Fixed Land Mobile Broadcasting	Verizon LTE
98	748.6 – 753.9	–88	97.25	48		Downlink
99	754.4 – 759.8	–90	48.32	43		
103	777.9 – 783.2	–111	0.48	1	Fixed Land Mobile Broadcasting	Verizon LTE
104	783.7 – 789.1	–114	0.34	1		Uplink
109	813.0 – 818.4	–126	0.48	3	Fixed Land Mobile Broadcasting	2G/3G Uplink
111	824.8 – 830.1	–105	2.77	3		Public Safety Radio Systems
112	830.6 – 836.0	–112	3.20	3		
113	836.5 – 841.9	–97	0.40	1		
114	842.3 – 847.7	–104	0.31	1		
115	848.2 – 853.6	–115	0.25	1		
118	865.8 – 871.2	–93	35.47	36	Fixed Land Mobile Broadcasting	Public Safety Radio Systems
119	871.7 – 877.1	–93	99.80	41		2G/3G Downlink
120	877.5 – 882.9	–96	91.75	42		
121	883.4 – 888.8	–96	99.96	46		
122	889.3 – 894.6	–92	90.91	44		
123	895.1 – 900.5	–113	11.26	17	Fixed Land Mobile Radiolocation	ISM
124	901.0 – 906.4	–110	5.31	8		RFID
125	906.9 – 912.2	–109	8.55	8		Amateur 33-cm band (secondary)
126	912.7 – 918.1	–114	19.90	11		Low-power unlicensed devices
127	918.6 – 924.0	–111	20.85	11		
128	924.4 – 929.8	–112	12.22	13		
131	942.0 – 947.4	–123	4.71	3	Fixed	Aural Broadcast
132	947.9 – 953.3	–116	36.34	12		Auxiliary Stations
133	953.8 – 959.1	–106	0.42	3		RFID

## Appendix D: SPLAT! User Control

Basic command-line instructions are pictured in Figure 99. To use SPLAT! in point-to-point mode, one needs to specify the Tx and Rx with the `-t` and `-r` switch respectively that reference the name, coordinates and antenna height in the `*.qth` file. The default is imperial units, so the metric switch must be used, `-metric` to return SI units. ITM is specified with the `-olditm` switch. Each SRTM file type has its own directory whose path is specified with the `-d` switch. The `*.lrp` contains the irregular terrain parameters and shares the name of the Tx designated in the `splat` command.

```
erin@museum-VM:~/splat/splat_prjs/grid/butte$ splat -t KWYB.qth -r Tech-Museum.qth
-metric -olditm -d $path

--==[ Welcome To SPLAT! v1.4.2 ]==--

Loading "/home/erin/splat/SRTM3/46:47:112:113.sdf" into page 1... Done!
Site analysis report written to: "KWYB-site_report.txt"
Path Loss Report written to: "KWYB-to-Tech-Museum.txt"
```

Figure 99: SPLAT! Command Line for ITM non-HD

The required elevation files are found and loaded into memory, then a Tx site report is generated. This report returns the coordinates, ground elevation and antenna heights. The path loss report is of most interest in Figure 100.

--=[ SPLAT! HD v1.4.2 Path Analysis ]=--

-----  
 Transmitter site: KWYB  
 Site location: 46.0067 North / 112.4417 West (46° 0' 24" N / 112° 26' 30" W)  
 Ground elevation: 2476.00 meters AMSL  
 Antenna height: 86.30 meters AGL / 2562.30 meters AMSL  
 Distance to Tech-Museum: 8.91 kilometers  
 Azimuth to Tech-Museum: 272.90 degrees  
 Depression angle to Tech-Museum: -5.0584 degrees  
 -----

Receiver site: Tech-Museum  
 Site location: 46.0107 North / 112.5569 West (46° 0' 38" N / 112° 33' 24" W)  
 Ground elevation: 1766.00 meters AMSL  
 Antenna height: 17.00 meters AGL / 1783.00 meters AMSL  
 Distance to KWYB: 8.91 kilometers  
 Azimuth to KWYB: 92.82 degrees  
 Elevation angle to KWYB: +4.9786 degrees  
 -----

Longley-Rice Parameters Used In This Analysis:

Earth's Dielectric Constant: 15.000  
 Earth's Conductivity: 0.005 Siemens/meter  
 Atmospheric Bending Constant (N-units): 301.000 ppm  
 Frequency: 503.000 MHz  
 Radio Climate: 5 (Continental Temperate)  
 Polarization: 1 (Vertical)  
 Fraction of Situations: 50.0%  
 Fraction of Time: 50.0%  
 Transmitter ERP: 46.000 kilowatts (+76.63 dBm)  
 Transmitter EIRP: 75.294 kilowatts (+78.77 dBm)  
 -----

Summary For The Link Between KWYB and Tech-Museum:

KWYB antenna pattern towards Tech-Museum: 0.495 (-6.10 dB)  
 Free space path loss: 105.49 dB  
 Longley-Rice path loss: 105.43 dB  
 Attenuation due to terrain shielding: -0.06 dB  
 Total path loss including KWYB antenna pattern: 111.54 dB  
 Field strength at Tech-Museum: 98.52 dBuV/meter  
 Signal power level at Tech-Museum: -32.77 dBm  
 Signal power density at Tech-Museum: -47.26 dBW per square meter  
 Voltage across a 50 ohm dipole at Tech-Museum: 6577.71 uV (76.36 dBuV)  
 Voltage across a 75 ohm dipole at Tech-Museum: 8056.02 uV (78.12 dBuV)  
 Mode of propagation: Line-Of-Sight Mode  
 Longley-Rice model error number: 0 (No error)  
 -----  
 -----

No obstructions to LOS path due to terrain were detected by SPLAT! HD

The first Fresnel zone is clear.

60% of the first Fresnel zone is clear.

---

**Figure 100: SPLAT! Path Loss Report**

If there were obstructions, SPLAT! lists their coordinates, distance from Rx and the elevation. Then it gives the required height of the antenna heights for the Rx to clear the obstruction as pictured in Figure 101:

```
-----
Between Tech-Museum and K27CD-D, SPLAT! HD detected obstructions at:
```

```
46.0186 N, 112.5441 W, 1.32 kilometers, 1781.00 meters AMSL
46.0187 N, 112.5439 W, 1.34 kilometers, 1784.00 meters AMSL
46.0189 N, 112.5437 W, 1.37 kilometers, 1787.00 meters AMSL
46.0190 N, 112.5434 W, 1.39 kilometers, 1789.00 meters AMSL
46.0192 N, 112.5432 W, 1.42 kilometers, 1790.00 meters AMSL
46.0193 N, 112.5429 W, 1.44 kilometers, 1790.00 meters AMSL
46.0194 N, 112.5427 W, 1.47 kilometers, 1793.00 meters AMSL
46.0196 N, 112.5425 W, 1.49 kilometers, 1798.00 meters AMSL
46.0197 N, 112.5422 W, 1.51 kilometers, 1798.00 meters AMSL
46.0199 N, 112.5420 W, 1.54 kilometers, 1802.00 meters AMSL
46.0200 N, 112.5418 W, 1.56 kilometers, 1803.00 meters AMSL
46.0202 N, 112.5415 W, 1.59 kilometers, 1807.00 meters AMSL
46.0203 N, 112.5413 W, 1.61 kilometers, 1808.00 meters AMSL
46.0205 N, 112.5411 W, 1.64 kilometers, 1812.00 meters AMSL
46.0208 N, 112.5406 W, 1.68 kilometers, 1815.00 meters AMSL
46.0210 N, 112.5401 W, 1.73 kilometers, 1818.00 meters AMSL
```

```
Antenna at Tech-Museum must be raised to at least 1916.51 meters AGL
to clear all obstructions detected by SPLAT! HD.
```

```
Antenna at Tech-Museum must be raised to at least 2090.86 meters AGL
to clear the first Fresnel zone.
```

```
Antenna at Tech-Museum must be raised to at least 2021.06 meters AGL
to clear 60% of the first Fresnel zone.
```

**Figure 101: SPLAT! Path Loss Report if Obstruction Detected**

To run an HD prediction, change the path to the SRTM1 directory, then add `-hd` after the `splat` call as pictured in Figure 102 below:

```
erin@museum-VM:~/splat/splat_prjs/grid/butte$ path=/home/erin/splat/SRTM1
erin@museum-VM:~/splat/splat_prjs/grid/butte$ splat-hd -t KQWB.qth -r Tech-Museum.qth
-metric -olditm -d $path
```

**Figure 102: SPLAT! Command Line for ITM HD**

Optional parameters are antenna pattern for azimuth and elevation. Most antenna patterns (in the azimuth direction) can be found on the FCC TV Query database [59]. These antenna patterns are normalized field strength patterns, which span from 0 to 1. Elevation patterns do not appear to be available publically. This work extracted these files, then generated an interpolation

to meet SPLAT!'s structure requirements. Figure 103 depicts the antenna pattern for KWYB in Butte. The rest of the known antenna patterns may be found in Appendix E.

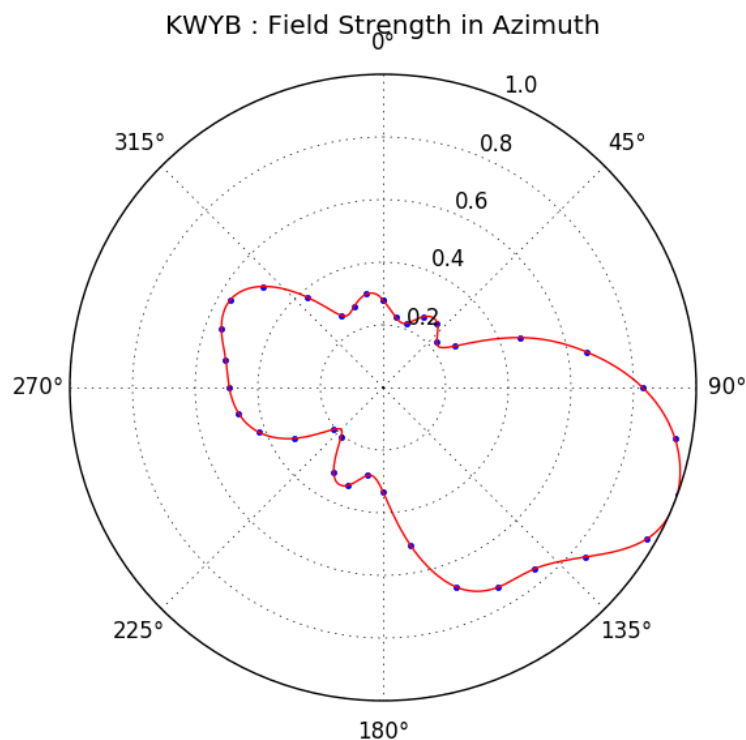


**Figure 103: KWYB Normalized Field Strength in Azimuth**

To determine the loss in decibel due to orientation, treat the normalized field strength like voltage measurements:

$$G_{azimuth}[dB] = 10 \times \log_{10}(E_{azimuth}^2) \quad (67)$$

Since a large set of path loss predictions were required for this work and SPLAT! is used from the command line, various bash scripts were employed. Only the basic structure of one, `run_grid.sh` will be discussed in detail. This script is pictured in Figure 104.

```

#!/bin/bash

mode=non-hd
mode=hd

# Extension
q=.qth

mapfile -t TX_array < TX_names.txt
mapfile -t RX_array < RX_names.txt
mapfile -t bug < buggy_loc.txt

for TX in ${TX_array[@]}
do
  for RX in ${RX_array[@]}
  do
    flag=0
    for rx in ${bug[@]}
    do
      if [ $rx == $RX ]
      then
        flag=1
      fi
    done

    if [ $flag == 0 ]
    then
      if [ $mode == hd ]
      then
        # Path to SDF files
        path=/home/erin/splat/SRTM1
        splat-hd -t $TX$q -r $RX$q -metric -olditm -d $path
      else
        path=/home/erin/splat/SRTM3
        splat -t $TX$q -r $RX$q -metric -olditm -d $path
      fi
    fi
  done
done

```

Figure 104: Example SPLAT! Bash Script

SPLAT! will generate a site report for each Tx and Rx combination.

The average path loss was found for WK9XUC operating at 500 MHz and 560 MHz. For most locations, the maximum difference was 3 dB and the average difference was 2 dB. Once the receive power is determined for the Rx location on the grid. The SNR was determined for the TV stations, and the SINR was determined by adjusting the power level of WK9XUC.



The names of the Tx are stored in a text file called Tx\_names.txt, the names of the Rx are stored in text file, Rx\_names.txt. Each site has its own line. Figure 105 depicts the Rx\_names file of the first 22 sites in the Butte grid. The Haversine formula was used to create these grids (Equation 41).

```
Butte_000
Butte_001
Butte_002
Butte_003
Butte_004
Butte_005
Butte_006
Butte_007
Butte_008
Butte_009
Butte_010
Butte_011
Butte_012
Butte_013
Butte_014
Butte_015
Butte_016
Butte_017
Butte_018
Butte_019
Butte_020
Butte_021
Butte_022
```

**Figure 105: Rx\_names.txt Example**

These names and location files may be generated by the user or some scripting program. One unresolved bug is that certain latitudes cause the SPLAT! program to hang indefinitely. Known latitudes are listed in the Table XXIII.

**Table XXIII: Incompatible Latitudes for SPLAT!**

Latitude
47.1111°
46.9333°
46.4000°
44.0000°

Any Rx located at one of these latitudes is saved to file called `buggy_loc.txt` and the bash script will raise a flag that prevents the SPLAT! program from being called.

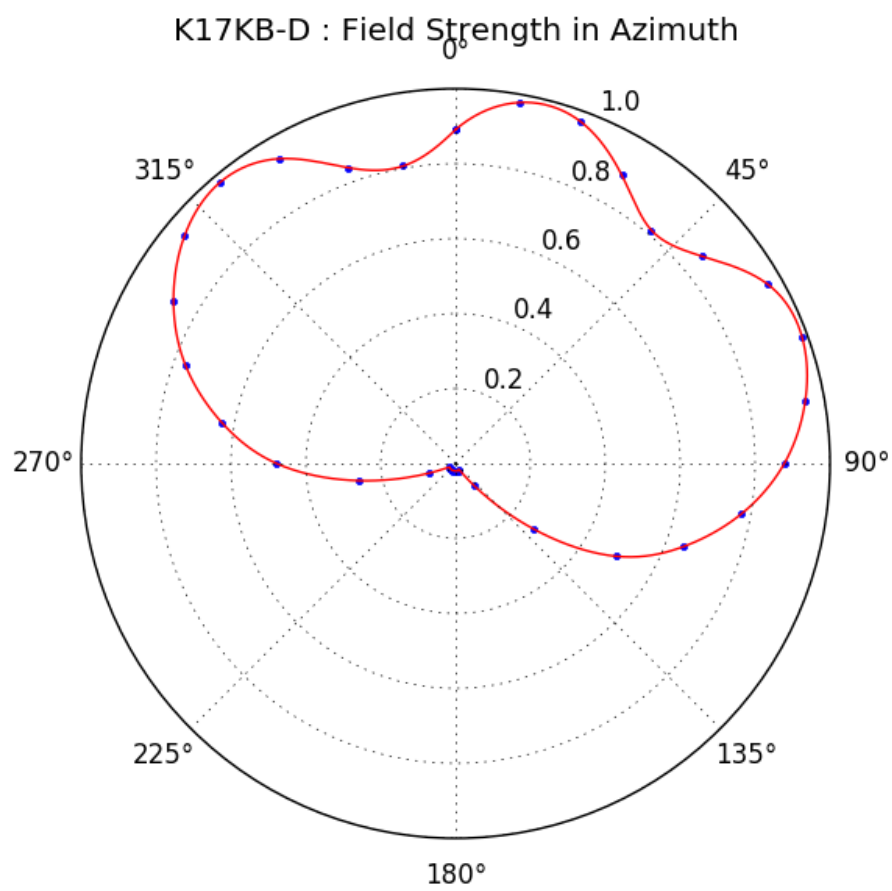
To run a bash file from the command line permission must first be given to make the bash script executable (`chmod +x`), then simply call the bash file in the current working folder as pictured below in Figure 106.

```
erin@museum-VM:~/splat/splat_prjs/grid/boulder$ chmod +x ./run_grid.sh
erin@museum-VM:~/splat/splat_prjs/grid/boulder$ ./run_grid.sh
```

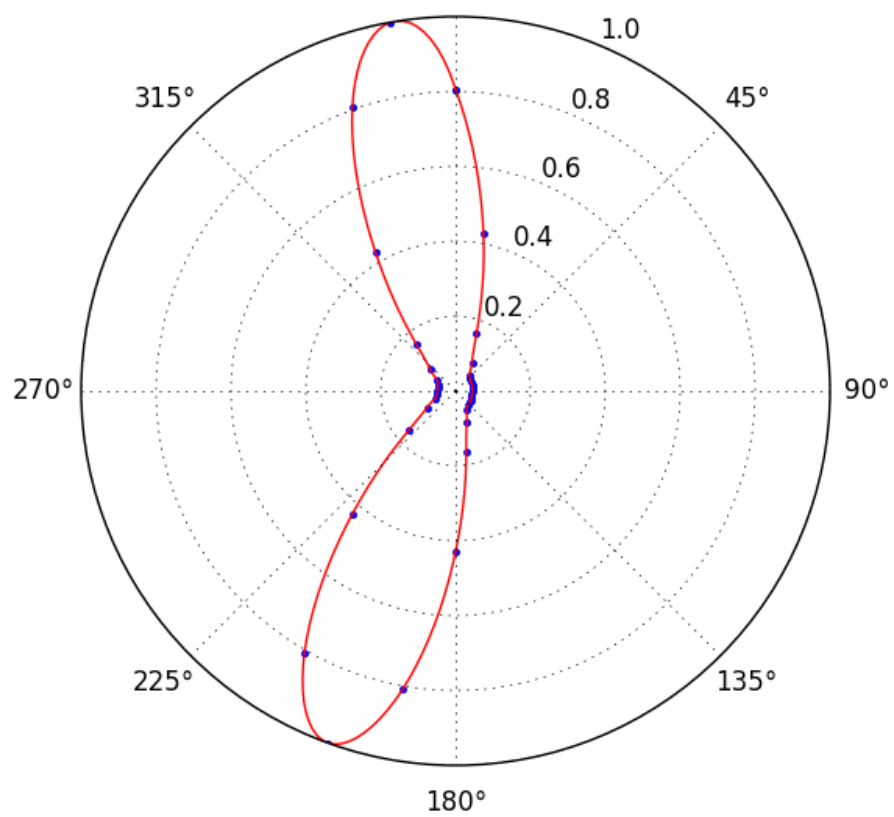
**Figure 106: Grant Permission and Run Bash Script**

This work employs another python script, `read_report.py` to parse the report for the path loss prediction and gain loss due to azimuth pattern of the TV transmitter. These variables are used to determine the received power at the Rx. It finds the appropriate string, then converts it to a numerical value and saves it to binary file.

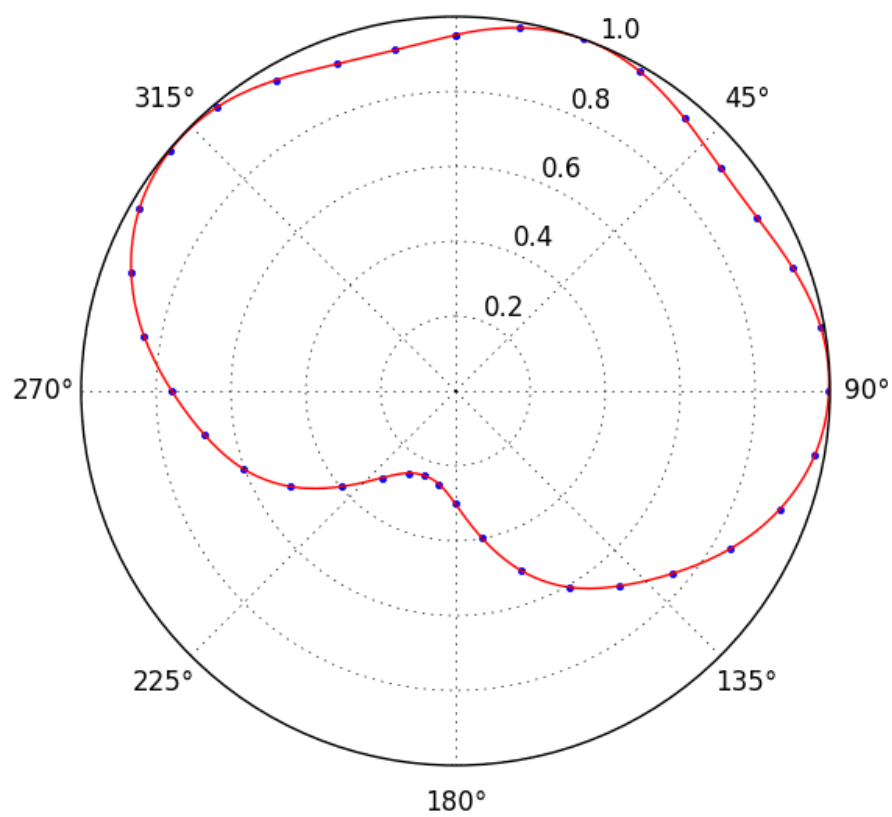
## Appendix E: Antenna Patterns

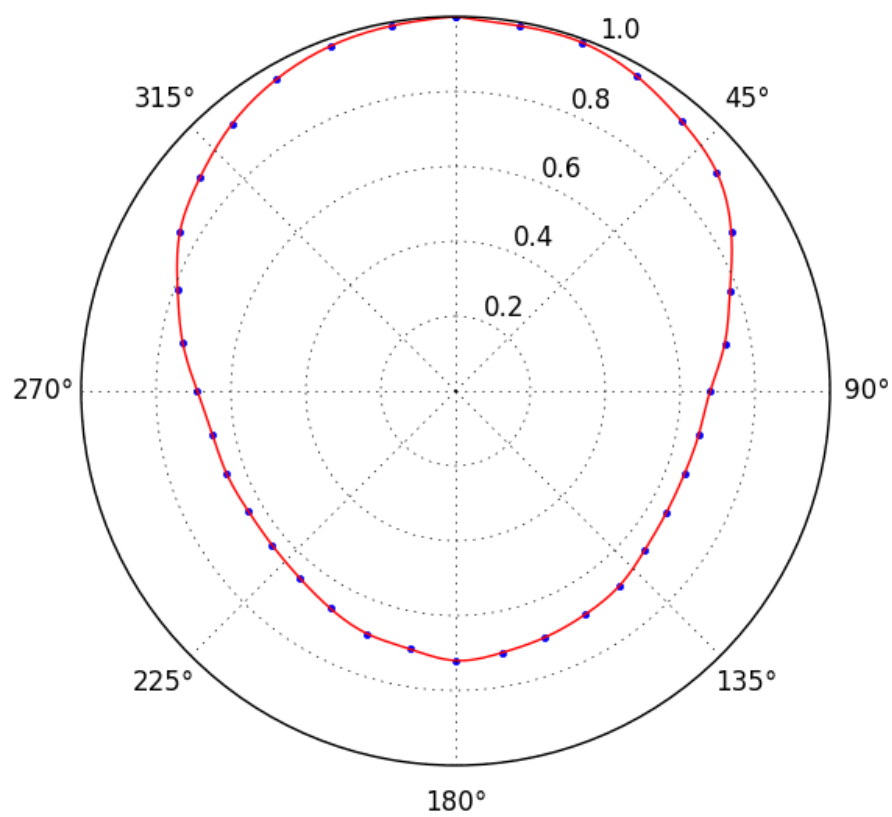


K20KQ-D : Field Strength in Azimuth

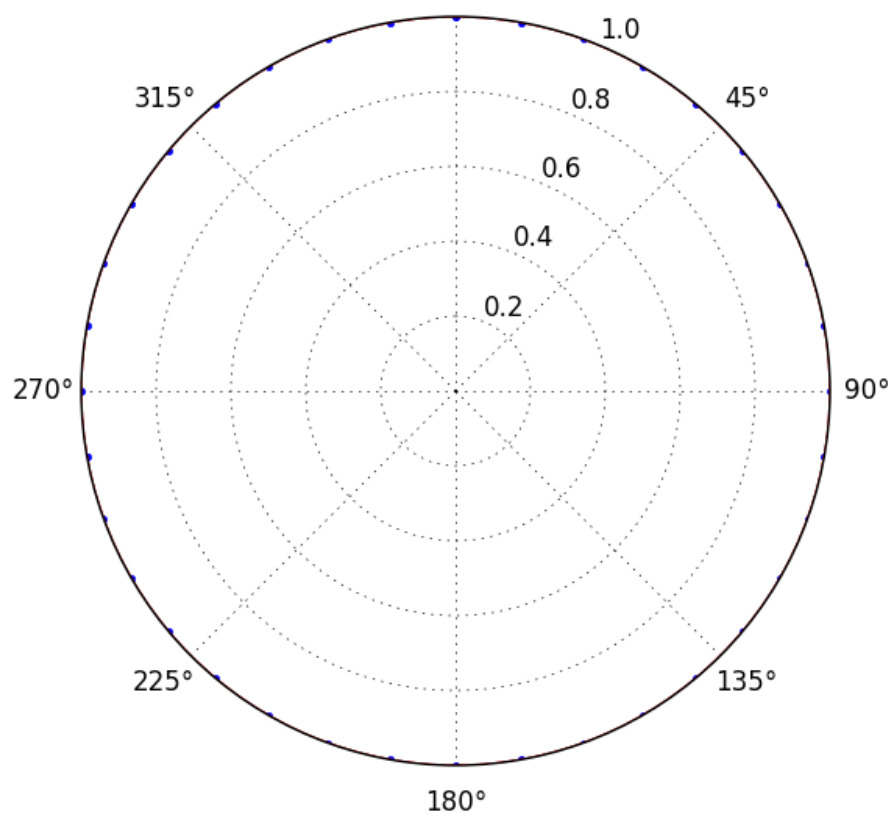


K26DE-D : Field Strength in Azimuth

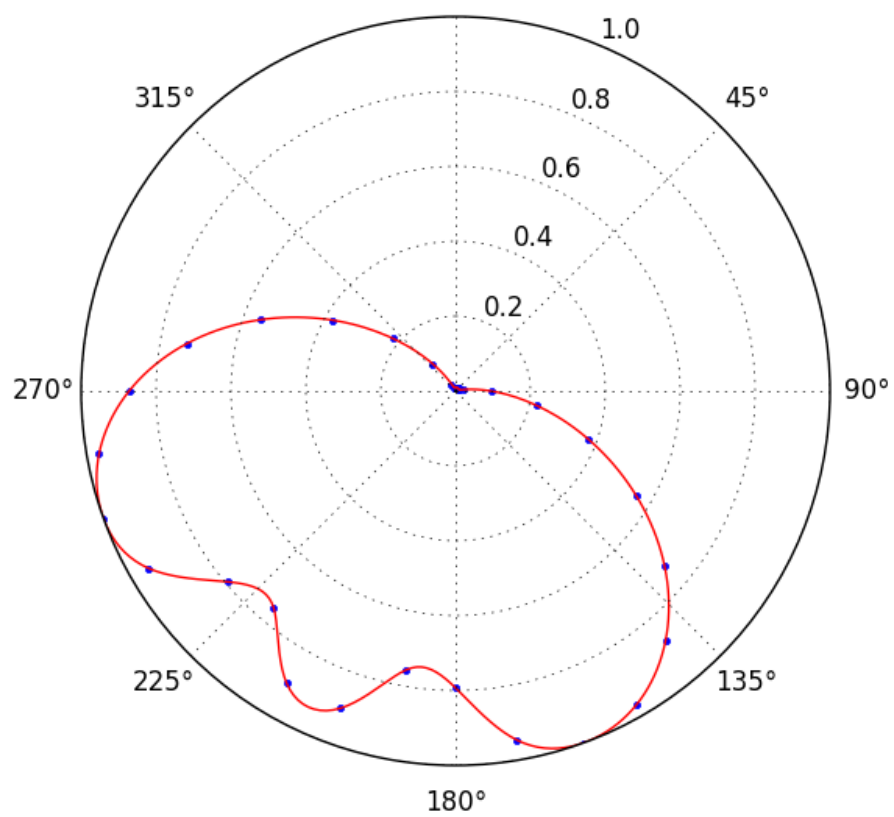


K27CD-D : Antenna<sub>0</sub> Pattern in Azimuth

K31KR-D : Antenna Pattern in Azimuth

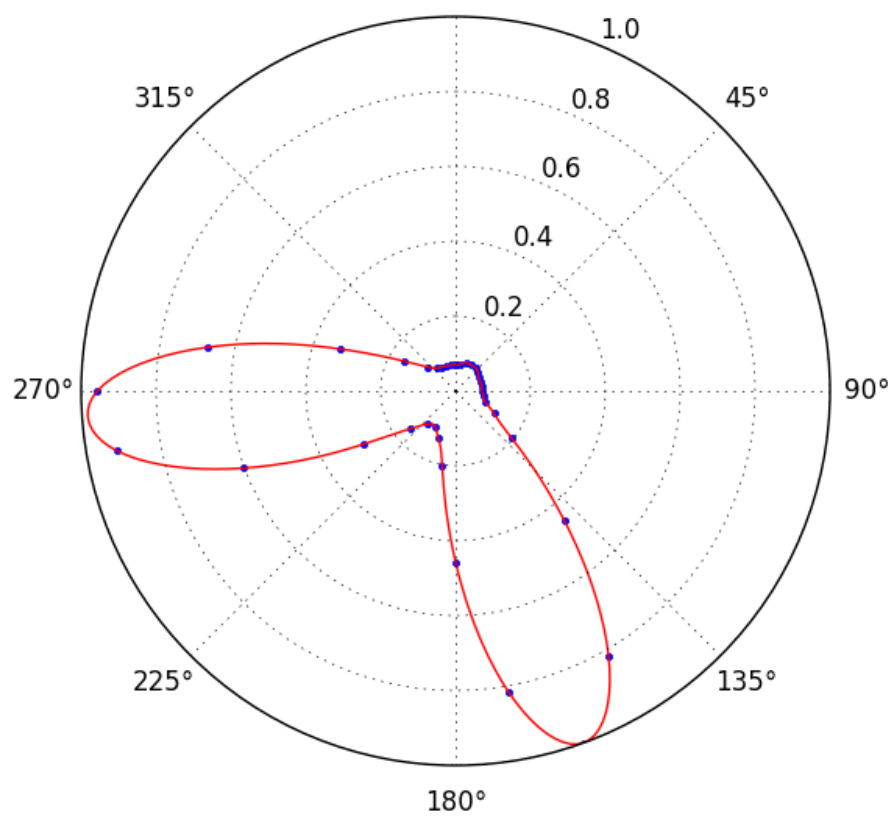


K39JC-D : Field Strength in Azimuth

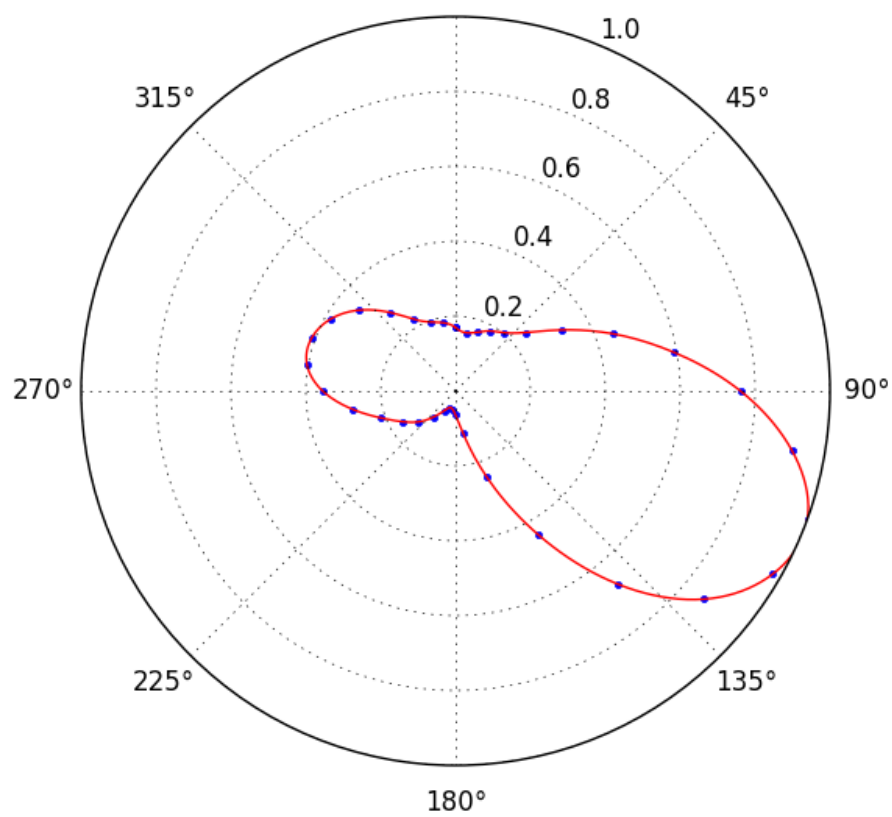




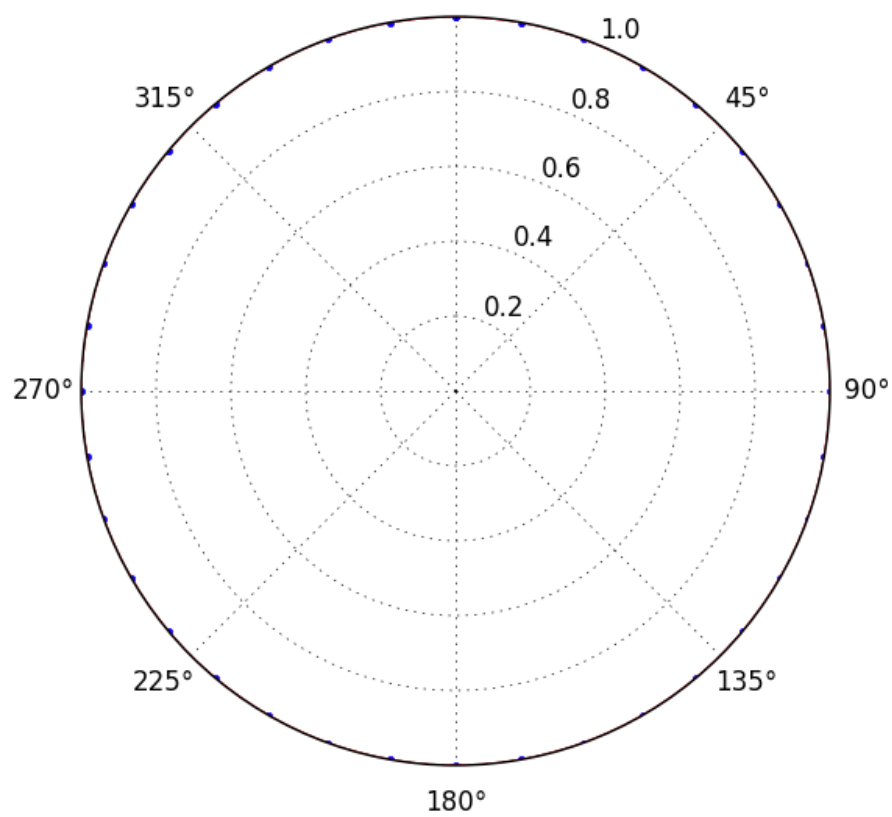
K40HL-D : Antenna Pattern in Azimuth



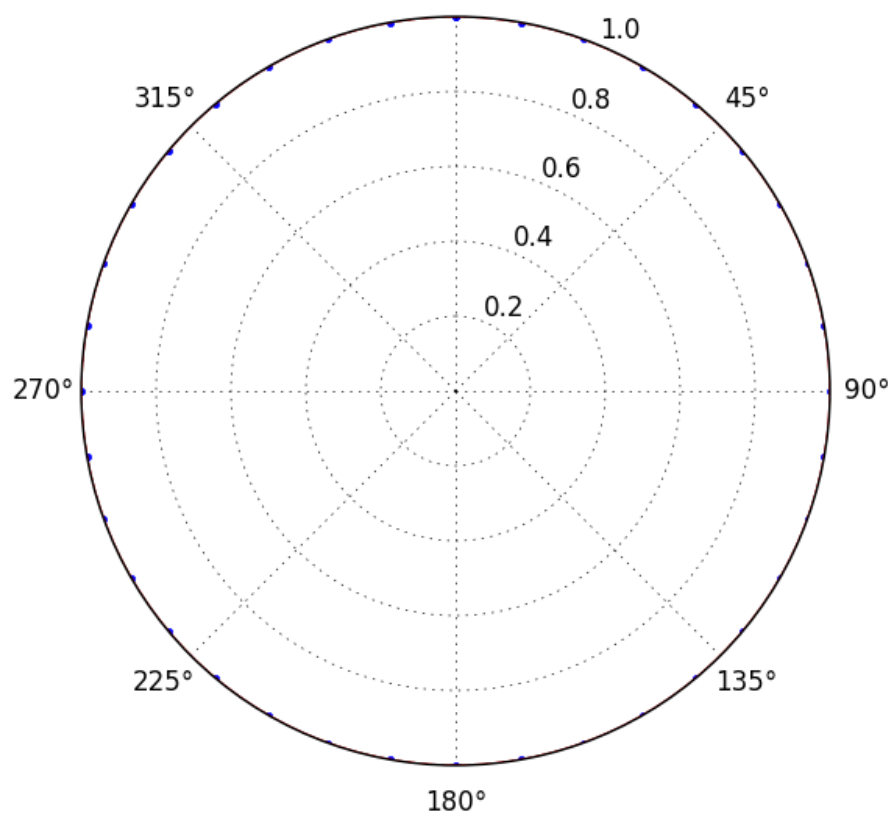
K43DU-D : Field Strength in Azimuth



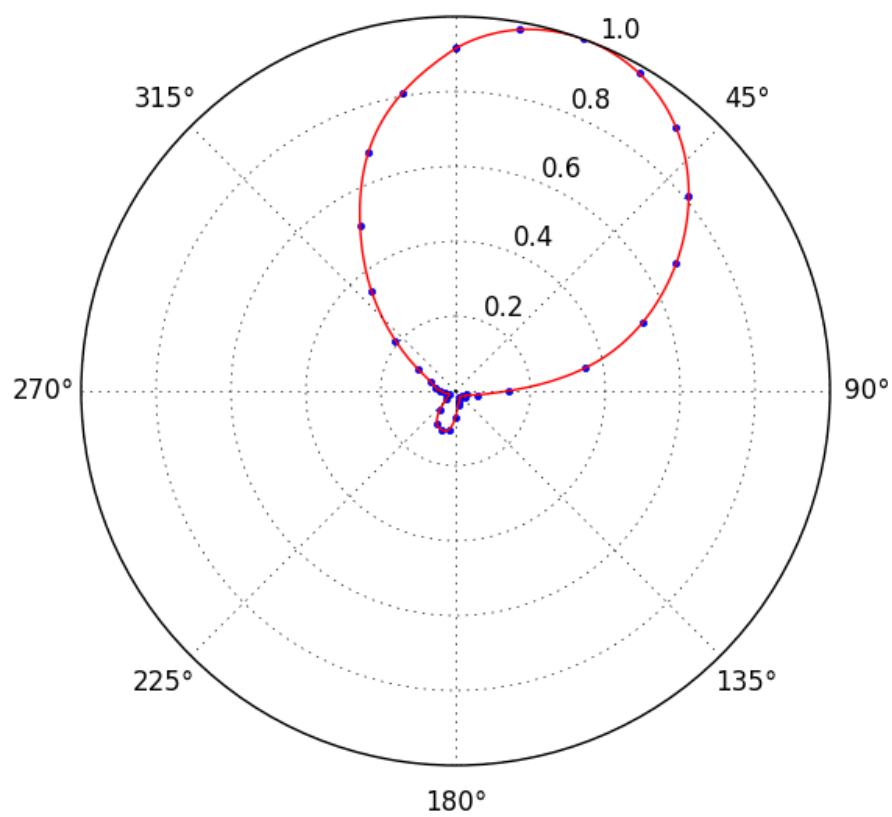
K44JW-D : Antenna Pattern in Azimuth



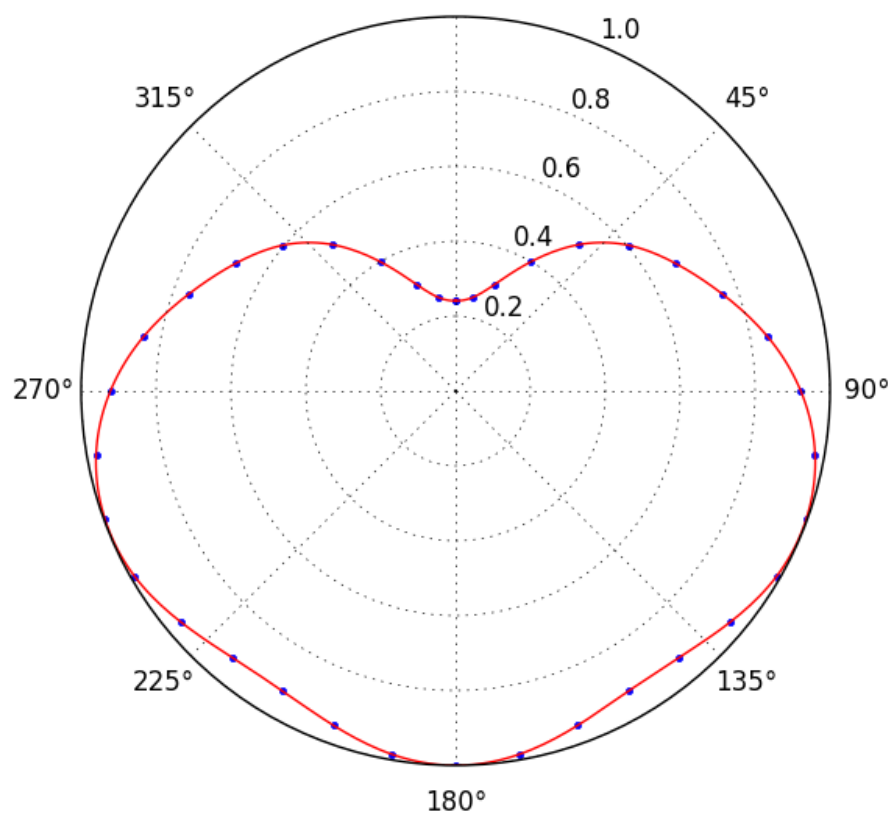
K48LV-D : Antenna Pattern in Azimuth



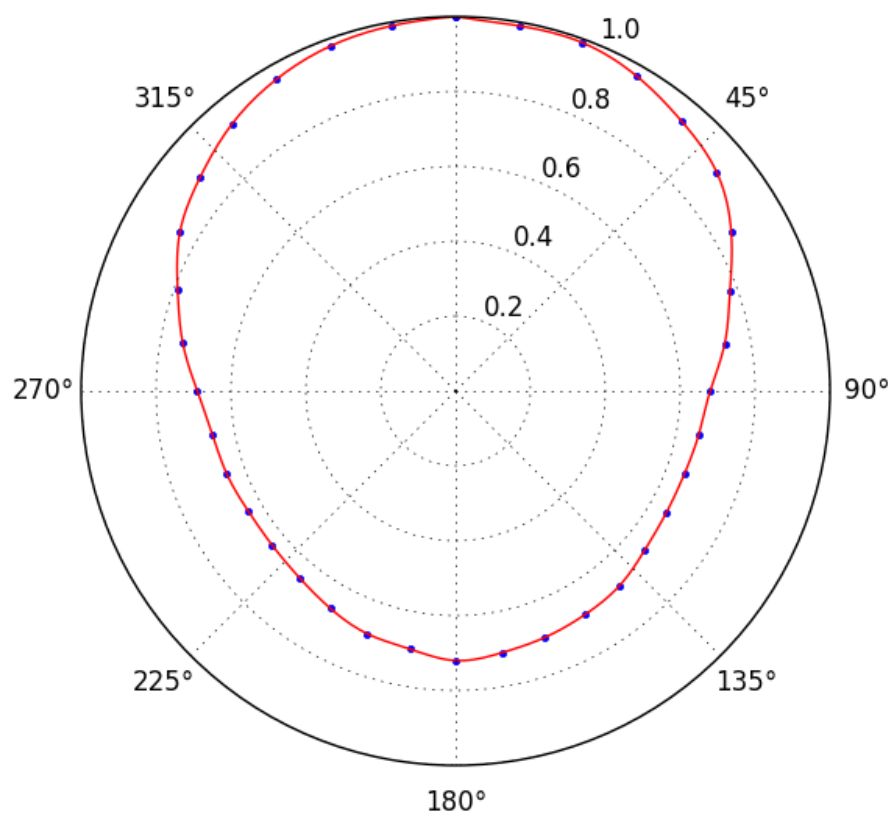
K48MM-D : Field Strength in Azimuth



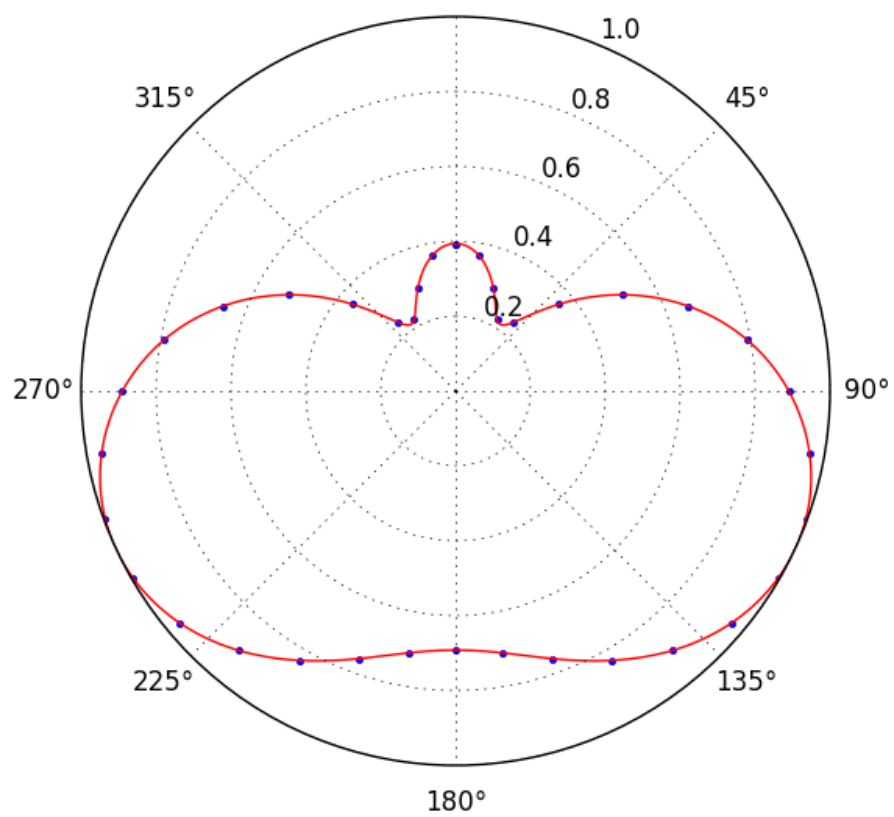
K49EH-D : Field Strength in Azimuth



K49KA-D : Antenna Pattern in Azimuth

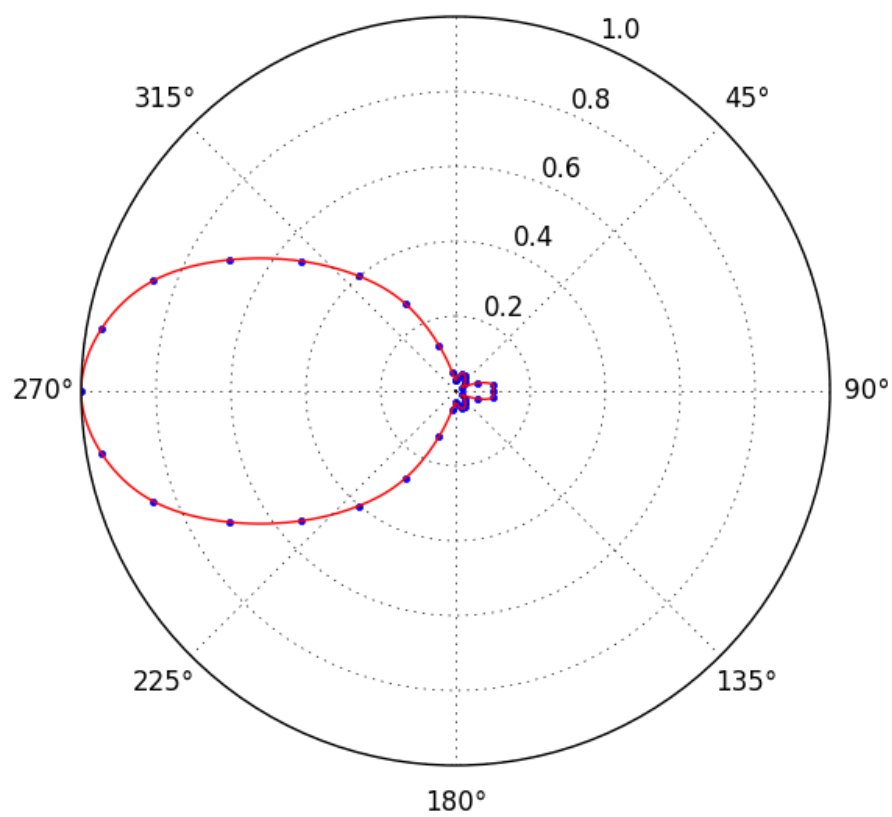


KBGF-LD : Field Strength in Azimuth

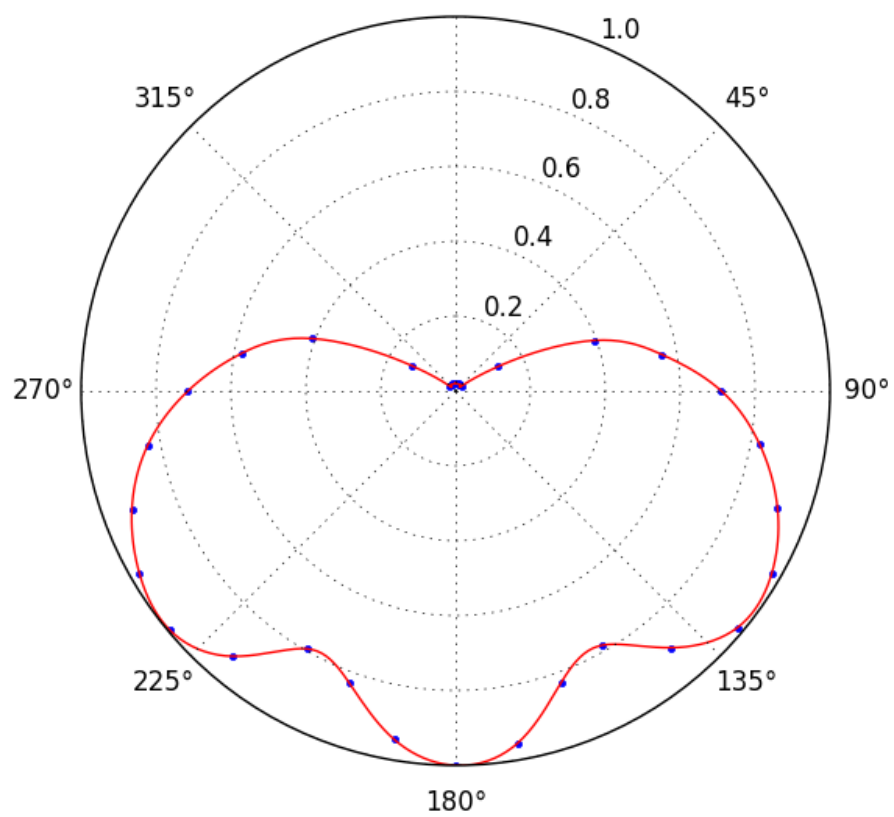




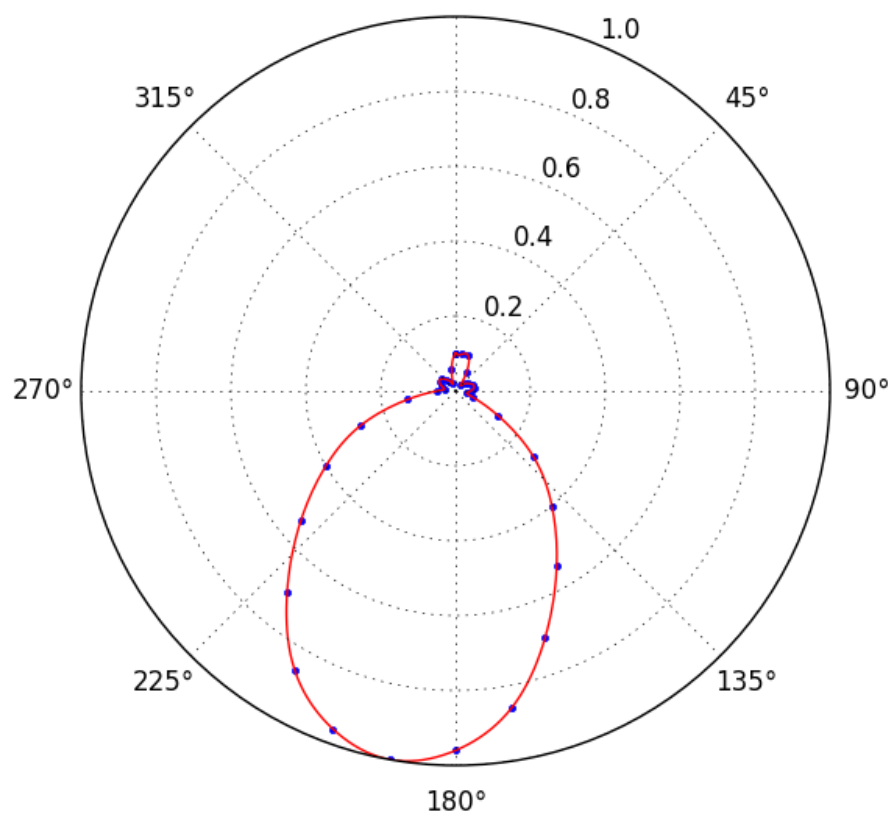
KDBZ-CD : Field Strength in Azimuth



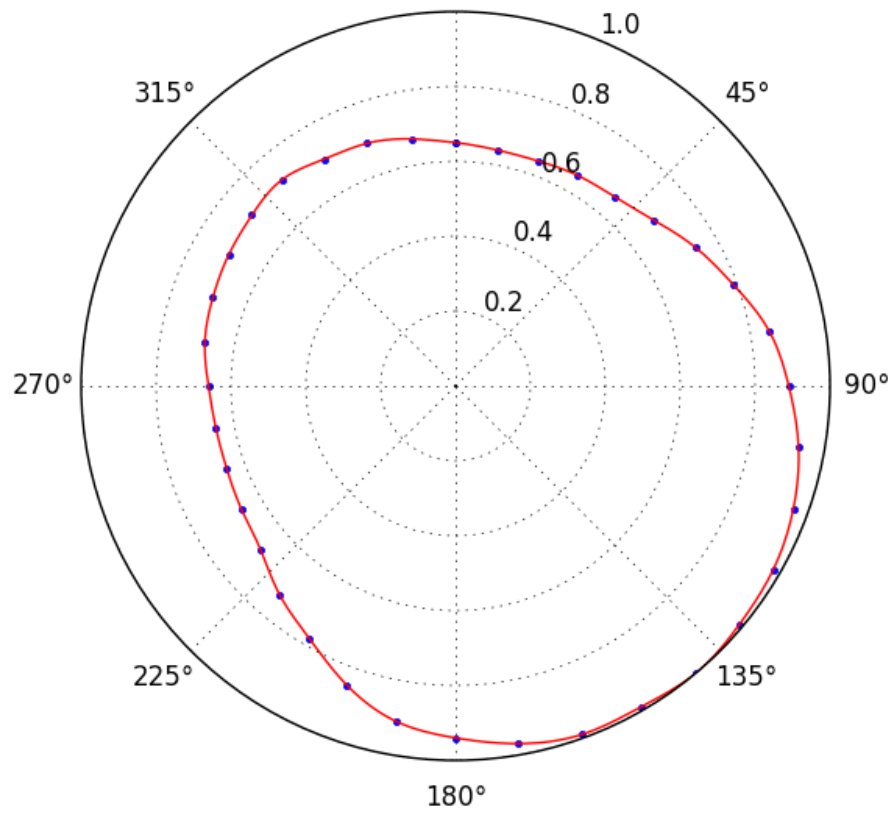
KHBB-LD : Field Strength in Azimuth

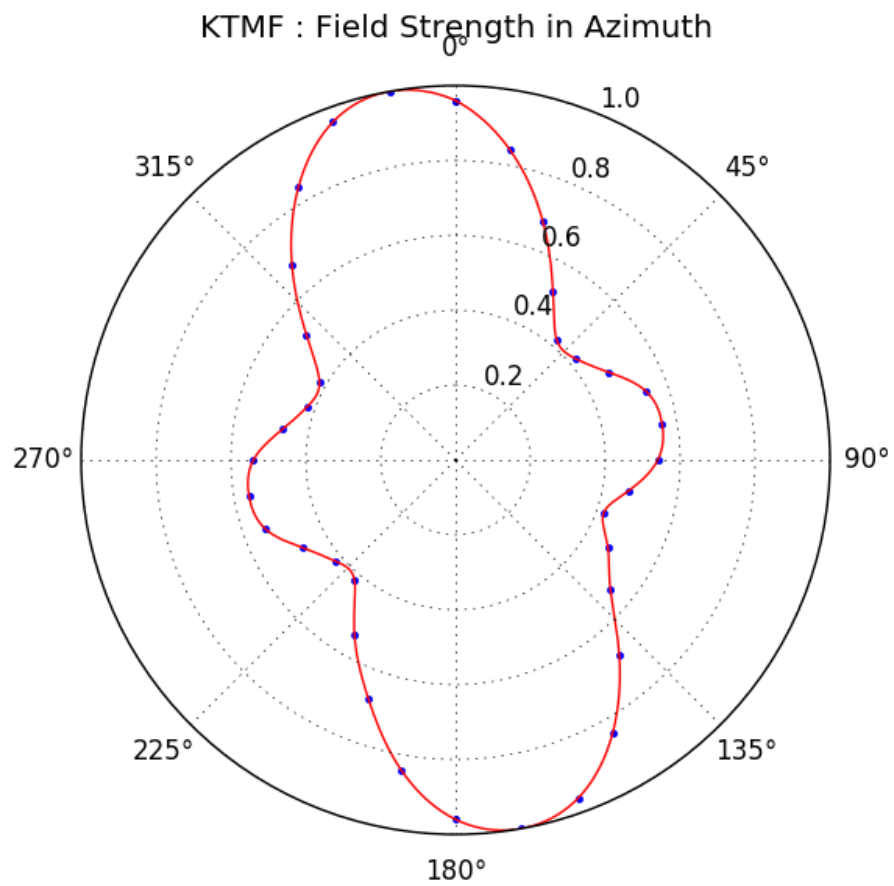


KSKC-CD : Field Strength in Azimuth

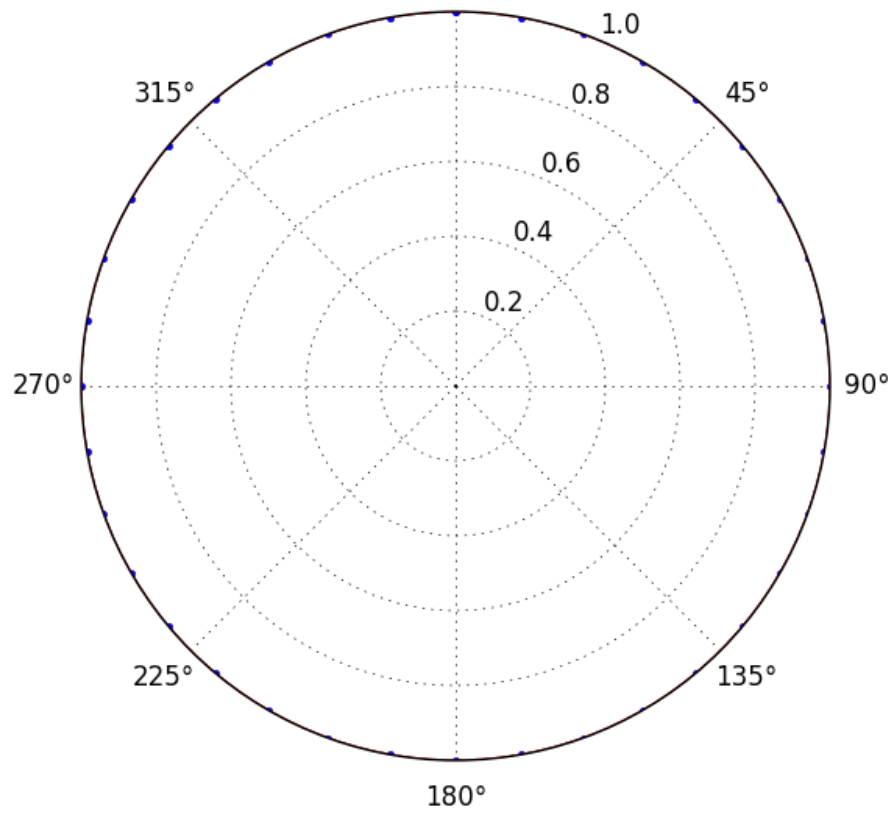


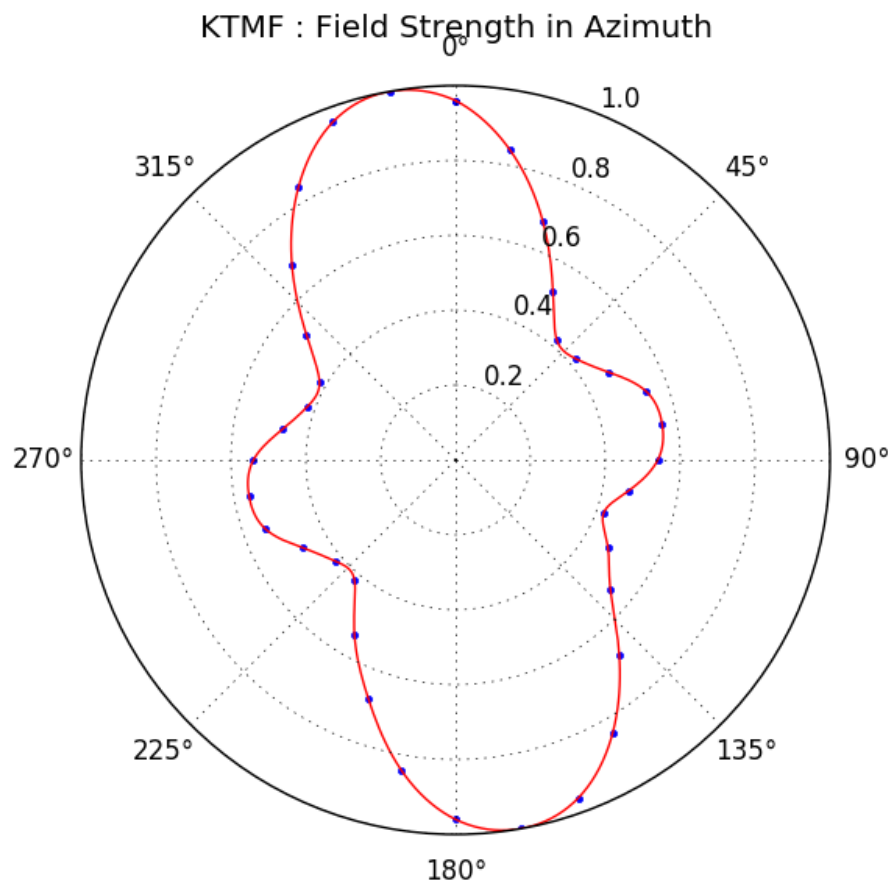
KTGF : Field Strength in Azimuth



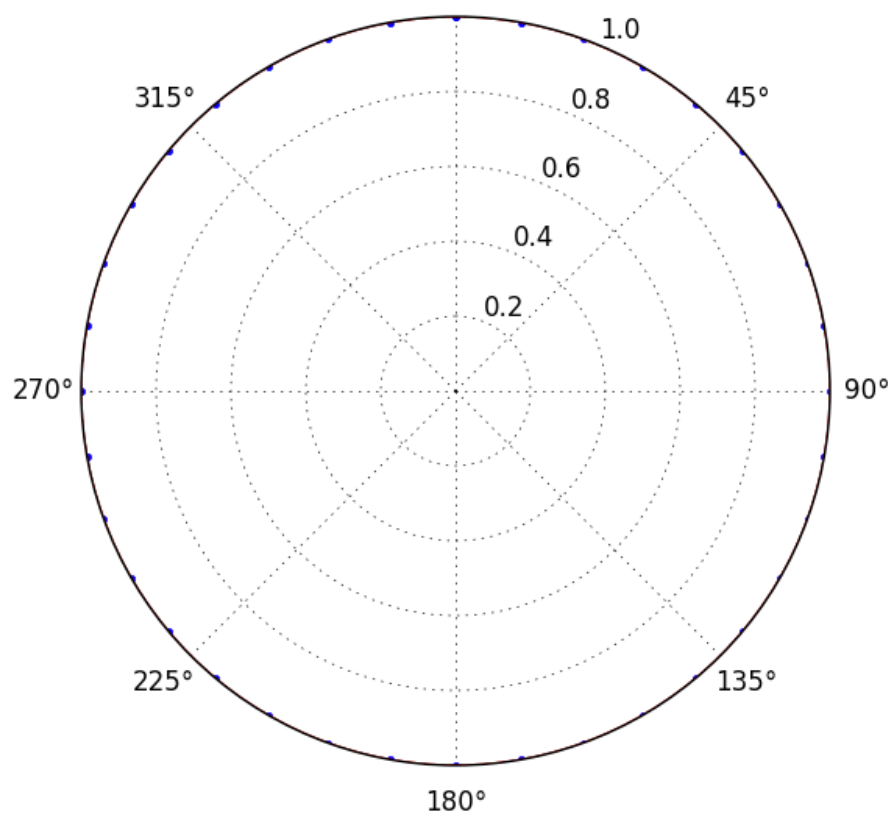


KUGF-TV : Antenna Pattern in Azimuth



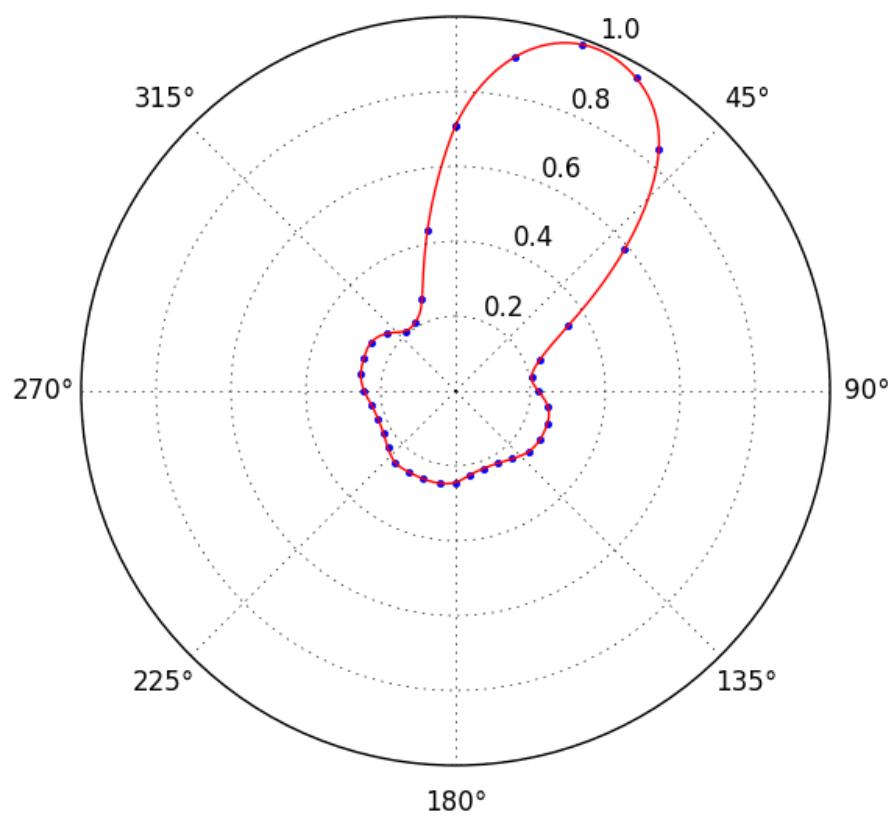


KUGF-TV : Antenna Pattern in Azimuth

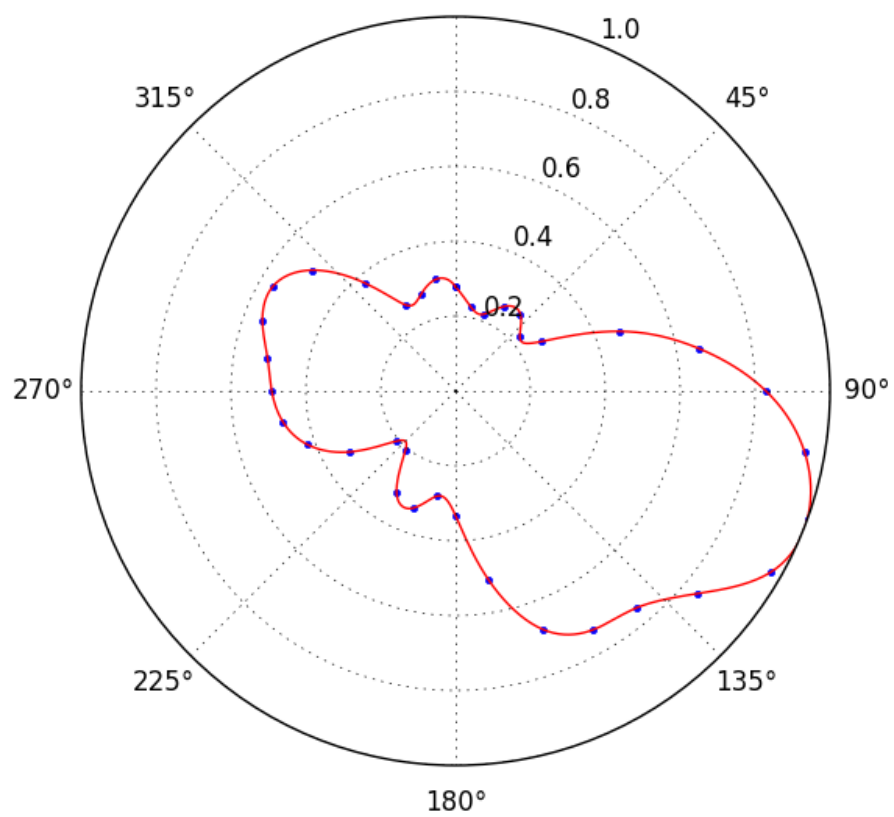




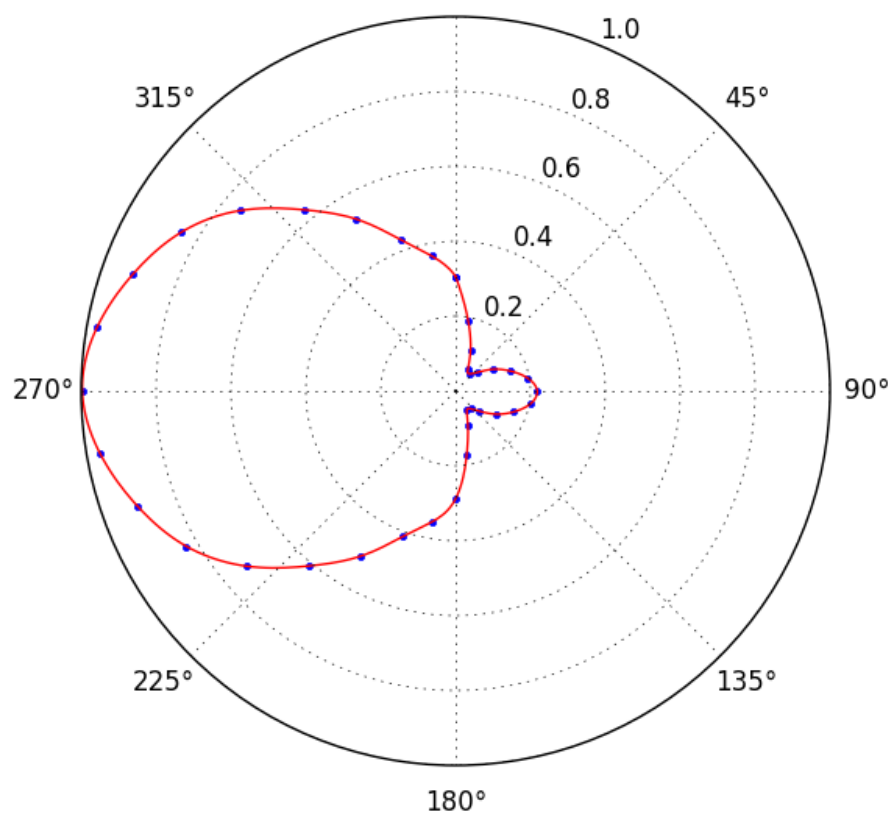
KUHM-TV : Field Strength in Azimuth



KWYB : Field Strength in Azimuth

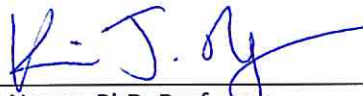


KWYB-LD : Field Strength in Azimuth



## SIGNATURE PAGE

This is to certify that the thesis prepared by Erin Wiles entitled "Rural Broadband Mobile Communications: Spectrum Occupancy and Propagation Modeling in Rural Western Montana" has been examined and approved for acceptance by the Department of Electrical Engineering, Montana Tech of The University of Montana, on this 25th day of April, 2017.



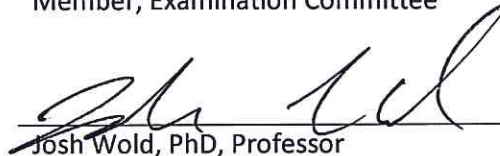
---

Kevin Negus, PhD, Professor  
Department of Electrical Engineering  
Chair, Examination Committee



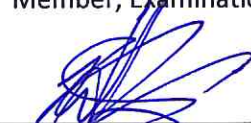
---

Dan Trudnowski, PhD, Professor and Department Head  
Department of Electrical Engineering  
Member, Examination Committee



---

Josh Wold, PhD, Professor  
Department of Electrical Engineering  
Member, Examination Committee



---

Hilary Risser, PhD, Professor  
Department of Mathematical Sciences  
Member, Examination Committee